# PROCEEDINGS
# OF THE INTERNATIONAL SYMPOSIUM
## CEMC 2014

Czech Geological Society

4th Central European Mineralogical Conference
Skalský Dvůr 2014

1919
ČESKÁ GEOLOGICKÁ SLUŽBA

UNIVERSITAS · MASARYKIANA BRUNENSIS

Skalský Dvůr, Czech Republic     23–26 April, 2014

4<sup>th</sup> CENTRAL EUROPEAN MINERALOGICAL CONFERENCE (CEMC)

Skalský Dvůr, Czech Republic, 23–26 April 2014

# Proceedings of the international symposium CEMC 2014

**Masaryk University**
**Czech Geological Society**

# Organizers

**Milan Novák**

**Petr Gadas**

**Zbyněk Buřival**

**Radek Škoda**

**Renata Čopjaková**

**Zdeněk Losos**

**Ivo Macek**

**------------------------------**

Masaryk University
Brno


**David Buriánek**

**František Veselovský**

**---------------------------**

Czech Geological Survey


**Stanislav Houzar**
**Vladimír Hrazdil**

**------------------------------**

Moravian Museum
Brno


**Jakub Plášil**
**-----------------------------**
Czech Academy of Science
Czech Republic

# Table of contents

# DISORDER AMONG OCTAHEDRAL SITES IN TOURMALINES OF SCHORL-DRAVITE SERIES

[1]Peter Bačík[#]

[1] Comenius University in Bratislava, Faculty of Natural Sciences, Dpt. of Mineralogy and Petrology, Mlynská dolina, 842 15 Bratislava, Slovakia, [#]bacikp@fns.uniba.sk

Key words: tourmaline supergroup, crystal chemistry, disorder, octahedral sites

## INTRODUCTION

Tourmaline-supergroup minerals are silicates crystallizing in $R3m$ spacegroup with following general formula $XY_3Z_6(T_6O_{18})(BO_3)_3V_3W$, where octahedral $Y$ and $Z$ sites are the most variable in occupying cations: $Y$ = $Fe^{2+}$, Mg, Mn, Al, Li, $Fe^{3+}$, and Cr; $Z$ = Al, $Fe^{3+}$, Mg, V and Cr (Henry et al. 2011).

Significant amounts of Mg (up to 2 *apfu*) can enter the $Z$ site due to Al-Mg disorder even if the Al content is higher than 6 apfu and could be sufficient for entire occupation of the $Z$ site (Grice and Ercit 1993). Similar $Fe^{2+}$-Al and $Fe^{2+}$-$Fe^{3+}$ disorders were also described (Bosi 2008) but latest works gave no proof of $^{Z}Fe^{2+}$ disorder (Bačík et al. 2011; Ertl et al. 2012).

The reason of these order-disorder reactions is still not yet clear. The deprotonization in the O1 ($W$) site and subsequent change in the valence of $Y$-O1 bond was proposed as the trigger factor for Al-Mg disorder (Hawthorne 2002). However, there are indications that the structural mechanism involving disorder is more complex. The statistical approach based on published data can shed a light on this topic. Moreover, the application of bond-valence theory and bond topology also helps to describe structural mechanisms producing disorder.

## DEPENDENCE OF ATOMIC PROPORTIONS AND STRUCTURAL PARAMETERS

Published data on the chemical composition and lattice parameters were collected from 46 samples of tourmalines with dravite-to-schorl composition. Lattice parameters from the most of them were determined from structural refinement (SREF); some of them were calculated from powder X-ray diffraction data (PXRD). To avoid the influence of errors caused by any handling with crystallographic or crystal-chemical data, the data as raw as possible including lattice parameters, bond lengths and total amounts of cations were used.

The size of the $a$ and $c$ parameters have a good positive correlation to the <$Y$-O> and <$Z$-O> bond length, respectively, which allows indirect determination of octahedral distortions. The dependence of the $a$ parameter and cation contents is less pronounced than in case of $c$ parameter. Al and Mg have a weak negative correlation to $a$ which is conform to their smaller ionic radii. In contrast, Fe has a weak positive

correlation to $a$ which is the result of its larger ionic radius compared to Al and Mg. It suggests that all three cations occupy the $Y$ site and have influence on its distortion.

The negative correlation of Al to $c$ is not surprising since Al is the most abundant cation in the $Z$ site and has smaller ionic radius compared to Mg. In contrast, the positive correlation of larger Mg cation to $c$ proves that increase in Mg content is proportional to the enlargement of $c$ size and dilatation of the $ZO_6$ octahedra. Consequently, we can assume that the total content of Mg is proportional to the Mg content in the $Z$ site. Ferrous iron has a negative correlation to the $c$ size. It may seem strange since $Fe^{2+}$ has larger ionic radius than Mg or Al. It suggests that none or only negligible proportion of $Fe^{2+}$ can be fixed at the $Z$ site.

Similar dependence of cation occupancy and octahedral distortions revealed from the study of selected bond lengths. $Fe^{2+}$ induces an increase in all bond lengths in $Y$ site except $Y$-O2 while Mg has a completely opposite effect. It corresponds to their ionic radii. Aluminium has no significant effect except the contraction of $Y$-O2 bond length. In the $Z$ site Al induce the contraction of all bond lengths, Mg has opposite effect. $Fe^{2+}$ has illogical negative correlation to bond lengths which suggest that $Fe^{2+}$ do not enter the $Z$ site in any significant amount. Consequently, the Al-Mg disorder is likely very common in tourmalines of Mg-bearing tourmalines whereas any disorder involving $^{Z}Fe^{2+}$ seems to be unlikely.

BOND-TOPOLOGICAL STUDY

Local arrangement of one $Y$ site and two $Z$ sites was inspected and bond valences for each bond in graphs for 12 different local arrangements were calculated. The first group includes graphs of 4 arrangements with various $Z$ and $Y$ occupancy and $^{W}OH$ and $^{V}OH$, second includes 4 graphs with $^{W}O$ and $^{V}OH$, and third has $^{W}OH$ and $^{V}O$.

Bond-topology graphs revealed that $^{Z}R^{2+}$ induces an increase in valence and decrease in length of $Y$-O6 bond. Consequently, the valence of $Y$-O2 bond decreases and its length increases. This corresponds to variations in bond lengths dependent on the site occupancy.

Moreover, $^{Y}R^{2+}$ requires the presence of $R^{3+}$ in neighboring $Y$ sites. On the other hand, $^{Y}R^{3+}$ can be stable in arrangement with $^{Z}R^{2+}$ and $^{X}Na$ while $^{Y}R^{3+}$ with $2^{Z}R^{3+}$ requires the $X$-site vacancy. These bond-valence requirements are the structural factor producing the Al-Mg disorder very likely.

REFERENCES

Bačik, P., Ozdín, D., Miglierini, M., Kardošová, P., Pentrák, M., and Haloda, J. (2011): Crystallochemical effects of heat treatment on Fe-dominant tourmalines from Dolní Bory (Czech Republic) and Vlachovo (Slovakia). *Phys. Chem. Min.* **38**, 599-611.

Bosi, F. (2008): Disordering of $Fe^{2+}$ over octahedrally coordinated sites of tourmaline. *Am. Mineral.* **93**, 1647-1653.

Ertl, A., Kolitsch, U., Darby Dyar, M., Hughes, J. M., Rossman, G. R., Pieczka A., Henry, D.J., Pezzotta, F., Prowatke, S., Lengauer C. L., Körner, W., Brandstätter, F., Francis, C. A., Prem M., Tillmanns E. (2012): Limitations of $Fe^{2+}$ and $Mn^{2+}$ site occupancy in tourmaline: Evidence from $Fe^{2+}$- and $Mn^{2+}$-rich tourmaline. *Am. Mineral.* **97**, 1402-1416.

Grice, J. D. & Ercit, T. S. (1993) Ordering of Fe and Mg in tourmaline: The correct formula. *N. Jahrb. Mineral. Abh.* **165**, 245-266.

Hawthorne, F. C. (2002): Bond-valence constraints on the chemical composition of tourmaline. *Can. Mineral.* **40**, 789-797.

Henry, D., Novák, M., Hawthorne, F. C., Ertl, A., Dutrow, B., Uher, P. & Pezzotta, F. (2011): Nomenclature of the tourmaline-supergroup minerals. *Am. Mineral.* **96**, 895-913.

# PETROGRAPHIC STUDY OF EARLY MEDIEVAL MORTARS FROM THE CASTLE IN OSTRÓW TUMSKI (WROCLAW, SW POLAND)

[1]Wojciech Bartz[#], [2]Małgorzata Chorowska,
[3]Maria Gąsior, [4]Jacek Kościuk

[1] Institute of Geological Sciences, University of Wroclaw, Poland, [#]wojciech.bartz@ing.uni.wroc.pl
[2,4] Institute of History of Architecture, Art and Technology, Wroclaw University of Technology, Poland
[3] Laboratory for Technological and Conservation Research, Faculty of Architecture, Wroclaw University of Technology

The first dukal castle in Wrocław was erected after 1175, built on the site of the former stronghold. It was situated on a river island called Ostrów Tumski. The results of archaeological research, conducted in the years 1980-1989 and 2011-2012, shows that the oldest part was a huge brick building, which was the 18-side tower house. Probably it was a residential tower, situated on the northern side of a castle, in the vicinity of the wooden – earth walls. At the turn of the 12th and 13th century it was flanked from the North-East of a curtain wall. During the reign of Prince Henry I Bearded (1201-1238) the building was partially demolished, and replaced by the Brick Palace with a length of more than 40 m, with adjacent Palatine Chapel. In the mid-13th century the castle was surrounded by a fortified wall. In the next phase (80's of the 13th century) its residential core was again rebuilt and replaced by another Palace, with a length of 50 m. It is peculiarity was 8-side Hall, built in the middle of the Palace. It was built at the site of the 18-side Tower, previously demolished to the ground.

The castle on the Ostrów Tumski was important Dukes residence to the beginnings of the 14th century, when the new castle was created on the left bank of the river, close to the city. Abandoned first, the Castle were occupied by the clergy of the Collegiate Church of St. Cross and almost completely dismantled.

Nowadays, the remains of the Castle are located below the ground level and are the subject of an extensive archaeological research. These relics are extremely valuable, because they are the only source of knowledge of the history of the Piast Castle in Wrocław. However, the investigations are difficult to perform due to numerous conversion of the Castle and the lack of continuity of the archaeological layers. Thus, the aim of our project is a detailed mineralogical analysis of historic mortars sampled from particulars constructing phases of the castle. We expect that it will help us assign the individual relics to the proper building phases.

Twenty one mortar samples, originating from all distinguished construction phases were analyzed, according to methodology proposed by Middendorf et al. (2000). They were investigated by means of: optical polarising microscopy (OPM), simultaneous thermal analysis (DTA-TG), X-ray powder diffraction (XRD), sieve analysis, and electron microscopy (SEM-EDX).

The petrographic data shows that the aggregate represents moderately to poorly sorted, coarse- to less common medium-grained sand. Against this background, only few samples, taken from the 18–side tower house, are slightly coarser-grained. Typically, the aggregate consists mainly of quartz, with subordinate feldspars and lithic grains. Accessories are: rutile, glauconite, amphibole, zircon, garnet, epidote, staurolite. Their distribution among individual samples is generally scattered. However, samples from the Brick Palace show slight enrichment in accessory minerals. Moreover, these mortars contain distinctive quartz grains. They exhibit signs of heat treatment. Inside these grains an irregular fracture network, healed with optically isotropic substance, was observed. Mortars from the Brick Palace are distinguished from the other by the presence of brownish patches of microcrystalline goethite, located in the binding mass, and most of all inside the lime lumps (underburnt fragments of carbonate rocks). Their occurrences imply production of a lime from carbonate rocks rich in ferrous minerals. One of the characteristics is the presence of brick fragments, charcoal and silicate sinters, presumably remnants of lime calcination process. They occur in mortar samples from the Brick Palace, the fortifying wall and the 8-side Hall, with an exception of mortars from 18–side tower house. The petrographic analysis permits to calculate the binder: aggregate ratio. It is estimated as 1:1 (by volume) for all samples.

The binder is an air-hardening lime, present as microcrystalline calcium carbonate (micrite). It is relatively homogenous, lime lumps are preset but very scarce. It implies that the lime burning process was conducted carefully, within its temperature optimum or slightly above. An indication of the latter thesis is the presence of siliceous sinters. Most samples are affected by autogeneous healing of their binder. Small cracks, voids are filled with neo-formed sparitic euhedral calcite crystal, mostly in rhombohedral form.

Summing up, the petrographical data partly allowed us to identify different building materials with similar compositional characteristics, which can be related to different building phases.

REFERENCES

MIDDENDORF, B., BARONIO, G., CALLEBAUT, K., HUGHES J. J. (2000): Chemical-mineralogical and physical-mechanical investigations of old mortars. *In Proceedings of the International RILEM-workshop "Historic mortars: characteristics and tests"* (Bartos, P., Groot, C. and Hughes, J. J. eds.), Paisley, 53-59.

# VESUVIANITE FROM THE DUBOVÁ AND MODRA-HARMÓNIA SKARNS (MALÉ KARPATY MTS., SLOVAKIA): COMPOSITION AND ALTERATION PRODUCTS

[1]Vladimír Bolohuščin[#], [1]Pavel Uher,
[1]Peter Ružička

[1]        Dept. of Mineralogy and Petrology, Comenius University, Mlynská dolina G, 842 15 Bratislava, Slovakia, [#] v.bilohuscin@gmail.com

Key words: vesuvianite, clinozoisite, allanite-(Ce), REE, Th, Ca-skarn, Malé Karpaty Mts., Slovakia

## INTRODUCTION

Ca-skarns are the contact metamorphic rocks, which were created on contact zone between magmatic rocks and carbonate sedimentary or metamorphic rocks, mostly on contacts between granitic rocks and limestones. We investigated the Ca-skarns located at the contact between Devonian limestones and Hercynian granitic rocks of the Modra Massif from Dubová and Modra-Harmónia near Modra town, the Malé Karpaty Mountains, Central Western Carpathians, SW Slovakia. The skarns and their minerals were studied by several authors (e.g., Cambel 1954, Čajková and Šamajová 1960, Cambel et al. 1989) but their detailed mineralogical examination is still missing. The aim of this contribution is compositional study of vesuvianite, including its texture and alteration products using the electron microprobe. The vesuvianite compositions were calculated on 50 cations and 78 anions (Groat et al. 1992); clinozoisite and allanite analyses were normalized on 8 cations according to procedure of Armbruster et al. (2006).

## RESULTS

The rock-forming minerals of the studied Ca-skarns are calcite, diopside to hedenbergite, grossular, vesuvianite, locally wollastonite, epidote, titanite, and alkali feldspars. Vesuvianite forms subhedral to euhedral crystals and aggregates, usually up to 1 cm across, in association with calcite, grossular and diopside to hedenbergite. In some cases, vesuvianite contains tiny inclusions of Ba-rich feldspars (hyalophane to celsiane with 7-39 wt. % BaO), albite, orthoclase, barite, and zircon. Vesuvianite crystals from the Dubová, Horné Trávniky skarn locally shows tiny oscillatory zoning due to variations of heavy elements, mainly REE`s and Th. The REE and Th enriched zones attain up to 5.3 wt. % of total $REE_2O_3$ (up to 0.96 *apfu* REE) and up to 1.8 wt. % $ThO_2$ ($\leq$ 0.21 *apfu* Th). Light REE`s (La to Eu) show clear dominancy over heavy REE`s (Gd to Lu); the maximum concentration of $Ce_2O_3$ attains 2.5 wt. %, $Nd_2O_3 \leq 1.4$ wt. %, and $La_2O_3 \leq 1.1$ wt. %. Thorium generally reveals a positive correlation with REE`s; the best correlations show Th vs. Nd and Th vs. Sm, due to the highest similarity of their ionic radii. Titanium content varies in a

broad interval: 0.20 to 5.4 wt. % $TiO_2$ (up to 1.97 *apfu* Ti). Compositional variations indicate following possible substitutions in the studied vesuvianite: $(Fe,Mg)TiAl_{-2}$, $Ca(Fe,Mg)Na_{-1}Al_{-1}$, $REEAlCa_{-1}Ti_{-1}$, and $ThO_2Ca_{-1}(OH)_{-2}$.

In some places, vesuvianite is partly replaced by anhedral veinlets and grains of secondary REE-rich clinozoisite to allanite-(Ce). The clinozoisite to allanite contains 12 to 23 wt. % $REE_2O_3$ (0.39 to 0.79 *apfu* REE), low concentrations of Th (max. 0.7 wt. % $ThO_2$; 0.015 *apfu* Th) and Ti (≤ 0.5 wt. %; 0.035 *apfu* Ti).

## CONCLUSIONS

Textural and compositional data indicate an origin of vesuvianite + grossular + diopside to hedenbergite ± wollastonite association near peak P-T conditions of the contact-thermal metamorphism (~ 200 MPa and ~ 600 °C), during intrusion of the Hercynian granitic rocks of the Modra Massif into Devonian limestones, ca. 345 Ma ago. Vesuvianite is the main carrier of light REE`s and Th in the absence and possible unstability of common primary REE,Th-rich phases (allanite or monazite), probably due to low concentration of these elements in the host metacarbonate rocks. Minerals of the vesuvianite group usually contain only negligible concentrations of REE`s (up to 0.5 wt. % $REE_2O_3$; Groat et al. 1992; Galuskin 2005). Conversely, the highest known REE concentration shows vesuvianite in altered greenstone from San Benito County, California: ca. 14.7 to 20.6 wt. % $REE_2O_3$; ~ 3.0 to 4.1 *apfu* REE (Murdoch and Ingram 1966; Crook and Oswald 1979; Fitzgerald et al. 1987; Groat et al. 1992). On the contrary, the highest known Th content in vesuvianite from Seward Peninsula, Alaska attains only 1.5 wt. % $ThO_2$ or 0.18 *apfu* Th; this vesuvianite is also REE-rich (Groat et al. 1992). Consequently, vesuvianite from the Dubová skarn shows the most Th-rich composition in this mineral yet reported.

Alteration and partial replacement of the contact-metamorphic vesuvianite by late retrograde fluids led to formation of secondary REE-rich clinozoisite to allanite-(Ce), which documents mobility and evolution of REE`s in metamorphic prograde versus retrograde processes.

REFERENCES

ARMBRUSTER, T., BONAZZI, P., AKASAKA, M., BERMANEC, V., CHOPIN, C., GIERÉ, R., HEUSS-ASSBICHLER, S., LIEBSCHER, A., MENCHETTI, S., PAN, Y. & PASERO, M. (2006): Recommended nomenclature of epidote-group minerals. *Eur. J. Mineral.* **18**, 551-567.

ČAJKOVÁ, M. & ŠAMAJOVÁ, E. (1960): Contribution to topographic mineralogy of the Malé Karpaty Mountains. *Acta Geol. Geogr. Univ. Comen. Geol.* **4**, 51-67 (in Slovak).

CAMBEL, B. (1954): Geological-petrographical problems of north-east part of the Malé Karpaty crystalline basement. *Geol. Práce Zoš.* **36**, 3-74 (in Slovak).

CAMBEL, B., KORIKOVSKY S.P., MIKLÓŠ, J. & BORONIKHIN, V.A. (1989): Calc-silicate hornfelses (erlans and Ca-skarns) in the Malé Karpaty Mts. region. *Geol. Zbor. Geol. Carpath.* **40**, 281-304.

CROOK, W.W.III & OSWALD, S.G. (1979): New data on cerian vesuvianite from San Benito County, California. *Am. Mineral.* **64**, 367-368.

GALUSKIN, E. (2005): Minerals of the vesuvianite group from the achtarandite rocks (Wiluy River, Yakutia). *Wyd. Uniw. Śląskiego, Katowice*, 192 p. (in Polish).

Groat, L.A., Hawthorne, F.C. & Ercit, T.S. (1992): The crystal chemistry of vesuvianite. *Can. Mineral.* **30**, 19-48.

FITZGERALD, S., LEAVENS, P.B., RHEINGOLD, A.L., NELEN, J.A. (1987): Crystal structure of a REE-bearing vesuvianite from San Benito County, California. *Am. Mineral.* **72**, 625-628.

MURDOCH, J. & INGRAM, B. (1966): A cerian vesuvianite from California. *Am. Mineral.* **51**, 381-387.

# 3D VISUALIZATION OF ORE MINERALIZATION, K-SILICATE ALTERATION AND CA-NA ALTERATION AT THE PORPHYRY GOLD DEPOSIT BIELY VRCH (SLOVAKIA)

[1]Jana Brčeková[#], [1]Michal Jánošík,
[1]Peter Koděra, [1]Peter Uhlík, [12]Jaroslav Lexa, [3]Andrej Biroň

[1] Comenius University, Faculty of Natural Sciences, Department of Geology of Mineral Deposits, Mlynská Dolina, 842 15 Bratislava, Slovakia [#]michnova@fns.uniba.sk
[2] Geological institute, Slovak Academy of Sciences, Dúbravská cesta 9, 840 05 Bratislava, Slovakia
[3] Geological institute, Slovak Academy of Sciences, Severná 5, 974 01 Banská Bystrica, Slovakia

Key words: Au-porphyry, Biely vrch, alteration, 3D modelling, ore body, GIS, gold

## INTRODUCTION

In the year 2006 at the locality Biely Vrch near Detva the company EMED Slovakia discovered the presence of a new type of porphyry mineralisation with a relatively high Au/Cu ratios, which is typical for porphyry gold type of mineralisation (Koděra et al. 2010). The deposit is situated in the central zone of the Javorie stratovolcano. Parental intrusion of diorite to andesite porphyry is emplaced into andesitic volcanic rocks. Gold mineralization occurs in the vicinity of quartz veinlets (down up to about 750 m). K-silicate alteration situated in the central part of the porphyry intrusion is probably the primary source of gold (Bakos et al. 2012). High Au grades occur in the vicinity of quartz veinlets, in altered rocks with clays, chlorite and K-feldspar, sometimes attached to sulphides or Fe-Ti minerals (Koděra et al. 2010).

The purpose of our study was to visualize zones with high grade gold mineralization and their correlation with distribution of K-silicate and Ca-Na alteration. Definition of alteration boundaries based only on chemical composition is difficult and therefore 3D modelling was supplemented by results of mineralogical research.

## DATA PREPARATION AND METHODS

The database in PostgreSQL format with drill holes collar, survey, assay and litological data has been provided by EMED Mining Ltd. The database contains detailed documentation of 52 inclined drill holes with length ranges to 782 m. Drill holes are sampled in 1 or 2 meters step. Geochemistry data are determined in ppm or wt. % and mineralogy and alteration data in estimated intensity from 0 to 5.

3D Element grade distribution block models were generated via ordinary kriging method (Matheron 1971) using Encom Discover 3D software. Estimation of domains was modelled based only on metal grade, with statistically defined "cut-off" grade and "top cut" grade values. Modelled variograms for three principal directions were comprised of structure-nested spherical models. Validation of the block model by statistical comparison of

composite grades versus block grades, inspection of the block model in plain and in section and visual comparison of block grades to drill data were done. Mineralogical characterization of studied samples was realized by XRD analyses of clay fraction and random specimens using a Philips PW 1710. Samples for quantitative analyses were milled in a McCrone Micronizing Mill with internal standard $Al_2O_3$ to < 20 μm size. The XRD data were converted into wt. % minerals using the RockJock software.

## INTERPRETATION OF ALTERATION ZONES BASED ON CHEMICAL AND MINERAL COMPOSITION

Geochemistry of rock is one of the most prominent features for determination of individual types of hydrothermal alteration. In general, K-silicate and Ca-Na alteration are represented by the increased amount of K or Ca-Na, respectively. Mineralogical studies (XRD analyses of whole-rocks combined with thin section study) show that rocks with increased amount of K and K/(Ca+Na) ratio contain increased amount of secondary K-feldspar and/or secondary biotite (biotite up to 21 %, K-feldspar up to 27 %; in studied samples). For the purpose of 3D modeling the K-silicate zone was fixed to have the following properties: K > 1.34 wt. %, Al < 7.66 wt. %, Fe > 4.55 wt. %, Mg < 1.33 wt. %. On the other hand, rocks with high amount of Ca+Na and low K/(Ca+Na) ratio contain increased amount of basic plagioclase and amphibole (plagioclase up to 53%, amphibole up to 15%) that can be of hydrothermal origin, but also predominantly of magmatic origin (as seen in the relatively fresh rock below ~ 700 m depth in DVE-51 drill hole). For the purpose of 3D modelling of the Ca-Na-silicate zone, the following properties were fixed: Ca > 3.34 wt. %, Na > 0.9 wt. %, minimum amount of plagioclase > 5 %. In general, the K-silicate alteration zone is preserved mostly in the form of fragments within heavily argillised rock (intermediate argillic and advanced argillic alteration) from the surface down to the depth of about 400 m. Intermediate argillic alteration generally does not change the whole-rock geochemistry, but advanced argillic alteration results in decrease of most elements (including Ca, Na, K). Below ~ 400 m, Ca-Na silicate zone prevails, but locally with distinct zones of K-silicate alteration that roughly correlate with increased amount of gold and are interpreted to represent former feeder zones of the hydrothermal system. In contrast to K-silicate zone, the Ca-Na silicate alteration zone also shows increased content of Mn and Sr and relatively decreased content of Mg, Al, Ti and Au.

3D GIS modelling shows correlation of high grade ore distribution in the central part of the porphyry system with quartz stockwork. The upper part of this zone is characteristic with advance argillic alteration associated with highest grades of Au. In the deeper part of system (> 500m), gold positively correlates with K-silicate alteration within Ca-Na silicate zone of alteration.

## REFERENCES

BAKOS, F., KODĚRA P., JÁNOŠÍK M. (2012): Geochémia Au porfýrových mineralizácií v stredoslovenských neovulkanitoch v praxi. *Abstracts of the conference Geochémia 2011, Bratislava*, 16-18.

KODĚRA, P., HEINRICH, C. A., WÄLLE, M., LEXA, J. (2014): Magmatic salt melt and vapor: Extreme fluids forming porphyry gold deposits in shallow subvolcanic settings. *Geology, doi:10.1130/G35270.1*

KODĚRA, P., LEXA, J., BIROŇ, A., ŽITŇAN, P. (2010): Gold mineralization and associated alteration zones of the Biely Vrch Au-porphyry deposit, Slovakia. *Min. Slov.* **42**, 33-56.

# SCHORLITIC TOURMALINE FROM ECLOGITE- HOSTING GNEISSES IN THE TSO MORARI UHP METAMORPHIC TERRANE (LADAKH HIMALAYA, INDIA)

[1]Igor Broska[#], [1]Marian Janák,
[2]Peter Bačík

[1] Geological Institute Slovak Academy of Sciences, Dúbravská cesta 9, 840 05 Bratislava,
[#]:igor.broska@savba.sk

[2] Comenius University in Bratislava, Faculty of Natural Sciences, Dpt. of Mineralogy and Petrology, Mlynská dolina, 842 15 Bratislava, Slovakia

Key words: tourmaline, UHP metamorphism, orthogneiss

## INTRODUCTION

Tourmaline is stable at wide P-T conditions including high- to ultrahigh-pressure metamorphism (Ertl et al. 2010). Generally, tourmaline composition in metamorphic rocks is related to the character of the host rock and this contribution points to variability of tourmaline generations in eclogite-hosting gneisses from the Tso Morari UHP metamorphic terrane (Eastern Ladakh, Indian Himalaya).

## GEOLOGICAL SETTING

Tourmaline-bearing gneiss, named as Puga gneiss, belongs to the Tso Morari complex which is one of the Himalayan domes exposed in the northern part of Indian plate (Steck 2003). Puga gneisses (both ortho- and para-gneisses) host several eclogite lenses and boudins. Coesite found in these eclogites indicates UHP metamorphism in the Tso Morari complex is related to deep subduction of the Indian plate during India-Asia collision in the Eocene (Sachan et al. 2004)

The studied locality (a cliff of ca. 100 m high near Sumdo village), exposes several metre-scale eclogite boudins in a compositionally-heterogeneous sequence of tourmaline- bearing gneisses.

## TOURMALINE GENERATIONS

Tourmalines in the Puga orthogneiss form scattered disintegrated black grains visible by naked eye. In contrast, intercalating paragneiss contains euhedral, green brown grains of tourmaline which is much smaller (up to 500 μm) than in orthogneiss. Secondary quartz and tourmaline-bearing veins cutting the whole system are several cm wide, forming a fluidal structure.

The composition of tourmaline in felsic orthogneiss with the MgO content of ca. 1.5 wt. %, defines a presence of schorlitic component with a very low dravitic one. The schorlitic tourmaline can be characterised as slightly Al-deficient, with a slight vacancies on the X- site. However, Al- deficient tourmaline is present in

paragneiss and secondary veins as well. Tourmalines from paragneiss are dravitic in composition, containing ca. 8 wt. % of MgO. They form zonal crystals with more schorlitic rims. Schorlitic tourmaline in veins creating fluidal growth structure contains up to ca. 3 wt. % of MgO.

Tourmaline in orthogneiss is strongly disintegrated, which indicates that it is the oldest tourmaline generation in the investigated gneisses. A specific textural phenomenon of this tourmaline is its graphic intergrowth with quartz. This quartz is enriched in Fe (ca. 0.3 wt. % FeO) and slightly also in Ti and Al, compared to intergranular quartz.

## X-RAY DATA OF SCHORLITIC TOURMALINE

Lattice parameters $a = 16.0093(11)$ Å, $c = 7.2071(6)$ Å, $V = 1599.7(3)$ Å$^3$ of tourmaline from the Tso Morari allowed to calculate average bond lengths in the octahedral sites based on empirical equations (Bačík *in prep.*). Both of them have a relatively large values compared to common tourmalines of the schorl-dravite series. The <$Y$-O> bond length of 2.06 Å suggests a dominance of Fe$^{2+}$ in the $Y$ site but it probably does not exceed 2 *apfu*, the rest of Fe may be in trivalent form. The <$Z$-O> bond length of 1.93 Å reflects the significant proportion of cations larger than Al in the $Z$ site. It can attain up to 1 *apfu*. A part of it may be attributed to Mg but it seems to be insufficient to balance such disorder according to EMPA and consequently Fe$^{3+}$ may also occupy the $Z$ site.

## DISCUSSION

The graphic intergrowth of quartz and tourmaline is known in pegmatites (e.g. Wadoski et al. 2011). However, the intergrowth of quartz with tourmaline in orthogneiss from the Tso Morari rather resembles the exsolution phenomena. Taking into account the UHP conditions in the Tso Morari complex, tourmaline could

have been stable at such peak-pressure conditions but strongly disintegrated during decompression and exhumation. In spite of missing typical UHP inclusions such as coesite, the observed microtexture of quartz exsolved from tourmaline may indicate primary excess of silica in tourmaline. Fixation of silica to octahedral site is highly possible at UHP conditions, as proposed Finger and Hasen in 2005. At HP/UHP conditions, silica may enter the octahedral Z-site of the tourmaline crystal structure via several substitutions. During decompression the exsolution of silica from the tourmaline octahedral site could have formed new quartz stabilizing the whole system. Silica released from $Z$ site may have been replaced by excess of Fe$^{3+}$. On the other hand, the formation of well-preserved, euhedral tourmaline in paragneiss and veins could have resulted from retrograde stage of metamorphism.

## REFERENCES

ERTL, A. MARSCHALL, H. R., GIESTER, G., HENRY, D. J., SCHERTL, H. P., NTAFLOS, T., LUVIZOTTO, G. L., NASDALA, L., & TILLMANS, E. (2010): Metamorphic ultrahigh-pressure tourmaline: Structure, chemistry, and correlations to *P-T* conditions. *Am. Mineral.* **95**, 1-10.
SACHAN, H., MUKHERJEE, B., OGASAWARA, Y., MARUYAMA, S., ISHIDA, H., MUKO, A. & YOSHIOKA, N. (2004): Discovery of coesite from Indus Suture Zone (ISZ), Ladakh, India: Evidence for deep subduction. *Eur. J. Mineral.* **16**, 235-240.
STECK, A., (2003): Geology of the NW Indian Himalaya. *Eclogae Geologicae Helvetiae,* **96**, 147–196.
WADOSKI, E. R., Grew, E. S. & YATES M., G. (2011): Compositional evolution of tourmaline-supergroup minerals from granitic pegmatites in the Larsemann hills, east Antarctica. *Can Mineral.* **49**, 381-405.

# MINEROLOGICAL DIVERSITY OF SULFIDES FROM CHROMITE ORE FROM THE CZERNICA AND GROCHOWIEC HILL, CENTRAL-SUDETIC OPHIOLITE (SW POLAND)

[1]Michał Bukala[#], [1]Piotr Wojtulek,
[1]Jacek Puziewicz, [2]Theodoros Ntaflos

[1]   Department of Experimental Petrology, Institute of Geological Sciences, University of Wrocław, Maksa Borna 9, 50-204 Wrocław; [#] michal.bukala91@gmail.com
[2]   Department of Lithospheric Research, University of Vienna, Althanstasse 14, 1090 Vienna

## GEOLOGICAL SETTING

The Gogołów – Jordanów Serpentinite Massif (GJSM) and the Braszowice-Brzeźnica Massif (BBM) are recognized as the parts of the Central-Sudetic Ophiolite (Kryza and Pin 2010). The GJSM serpentinites recorded both low temperature serpentinization and greenschist facies metamorphism (Dubińska and Gunia 1997, Wojtulek et al. 2013). Chromitite veinlets and pockets occur in the Czernica Hill (in the GJSM) and in the Grochowiec Hill area (in the BBM) within strongly serpentinized harzburgites. Chromitites are not associated with specific serpentinite lithology and they occur within both lizardite and antigorite serpentinites.

## PETROGRAPHY

The chromitites from the GJSM and the BBM occur as (1) massive, (2) laminated, (3) nodular, (4) disseminated ore and (5) veinlets within serpentinite. Chromitites contain frequently sulfide minerals that form anhedral and subhedral grains up to 120 μm, included in (1) chlorite-serpentinite groundmass or at (2) the chromite grain margins. The most frequently occurring sulfides are millerite, polydymite-ss, godlevskite, whereas carrollite and sugakite occur rarely.

Millerite forms anhedral and subhedral grains up to 50 μm. It occurs as individual grains and in association with godlevskite and polydymite-ss. Millerite has atomic metal/sulfur ratio $= 0.76 – 1.01$. Millerite occurring in the vicinity of chromite grains includes greater amounts of Fe (2.3 % mol). It contains also low contents of Cu and Co (up to 0.31 and up to 0.43 mole %, respectively).

Polydymite forms anhedral and subhedral grains up to 100 μm. Polydymite atomic metal/sulfur ratio ranges between $0.75 – 0.80$, it contains Fe (0.54 – 6.03 % mol) and Co (up to 1.74 mole %). Only one grain of violarite has been found at chromite grain margin in association with polydymite and millerite (Fig.2) Violarite has atomic metal/sulphur ratio $= 0.82$,

containg Fe (12.4 mole %) and Co (0.7 mole %).

Godlevskite forms subhedral grains up to 30 μm. Godlevskite has atomic metal/sulfur ratio = 1.06 – 1.16, Ni and Fe content is variable over a wide range. Godlevskite contains Co (up to 3.93 mole %), furthermore, one grain contains Cu (5.46 mole %). Locally godlevskite is intergrown with millerite and rimmed by polydymite. The boundary between godlevskite and polydymite is gradual. (Fig. 1).
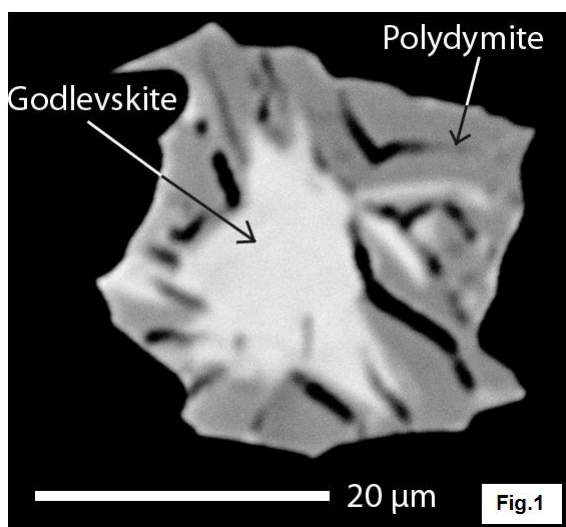


Fig. 1. BSE image of godlevskite relic rimmed by secondary polydymite.

Carrollite and sugakiite form individual, anhedral grains up to 15 μm. Carrollite has atomic metal/sulfur ratio = 0.85, contain Co (1.6 % mol). Sugakite atomic metal/sulfur ratio is 0.81.

## CONCLUSIONS

The sulfides provide informations about the conditions of serpentinization and other alteration processes affecting ultrabasic rocks. The sulfides are heterogeneous and altered in the GJSM chromitites. Typically, polydymite replaces godlevskite and millerite (Fig. 1, 2). This fits the interpretation of Klein and Bach (2008) that sulfur metasomatism leads to replacement of S-poor sulfides by S-rich ones. Such alteration tooks place if the fluids rich in sulfur penetrate the peridotite at serpentinite and steatization conditions.
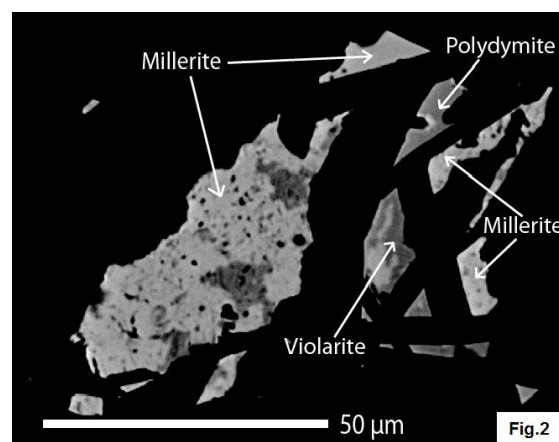


Fig. 2. BSE image of sulfide mineral assemblage in a highly altered chromitite

## REFERENCES

DUBIŃSKA, E., Gunia, P. (1997): Sudetic ophiolite: current view on its dynamic model. *Geological Quarterly,* **41**, 1-20.

GONZÁLEZ-JIM ÉNEZ, KERESTEDJIAN, J.M., PROENZA, K., GERVILLA, J.A. (2009): Metamorphism on Chromite Ores from the Dobromirtsi Ultramafic Massif, Rhodope Mountains (SE Bulgaria). *Geologica Acta* **7**, 413-429.

KLEIN, F., BACH, W. (2008): Fe-Ni-Co-O-S Phase Relations in Peridotite- Seawater Interactions, *Journal of Petrology,* **50**, 37-59.

MAJEROWICZ, A. (1979): Grupa górska Ślęży a współczesne problemy geologiczne ofiolitów. Wybrane zagadnienia stratygrafii, petrografii i tektoniki wschodniego obrzeżenia gnejsów sowiogórskich i metamorfiku kłodzkiego. (T. Gunia, ed.). *Field Conference*, *Sept 8-9 1979, Nowa Ruda*, 9-34. (in Polish).

WOJTULEK, P. PUZIEWICZ, J., NTAFLOS, T. (2013): The origin of the non-serpentinic phases of the Gogołów-Jordanów serpentinite massif (SW Poland). *European Geosciences Union, General Assembly 2013, conference abstract.*

# TEXTURAL AND COMPOSITIONAL EVIDENCES FOR A POLYPHASE SATURATION OF TOURMALINE FROM PERALUMINOUS GRANITES AND PEGMATITES ENCLOSED IN THE TŘEBÍČ PLUTON (BOHEMIAN MASSIF)

[1]David Buriánek[#], [2]Zdeněk Dolníček,
[3]Milan Novák

[1]     Czech Geological Survey, Leitnerova 22, 602 00 Brno, [#]david.burianek@geology.cz
[2]     Department of Geology, Palacký University, 17. listopadu 12, 771 46 Olomouc
[3]     Department of Geological Sciences, Faculty of Science, Masaryk University, Kotlářská 2, 611 37. Brno, Czech Republic

Key words: tourmaline, peraluminous granite, pegmatite, P-T conditions, Třebíč Pluton

## INTRODUCTION

Dykes of peraluminous granites common predominantly oriented in the NE-SW to NNE-SWW direction crosscut the Třebíč Pluton (Buriánek and Novák 2007). Dykes, about 1–6 m thick and up to 15 m long, have heterogeneous internal structure and typically sharp contacts to host durbachites.

## CHEMICAL COMPOSITIONS OF TOURMALINE

Large diversity of the textural types of tourmalines is also reflected in high variability of chemical compositions. The occupation of T-site is variable (5.71–6.05 *apfu* Si), but commonly close to the ideal stoichiometry 6 Si. Almost all analyses comprise Z-site fully occupied by Al ($\geq$ 5.98 *apfu*) and Al content in Y-site ranged from 0.00 to 1.00 *apfu*. Tourmaline also displays considerable variations in Mg (0.03 to 1.51 *apfu*) and Fe (0.89 to 2.18 *apfu*) but low contents of Mn ($\leq$ 0.06 *apfu*) and Ti ($\leq$ 0.21 *apfu*). The Na content is varying from 0.31 to 0.76 *apfu*; Ca ($\leq$ 0.10 *apfu*) and K ($\leq$ 0.05 *apfu*) are low. The majority of tourmalines are F-poor to F-moderate (0.00–0.34 *apfu*).

The compositional changes are a result of combination of four main substitutions. The homovalent substitution (1) $Fe\,Mg_{-1}$ is dominant. Alkali-deficiency can be explained by the heterovalent substitutions (2) $^{X}Na\,^{Y}R^{2+W}F$ $^{X}\square\,^{Y}Al_{-1}{}^{W}OH_{-1}$ or (3) $^{X}Na\,^{Y}R^{2+}$ $^{X}\square\,^{Y}Al^{-1}$, which is usually combined with the substitution (4) $^{Y}R^{2+W}O$ $^{Y}Al_{-1}{}^{W}OH_{-1}$.

## TEXTURAL AND MINERALOGICAL EVOLUTION OF GRANITE MELT

During crystallization of granite dykes several textural types of granites and pegmatites have been formed. Along contact with surrounding durbachites there is locally present aplitic zone several cm to dm thick (locally with comb structures). In the central part of the dykes medium-grained muscovite-biotite granite with tourmaline-rich nodules dominates.

Younger tourmaline granites and pegmatites crosscut both textural types. Polyphase evolution is suggested in these dykes.

**The first stage** is related to the emplacement of granite melt into the durbachites. The P-T conditions of emplacement of the peraluminous granite have been estimated using the zircon and monazite saturation thermometry (Montel 1993) and the andalusite stability field (Clarke et al. 2005) at T = 672–736 °C and P = 0.1–0.4 GPa. A boron-rich melt was exsolved from fluid-rich melt containing crystals of feldspars and concentrated in the spherical bubbles – nodules. They agglutinated sporadically and formed ring structures or large pockets, which produced tourmaline granites. Tourmaline in nodules evolved from early schorl to hydrothermal foitite. Usually these systems froze very quickly and pockets of the fluid-rich melt were closed in the muscovite granites with higher solidus temperature. We assumed a temperature of 650–680°C for the near-solidus conditions of volatile-rich melt forming tourmaline nodules.

**The second stage** of magmatic crystallization represents formation of coarse-grained pegmatite veins and pockets often containing tourmaline. Tourmaline in pegmatite evolved from the magmatic schorl to late hydrothermal dravite.

During **the third stage** of evolution the boron-rich melts in tourmaline nodules may exsolved boron-rich aqueous fluids, which reacted with earlier magmatic minerals, namely biotite and feldspars at temperatures of 630 to 450 °C and pressure of 0.2 GPa. During this period the leucocratic halo around the nodules was formed and tourmaline in the nodules crystallized at the expense of K-feldspar, plagioclase and biotite. Fluid inclusions suggest that external parts of tourmaline grains in nodules crystallized from hydrothermal fluids. The presence of aqueous fluids also is indicated by low K/Rb ratios (54–155) in nodules. Nodules crystallized in the closed system conditions. The same leucocratic halo is sometimes present along coarse-grained tourmaline-quartz aggregates in the marginal parts of veins of tourmaline granites.

During **the final stage** the pegmatite system was probably opened for fluid phase from surrounding rocks, because surrounding granite is solidified and brittle.

REFERENCES

BURIÁNEK, D., & NOVÁK, M. (2007): Compositional evolution and substitutions in disseminated and nodular tourmaline from leucocratic granites: Examples from the Bohemian Massif, Czech Republic. *Lithos,* **95**, 1-2, 148-164.

CLARKE, D.B., DORAIS, M., BARBARIN, B., BARKER, D.A.N., CESARE, B., CLARKE, G., EL BAGHDADI, M., ERDMANN, S., FORSTER, H.-J., GAETA, M., GOTTESMANN, B., JAMIESON, R.A., KONTAK, D.J., KOLLER, F., LEAL GOMES, C., LONDON, D., MORGAN, G.B.V., NEVES, L.J.P.F., PATTISON, D.R.M., PEREIRA, A.J.S.C., PICHAVANT, M., RAPELA, C.W., RENNO, A.D., RICHARDS, S., ROBERTS, M., ROTTURA, A., SAAVEDRA, J., SIAL, A.N., TOSELLI, A.J., UGIDOS, J.M., UHER, P., VILLASECA, C., VISONA, D., WHITNEY, D.L., WILLIAMSON, B.E.N., & WOODARD, H.H. (2005): Occurrence and Origin of Andalusite in Peraluminous Felsic Igneous Rocks. *J. Petrol.* 46(3), 441-472.

MONTEL, J. – M. (1993): A model for monazite/melt equilibrium and application to the generation of granitic magmas. *Chem. Geol.* **110**(1-3), 127-146.

# HYDROTHERMAL REPLACEMENT OF GARNET BY TOURMALINE – AN EXAMPLE FROM LCT PEGMATITES IN THE SAHATANY VALLEY, MADAGASCAR

[1]Zbyněk Buřival[#], [1]Milan Novák

[1] Department of Geological Sciences, Kotlářská 2, 611 37, Brno, Czech republic
[#] zbynek@burival.com

Key words: LCT pegmatite, subsolidus, alteration, replacement, garnet, tourmaline

## INTRODUCTION

In the late stages of pegmatite crystallization residual fluids rich in volatiles and some incompatible elements ($H_2O$, F, B, P, Li, Rb, Cs) appear (London 2005). Rarely also fluids derived from host rock rich in Mg, Ca and Ti may income a pegmatite system (Novák 1998). Both types of fluids react with some early crystallized minerals (e.g., cordierite, garnet) and replacement of garnet by a mixture of secondary tourmaline and Li-rich micas in some LCT pegmatites from Czech Republic described by Němec (1983) is a typical product of such reactions. In the pegmatites Tsarafara Nord and Tamponilapa, both tending to elbaite subtype, garnet and albite located close to Li-mineralized zone were partially replaced by a mixture of blue tourmaline and quartz: We examined these assemblages to reveal composition of residual fluids.

## MINERAL ASSEMBLAGES AND CHEMISTRY

Spessartine-dominant garnets from the pegmatites Tsarafara Nord ($Sps_{48-60}Alm_{32-42}Grs_{8-10}$) and Tamponilapa ($Sps_{43-62}Alm_{2244}Grs_{3-21}Prp_{0-3}$) (see Fig. 1) are associated with primary tourmaline (schorl to Mg-rich schorl) showing Mg (0.13–0.46; 0.32–1.13), Al (5.78–6.45; 4.77–5.26), Mn (0.05–0.15; 0.04–0.12), Ti (0.10–0.12; 0.08–0.18), Ca (0.13–0.18;
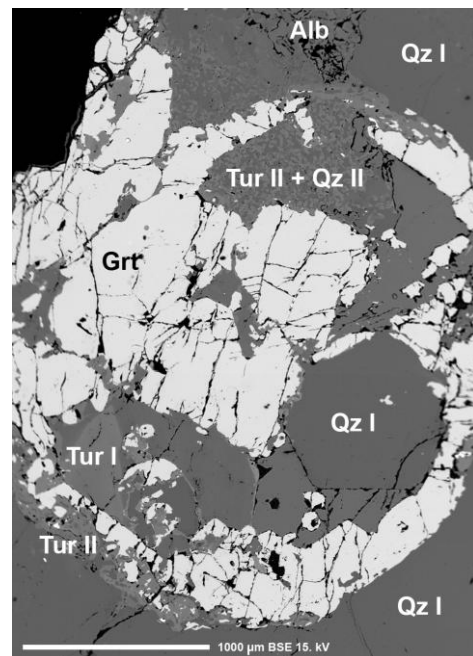


Fig. 1. Skeletal crystal of garnet (Grt) with primary tourmaline (Tur I), quartz (Qz I) and albite (Alb) partially replaced by mixture of secondary tourmaline (Tur II) and quartz (Qz II) from the locality Tamponilapa.

0.14–0.38) and F (0.13–0.48; 0.05–0.08) respectively.

Secondary tourmaline replacing garnet (schorl to Fe-rich fluor-elbaite) is Li, Al and F enriched showing Mg (0.00–0.01; 0.00–0.23), Al (6.92–7.53; 6.68–7.67), Licalc. (0.83–1.32; 0.00–0.97), Mn (0.03–0.47; 0.10–0.49), Fe (0.01–0.87; 0.15–1.76), Ca (0.24–0.43; 0.10–0.26), F (0.49–0.84; 0.06–0.18) (all values above are given in apfu and in the order Tsarafara Nord and Tamponilapa). Albite is close to the end member composition. The minerals from the Tsarafara Nord are slightly more fractionated with higher (Li, Mn, F) and less contaminated (elevated Ca, Mg, Ti) from host rock relative to the Tamponilapa.

### POTENTIAL REPLACEMENT REACTION

Textural relations showing replacement of garnet and albite by tourmaline and quartz (Fig. 1) suggest the simplified reaction:

$$24\ NaAlSi_3O_8 + 3\ (Mn_{1.6}Fe_1Ca_{0.4})\ Al_2Si_3O_{12} + 12\ H_3BO_3 + 2\ LiF =>$$
$$4\ (Na_{0.5}Ca_{0.3}\square_{0.2})\ (Al_{1.5}Fe_{0.75}Li_{0.5}Mn_{0.25})\ Al_6\ (Si_6O_{18})\ (BO_3)_3\ (OH_{3.5}F_{0.5}) + 46\ SiO_2 + 11\ Na_2SiO_3 + 3.8\ MnO_2 + 0.4\ O + 9\ H_2O + 4\ H^+$$
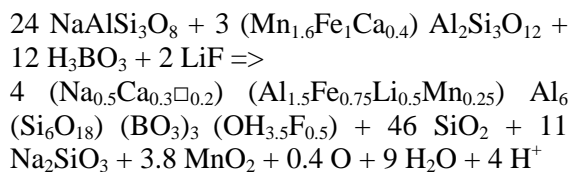
It is calculated based on stable = immobile Al, Fe and Ca and idealized compositions of primary garnet, albite and secondary tourmaline, which is generally enriched in Al, F, Li, and Mn and depleted in Ti, Mg and Fe compared to primary tourmalines. They are only sporadically associated with garnet and very likely do not participate in the replacement reaction (Fig. 1). Because we assume a direct replacement of primary garnet and albite (Fig. 1), the elevated contents of Al, Mn and Ca in secondary tourmalines reflects the compositions of primary garnet (Mn, Al, Fe, Ca) and of residual fluids (B, F, Li, H_2O). Very low to negligible concentrations of Mg in secondary tourmaline suggest closed system to host rock during this alteration. The excess of Na and Mn may be dissolved in fluids and transported away as e.g., soluble sodium silicates. Apparently, no Mn-bearing minerals occur close to garnet as well.

### CONCLUSIONS

The replacement of garnet and albite generally resulted in origin of zoned secondary tourmaline with quartz which reflects the composition of primary minerals and composition of residual fluids (B, F, Li) whereas Mn and Na were mobile and left the system. However, due to negligible volume of this replacement process in the whole pegmatites, the released Na and Mn can hardly be identified in later subsolidus mineral assemblages.

### REFERENCES

LONDON, D. (2005): Geochemistry of alkalis and alkaline earths in ore-forming granites, pegmatites and rhyolites. In: Linnen R. L., Samson I. M. (2005): Rare-elements geochemistry and ore deposits. *Geological Association of Canada Short Course Notes* 17.

NĚMEC, D. (1983): Masutomilite in lithium pegmatites of West-Moravia, Czechoslovakia. *N. Jb. Miner. Mh. H.*, **12**, 537-540.NOVÁK, M. (1998): Blue dravite as an indicator of fluid composition during subsolidus replacement processes in Li-poor granitic pegmatites in Moldanubicum, Czech Republic. *J. Czech Geol. Soc.* **43**, 1-2, 24-30.

# EFFLORESCENCES AND GAS COMPOSITION EMITTED FROM THE BURNING COAL – WASTE DUMP IN SŁUPIEC, LOWER SILESIAN COAL BASIN, POLAND

[1]Justyna Ciesielczuk[#], [2]Łukasz Kruszewski,
[1]Monika J. Fabiańska, [1]Magdalena Misz-Kennan, [3]Adam Kowalski, [3]Bartosz Mysza

[1]  University of Silesia, Faculty of Earth Sciences, Będzińska 60, 41-200 Sosnowiec, Poland
[#]justyna.ciesielczuk@us.edu.pl

[2]  Polish Academy of Science, Institute of Geological Sciences, Twarda 51/55, 00-818 Warszawa, Poland

[3]  University of Science and Technology, Mickiewicza 30, 30-059 Kraków, Poland

## INTRODUCTION

The coal-waste dump at Słupiec in the Lower Silesian Coal Basin undergoes self-heating notwithstanding the extensive preventative measures undertaken there. Symptoms of thermal activity were found in 10 areas within the dump. The main fire indicator was a smell perceptible from a distance. An additional indicator, especially at winter time, is the growth of mullein (*Verbascum* L.) in the poor but heated soil. In most active areas, charred venting cracks were present with gray smoke escaping from some. At all sampling points, temperature was measured at the surface and at 30 cm subsurface, and efflorescences blooming around the fissures and gas samples from different depths collected. The aim of the study was to identify efflorescences and gas composition emitted from burning coal-waste dump in Słupiec.

Samples were collected on December, 10th, 2013 after rainfall on what was a cloudy day. The air temperature was +2 C. Temperatures measured in thermally-active areas ranged from 8-75 $^{o}$C at the surface and from 28-88 $^{o}$C at 30 cm subsurface. Corresponding temperatures measured at a reference point were 3 $^{o}$C and 5 $^{o}$C.

Efflorescences were identified by XRD and SEM-EDS and gas composition was determined by GC-FID and GC-TCD.

## MINERAL EFFLORESCENCES

Efflorescences blooming at the fissure openings are scarce except for one sampling point on the slope of the dump. As they crystallize directly on the soil and on plants, samples tend to be contaminated by quartz, kaolinite, illite, muscovite, feldspars, mullite and amphiboles.

The most frequent mineral phases present are elemental sulphur, gypsum, and other sulphates such as mohrite-boussingaultite solid solution $(NH_4)_2(Fe, Mg[SO_4]_2 \cdot 6H_2O$, and halotrichite-group

minerals. Tschermigite $(NH_4)Al(SO_4)_2 \cdot 12H_2O$, alum-(K) $KAl(SO_4)_2 \cdot 12H_2O$, mascagnite $(NH_4)_2SO_4$, rosenite $FeSO_4 \cdot 4H_2O$, and probable hydronium jarosite $(H_3O)Fe_3^{3+}(SO_4)_2(OH)_6$ are less common. Species as yet unconfirmed include alum-(Na) $NaAl(SO_4)_2 \cdot 12H_2O$, tamarugite $NaAl(SO_4)_2 \cdot 6H_2O$, hexahydrite $MgSO_4 \cdot 6H_2O$, starkeyite $Mg(SO_4) \cdot 4H_2O$, melanterite $Fe(SO_4) \cdot 7H_2O$, mikasaite $Fe_2(SO_4)_3$, and copiapite $FeFe_4[(SO_4)_6|(OH)_2 \cdot 20H_2O$. Halotrichite-group minerals likely represent two crystallochemical types, one Fe- and Mn-rich with minor Mg and trace Al, likely corresponding to bílinite-apjohnite, and a second rich in Al and Fe, representing Mg- and Mn-bearing halotrichite.

Native sulphur is chemically pure; no As or Se admixtures were confirmed. Its habit is rather invariable over the area of the dump. Sal ammoniac, which is typically ubiquitous in the burning coal-waste dumps, was found only in a 10 cm in diameter niche above the venting crack. As nitrogen is concentrated in the gases and is present in other minerals collected from various other sampling points, it is possible, that this mineral was dissolved by rain. However, it was also not found in April 2011 (Fabiańska et al. 2013). On the other hand no fluorosilicate minerals, found on this earlier date (opus cit), were recognized in the samples collected in December 2013. This may indicate a slight change in the chemistry of the Słupiec fire gas.

Carbonates, namely, aragonite, calcite, and nesquehonite $MgCO_3 \cdot 2H_2O$ were found in samples located at the foot of a nearby cone.

## Gas composition

Twenty one gas samples collected from different depths at 11 locations at the top or at the slope of the Słupiec dump were analysed.

There is a lack of oxygen in favor of nitrogen and carbon dioxide. In most cases, $N_2/O_2$ exceeds values for air by a factor of eight. Carbon dioxide concentrations are high (14 % vol.) in most samples. There is no correlation between gas composition and its temperature.

## References

Fabiańska, M. J., Ciesielczuk, J., Kruszewski, Ł., Misz-Kennan, M., Blake, D. R., Stracher, G., Moszumańska, I. (2013): Gaseous componds and efflorescences generated in self-heating coal-waste dumps – A case study from the Upper and Lower Silesian Coal Basins (Poland). *Int. J. Coal Geol.* **116-117**, 247-261.

# BEHAVIOR OF B AND LI DURING THE EVOLUTION OF THE KRACOVICE PEGMATITE RELATED TO THE FORMATION AND STABILITY OF TOURMALINE AND GARNET

[1]Renata Čopjaková[#], [1]Radek Škoda,
[2,3]Michaela Vašinová Galiová, [1]Milan Novák

[1]    Institute of Geological Sciences, Masaryk University in Brno, Kotlářská 2, 611 37 Brno, Czech Republic, [#]copjakova@sci.muni.cz
[2]    CEITEC, Masaryk University, Kamenice 5, 625 00 Brno, Czech Republic
[3]    Department of Chemistry, Masaryk University, Kotlářská 2, 611 37 Brno, Czech Republic

Key words: tourmaline, schorl, elbaite, garnet, Li,F,B-rich pegmatitic fluids, Kracovice pegmatite

## INTRODUCTION

Enrichment in B and Li is known from many evolved granites and pegmatites. The Kracovice pegmatite represents the most evolved body with mixed LCT-NYF signature related to the Třebíč Pluton (Novák et al. 2012). From the contact inwards, the pegmatite consists of a granitic unit, graphic unit, blocky K-feldspar, albite unit and a small quartz core. Tourmaline and garnet represent the only important AFM silicate minerals which occur in majority of textural-paragenetic units (graphic, blocky K-feldspar and albite). We studied compositional evolutions and behavior of B and Li in tourmaline and garnet using the Cameca SX100 electron microprobe and LA-ICP-MS.

## MAGMATIC EVOLUTION OF TOURMALINE AND GARNET

Black magmatic tourmaline (Tur1) forms isolated prismatic crystals, up to 3 cm in diameter, chemically rather homogeneous (Fig. 1) corresponding to schorl to fluor-schorl (6.56-7.52 $apfu$ Al; 1.88-2.24 $apfu$ Fe; $Fe_{tot}/(Fe_{tot} + Mg) \sim 0.98$; 0.18-0.69 $apfu$ F) with moderate to high Na (0.49-0.72 $apfu$). Lithium contents in magmatic tourmaline are rather low but variable (75-1300 ppm). Magmatic tourmaline tends to be slightly enriched in Na, Fe, Mn, F, Li and depleted in Mg during its evolution from core to rim and from graphic to albite unit, respectively (Fig. 2).

Presence of early tourmaline as well as magmatic hambergite indicates B-rich melt. Crystallization of Tur1 was terminated probably owing to low content of B in the melt as a result of precipitation of both B-rich minerals and/or by partitioning of B into exsolved vapour.

Garnet ($Sps_{59-63}Alm_{35-40}$) forms euhedral grains (< 2 cm) commonly associated with magmatic schorl. The content of Li in the garnet increases from ~ 140 (graphic unit) to ~ 350 ppm (albite unit) and is only slightly lower compared to the associated tourmaline ($D_{Tu/Grt} \sim 1-2$).

## HYDROTHERMAL EVOLUTION

The activity of B in vapor increased with decreasing T until Li-tourmaline becomes stable (London 1986) which consequently crystallized as later hydrothermal tourmaline (Tur2). It overgrows (Tur2o) magmatic tourmaline from blocky K-feldspar and albite unit or it replaces
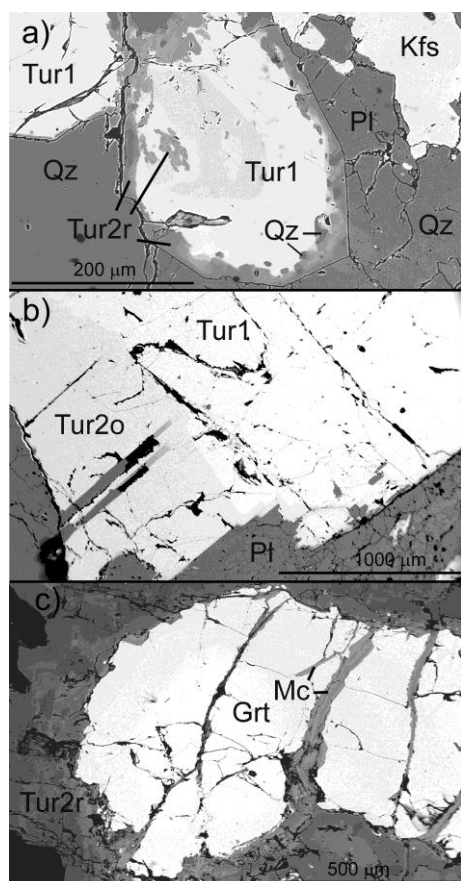


Fig. 1. BSE images; a) Tur1 replaced by Tur2r with micro-lobulated contact and quartz inclusions; b) Tur1 overgrown by Tur2o with straight contact; c) garnet replaced by fluor-elbaite and Li-rich mica.

(Tur2s) magmatic tourmaline or garnet usually in the graphic unit (Fig. 1). Both textural types show similar chemical composition and compositional trends (Fig. 2) reflecting their rather coeval formation and correspond to rare fluor-schorl to major fluor-elbaite (0.1-1.4 wt. % Li; 6.96-7.41 *apfu* Al; 0.25-1.82 *apfu* Fe; 0.18-0.76 *apfu* Mn; 0.71-0.99 *apfu* Na; 0.67–1.05 *apfu* F). The contents of Fe decrease and Al, Mn, Na, F and Li increase towards the

rims reflecting the evolution of parent hydrothermal fluids. Textural differences (overgrowing Tur2o versus replacing Tur2r) reflect either degree of solidification of the melt or differences in local activity of B in fluids. Replacing fluor-elbaite formed as a result of temporal instability of schorl and garnet during their interaction with Li,F-rich, Fe-poor, highly alkaline, pegmatite-derived fluids. Coeval formation of chamosite + allanite together with fluor-elbaite was observed during the schorl replacement, and garnet was replaced by fluor-elbaite (Tur2r) and Li-rich mica during closely related process as well.
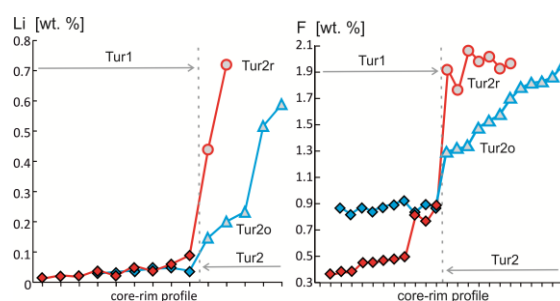


Fig. 2. Evolution of Li and F in tourmaline. Red – tourmaline from the graphic zone; blue – tourmaline from the albite zone.

REFERENCES

LONDON, D. (1986): Magmatic-hydrothermal transition in the Tanco rare-element pegmatite: Evidence from fluid inclusions and phase-equilibrium experiments. *Am. Mineral.* **71**, 376-395.
NOVÁK, M., ŠKODA, R., GADAS, P., KRMÍČEK, L. & ČERNÝ, P. (2012): Contrasting origins of the mixed (NYF + LCT) signature in granitic pegmatites, with examples from the Moldanubian Zone, Czech Republic. *Can. Mineral.* **50**, 1077-1094.

# URANIUM DISTRIBUTION OF SOUTHERN PART OF BOSKOVICE FURROW

[1]Šárka Dvořáková[#]

[1]  Department of Geological Sciences, Masaryk University, Brno, Czech Republic,
[#] dvorakovasarus@seznam.cz

Key words: Boskovice furrow, U (uranium), Th (thorium), Rokytná conglomerates, Oslavany formation, concentration, conglomerates

## INTRODUCTION

Boskovice furrow contains higher amount of uranium than its surroundings. Goal of this presentation was to determine distribution of uranium, thorium and potassium in south-east part of furrow – Rokytná conglomerates. Boskovice furrow is rift valley filled with Permo-Carboniferous sediments stretching from town Moravský Krumlov to town Boskovice in north northeast to south southwest direction (Műller et al. 2000). Studied area – south part of furrow – is situated in southeastern part of Czech Republic, 40 kilometres away from second largest city Brno, between towns Moravský Krumlov, Ivančice and Oslavany. Distribution of uranium in southern part of Boskovice furrow is irregular due to lithological differences between two main units forming the furrow. The clastic material from Oslavany formation was derived mainly from Moldanubian and Moravian crystalline units, mainly metamorphic and igneous rocks with higher amount of uranium. The clasts derived Brunovistulicum and culmian sediments of Drahany highlands, which display lower amount of uranium

form the substantial part of the Rokytná conglomerates.

Oslavany formation consists of alternating sandstone and siltstone layers. Its colour is mainly grayish. This formation contains high amount of organic matter. Rosice–Oslavany coalfield is situated in this area. The darkest layers with higher amount of organic matter are known for higher concentration values of uranium – up to 70 ppm (Jakubová 2011). Rokytná formation consists of unstratified reddish to brownish conglomerates (Chlupáč 2002). The rocks here are mainly breccias to conglomerates. Other characteristic features are angular clasts in size from 0.2 to 20 centimetres, though bigger clasts could be found. (Jaroš 1963).

## RESULTS

Object of my study are mainly reddish Rokytná formation, which have not been studied in detail before (Fig. 1). Field gamaspectrometer RS 230 and laboratory gamaspectrometry (device SG–1000 LAB) were used. The results are concentrations of uranium, thorium and potassium. Field gamaspectrometry was done around the town of Moravský Krumlov in six selected

outcrops with 60 obtained values. Field gamaspectrometry was done around the town of Moravský Krumlov in six selected outcrops with 60 obtained values. First outcrop was Svatý Florián hill with values from 2.0 to 2.6 % of K, from 1.8 to 4.2 ppm of U and from 9.2 to 11.9 ppm of Th.



Fig. 1. Rokytná conglomerates

Second was Křižák hill with values from 2.2 to 3.0 % of K, from 1.9 to 3.1 ppm of U and from 9.7 to 13.4 ppm of Th. Third were outcrops on the street Pod Hradbami with values from 2.6 to 4.1 % K, from 2.6 to 4.6 ppm U and from 9.2 to 14.0 ppm of Th. Fourth was Křepelčí hill with values from 2.9 to 3.4 % of K, from 2.4 to 3.5 ppm of U and from 12.7 to 15.0 ppm of Th. All of those are situated in town of Moravský Krumlov. Fifth locality was outcrops near village Budkovice with values form 3.5 to 3.8 % of K, from 3.2 to 3.9 ppm of U and from 11.2 to 13.2 ppm of Th. And six were outcrops near village Řeznovice with values from 2.2 to 2.7 % of K, from 1.6 to 4.6 ppm of U and from 11.6 to 12.2 ppm of Th. These outcrops are formed mainly by typical reddish Rokytná conglomerates with large clasts only outcrops of the street Pod Hradbami are formed by fine-grained sediments of grayish color. Values of concentration of uranium measured at this locality in grayish sediments were about 0.5 ppm higher than values of other localities. The distribution of U is more or less uniform. However, two anomalies were observed at the second locality Křižák hill (Fig. 2). The

first anomaly is characterized by values of 28.2 ppm of uranium, 4.6 ppm of thorium and 0 % potassium. Second one was 0.5 ppm of uranium, 9.8 ppm of thorium and 2.6 % of potassium. Both anomalies were detected on same side of hill, about 30 meters from each other.
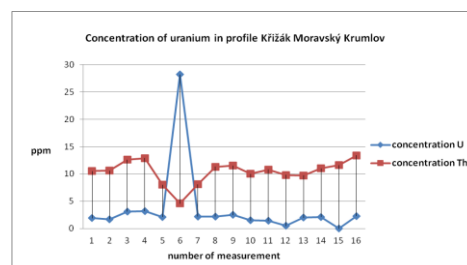


Fig. 2. Graph of concentration of uranium and thorium from profile of Křižák hill outcrops

## CONCLUSIONS

Discovered anomalies were interpreted as locally enriched domains and uranium depleted spot. These were considered as proof of uranium migration. Based on measurements from eastern part of furrow and known facts about western part may be said that distribution of uranium and thorium of Boskovice furrow is irregular depending on lithology and further conditions such as secondary migration or affecting by other processes.

## REFERENCES

CHLUPÁČ, I., BRZOBOHATÝ, R., KOVANDA, J., STRÁNÍK, Z. (2002): Geologická minulost České republiky, *Akademie věd ČR*. Praha. (in Czech)

JAKUBOVÁ, P. (2011): Charakteristika uranové anomálie v jižní části boskovické brázdy. *MS: diploma thesis*. Archive Faculty of Science, Masaryk University. Brno. (in Czech)

JAROŠ, J. (1963): Litostratigrafie permokarbonu Boskovické brázdy.- *Věst. Ústř. Úst. geol.*, **38**, 2, 115-118.(in Czech)

MÜLLER, P., NOVÁK, Z. (2000): Geologie Brna a okolí. – Český geologický ústav, Praha. (in Czech)

# MAGMATIC AND METAMORPHIC CRYSTALLIZATION HISTORY OF A CORONITIC GABBRO FROM THE MOLDANUBIAN ZONE (BOHEMIAN MASSIF) AND ITS GEOTECTONIC IMPLICATION

[1]Shah Wali Faryad[#], [2]Václav Kachlík

[1]     Institute of Petrology and Structural Geology, Charles University, Prague, # faryad@natur.cuni.cz
[2]     Institute of Geology and Paleontology, Charles University, Prague

Key words: coronitic gabbro, sapphirine, granulite facies

Coronitic gabbro from the Moldanubian Zone at border with the Brunovistulian Block is characterized by amphibole + spinel + sapphirine coronae around orthopyroxene that occurs in a medium-grained plagioclase matrix. Numberless diopside inclusions (1-10 micrometer, maximum 20 micrometers in size) are present in plagioclase of anorthite composition. They are abundant mostly in large porphyric grains and less common in the medium-grained plagioclase of the matrix. The inclusions are monomineralic and form columnar crystals without shape-preferred orientation. There is no evidence for the presence of former melt or polyphase inclusions in the plagioclase. The frequency of inclusions depends on their size; the smaller grain size, the larger number of inclusions in the plagioclase. Triple junctions of the plagioclase grains in the matrix are represented by amphibole. The corona consist of orthopyroxene in the core with two or three zones; the first represented by calcic amphibole, the second by symplectite of amphibole with spinel, sapphirine and accessory corundum and the third by garnet amphibole with relic of spinel. The orthopyroxene forms a monomineralic aggregates that may contain serpentine cluster in the core, suggesting its formation after olivine. Relic of clinopyroxene was observed within amphibole zone.

Based on the mineral and geochemical composition, the rock corresponds to olivine gabbro with normative anorthite = 55 %, olivine = 33 %, orthoclase = 3 %, albite 3 % and diopside = 6 %), where olivine was transformed into orthopyroxene and possible clinopyroxene in the matrix into amphibole. Because of low normative clinopyroxene content in the rock, the amphibole present around the coronae and in the triple junctions of plagioclase could form by the reaction between olivine (orthopyroxene) and plagioclase. The presence of tiny diopside ($X_{Mg}$ = 0.80) inclusions in plagioclase ($An_{98}$) suggest a rapid cooling after melt crystallization reached cotectic line between olivine and diopside and continued to the ternary eutectic point with plagioclase. The orthopyroxene in the core of corona has $X_{Mg}$ = 0.78 and the surrounding amphibole corresponds to alumino-tschermakite with $X_{Mg}$ = 0.76-0.85. Textural relations indicate that

amphibole around corona of orthopyroxene was followed by formation of symplectite of amphibole + spinel + sapphirine with corundum at granulite facies conditions and finally garnet ($Alm_{26-29}$, $Prp_{45-51}$, $Grs_{22}$, $Adr_2$, $Sps_1$) was formed during rapid cooling but still in granulite facies conditions. It contains inclusions of spinel. In addition to availability of water, stabilization of calcic amphibole instead of clinopyroxene in the granulite facies conditions was governed by the local mass-balance of Na, K and Al in adjacent plagioclase. Small amounts of talc after orthopyroxene and the presence of muscovite within plagioclase and chlorite at contact with amphibole belong among later alteration product in the rock.

Based on mineral textures the coronae in olivine gabbro were formed during three different stages. The first stage related to the reaction between olivine and anorthite to form orthopyroxene probably during the postmagmatic cooling. The amphibole formation in the second corona suggests fluid presence that resulted replacement of clinopyroxene in the matrix and governed the reaction orthopyroxene + anorthite = amphibole + spinel. The last stage of corona formation with amphibole + spinel + sapphirine indicates granulite facies conditions. Garnet enclosing spinel and its occurrence along the rim of corona at contact with anorthite suggests its formation either during cooling or both cooling and compression. Preliminary thermo-barometric calculations for the garnet – amphibole - plagioclase assemblage suggest medium pressure conditions for the granulite facies stage.

As most rocks from the Gföhl unit indicate an early high- to ultrahigh-pressure metamorphic history, the only granulite facies metamorphism in the olivine gabbro suggests that their tectonic emplacement within granulite and/ migmatite. It is not clear if the olivine gabbro shared the same granulite facies metamorphism, or they were tectonically emplaced during their exhumation.

# EPITHERMAL PRECIOUS METALS MINERALIZATION AT NOVÁ BAŇA – GUPŇA OCCURRENCE (POHRONSKÝ INOVEC MTS., SLOVAK REPUBLIC)

[1]Štefan Ferenc[#], [2]Peter Koděra,
[3]Rastislav Demko

[1] Dept. of Geography, Geology and Landscape Ecology, Fac. of Natural Sciences, University of Matej Bel, Tajovského 40, 974 01 Banská Bystrica, Slovak Republic, [#] stefan.ferenc@umb.sk

[2] Dept. of Geology of Mineral Deposits, Fac. of Natural Sciences, Comenius University, Mlynská dolina G, 842 15 Bratislava 4, Slovak Republic

[3] State Geological Institute of Dionýz Štúr, Mlynská dolina 1, 817 04 Bratislava 11, Slovak Republic

## INTRODUCTION

Nová Baňa is one of the most important silver-gold historical deposits in the Central Slovakia Volcanic Field. Mining activities started probably in the 13th Century, and continued with pauses until the year 1887 (Bergfest 1955). Later, unsuccessful exploration was carried out in the second half of 20th and at beginning of 21st centuries. A lot of mineral phases are known from the Nová Baňa deposit. Majority of mineral descriptions originated in the 19th. and beginning of 20th Century, in contrast with a lack of modern analytical tools. This contribution is dedicated to the results of new mineralogical and geochemical research of epithermal precious metals veins at Gupňa occurrence (SE part of the Nová Baňa ore field).

## GEOLOGICAL SETTING

Nová Baňa ore field is located within W part of the Banská Štiavnica stratovolcano. In upper parts of the deposit ore veins are developed in propylitized andesites (Badenian), and rhyolitic volcanic rocks of the Jastrabá Formation (11.9-12.2 Ma, Lexa and Pecskay 2013). Footwall of Miocene volcanics is formed by the Late Paleozoic clastic sediments of the Hronicum Unit, overthrusting the Mesozoic carbonates of the Veporicum Unit. Paleozoic and Mesozoic rocks are intruded by Miocene quartz-dioritic porphyre. Ore veins have N-S to NE-SW direction, with variable dip direction. Mineralization disappears with increasing depth (Lexa et al. 2000).

## RESULTS

In the past at Gupňa the Reissenschuch vein system was exploited, located predominantly in the adularized rhyolites. Vein system is about 1.7 km long, and consists of 80-400 m long partial veins.

Sampling was undertaken on three locations: I) mouth of the Hohen Klotzer adit, II) crest of the Gupňa Mt., III) Červená skala open cut. Vertical range of

samples from vein system is 170 m. One of the vein structures (dip direction 296°/65°, thickness 1.5 m) is well observable in outcrop at the mouth of Hohen Klotzer adit. Central vein part (15 cm thick) consists of limonitized fine-grained quartz with ore minerals disseminations. Fine-grained quartz zone is symetrically bordered by reddish brown jasper. Central vein part is accompanied by swarm of quartz veinlets (up to 20 cm long, about 1-2 cm thick) without ore mineralization. Au content in various vein structure parts ranges from 0.05 to 50 ppm, Ag content varies in the range 42-570 ppm. Mineralization at Gupňa originated in the following steps:

I. magmatic (?) Fe-Sn mineralization represented by local cassiterite and hematite disseminations in altered rhyolite.

II. ore mineralization stage:
a) base metals substage (quartz, pyrite, galena, sphalerite, gold)
b) precious metals substage (quartz II, pearceite, Sb pearceite, As polybasite, polybasite, uytenbogaardtite, acanthite?)
c) chalcedony substage (quartz II, chalcedony)

III. supergene stage, including products of the cementation (acanthite) and oxidation (goethite, corkite) processes. Wall rocks of ore veins are affected by hydrothermal alterations: silicification, pyritization and adularization. Fluid inclusions hosted in vein quartz are mainly liquid-rich, but vapor-rich inclusions are also sometimes present, indicating boiling of fluids. Analyses of fluid inclusions showed low salinities (0-1.6, mean 1.1 wt. % NaCl eq.), which is typical for low sulfidation epithermal systems. Eutectic temperatures ranged from -42 °C to -34 °C indicative of the system $NaCl-FeCl_2-H_2O$. Total homogenization temperatures ranged from 183 °C to 246 °C (average 226 °C). Boiling of fluids was the likely reason for precipitation of gold. Assuming hydrostatic pressures, boiling occurred from 17 to 28 bars, corresponding to paleodepth of boiling (today erosion level) 180 to 310 m.

Isotopic composition of vein quartz ranged from 6.4 to 7.7 ‰ $\delta^{18}O$, while illite-smectite from wall rock alteration had 1.9 to 6.9 ‰ $\delta^{18}O$ and -66 to -98 ‰ $\delta D$. Composition of fluids in equilibrium with quartz (-4.1 to -3.0 ‰ $\delta^{18}O$; -80 to -46 ‰ $\delta D$) indicate mostly meteoric origin of fluids affected by isotopic reequilibration with country rocks. The isotopic composition of fluids was calculated using temperatures based on fluid inclusions microthermometry and illite-smectite expandability (130–196 °C, Šucha et al. 1992; Harvey and Browne 2000).

REFERENCES

BERGFEST, A. (1955): Mining in Nová Baňa. Manuscript, Geofond archive, Bratislava, 130 p. (in Slovak)

HARVEY, C.C, BROWNE, P.R.L. (2000): Mixed layer clays in geothermal systems and their effectiveness as mineral geothermometers. *Proceedings of the World Geothermal congress*, Kyushu, Japan, 1201-1205.

LEXA, J., ŽÁKOVÁ, E., HOJSTRIČOVÁ, V, ROJKOVIČOVÁ, Ľ. (2000): Gold deposit Nová Baňa. Manuscript, Geofond archive Bratislava, 11 p. (in Slovak)

LEXA, J., PÉCSKAY, Z. (2013): K-Ar dating of the Jastrabá formation rhyolites and related mineralization in the Central Slovakia Volcanic Field. *In* Geological evolution of the Western Carpathians: new ideas in the field of inter-regional correlations (I. Broska and A Tomašových, eds.). *Geological Institute of the Slovak Academy of Sciences, Bratislava*, 80-81.

ŠUCHA, V., KRAUS, I., GERTHOFFEROVÁ, H., PETEŠ, J., SEREKOVÁ, M. (1992): Smectite to illite conversion in bentonites and shales of the East Slovak basin. *Clay Minerals* **28**, 243-253.

# GEMMOLOGICAL AND SPECTROSCOPIC STUDY
# OF GEM TOURMALINES

[1]Jana Fridrichová[#], [1]Peter Bačík,
[2]Ján Štubňa, [3]Peter Antal

[1] Comenius University in Bratislava, Faculty of Natural Sciences, Dpt. of Mineralogy and Petrology, Mlynská dolina, 842 15 Bratislava, Slovakia, [#] fridrichova@fns.uniba.sk

[2] Institute of Gemmology, of the Faculty of Natural Sciences of the Constantine the Philosopher University in Nitra, Nábrežie mládeže 91, 949 74 Nitra, Slovakia

[3] Comenius University in Bratislava, Faculty of Natural Sciences, Dpt. of Inorganic Chemistry, Mlynská dolina, 842 15 Bratislava, Slovakia

## INTRODUCTION

Heat treatment is routinely performed on gemstones to enhance optical properties, mainly colour and clarity, to make them more valuable and marketable (Castañeda et al. 2006; Bačík et al. 2011). The aim of this study is to use a nondestructive and noninvasive methods and devices to identify and describe faceted gemstones.

## RESULTS

All 8 samples except T4 are faceted gemstones and were described and analyzed before and after heating at 700 °C for 24 hours. Vis/NIR and Raman spectroscopy were performed at Dpt. of Inorganic Chemistry, Comenius University. Sample T1 is a rectangular cut, greyish green colour, its clarity is VVS, T2 is a cabochon of pale green colour with clarity grade SI (significant fissure viewed from the side). T3 is a brilliant of dark green colour, it is the darkest specimen from all. T4 is an angular shape tourmaline with VVS clarity grade, T5 is a dark green brilliant with VS clarity, T6 is a pear cut of pale green colour and VS clarity, T7 is yellowish green oval with VVS clarity, T8 is a pink pear with VVS clarity grade. Clarity was graded under 10x magnification. After heat treatment most of the samples did not change in colour and clarity, except T7 and T8. Both samples faded in saturation of colour, while T7 faded only in hue and T8 lost its colour almost completely. Tourmalines were identified and process of partial but not full heating-induced dehydration was confirmed with Raman analysis. However, for more detailed analysis is necessary to use other nondestructive techniques e.g. XRF for determination of chemical composition. In Vis/NIR spectra T1 sample shows broad absorption band at 730 nm. It corresponds to $Fe^{2+}$ (Laurs et al. 2008; Merkel & Breeding 2009). Significant absorption band is also visible at 970 nm and continues to higher wavenumbers. It can be an overtone of OH vibrations (Laurs et al. 2007). T1 specimen is likely elbaite since the green colour in elbaite is often caused by $Fe^{2+}$. Presence of $Cu^{2+}$ can be excluded, however $Cu^{2+}$ exhibits two significant peaks at 700 and 900 nm (Merkel & Breeding 2009). Spectrum of T2 and T3 have a similar pattern to T1, T2

displays significant peak around 710 nm a T3 shows two peaks at 680 and 750 nm. All of these peaks can be assigned to $Fe^{2+}$. There are no significant changes in spectrum before and after treatment in all three samples, it suggests that no oxidation process did not occur. Sample T4 is different to all previous, it exhibits significant peak at 730 nm, attributable to $Fe^{2+}$. In addition this sample displays two peaks at 440 and 600 nm which can be assigned to $V^{3+}$ (Merkel & Breeding 2009). T4 is probaly uvite or dravite, because colour in uvite and green dravite is caused by $V^{3+}$ and $Cr^{3+}$ (Schmetzer & Bank 1979) and both of them never occur in elbaite (Rossman et al. 1991). Spectra of T5–T8 samples shows no significant bands and can not be relevantly interpreted. These samples are faceted which produce reflections inside the specimens influencing absorption. Moreover, direct crystallographic orientation is almost impossible. It is recommended to measure in directions parallel or perpendicular to the $Z$ axis (Laurs et al. 2008; Merkel & Breeding 2009). This directions correspond to minimal (parallel to $Z$ axis) a maximal (perpendicular to $Z$ axis) absorption. Tourmaline has significant pleochroism (darkest colour is visible in the direction of ordinary ray – perpendicular to $Z$ axis, or paralel – but only in the direction of the ordinary ray). The darkest colour is the result of the highest absorption. This can be explained by geometrical arrangement of chromophore-bearing octahedral sites. In the view in the direction of $Z$ axis, octahedral positions occupy larger area than in the view perpendicular to the $Z$. Thus the probability of light absorption in the direction parallel to $Z$ on chromophores located in octahedral positions is higher than in the perpendicular direction, which explains the differences in absorption in different directions. This are reasons why spectroscopic methods may have limits in their use on faceted gemstones.Although it was not possible to determine the cause of decolourization in originally pink T8 spectroscopically, it can be attributed to change in Mn valence (Abduriyim et al. 2006).

## REFERENCES

ABDURIYIM, A., KITAWAKI, H., FURUYA, M., SCHWARZ, D. (2006): Paraíba-type copper-bearing tourmaline from Brazil, Nigeria, and Mozambique: Chemical fingerprinting by LA-ICP-MS. *Gems & Gemology*, **42**, 1, 4-21.

BAČÍK, P., OZDÍN, D., MIGLIERINI, M., KARDOŠOVÁ, P., PENTRÁK, M. & HALODA, J. (2011): Crystallochemical effects of heat treatment on Fe-dominant tourmalines from Dolní Bory (Czech Republic) and Vlachovo (Slovakia). *Phys. Chem. Min.* **38**, 599-611.

CASTAÑEDA, C., EECKHOUT, S.C., DA COSTA, G.M., BOTELHO, N.F. & DE GRAVE, E. (2006): Effect of heat treatment on tourmaline from Brazil. *Phys. Chem. Min.* **33**, 207-216.

LAURS, B.M., SIMMONS, W.B., ROSSMAN, G.R., FRITZ, E.A., KOIVULA, J.I., ANCKAR, B. & FALSTER, A.U. (2007): Yellow Mn-rich tourmaline from the Canary mining area, Zambia. *Gems & Gemology*, **43**, 4, 314-331.

LAURS, B.M., ZWAAN, J.C., BREEDING, C.M., SIMMONS, W.B., BEATON, D., RIJSDIJK, K.F., BEFI, R. & FALSTER, A.U. (2008): Copper-Bearing (Paraíba-Type) Tourmaline From Mozambique. *Gems & Gemology*, **44**, 1, 4-30.

MERKEL P.B., BREEDING C.M., 2009: Spectral differentiation between copper and iron colorants in gem tourmalines. *Gems & Gemology*, **45**, 2, 112-119.

ROSSMAN, G.R., FRITSCH, E. & SHIGLEY, J.E. (1991): Origin of color in cuprian elbaite from São José da Batalha, Paraíba, Brazil. *Am. Mineral.* **76**, 1479-1484.

SCHMETZER, K & BANK, H. (1979): East African tourmalines and their nomenclature. *Journal of Gemmology*, **16**, 5, 310-311

# CRYSTAL – CHEMICAL EFFECTS OF HEAT TREATMENT ON AQUAMARINES AND YELLOW BERYL FROM THANH HOA PROVINCE, VIETNAM

[1]Jana Fridrichová[#], [1]Peter Bačík,
[1]Petra Rusinová, [2]Marcel Miglierini, [3]Valéria Bizovská, [4]Peter Antal

[1] Comenius University in Bratislava, Faculty of Natural Sciences, Dpt. of Mineralogy and Petrology, Mlynská dolina, 842 15 Bratislava, Slovakia, [#]fridrichova@fns.uniba.sk

[2] Slovak University of Technology, Faculty of Electrical Engineering and Information Technology, Dpt. of Nuclear Physics and Technology, Ilkovičova 3, 812 19 Bratislava, Slovakia

[3] Slovak Academy of Sciences, Institute of Inorganic Chemistry, Dúbravská cesta 9, 845 36 Bratislava 45

[4] Comenius University in Bratislava, Faculty of Natural Sciences, Dpt. of Inorganic Chemistry, Mlynská dolina, 842 15 Bratislava, Slovakia

Key words: beryl, heat treatment, Powder X-ray diffraction, Infrared spectroscopy, Mössbauer spectroscopy, Electron microprobe, UV/Vis spectroscopy, DTA

## INTRODUCTION

Beryl, ideally $Be_3Al_2Si_6O_{18}$, space group $P6/mcc$, is a cyclosilicate mineral. The crystal structure was solved by Bragg and West (1926). Structure consists of two tetrahedral sites with Be and Si and one octahedral site with Al. $SiO_4$ tetrahedra form six-membered rings lying in planes paralel to (0001). The $SiO_4$ rings are linked together with $BeO_4$ tetrahedra and $AlO_6$ octahedra forming a three-dimensional framework. Structural channels parallel to the $Z$ axis are situated in the centre of the rings where alkali, transition-metal cations, $H_2O$ or $CO_2$ can be located. Alkali cations are also balancing deficiency in positive charge resulting from the replacement of octahedral Al and tetrahedral Be by cations with lower valence such as $Fe^{2+}$, $Mg^{2+}$, $Li^+$ (Aurisicchio et al. 1988; Wood and Nassau, 1968). The iron content in natural beryl is about 1 wt. %, but in blue or yellow varieties it can attain 3 wt. %. Ferric ion with ionic radii 0.55 Å prefers octahedral site, whereas ferrous ion with ionic radius 0.78 Å can occupy tetrahedral, octahedral site and channels. The blue, green and yellow colour of beryl gem stone varieties such as aquamarine and yellow beryl (heliodor) is caused by presence of divalent and trivalent iron and depend on their ratio in the crystal structure (Viana et al. 2002). The aim of this study is to determine optical and crystal-chemical changes in two beryl samples with different colour from Vietnam.

## RESULTS

All samples have a gemological quality and were heated at 300, 500, 700, 900, 1100 °C for 12 hours – changes in colour and clarity are demonstrated in Fig.1. Best improvement in colour and clarity applicable for gemological purposes was observed in aquamarine heated at 700 °C. Presuming radiation-induced colourization of yellow beryls (Huong et al. 2012), the heating at 500 °C resulted in resetting of artificial yellow to original very pale blue colour. Basic crystal-chemical properties of studied beryls were determined with EMPA and powder XRD. According to

*c/a* ratio (Aurisicchio et al. 1988), all studied beryls belong to normal beryls (*c/a* ratio 0.997-0.998).



Fig. 1. Beryl samples before and after heating.

Both Al octahedral ($Al^{3+} \leftrightarrow Me^{2+}$, where $Me^{2+} = Mg^{2+}$, $Fe^{2+}$) and Be tetrahedral substitution $Be^{2+} \leftrightarrow Li^{+}$) substitutions have a common effect on the beryl composition. Aquamarines are generally enriched in Fe (< 0.25 *apfu*) and alkali (< 0.08 *apfu*) than yellow beryls (< 0.07 *apfu* Fe, < 0.04 *apfu* alkali). Both beryl samples displayed only weak zoning in BSE images, but no changes in chemical composition were observed in heated samples. However, samples heated at 900 and 1100 °C show system of cracks which are very likely crystallographically oriented. The results from XRD and EMPA suggest that the heating had no effect on the structure of samples, since no significant changes of lattice parameters were observed during the heating.

Mössbauer spectroscopy could have been applied only on aquamarine samples due to insufficient Fe content in yellow beryl. In aquamarine, reduction of Fe was observed in samples heated at 300 to 700 °C (from 68:32 to 78:22 $Fe^{2+}$:$Fe^{3+}$ ratio) and subsequent oxidation from 900 to 1100 °C (to 8:92) which could induce changes in their colour and clarity. The results of Mössbauer spectroscopy were confirmed by data from Vis/NIR spectroscopy. In both samples, an increase in absorption of broad band at 810 nm occurring between 500 and 700 °C which can be attributed to $Fe^{2+}$ in octahedral (Wood & Nassau 1968). After the heating at 900 and 1100 °C, its absorption decreased with significant increase of total absorption as result of decrease in transparency. Moreover, small bands at 375 and 425 nm attributed to octahedral $Fe^{3+}$ (Wood & Nassau 1968) were pronounced.

The behaviour of water was studied with IR spectroscopy and DTA/TG. Two types of structural arrangement of water ($H_2O$ I – 3694 $cm^{-1}$, $H_2O$ II - 3655 and 3592 $cm^{-1}$) were detected by IR spectroscopy. The absorption of 3655 $cm^{-1}$ band distinctly decreases between 300 and 500 °C. It can be described as release of one of double coordinating $H_2O$ II and this event is confirmed also by decrease in TG curve. After the heating at 900 °C, the decrease in absorption displays at both 3694 and 3592 $cm^{-1}$ bands. Moreover, the 3655 $cm^{-1}$ band disappears at all. Finally all water from channels is released which is documented on samples heated at 1100 °C with no distinct absorption bands present. The release of water from channels in large crystals might be a relatively violent process which may be the reason of cracks development in samples heated at temperatures higher than 900 °C.

REFERENCES

AURISICCHIO, C., FIORAVANTI, G., GRUBESSI, O., ZANAZZI, P. F. (1988): Reappraisal of the crystal chemistry of beryl. *Am. Mineral.* **73**, 826-837.

BRAGG W. L. AND WEST J. (1926): The crystal structure of beryl. *Proceedings of the Royal Society London,* **3A**, 691-714.

HUONG L. T.-T., HÄGER T., HOFMEISTER W., HAUZENBERGER CH., SCHWARZ D., LONG V. P., WEHMEISTER U., KHOI N. N., NHUNG N. T. (2012): Gemstones from Vietnam: An Update. *Gems & Gemology*, **48**, 158-176.

VIANA R. R., DA COSTA G. M., DE GRAVE E., JORDT-EVANGELISTA H., STERN W. B. (2002): Characterization of beryl (aquamarine variety) by Mössbauer spectroscopy. *Phys. Chem. Min.* **29**, 78-86.

WOOD D. L. AND NASSAU K. (1968): The characterization of beryl and emerald by visible and infrared absorption spectroscopy. *Am. Mineral.* **53**, 777-800.

# ARCHAEOMETRIC STUDY OF BAROQUE STUCCOES FROM THE LUBIĄŻ ABBEY (SW POLAND) – PRELIMINARY RESULTS

[1]Maria Gąsior [#], [2]Wojciech Bartz,
[2]Jakub Kierczak

[1]     Laboratory for Technological and Conservation Research, Faculty of Architecture, Wroclaw
        University of Technology, Poland [#]maria.gasior@pwr.wroc.pl
[2]     Institute of Geological Sciences, University of Wroclaw, Poland

Key words: the Lubiąż Abbey, stuccoes, archaeometry, mineralogy

The study of historic mortars and plasters represents an important aspect in investigating historical buildings. Thanks to this scientific research, we can obtain a detailed information on their composition, expand our knowledge of historically used raw materials and applied technology, and finally learn the level of technological knowledge of ancient builders. Moreover, the information gathered on the ancient technology, degree of mortars and plasters weathering and state of their preservation play an important role in planning of future restoration.

In this work we present the preliminary results of the analysis of some stucco mortars, taken from the abbatial church of the Assumption of the Virgin Mary. It belongs to the post-Cistercian abbey in the Lubiaż (SW Poland), one of the largest Christian architectural complexes in the world. The Lubiąż Abbey was founded at the end of the twelfth century. In following centuries, during the Hussite Wars and the Thirty Years War, it was devastated and ruined. The end of the latter, the economic reform initiated by the Abbot Arnold Freiberg in 1649, enabled start of a great renewal of the whole complex in Baroque style. Since the Silesian Wars (1740-1763) the Lubiąż Abbey has started to fall into a decline, ended with a secularization in 1810.

The church of the Assumption of the Virgin Mary, belonging to the abbatial complex, was selected for sampling. The first selected area corresponds to the decorated domes of chapels: southern St. Benedict chapel and northern, St. Bernard chapel, with the frescoes painted in 1691-1692 by Karl Dankwart and Michael Willmann. The second area was the Monument of Eight Bishops, located in the western side of the ambulatory (behind the presbytery), linking the chapels of St. Benedict and St. Bernard, created between 1691-1693.

The characterization of stuccoes samples was carried out through different analytical techniques. They were: optical microscopy (OM), X-ray diffractometry (XRD), Simultaneous Thermal Analysis (DSC-TG and DTA-TG), Scanning Electron Microscopy with Energy Dispersive X-ray Spectroscopy (SEM-EDS).

The domes of the chapels are decorated with two-layered stuccoes, showing winged putti and acanthus scrolls. The rendering coat is made of aggregate, dominated with medium grained quartz and less abundant feldspars, lithic grains. The lime binder is microcrystalline calcite, with numerous lime lumps. The aggregate to binder ratio is 1:1 (by volume). As a finishing coat for more complicated details, a lime paste with small amounts of gypsum was used. The latter reduces drying shrinkage and prevent the decorative last layer from cracking, while lime reduces setting time, resulting in unhurriedly preparing relief. The filler is composed of fine grained quartz. This finishing coat is richer in binder, with aggregate to binder ratio 1:2 (by volume). Finishing coat of smaller bulge decorations additionally contain crushed brick, added intentionally, which serves as an artificial pozzolanic additive. It provides good resistance to damp and acts as a dye.

In the Monument of Eight Bishops, there are cartouches with inscriptions. They are richly decorated with stucco. All inscriptions on the cartouches, as well as decorative convex details, are gilded. These decorations are composed of three layers. The two rendering coats resemble those from the winged putti and acanthus scrolls, however they contain variable amounts of gypsum. The aggregate to binder ratio is similar, close to 1:2 (by volume). They are covered with lime plaster red or black with vein decoration, imitating marble (so-called marbleizing). The red marbleizing is lime stucco, consisting of fine grained quartz as filler, coloured with strongly dispersed red ochre as a dye. The binder is microcrystalline calcite mass, rich in lime lumps. The black marbleizing contains gypsum as an additive, whereas soot plays a role of a dye. The finishing coat is strongly enriched in binder. It has aggregate to binder ratio close to 1:4.

The grain size distribution of the filler, as well as the aggregate to binder ratio ranges widely, depending on the application of mortar. Generally, it can be said that for the rendering coats the filler is coarser grained, in comparison to finishing layers, containing much finer grained filler. It stays in good agreement with Middle Ages and Early Renaissance recipe (Salavessa et al. 2013). However, the vast majority of historic recipes give the aggregate to binder ratio varying from 2:1 up to 3:1 (by volume), differing much from our results. They are most similar to Renaissance recipe described by Italian artist G. Vasari, including 2:1 (by volume) of lime and marble dust, with an addition of little gypsum (op. cit.).

REFERENCES

SALAVESSA, E., JALALI, S., SOUSA, L., FERNANDES, L., DUARTE, A. M. (2013): Historical plasterwork techniques inspire new formulations. *Constr Build. Mater.* **48**, 858–867.

# STUDY OF THE TRILOBITES FROM THE LOCALITY HORNÍ BENEŠOV

[1]Sabina Giblová[#], [1]Nela Doláková

[1]     Department of Geological Sciences, Faculty of Science, Kotlářská 2, 611 37 Brno, Czech Republic;
[#]GiblovaS@eznam.cz

Key words: Devonian; Eifel; Stínava- Chabičov formation; Trilobites; Horní Benešov

## INTRODUCTION

Fragmented trilobite fauna of the Stínava-Chabičov formation (Devon – Eifel) from the locality Horní Benešov have been studied. Specimens have been retrieved from the collection of the IGS MU. This locality is the richest and basically the only site in Nízký Jeseník where unmistakably Eifelian trilobite faunas have been uncovered. Since the locality had been destroyed and an industrial compound had been built upon it, it has not been possible to acquire new material from the site. For this reason, only specimens stored in the collections of the Department of Geological Sciences of the Masaryk University Faculty of Science have been studied. All the fossils come from the original collections of Strnad and Kalabis from 1954, 1955.

In the studied locality, the trilobite fauna is contained in anchimetamorphic shales and to a lesser extent in intercalations of porous grey marlstone. The species of *Kettnerapsis pigra*, *Koneprusia* cf. *subterarmata* and *Chotecops* cf. *Auspex* have been identified before (Chlupáč 2000).

## RESEARCH

Twelve pieces of the pygidium, ten pieces of free cheeks and six pieces of the thorax separate segments have been identified. Synonyms of the species have been examined in great detail; including changes in the species classification from the original collections by various authors (Strnad 1956, Chlupáč 1969, Kupková and Pek 1985). The only one dominant species *Leonaspis (Kettneraspis) pigra* (Barrande 1872, Chlupáč 1967) has been identified on the basis of a comparison of different original synonyms.

The species was classified as *Leonaspis (Kettneraspis) moravika* by Strnad (1956), as opposed to the original Barrande's classification as *Acantholoma (Kettneraspis) pigra*, since the studied specimens from Horní Benešov are distinguished by a specific granulation of the pygidium. For this reason, Strnad designated it as a new species. Chlupáč (1969) claims that cheek granulation of the great majority of the specimens from Horní Benešov that Strnad studied does not differ significantly and therefore, he categorizes it as *Acantholoma (Kettneraspis) pigra* again.

Chlupáč also states that according to the description, *Odontolleura ?* n. sp. Strnad

tallies with the dominating species of *Leonaspis (Kettneraspis) pigra* (Barrande). Kupková and Pek (1985) thus used *Leonaspis (Kettneraspis) pigra* as a model and re-classified the specimens from Strnad's original collection for the Regional Museum (Krajské vlastivědné muzeum) in Olomouc. In his later work (2000), however, Chlupáč classified the species as *Kettneraspis pigra* (Barranade 1872), but since the work contains no rationale for the change of the generic name, neither does it include any description of the individuals or photographic documentation.

DISCUSSION AND CONCLUSION

Chlupáč (2002) described the species *Leonaspis (Kettneraspis) pigra* as very similar or identical to the species uncovered in chotečské souvrství (in the Barrandien area). This suggests that there was an open exchange (migration) between the Barrandien's and the Horní Benešov's faunas in the Eifelian period as well as it proves that there existed an oceanic region between the two areas, as some authors have already proposed.

Shallow-water bioclastic facies of chotečské souvrství are thanks to their oxygenated environment the very opposite of pelitic dark-shale facies of the Horní Benešov area. However, the analogy between the two trilobite faunas has led Chlupáč (2000) to assume that the character of the bed was not the deciding factor in the trilobite development. The deciding factor that was common to both the faunas is apparently the depth which was not big in case of both acanthopyge limestone and Eifelian strata from the Horní Benešov area.

According to literary data, trilobite specimens from Horní Benešov have been described with different scientific names Chlupáč (1969, 2000), Kupková and Pek (1985), Strnad (1956, 1960), Strnad and Kalabis (1954). After a meticulous analysis of their morphological features and a careful exploration of the literature, it appears that all these names are synonyms. All the studied trilobite fragments from the collections of the Department of Geological Sciences have been classified as the one dominating species *Leonaspis (Kettneraspis) pigra*, which is in accordance with previous research Barrande (1872), Chlupáč (1967), and Strnad and Kalabis (1954).

REFERENCES

BARRANDE, J. (1872): Trilobites, Extraid du Supplement au vol. I. du Systeme silurien du center de la Boheme.(Prague-Paris).

CHLUPÁČ, I. (1969): Revision of the Middle Devonian trilobites from Horní Benešov in the Nízký Jeseník Mts. (Moravia). *Sborník geologických věd*, **10**: 67-103.

CHLUPÁČ, I. (2000): Devonští trilobiti Moravy a Slezska, jejich výskyt a význam. *Přírodovědené studie Muzea Prostějovska*, 3, 5-24. (in Czech)

CHLUPÁČ, I. (2002): Explanatory remarks to reprinted Joachim Barrande: Système silurien du centre de la Bohême. vol. 1. Crustacés: Trilobites. Trilobit (Petr Materna), Praha, 47 p.

KUPKOVÁ, A., PEK, I. (1985): Typový materiál ve sbírkách Krajského vlastivědného muzea v Olomouci, *Trilobita*, 61 p. (in Czech)

STRNAD, V. (1956): O Devonských trilobitech z Horního Benešova. *Sborník Ústředního ústavu geologického*, **23**, 433-473. (in Czech)

STRNAD, V. (1960): O devonských trilobitech z Horního Benešova II. *Přírodovědný časopis slezský*, **21**, (3), 333-354. (in Czech)

STRNAD, V., KALABIS, V. (1954): Fauna východního devonského pruhu Šternberk-Horní Benešov. Trilobita I, *Sborník SLUKO*, A, 1/1951-1953, 81-87. (in Czech)

# TL-RICH MN OXIDES FROM ZALAS (CRACOW AREA, POLAND)

[1]Bożena Gołębiowska[#], [1]Grzegorz Rzepa,
[1]Adam Pieczka

[1]      AGH University of Science and Technology, Department of Mineralogy, Petrography and Geochemistry, al. Mickiewicza 30, 30-059 Cracow, [#] goleb@agh.edu.pl

Key words: thallium, manganese oxides, Callovian, sandy limestones.

## INTRODUCTION

Permian rhyodacites and andesites have been exploited in the Zalas quarry, located in the southern, marginal part of the Silesian-Cracovian Monocline. This area belongs to the Upper Silesian block, where large deposits of Zn-Pb-bearing dolomite of Triassic age have been mined for a few centuries in the region of Trzebinia and Olkusz. Volcanic rocks in Zalas are overlain by a Middle – Upper Jurassic sedimentary sequence with a total thickness of about 18 meters. Brecciated Callovian sandy limestones include hydrothermal mineralization developed within a fault zone. The encrustation, represented by chalcopyrite, pyrite, marcasite, Ag-bearing chalcocite, covellite, galena, native bismuth, Fe and Mn oxides (Gołębiowska et al. 2010), is most likely connected with rejuvenation of Old–Paleozoic faults of the Alpine orogeny on the Oligocene–Miocene boundary. Supergene alteration of the primary minerals resulted in a diversified assemblage of secondary phases: malachite, cuprite, Fe- and Mn-dominant oxides, Cu sulfates, barite and iodargyrite (Gołębiowska et al. 2010). In this paper, we present chemical variability of Mn oxides, focusing on the causes of the strong Tl, Pb, Co and Ni enrichment. The SEM–BSE observations and preliminary EDS analyses were performed using a FEI Quanta 200 FEG scanning electron microscope. The chemical compositions were determined applying Cameca SX 100 electron microprobe under following conditions: accelerating voltage 20 kV, beam current 15 nA, peak count-time 20 s, and background time 10 s.

## RESULTS

The Mn oxides present in the thrust zone exhibit wide chemical variations. They commonly form cryptocrystalline, massive or rosette < 0.5 cm assemblages that include grains of < 20 μm. The Mn oxides contain variable admixtures of Fe, Ca, Ba, Si, Al, Mg, K, Co, Ni, Ti, Pb and Tl. Asbolane-type Co-Ni bearing phases (Co up to 13 wt. %, Ni up to 7.47 wt. %, Mn up to 30 wt. %) were observed as well. High concentrations of Co and Ni in Mn oxide are accompanied by elevated Cu content reaching 8.5 wt. %. The most interesting, but rarely occurring, are Mn oxides enriched in Tl. These fill small fractures and cracks in the thrust zone rocks, and are commonly intergrown with single flakes of

phyllosilicates. Spherulitic Ni-Co bearing Mn oxides, with bright in BSE imaging rims of Tl-Pb bearing Mn oxides occur also. The highest Tl concentration in the Mn oxides reaches 18.79 wt. %. The Mn oxides show also elevated content of Cu and Ba, reaching 5.56 wt. % and 4.39 wt. %, respectively.

## DISCUSSION

The admixtures in hypergenic Mn oxides from Zalas suggest that primary ore assemblage must have contained Ni-, Co-, Pb-, and Tl-bearing minerals. In the Silesian-Cracovian Monocline region, Co and Ni sulfides are known from Karniowice, in the ore veins cutting the Old-Paleozoic basement, in the Myszków and Zawiercie areas and in the Będkowska valley (e.g. Muszyński 1991; Czerny 1992; Koszowska 2004). Sawłowicz (1981) documented pyrite containing up to 1.5 wt. % Tl, while Kucha and Viene (1993) reported almost 2.3 wt. % Tl in oxysulfides. The latter ones were not documented in Zalas, probably due to used sample preparation, because the oxysulfides are well water soluble. It is highly probably that these are a source of high Tl concentrations in the secondary minerals. The process of Tl-enrichment in Mn oxides may be related to well known process of concentration of trace elements in the weathering zones. Although relatively low content in primary mineralization, the Tl concentration can be elevated up to over a dozen percent in hypergene zone. The studied zone in Zalas is most probably an example of such situation.

It has to be noted that Tl forms numerous own minerals, and occurs in elevated concentrations in other phases, such as sulphides (e.g. John Peter and Viraraghavan 2005). However, such high concentrations of Tl as reported in the Mn oxides from Zalas exceed more than two orders of magnitude those reported in similar minerals before (Critteden et al.

1962), making them unique in a world scale.

## REFERENCES

CRITTEDEN, M.S., CUTTITTA, F., ROSE, H.D. & FLEISCHER, M. (1962): Studies on manganese oxide minerals VI. Thallium in some manganese oxides. *Am. Mineral.* **47**, 1461–1467.

CZERNY, J. (1992): Hydrothermal mineralization phenomena in Karniowice travertine near Cracow. *Mineralogia Polonica*, **23**, 2, 3–13.

GOŁĘBIOWSKA, B., PIECZKA, A., RZEPA, G., MATYSZKIEWICZ, J. & KRAJEWSKI M. (2010): Iodargyrite from Zalas (Cracow area, Poland) as an indicator of Oligocene–Miocene aridity in Central Europe. *Palaeogeogr., Palaeoclimat., Palaeoecol.* **296**, 1-2, 130–137.

JOHN, PETER, A. L., VIRARAGHAVAN, T. (2005): Thallium: a review of public health and environmental concerns. *Environment International,* **31**, 493–501.

KOSZOWSKA, E. (2004): Preliminary report on tellurian and bismuth mineralization in skarn from Zawiercie, southern Poland. *Polskie Towarzystwo Mineralogiczne Prace Specjalne*, **24**, 231–234.

KUCHA, H., VIAENE W. (1993): Compounds with mixed and intermediate sulfur valences as precursors of banded sulfides in carbonate-hosted Zn–Pb deposits in Belgium and Poland. *Mineralium Deposita*, **28**, 13–21.

MUSZYŃSKI, M. (1991): Żyły mineralne w skałach poddewońskiego podłoża monokliny śląsko–krakowskiej. *Zeszyty naukowe AGH*, **52**, 7–129.

SAWŁOWICZ, Z. (1981): Forma występowania domieszek Pb, As, Tl i Zn w pirycie ze złóż śląsko–krakowskich. *Rudy Metale*, **26**, 7, 355–362.

# P-T EVOLUTION OF DIAMOND-BEARING INTERMEDIATE GRANULITES FROM NORTH BOHEMIA: FIRST RESULTS

[1]Jakub Haifler[#], [1,2]Jana Kotková,

[1] Department of Geological Sciences, Masaryk University, Brno, Czech Republic,
[#] haifler.j@mail.muni.cz
[2] Czech Geological Survey, Praha 5 – Barrandov, Czech Republic

Key words: granulite, Eger Crystalline Complex, geothermobarometry

Diamond and coesite inclusions discovered within garnet and kyanite in felsic and intermediate granulites of the Eger Crystalline Complex document ultrahigh-pressure conditions experienced by the rocks (Kotková et al. 2011). Such conditions significantly exceed previously determined peak metamorphic conditions (Kotková 1993) and they rather correspond to eclogite facies. However, these rocks later equilibrated under granulite facies. We investigated intermediate granulites from outcrops in Stráž nad Ohří in order to constrain their P-T evolution.

The rocks have porphyroblastic texture with mostly anhedral poikiloblastic garnet porphyroblasts and matrix comprising clinopyroxene, plagioclase (antiperthite) and quartz. Kyanite is less common and rutile is the most common accessory phase. Biotite, amphibole and epidote represent retrograde phases.

Large garnets (0.7-3 mm in diameter) contain numerous inclusions of plagioclase, K-feldspar, clinopyroxene, quartz and also rutile, diamond and graphite. Rare symplectites of clinopyroxenene and plagioclase and an omphacite grain were also observed in garnet. Garnets are zoned with homogeneous cores having composition of $Prp_{33}Alm_{37}Grs_{27-28}$ and rims poorer in grossular component ($Prp_{34-41}Alm_{44-48}Grs_{15-20}$). Diamond inclusions are located in the marginal zone of the high-Ca cores. Smaller garnets occuring in the matrix and surrounding kyanite have composition similar to the large garnet rims. Matrix clinopyroxenes are single grains up to 0.3 mm in diameter or aggregates of such grains and have mostly diopsidic composition ($En_{41-43}Fs_{10-13}Wo_{45-48}$) similar to that of clinopyroxene from plagioclase-bearing symplectite within garnet. Such symplectites are commonly products of omphacite breakdown, however, the reintegrated bulk composition of this symplectite does not correspond to that of the analyzed omphacite inclusion ($Jd_{36}Aeg_1Quad_{63}$).

The peak metamorphic temperatures can be constrained by Ti-in-zircon (Ferry and Watson 2007) and Zr-in-rutile (Tomkins et al. 2007) thermometry. The average content of Ti in diamond-bearing zone in zircon determined by SIMS is 150 ppm that gives temperature of 1085°C. The analyzed rutile shows variable Zr contents which cannot be simply correlated with their textural position. Matrix rutile

contains 0.25-0.35 wt. % Zr, whereas individual inclusions in garnet cores contain 0.15 (in contact with a diamond inclusion), 0.5 and even 0.77 wt. % Zr. These values yield temperatures of 900°C (0.15 wt. % Zr) up to 1130°C (0.77 wt. % Zr) for pressures of 3 GPa. However, the usability of Zr-in-rutile thermometer strongly depends on communication between rutile, zircon and $SiO_2$ phase. Grt-Cpx thermometry (Ravna 2000) for the most calcic garnet core and the omphacite inclusion yielded about 890°C at 2.5 GPa, which corresponds to minimum temperature of this stage due to garnet core homogenization. Further work will be focused on explanation of the scattered Zr contents in rutile and further precision of the exhumation path using both conventional and thermodynamic modeling.

## REFERENCES

FERRY, J. M, WATSON, E. B. (2007): New thermodynamic models and revised calibrations for the Ti-in-zircon and Zr-in-rutile thermometers. *Contributions to Mineralogy and Petrology*. **154**, 429-437.

KOTKOVÁ, J. (1993): Tectonometamorphic history of lower crust in the Bohemian Massif – example of North Bohemian granulites. *Czech Geological Survey Special Papers,* **2**, 1-42.

KOTKOVÁ, J., O'BRIEN, P., ZIEMANN, M.A. (2011): Diamond and coesite discovered in Saxony-type granulite: Solution to the Variscan garnet peridotite enigma. *Geology*, **39**, 667-670.

RAVNA, E.K. (2000): The garnet–clinopyroxen $Fe^{2+}$ –Mg geothermometer: an updated calibration. *Journal of Metamorphic Geology*. **18**, 211-219.

TOMKINS, H.S., POWELL, R., ELLIS, D.J. (2007): The pressure dependence of the zirconium-in-rutile thermometer. *Journal of Metamorphic Geology*. **25**, 703-713.

# CHARACTERIZATION OF THE ALTERATION PROCESSES OF THE METAMICT ZIRCONOLITE

[1]Jakub Haifler[#], [1]Radek Škoda

[1] Department of Geological Sciences, Masaryk University, Brno, Czech Republic
[#] haifler.j@mail.muni.cz

Key words: zirconolite, hydrothermal alteration, metamict, experiment, annealing

## INTRODUCTION

Zirconolite, $CaZrTi_2O_7$, is a mineral with excellent resistance to hydrothermal alterations. It usually remains unaltered in geological environments for hundreds of millions of years or even longer periods despite of high contents of unstable elements like U and Th. For this reason synthetic analogue of zirconolite doped with components of spent nuclear fuel is suggested to be used as a form for immobilisation of high level nuclear waste. In this work we studied both the natural and experimental alterations of metamict zirconolites from Håkestad and Stålacker quarries in Norway in order to describe behaviour of this phase in contact with hydrothermal fluids – the mobility of elements and the alteration features.

## CHEMICAL COMPOSITION AND XRD MEASUREMENT

Zirconolites are highly enriched in REE (Ce, Nd, Y, La), Nb, Th, U and Fe relative to ideal composition. Natural alteration features are quite rare among zirconolites, although in case of here-described samples the alteration zones are observed at some rims or along cracks. They are depleted in Ca, Fe, Zr and Ti and enriched in Si and $H_2O$ compared to unaltered parts. The contents of heavy elements U, Th and REE, however does not change significantly. Metamict state of zirconolite caused by high content of U and Th was confirmed by XRD-powder diffraction analysis. The annealing at temperatures between 400 and 800°C in a reaction chamber gave rise to a recrystallization of a cubic phase (*Fm-3m* space group with cell parameter a=5.104(3) Å). During annealing at 900°C, zirconolite-3O polytypoid was formed.

## EXPERIMENTS

The fragments of metamict zirconolite were experimentally altered in three solutions (1M HCl; 1M HCl + 0.2 g of silica powder; 1M HCl + 1 g of uranium acetate) at 200°C for 30 days. Complex alteration zones rich in Zr, Nb, Ti were formed by a dissolution-reprecipitation process. Uranium, thorium and REE were not immobilised in solid products. Further experiments were performed on powdered samples - 1570 mg of powder were altered in 15 ml of 1M HCl solution and 795 mg of powder were altered in 15 ml of 1M NaOH solution at 200°C for 30 days.

There were 15.31 mg Ca; 0.01 mg Zr; 0.25 mg Ti; 6.39 mg Th; 2.25 mg U; 15.15 mg Ce and 5.88 mg Nd dissolved in the acid after the termination of the experiment. The relative mobility of selected elements from mineral to acidic fluid in descending order is as follows: U > Nd > Ca > Ce > Th > Ti > Zr > Nb. There were 0.04 mg Ca; 0.005 mg Zr; 0.005 mg Ti; 0.003 mg Nb; 0.056 mg U and 0.0005 mg Ce dissolved in the hydroxide. The relative mobility of the selected elements in descending order is as follows: U > Ca > Ti > Nb > Zr > Ce > Th, Nd. The complex zones of products observed within the altered fragments did not form in powders altered in HCl, but two separated products were formed. Powders altered in NaOH solution were not covered by products; they had rounded edges indicating a dissolution process only in contrast with HCl experiments, where the dissolution and reprecipitation were spatially coupled. Anatase and zircon were determined as products of alteration in HCl solutions. Zircon was determined as products of alteration in NaOH solutions and monazite overgrowth on zirconolite was observed despite the fact that phosphorus was not input deliberately. Many further unidentified phases were discovered.

## CONCLUSIONS

In case of natural alterations of metamict zirconolite the heavy elements U, Th and REE are commonly preserved in solids (this work; Lumpkin 2001; Williams et al. 2001; Bulakh et al. 1998; Bulakh et al. 2006), while when the strongly corrosive solutions of HCl and NaOH were applied, these elements were released into solution. The completely metamict state of zirconolite together with hot and aggresive acidic or basic fluid disrupt the usual retention of U, Th, REE previously observed among naturally altered samples (cited above), experimentally altered crystalline samples (Pöml et al. 2011) or those altered by less corrosive fluid or at lower temperature (Leturcq et al. 2005; Pöml et al. 2011).

## REFERENCES

BULAKH, A., NESTEROV, A., ANISIMOV, I., WILLIAMS, C.T. (1998): Zirkelite from the Sebl'yavr carbonatite complex, Kola Peninsula, Russia; an X-ray and electron microprobe study of a partially metamict mineral. *Min. Mag*. **626**, 837-846.

BULAKH, A., NESTEROV, A., WILLIAMS, C.T. (2006): Zirconolite, $CaZrTi_2O_7$, re-examined from its type locality at Afrikanda, Kola Peninsula, Russia and some SYNROC implications. *N. Jh. Min. Ab*. **182**, 109-121.

LETURCQ, G., McGLINN, P., BARBE, C., BLACKFORD, M., FINNIE, K. (2005): Aqueous alteration of nearly pure Nd-doped zirconolite $(Ca_{0.8}Nd_{0.2}ZrTi_{1.8}Al_{0.2}O_7)$, a passivating layer control. *Applied Geochemistry*. **20**, 899-906.

LUMPKIN, G. (2001) Alpha-decay damage and aqueous durability of actinide host phases in natural systems. *Journal of Nuclear Materials.* **289**, 136-166.

PÖML, P., GEISLER, T., COBOS-SABATÉ, J., WISS, T., RAISON, P., SCHMIDT-BEURMANN, P., DESCHANELS, X., JÉGOU, C., HEIMINK, J., PUTNIS, A. (2011): The mechanism of the hydrothermal alteration of cerium- and plutonium-doped zirconolite. *Journal of Nuclear Materials*. **410**, 10-23.

WILLIAMS, C.T., BULAKH, A., GIERÉ, R., LUMPKIN, G., MARIANO, A. (2001): Alteration features in natural zirconolite from carbonatites. *In* (K.P. Hart, G. Lumpkin, eds.). *MRS Proceedings*. **663**, 945-952.

# PROGRADE AND RETROGADE MINERAL ASSOCIATION IN METAULTRAMAFICS IN THE SIEGGRABEN AND SCHWARZENBACH AREA, EASTERN ALPS

[1]Samila Hrvanović[#], [1]Marián Putiš,
[1]Peter Bačík

[1] Comenius University in Bratislava, Faculty of Natural Sciences, Dpt. of Mineralogy and Petrology, Mlynská dolina, 842 15 Bratislava, Slovakia, [#] hrvanovic@fns.uniba.sk

Key words: metaultramafics, electron microprobe, petrography, mineral chemistry, prograde, retrograde, mineral assemblage, Eastern Alps

## INTRODUCTION

The Sieggraben structural complex belongs to the Middle Austro-Alpine basement unit in the Eastern Alps (Tollman 1980). It is located in the Rosalien Mountains between villages of Sieggraben and Schwarzenbach (ca. 80 km south of Vienna). The main goal of study is to identify petrographic and mineralogical properties of prograde and retrograde mineral assemblage of serpentinized metaultramafics.

Metaultramafics occurs as individual lensoidal bodies in metapelites (micaschists to gneisses, migmatitic gneisses), metabasites (eclogites, amphibolites, metagabbros), impure metacarbonates and calc-silicate rocks (marbles), crosscut by veins of granitic orthogneisses (leucocrate metagranites, metapegmatites) in a pre-Alpine basement complex (Putiš et al. 2000).

Metaultramafics preserve mineral assemblages characterized by olivine (forsterite) and orthopyroxene (enstatite) relics from eclogite facies metamorphic stage, overprinted by serpentine minerals (antigorite and chrysotile), Cr-spinel, chromite, Ca-amphibole (tremolite), Mg-rich chlorite and rare talc and carbonates. Clinopyroxene is characteristically absent but a large amount of Cr-spinel to chromite and Ca-amphibole is present (Hrvanović et al. 2013a, b). Metaultramafics represent mantle fragments emplaced in the subducted lower continental crust during Cretaceous orogeny. Mineral abbreviations in text, figures: Amp – amphibole, Atg – antigorite, Chl – chlorite, Chr – chromite, Ctl – chrysotile, Ol – olivine, Opx – orthopyroxene, Spl – spinel, Srp – serpentine group, Tlc – talc, Tr – tremolite (Whitney et al. 2010).

## RESULTS

Serpentinites from the MAA SSC occur as lenses in eclogitic amphibolites, gneisses or marbles. Macroscopically (Fig. 1. a), a typical studied serpentinite is a dark grey to dark green massive fine grained to schistose rock with pale pseudomorphs of Srp after coarse-grained orthopyroxenes (bastite) randomly oriented in serpentine matrix.

Microscopically identified phases include olivine, orthopyroxene, spinel group (Chr, 0.1 mm in size), amphibole, surrounded by matrix minerals of serpentine group (Atg and Ctl), chlorite, rare talc and opaque minerals (magnetite, hematite) (Fig. 1. b). Clinopyroxene was not found in these samples. Calcite veinlets were found in one sample. Olivine occurs in relic aggregates as subhedral high-relief grains, partly replaced by Srp in typical mesh structure. The olivine grains show homogeneous chemical composition and have no inclusions (Fig.1. b-c).
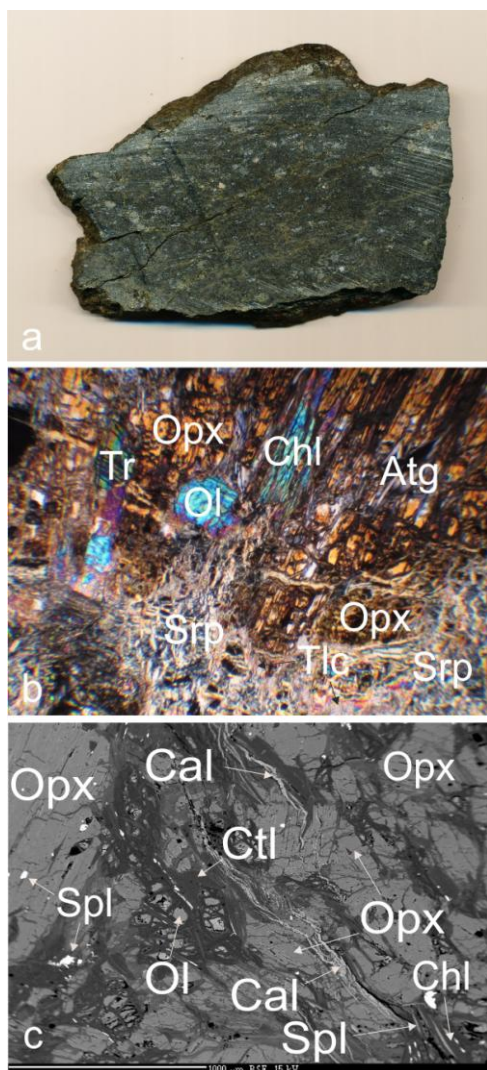
Fig. 1.a) Scanned cutted surface of serpentinite hand sample SW-4-1, b) Microphotographs of sample S-201-2a and c) BSE image of S-200f.

According to the end-member composition, Ol contains from 90.21 to 90.38 mol. % of forsterite component.

Pyroxene in investigated metaultramafics is magnesium-rich pyroxene, enstatite (Fig. 1b-c), with Mg in range from 1.81 to 1.93 *apfu*. It occurs as big relic grains with inclusions of spinel (Fig. 1b-c). It is partly altered by minerals of serpentine group (Fig. 1b, c).

Spinel group occurs as opaque anhedral grains in matrix and also as needleous inclusions in enstatite. According to end member calculation it is chromite with Cr from 1.65 to 1.72 *apfu*.

Amphibole occurs as prismatic non-pleochroic grains. Amphibole has chemical composition of tremolite with $X_{Mg}$ between 0.94 and 0.96 and $^B$Na up to 0.19 *apfu*.

Minerals of serpentine group occur in metamorphic matrix or they make pseudomorphs replacing Ol and Opx. Flakes of Atg (Fig. 1a) show a higher Fe and also Al contents, however a lower Si content in comparison with Ctl fine-flake aggregates.

Chlorite occurs as randomly oriented flakes. It is an alteration product of Ol, Opx, tremolite and spinel (Fig. 1b, c). In calculated structural formula value, Mg is in range from 4.5 to 4.8 *apfu*.

Talc is present in a small amount in matrix, mixed with minerals of serpentine group (Fig. 1b). It occurs as colourless grains with low relief and characteristic high interference colours.

CONCLUSIONS

The studied serpentinites recorded two metamorphic stages – a prograde and retrograde one. The prograde metamorphic mineral assemblage consists of Ol, Opx and Atg, most likely due to eclogite facies conditions. The retrograde assemblage contains Tr, Mg-Chl, Ctl, Chr, ±Tlc and ±Carb due to superimposed amphibolite- to greenschist-facies.

REFERENCES

TOLLMAN, A. (1980): Geology and tectonics of the Eastern Alps (Middle Sector). *Abh. Geol. Bundesanst. Wien,* **34,** 197-255.

PUTIŠ M., KORIKOVSKY S. P., PUSHKAREV D. Y. (2000): Jahrb. Geol. Bundesanst. 142 (3), 73 p.

HRVANOVIĆ S., PUTIŠ M., BAČÍK, P. (2013a): Metaultramafics in the eclogitic Sieggraben complex (Eastern Alps), *ŠVK PriF UK 2013 Zborník recenzovaných príspevkov,* 1253-1258.

HRVANOVIĆ S., PUTIŠ M., BAČÍK, P., KROMEL J. (2013b): Petrological characterization of metaultramafics in the Sieggraben complex (Eastern Alps). *Univerzita Komenského v Bratislave, MINPET 2013.*

Whitney, D.L., Evans, B.W. (2010): Abbreviations for names of rock-forming minerals. Am. Mineral. 95, 185.

# APPLICATIONS OF GEOSCIENCES IN THE STUDY OF ARCHAEOCERAMICS: ARCHAEOMETRIC STUDIES IN ROMANIA

[1]Corina Ionescu[#], [2]Volker Hoeck

[1] Depart. Geology Babes-Bolyai University Cluj-Napoca, Romania, [#] corina.ionescu@ubbcluj.ro
[2] Paris Lodron University Salzburg, Austria

Key words: archaeometry, ancient ceramics, geoscience

The last decades had witnessed the study of archaeological artifacts in particular ceramics, due to their potential in reconstruction the technological level of the ancient human societies. The fired ceramic body can be regarded as an "artificial rock" and therefore a geoscientific approach is necessary in obtaining information on composition and fabric. Nevertheless, as a product of the „anthropogenic metamorphism", ceramics may contribute to a better understanding of the mineral reactions taking place in complex systems at high temperature, atmospheric pressure and short time of heating. Due to the richness of ceramic shards ranging from Neolithic to medieval times, discovered within its territory, Romania represents an ideal field for study. Our research is focused on identification of composition, microfabric and chemistry of the ceramic body. Polarized light optical microscopy, electron microprobe analysis (EMPA), X-Ray powder diffraction, scanning electron microscopy, ICP-MS and ICP-ES are analytical methods applied. The studied archaeological ceramics belongs to Copper Age (Cucuteni-Ruginoasa, Cerişor Cave), Bronze Age (Palatca, Derşida, Copăceni, Lăpuş, Siliştea), Dacian and Roman period (Napoca, Micăsasa, Sarmizegetusa), Roman-Byzantine period (Ibida, Argamum, Noviodunum).

From these, the result of EMPA and chemical investigation on Copper Age ceramic shard from Cucuteni-Ruginoasa will be presented. The pots were painted and fired at various temperatures. Upon firing, several new phases formed, *e.g.* Ca-rich illite, K-feldpar, clinopyroxene, NaK-feldpar, CaAl silicates and glass.

The archaeometric interpretation of the data includes a certain range of firing temperature, between 850ºC and 950ºC. The used raw material was a calcareous illitic Sarmatian mudstone cropping out in the immediate neighborhood of the site. This clay was processed by levigation and was modeled a various pots.

# URANIUM AND SULPHIDE MINERALIZATION FROM THE 21ST LEVEL OF THE ROŽNÁ MINE

[1]Michaela Jakubcová[#], [1]Jaromír Leichmann

[1] Department of Geological Sciences, Masaryk University, Kotlářská 2, 611 37 Brno, Czech Republic; [#] 357453@mail.muni.cz

Key words: uranium, sulphide mineralization, Rožná

## INTRODUCTION

The lenses of Pb-Zn sulphide mineralization with uraninite-coffinite veins were found during mining on the 21st level. These mineralizations were hosted in metasomatites. The sulphide mineralization consists mainly of sphalerite and galena. Pyrite, pyrrhotite (from which marcasite originates) and chalcopyrite are less common. Uraninite and coffinite are typical for uranium mineralization. A mineral assemblage of Fe, Mn-sphalerite, galena, pyrite and pyrrhotite is characteristic for some of the silicate-rich marbles at the Rožná uranium deposit region, western Moravia, Czech Republic. Remarkable accessory of this assemblage is a Ba-rich feldspar and barite (Doležalová et al. 2006).

## SULPHIDE MINERALIZATION

Sphalerite occurs with pyrite and galena. In some parts it forms rounded grains. In other parts it is brecciate and penetrated with chlorite-calcite matrix. Sphalerite is enriched in Fe (8.7 wt. %) and Mn (1.9 wt. %).
Galena partly occurs as inclusions in pyrite and uraninite. Radial aggregates of Pb-rich chlorite were found in galena. Two types of pyrite were found. The massive one, which is older, and the porous, which is younger. Pyrite is partly replaced by uranium phases. This feature indicates that it served as a reducing agent for the U-bearing fluids.

Pyrrhotite forms needle-like aggregates in carbonate and is transformed into marcasite.

## URANIUM MINERALIZATION

Younger uraninite-coffinite veins crosscut the older suplhide mineralization (Fig. 1).
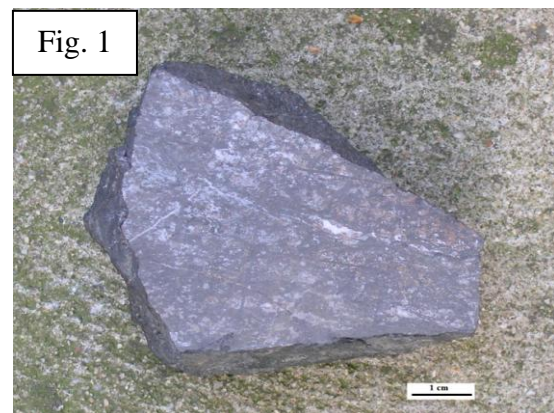


Fig. 1. Younger uraninite-coffinite veins crosscut the older suplhide mineralization.

Uraninite forms botryoidal greins with coffinit rims. The BSE study showed the presence of two types of coffinit rims – chlorite-coffinite (darker) and zirconium-coffinite (lighter) (Fig. 2).

Sulphide and uranium mineralization are genetically independent. The older sulphidic mineralization could locally reduce $U^{6+}$ ions from the fluids and induce the precipitation of uranium ores.
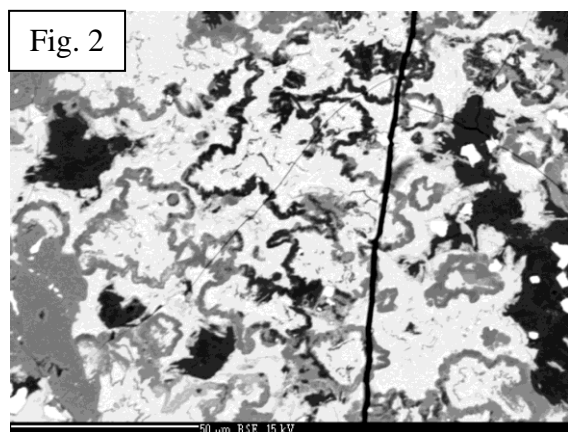


Fig. 2. BSE-images: Two types of coffinit rims. Chlorit-coffinit (darker) and zirconium-coffinit (lighter). Photo-R.Škoda.

## NON-METALLIC MINERALS

Carbonates occur as greins, veins or with chlorite as chlorite-calcite matrix. The BSE analyses documented two types of carbonates – calcite and siderite.

The BSE analyses show high content of BaO in feldspar (35 wt. %), which could be therefore classified as hyalofan and celsian. Barite is another Ba-bearing phases.

The studied sulphide mineralization could be therefore interpreted as a continuation of stratiform barite-hyalophane-sulphide mineralization described by Kříbek (2005) and also of the stratidependent disseminated sulphide mineralization with Ba-mica studied by Doležalová et al. (2006). Both mineralizations studied by Kříbek (2005) and Doležalová et al. (2006) were found on higher level of the Rožná mine. The results presented here indicate that mineralization continues into depth.

Further evidence supporting this interpretation is the chemistry of sphalerite, which corresponds to chemistry of sphalerites of stratidependent disseminated suplhide mineralization (Doležalová et al. 2006).

The Ba-Pb-Zn mineralization from Rožná could be therefore considered as highly metamorphosed equivalent of similar mineralizations known from Křižanovice and Horní Benešov in Bohemain Massif.

REFERENCES

DOLEŽALOVÁ, H., HOUZAR, S., LOSOS, Z. & ŠKODA, R. (2006): Kinoshitalite with a high magnesium content in sulphide-rich marbles from the Rožná uranium deposit, Western Moravia, Czech Republic. *N. Jb. Miner. Abh.* **182/2**, 165-171.

KŘÍBEK, B. (2005): Types, stages and mineralogy of paragenesis at Rožná deposit. *In* The Rožná uranium deposit: model of late Variscan and post-Variscan mineralization (KŘÍBEK, B. & HÁJEK, A., eds), 25-32.

# MORPHOLOGY OF MICRODIAMONDS FROM THE NORTH BOHEMIAN GRANULITES

[1]Petra Jakubová[#],[1,2]Jana Kotková,
[1]Jaromír Leichmann

[1]  Department of Geological Sciences, Masaryk University, Kotlářská 2, CZ-611 37 Brno,
   [#]petra.jakubova@centrum.cz
[2]  Czech Geological Survey, Klárov 3, CZ-118 21, Praha 1

## INTRODUCTION

In-situ diamond is one of the best indicators of ultrahigh–pressure (UHP) conditions. The UHP granulites from the northern Bohemia contain well-preserved diamonds not coated with graphite, which makes them ideal objects to study their morphology, i.e. crystal shape and character of crystal surfaces. Until now such data exist only for microdiamonds from Kokchetav Massif and Saxonian Erzgebirge, Germany (Dobrzhinetskaya 2012). Experiments and studies from these terrains provided data suggesting that different morphologies of diamond (e.g. perfect vs. imperfect crystal shape, diamond size, etc.) reflect the growth conditions and are influenced by many factors such as supersaturation or presence of solid impurities (Dobrzhinetskaya 2012).

The occurrence of diamonds in both felsic (Grt-Ky-Fs-Qtz) and in intermediate (Grt-Cpx-Fs-Qtz) granulite in North Bohemia, which formed at comparable P-T conditions, allows studying the influence of the bulk rock composition on the diamond morphology. In our study,

scanning electron microscope (SEM) MIRA3 equipped with back-scattered electron detector (BSE) was used and AFM imaging using Dimension Icon microscope (Bruker) in ScanAsyst mode with Scanasyst-Air probes was executed.

## DIAMOND MORPHOLOGY

Diamonds present as inclusions in kyanite, garnet and zircon were examined in thin sections and epoxy mounts prepared from separated host mineral grains. The samples were polished using the colloidal $SiO_2$ of 0.04 µm grain size so that the diamonds stand out above the surface of host minerals.

North Bohemian microdiamonds exhibit diverse morphologies, depending upon the host rock type.

Three polished thin sections (30 and 300 µm thick) of felsic granulite containing diamonds within kyanites, one garnet and one zircon have been examined. Out of 470 studied kyanite grains only 30 % contain diamond, and 30 % of these enclose more than 1 diamond grain. In total, 200 grains of single diamonds enclosed at variable depths and only

exceptionally found on the sample surface have been detected. Only one grain of garnet containing diamond has been observed. The size of diamonds ranges from 5 to 20 μm, rarely up to 40 μm and the shape is exclusively octahedral; octahedral diamond was also observed in zircon in thin-section.

In contrast to felsic granulite, diamonds in intermediate granulite are enclosed mainly in garnet and zircon. Again, three thin sections (30 and 300 μm thick) have been examined. Out of 200 garnet grains only 24 % contain 75 single diamonds and 9 diamond clusters. The size of diamonds ranges from 5 to 15 μm and the shape is mostly cubo-octahedral. Similarly, shape of diamonds enclosed in 30 out of 210 separated zircon grains, i.e. 14 %, is cubo-octahedral and size of the grains ranges from 4 to 20 μm.

Diamonds enclosed in felsic granulite (kyanite, garnet, zircon) occur exclusively as single crystals; several twins have been also observed. The diamonds have exclusively octahedral shape. However, only few crystals have form of an ideal octahedron with smooth surfaces and sharp edges. Instead, most of the crystals are distorted. Such diamonds have additional edges instead of pointed corners or edges of unequal lengths. Several crystals are imperfect with sharp corners and hillocks and cavities. Some octahedral crystal faces have triangular growth surfaces that develop a stepped appearance. The development of an octahedral habit indicates slow growth of the grain under stable conditions.

The shape of diamonds enclosed in intermediate granulite (garnet and zircon) is characterized by combination of cubic and octahedral faces, resulting in a cubo-octahedron. None of the crystals has smooth faces; each of them is imperfect with sharp truncated corners and more or less developed hillocks or cavities. Imperfect diamond morphologies suggest that they were formed in a medium oversaturated with impurities. (Dobrzhinetskaya et al. 2007).

Indicators of resorption, such as rounded corners and edges along with rarely observed etch pits (trigons on octahedrons, and both trigons and tetragons on cubo-octahedrons) can be observed on the diamonds. These probably develop from etching of the crystal faces by fluids at high temperatures.

No polyphase crystal growth which would suggest that the diamonds were formed in two distinct stages (Ishida et al. 2003) has been detected.

To summarize, based on morphology of diamond enclosed in kyanite, garnet and zircon we may assume that the diamonds were formed in one stage at stable conditions and some of them were affected by the later resorption. Different diamond morphology may be controlled by impurities available in the medium of crystallization (in our case K- vs. Ca-bearing fluids or melts for the two lithologies, respectively). Nevertheless, it is necessary to emphasize that perfect and imperfect diamonds lie in the host mineral grains next to each other.

REFERENCES

DOBRZHINETSKAYA, L. F. (2012): Microdiamonds–Frontiers of ultrahigh-pressure metamorphism: A review. *Gondwana Research*, **21**, 207-223.
DOBRZHINETSKAYA, L. F., WIRTH, R., GREEN, H. W. (2007): A look inside of diamond-forming media in deep subduction zones. *Proceedings of the National Acadamy of Sciences of the USA*, **104**, 9128-9132.
ISHIDA, H., OGASAWARA, Y., OHSUMI, K., SAITO, A. (2003): Two stage growth of microdiamond in UHP dolomite marble from Kokchetav Massif, Kazahstan. *J. metamorphic Geol.* **21**, 515-522.

# EVIDENCE OF TWO DIFFERENT METAMORPHIC GARNETS IN FELSIC GRANULITE FROM THE KUTNÁ HORA CRYSTALLINE COMPLEX (BOHEMIAN MASSIF) BY ZONING OF RARE EARTH ELEMENTS

[1]Radim Jedlička[#], [1]Shah Wali Faryad,
[2]Christoph Hauzenberger

[1]      Institute of Petrology and Structural Geology, Charles University, Prague, 12843, Czech Republic, [#]radim.jedlicka@natur.cuni.cz

[2]      Institute of Mineralogy and Petrology, Karl-Franzens University, Universitätplatz 2, 8010, Graz, Austria

Key words: rare Earth elements, garnet zonation, multiple zoning, felsic granulites

## INTRODUCTION

Preservation of compositional zoning in metamorphic garnet is considered as powerful tool to reconstruct P-T paths in metamorphic rocks. This is due to the slow diffusion coefficients of some major but mainly of trace elements, that include Y and heavy rare Earth elements (HREEs), which show strong partitioning in garnet.

In this study we present the results of laser-ablation ICP-MS, which was used to analyze the heavy and middle REEs and Y concentration in garnet crystals from felsic granulites of the Kutná Hora crystalline complex.

## CHAPTER 1

Felsic granulites with lenses and boudins of garnet peridotites and eclogites from the Kutná Hora complex, for which UHP metamorphic conditions were estimated (Medaris et al. 2006; Faryad 2009), are common in the Moldanubian Zone of the Bohemian Massif. However, it is not always clear when and how the HP-UHPM

rocks were emplaced into the host granulites. The most important question that remains is, whether HP-UHP mafic and ultramafic bodies emplaced during or even after granulite facies metamorphism into the felsic granulites also experienced UHP metamorphism. By studying of compositional zoning of both major and trace elements in garnet, we provide evidence of metamorphic event in felsic rocks prior to their granulite facies overprint.

## CHAPTER 2

LA-ICP-MS profile analyses reveal two different varieties of zoning of trace and middle and heavy rare Earth elements. First variety was found in about 1.3 cm large garnet crystal having irregular shape. In the core segment of this crystal, we observe bell-shaped distribution of yttrium and REE with maximum content in the middle, which is mostly attributed to Rayleigh fractionation during garnet growth (Hollister 1966). The concentration of these elements is high in the core and

after decreasing in the mantle segment it reaches the second maximum. At rim section the concentration of Y and HREE shows decrease back to the minimum values.

The second variety of zoning occurs in a regular shaped garnet crystal of about 0.96 mm in diameter. The lowest concentration of Y and REE is in the core segment. In the mantle segment the concentration increases and reaches its maximum values near the rim section and finally decreases back at the most rim part.

## CONCLUSION

Compositional zoning in garnets from felsic granulite in the Kutná Hora complex indicate two distinct metamorphic events. The core of large garnet with relatively high Ca content was probably formed during prograde low- to medium-temperature metamorphic event that could be coeval with HP-UHP metamorphism in the Bohemian Massif. After reaching maximum pressure conditions, cooling and decompression led to partial resorption of garnet along its rims. New garnet growth occurred at higher temperatures in granulite facies event. Therefore, the core and the annular maximums indicate the evidence for two-stage metamorphic evolution of the rock. Compositional profile of the smaller garnet crystal is similar to the mantle segment of a large garnet that indicates only the granulite facies metamorphic event.

## REFERENCES

MEDARIS, L. G., BEARD, B. L. & JELÍNEK, E. (2006): Mantle-derived, UHP garnet pyroxenite and eclogite in the Moldanubian Gföhl Nappe, Bohemian Massif: a geochemical review, new P-T determinations and tectonic interpretation. *International Geology Review*, **48**, 765-777.

FARYAD, S. W. (2009): The Kutná Hora Complex (Moldanubian Zone, Bohemian Massif): A composite of crustal and mantle rocks subducted to HP/UHP conditions. *Lithos*, **109**, 193-208.

HOLLISTER, L. S. (1966): Garnet zoning: an interpretation based on Rayleigh fractionation model. *Science*, **154**, 1647-1651.

# AN INFLUENCE OF SAMPLE PREPARATION ON MICROSTRUCTURE OF DENTAL HYDROXYLAPATITE

[1,2]Anna Kallistová[#], [1,2]Roman Skála,
[3,4]Radana Malíková, [5]Ivan Horáček

[1] Institute of Geochemistry, Mineralogy and Mineral Resources, Faculty of Science, Charles University, Albertov 6, 128 43 Prague 2, Czech Rep., [#] kallistova@gli.cas.cz
[2] Institute of Geology, AS CR, v.v.i., Rozvojová 269, 165 00 Prague 6, Czech Rep.
[3] Department of Mineralogy and Petrology, National Museum, Cirkusová 1740,193 00 Prague 9, Czech Rep.
[4] Department of Geological Sciences, Masaryk University, Kotlářská 2, 611 37, Brno, Czech Rep.
[5] Department of Zoology, Faculty of Science, Charles University, Viničná 7, 128 44, Prague 2, Czech Rep.

Key words: hydroxylapatite, crystallite size, crystallite microstrain, sample preparation

## INTRODUCTION

Dental hydroxylapatite (HAP) has been frequently studied by X-ray powder diffraction (XRD) to obtain essential information about the lattice and microstructure parameters; the latter have significant effects on the mechanical properties of the tooth (Kantola et al. 1973, Oktar et al. 1999, Kallaste and Nemliher 2005). Various methods have been adopted to prepare the specimens for XRD, however, there is no systematic study of their critical influence on the sample itself. This research compares the influence of specimen preparation on the microstructure of dental HAP.

## MATERIALS AND METHODS

The first molars of three miniature pig´s were cut into six slices perpendicular to the occlusal surface. These slices were then subjected to six different techniques of preparation to obtain pure enamel: (1) enamel and dentin were separated mechanically; (2) enamel was drilled off with drilling rotary micro-drill equipped with a 1 mm diamond spike; (3) enamel was retained after drilling off the dentin; (4) enamel was drilled off under cooling medium [water]; (5) teeth were deproteinated with hydrazin monohydrate ($NH_2.NH_2.H_2O$); and (6) sample was cooled in liquid nitrogen with subsequent immersion in boiling water.

X-ray powder diffraction data were collected with a Bruker D8 diffractometer ($CuK\alpha_1$). Calculation of the average crystallite size and microstrain was performed with the FullProf program (Rodríguez-Carvajal 2001).

## RESULTS

The influence of sample preparation on microstrain cannot be evaluated because its low overall size is invariant within experimental errors.

In the past, it has been shown that HAP crystallites are elongated along the [001] direction (Daculsi and Kerebel 1978,

Warshawsky 1987). Our results demonstrate that preparation technique influences the shape of crystallites mainly in this direction. The diameter of section perpendicular to the *c* axis remains almost unaffected. To involve quantitative data on both crystallite average size and its shape we employed its volume to evaluate the role of sample handling.

Mechanically prepared samples always correspond to the crystallite size obtained from literature (Fig. 1). On the contrary, drilling methods provide data off the range. In several cases new phases such as calcite and $CaH_2P_2O_7$ appear. In M1 and M2 the deproteinated and nitrogen treated samples cluster around the upper limit of the previously published crystallite size. The M3 sample, on general, shows much higher crystallite volume than the previous two.

CONCLUSIONS

The refined size of crystallites best corresponds to the literature data for specimens prepared by mechanical separation of enamel and dentin making this approach most suitable for sample preparation.

REFERENCES

DACULSI, G., KEREBEL, B. (1978): HRTEM study of human enamel crystallites: size, shape and growth. *J. Ultrastructure research.* **65**, 163-172.

GROVE, C.A., JUDD, G AND ANSELL, G. S. (1972): Determination of hydroxyapatite crystallite size in human dental enamel by dark-field electron microscopy.*J. Dent.Res.* **51**, 22-29.

KALLASTE, T., NEMLIHER, J. (2005): Apatite varieties in extant and fossil vertebrate mineralized tissues. *J. Appl. Cryst.* **38**, 587-594.

KANTOLA, S., LAINE, E. AND TARNA, T. (1973): Laser-induced effects on tooth structure VI. X-ray diffraction study of dental enamel exposed to a CO2 laser. *Acta Odontologica Scandinavica.* **31**, 369-379.

OKTAR, F. N, KESENCI, K. AND PISKIN, E. (1999): Characterization of processed tooth hydroxyapatite for potentional biomedical implant applications. *Artificial Cells, Nanomedicine and Biotechnology.* **27**, 367-379.

RODRÍGUEZ-CARVAJAL, J. (2001): Recent developments of the program FullProf. *Commission on Powder Diffracton (IUCr) Newsletter.* **26**, 12-19.

WARSHAWSKY, H. (1987): Enamel crystal shape: history of an idea. *Adv. Dent. Res.* **1**, 322-329.
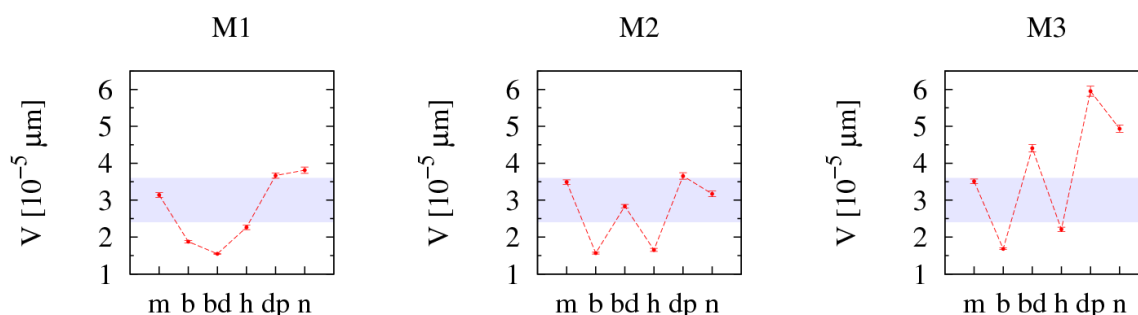


Fig. 1. Variations in volume size . Letters indicate methods of preparation: m - mechanically, b - drilled off enamel, bd - drilled off dentin, h - drilled off enamel when cooling, dp - deproteinized, n - nitrogen treated. The blue rectangle indicates the range of crystallite volume as published by Daculsi and Kerebel (1978).

# HISTORICAL COPPER SLAGS FROM THE VICINITY OF LESZCZYNA (LOWER SILESIA) – MINERALOGY AND CHEMICAL COMPOSITION

[1]Jakub Kierczak[#], [2]Tomasz Stolarczyk

[1]     University of Wrocław, Institute of Geological Sciences, Pl. M. Borna 9, 50-204 Wrocław, Poland, [#]jakub.kierczak@ing.uni.wroc.pl

[2]     Museum of Copper, ul. Partyzantów 3, 59-220 Legnica, Poland

Key words: North-Sudetic Basin, stratabound Cu deposits, glass, environmental impact

## INTRODUCTION

Three main types of Cu ores are distinguished on the basis of general geological settings. The most common are porphyry deposits, where Cu is associated with sulfide minerals disseminated in igneous intrusive rocks. In strata-bound deposits Cu occurs in silicates, carbonates, and sulfides within sedimentary rocks (e.g., shales, sandstones). Cu ores with the least economic importance are represented by massive sulfide deposits, where Cu-bearing sulfides occur as veins and massive replacements in limestones or as large bodies within volcanic rocks.

Copper ores exploited in Poland belong to the strata-bound type. They are located in Lower Silesia within two geological units: Fore-Sudetic Monocline and North Sudetic Basin and related to the Zechstein Kupferschifer formation. Polish Cu ores having largest economic importance are situated on the Fore-Sudetic Monocline. The first written references about the exploitation and smelting of Cu ores in the vicinity of Leszczyna (North Sudetic Basin) come from the 16th century (CDS XX-XXI). However, the history of metallurgy of Cu ores in this area dates back presumably to the Middle Ages (Stolarczyk 2012).

Copper ores in the Leszczyna region are associated with the Lower Permian marls (slate marls). These deposits were relatively poor, containing 0.5 to 1.8 % Cu. However, their occurrence in the form of relatively regular strata of approximately 2.8 meters thick, facilitated their exploitation (Stolarczyk 2012).

The major Cu-bearing minerals of these deposits included: bornite ($Cu_5FeS_4$), chalcocite ($Cu_2S$), and chalcopyrite ($CuFeS_2$) accompanied by minor covellite, native Cu, malachite and azurite (Stolarczyk 2012).

Copper ores mined in the vicinity of Leszczyna were subsequently smelted in a nearby smelters. As a result of this industrial activity important quantity of wastes – pyrometallurgical slags, were produced and deposited in the vicinity of the smelters.

This study presents mineralogical and chemical composition of historical slags resulted from Cu smelting in the vicinity of Leszczyna. We pay special attention to the identification of metal bearing phases which may constitute an environmental risk.

## RESULTS

Two sampling sites were chosen for this study. One is located in the area of former Cu smelter in Leszczyna (site 1; active 1865-1882) whereas second is situated approximately five kilometers south from site 1 near Kondratów (site 2; active 1751-1759). Slag samples from studied sites have different macroscopic characteristic. These from site 1 occur on the ground surface as single, highly porous blocks, which have the maximum diameter of 50 centimeters. Additionally, ruins of buildings with walls built of slag blocks are present at the site 1. Slags from site 2 are generally smaller (up to 20 centimeters in diameter) and characterized by lower porosity than the porosity of slags from site 1. Chemical composition of studied wastes from both sites is also slightly different. Slags from site 1 are composed of silica, lime and alumina as major oxide components with average concentrations of 46 wt. % $SiO_2$, 19 wt. % $CaO$ and 18 wt % $Al_2O_3$. Slags from site 2 have similar silica and lime contents (46 wt. % and 17 wt. % respectively) to these in slags from site 1. However, they also contain important amounts of iron (14 wt % of $Fe_2O_3$) and lower concentrations of alumina (12 wt. % of $Al_2O_3$) compared to the slags from site 1. Slags from both localities contain potassium (up to 6 wt. % of $K_2O$) and magnesia (up to 3 wt. % of $MgO$) as minor components. In terms of metallic element concentrations, both slags contain important amounts of Cu. However, average concentration of Cu in slags from site 1 is approximately 3000 mg $kg^{-1}$, whereas slags from site 2 contain on average 20000 mg $kg^{-1}$ Cu.

Mineral composition of studied slags from both sites is similar. They comprise silicate glass and leucite as major constituents with subordinate pyroxene, wollastonite and plagioclase. Sulfides and intermetallic compounds are common accessory phases in the studied slags. They are represented by: chalcocite, bornite, pyrrhotite, metallic Cu and various non stoichiometric intermetallic compounds of Pb, As, Cu, Fe and Ni. Sulfides and metallic Cu are volumetrically minor components of the studied material, but they constitute the most important Cu carriers. Furthermore, sulfides from studied slags often display clear signs of weathering (e.g., replacements of primary sulfides and metallic Cu by secondary cuprite). Thus, sulfides and metallic phases are considered as the most environmentally important phases in the studied slags.

## CONCLUSIONS

Our study revealed that historical Cu slags located in the vicinity of Leszczyna (North Sudetic Basin) still contain considerable concentrations of some metals (especially Cu) and may constitute a potential source of contamination. Furthermore, differences in chemical composition of studied slags from two sites indicate that they were formed as a result of two different smelting processes. Based on total Cu concentration measured in slags we can hypothesize that smelting process that led to the formation of slag from site 2 was less efficient than the process that produced the slag from site 1.

## REFERENCES

STOLARCZYK, T. (2012): Wyniki badań archeologicznych dawnego górnictwa i hutnictwa miedzi na terenie Pogórza Kaczawskiego i Rudaw Janowickich w 2012 r. *Szkice Legnickie,* **33**, 207-239.

CDS XX (1900): Codex Diplomaticus Silesiae, Band XX: Schlesiens Bergbau und Hüttenwesen. Urkunden und Akten (1136–1528). K. Wutke (hrsg.), Breslau 1900.

CDS XXI (1901): Codex Diplomaticus Silesiae, Band XXI: Schlesiens Bergbau und Hüttenwesen. Urkunden und Akten (1529-1740). K. Wutke (hrsg.), Breslau 1901.

# GEOCHRONOLOGY AIMED PRE-EXAMINATION OF ZIRCON FROM TWO VARISCAN ULTRAPOTASSIC PLUTONIC COMPLEXES

[1]Annamária Kis[#], [1]Tamás G. Weiszburg,
[2]Petr Gadas, [1]Tamás Váczi, [1]György Buda

[1] Department of Mineralogy, Eötvös L. University, Budapest, Hungary, [#]annamari.kis@gmail.com
[2] Department of Geological Sciences, Masaryk University, Brno, Czech Republic

Key words: durbachite, Mórágy, Rastenberg, zircon, morphology and texture of zircon, EPMA, SEM-BSE/CL, Raman spectroscopy

## INTRODUCTION

High-potassic mafic enclaves are widespread within the magnesio-potassic granitoids (local names: durbachite) of the Variscan collision belt in Europe (Massif Central, Vosges, Schwarzwald, Central and South Bohemian Plutonic Complexes (CSBPC)).

From petrographical and geochemical viewpoint, these mafic enclaves correspond to lamprophyre-derived rocks and a late/postmagmatic overprinting effect, connected possibly to the potassium enrichment of three rock-types: mafic enclaves, hybrid rocks and the hosting microcline megacryst-bearing granitoids. The origin (restitic or in situ unmixing) of mafic enclaves in these Variscan granitods has been debated widely, based mainly on geochemical constraints. Comparative age determination could provide independent arguments to that debate, but previous age determination trials left open basic questions, mainly because of the ambiguity caused by the uncontrolled heterogeneity of the zircon crystals studied.

Our zircon samples were separated from two granitoid bodies at the easternmost margin of the Western-Central-European Variscan collision zone. Mórágy, Hungary is the easternmost, tectonically detached continuation of the Moldanubian zone, while Rastenberg, Austria connects directly to the South Bohemian Batholith.

At the moment no local, texture related (core vs. rim; zoning within core and/or rim) LA-ICP-MS zircon age data are available for these two magmatic complexes. Költzli at al. (2004) reported zircon age data, based mainly on evaporation Pb/Pb analyses, where the core and the rim ages of the crystals could not be separated on a controlled way, for the hosting granitoids. For the two other rock types no data is available.

Taken into account the limited size and the typical, frequent, complex zoning of both the Mórágy and the Rastenberg zircon crystals SHRIMP and/or LA-ICP-MS methods may give good U-Pb, Th-Pb age data, provided we can prepare zircon crystals for these measurements careful enough.

## PRE-EXAMINATION OF ZIRCONS

Our methodology consists of four steps for the pre-examination of zircon crystals:

1. determination of morphology-types of zircon (Pupin 1980); 2. determination of internal texture-types (example: zoning) of zircon; 3. determination of the structural state (Nasdala et al. 2006) and chemical composition of zircons zones (Finch and Hanchar 2003); 4. identification of mineral inclusions in zircon. These four types of information are then evaluated together zone by zone in order to define those spots in zircon from where the most undisturbed age data characteristic for the geological processes can be expected. The particular texture features of these spots give the same time the maximum size limits of local probe to be applied.

Zircons of all rock the three types from both localities were processed by that pre-examination methodology. Three major zircon morphology types were distinguished in all samples: normal prismatic ($S_{24}$, $S_{25}$); flat prismatic ($AB_5$) and elongated prismatic ($P_5$). Zircons show both primary (growth/sector zoning $\pm$ xenocryst core) and secondary (convolute) zoning features on SEM-CL and SEM-BSE images. Raman spectroscopy was used for determining the structural state (FWHM) of the individual zircon zones found by SEM-CL/SEM-BSE imaging. Normal and flat zircon crystals show zones of all structural states (well crystallized, intermediate, metamict), while the elongated zircon crystals are not metamict. Chemical composition of the zones was measured by EMPA. The data confirm that SEM-BSE contrast may predominantly depend on structural state of the zircon zones (Nasdala et al. 2009), if strong differences in structural state are present, however if that variation is limited (within $\pm$ 1–2 cm$^{-1}$ FWHM) the SEM-BSE contrast depends mainly on changes in chemical composition (e.g. elevated U, Y, P, REE concentrations).

The studied zircons are rich in both single phase and multiphase mineral inclusions. The latter type, consisting Na free K-feldspar, albite and quartz (found most commonly in elongated zircons),

indicates the lowest crystallization temperature for Si-rich granite melt, confirming that zircon was crystallizing continuously in a wide temperature range during the consolidation of the granitoid magma.

CONCLUSION

Based on these measurements about 190 well characterized, undisturbed measuring areas (varying in diameter between several ten and one micrometer) in 96 crystals have been selected for future SHRIMP and LA-ICP-MS studies. These areas cover all the three expected geological processes and give a potential for determining the 1) age of inherited zircon of crustal origin (xenocrystic core), 2) crystallization age of rock (growth zoning), 3) the age of the overprinting effect (convolute zoning).

REFERENCES

FINCH, J. R., HANCHAR, J. M. (2003): Structure and chemistry of zircon and zircon-group minerals. *In* HANCHAR, J. M., HOSKIN, P. W. O. (Eds.), Zircon. *Rev. Mineral. Geochem,* **53**, 1–25.

KLÖTZLI, U., BUDA, GY., SKIÖLD, T. (2004): Zircon typology, geochronology and whole rock Sr-Nd isotope systematics of the Mecsek Mountain granitoids in the Tisia Terrane (Hungary). *Mineralogy and Petrology*, **81**, 113–134.

NASDALA, L., KRONZ, A., HANCHAR, J. M., TICHOMIROWA, M., DAVIS, D. D., HOFMEISTER, W. (2006): Effects of natural radiation damage on back-scattered electron images of single-crystals of minerals. *Am. Mineral.* **91**, 1738–1746.

NASDALA L., KRONZ A., WIRTH R., VÁCZI T., PÉREZ-SOBA C., WILLNER A., KENNEDY A. K. (2009): The phenomenon of deficient electron microprobe totals in radiation-damaged and altered zircon. *Geochimica et. Cosmochimica Acta,* **73**, 1637–1650.

PUPIN, J. P. (1980): Zircon and granite petrology. *Contrib. Mineral. Petr.* **73**, 207–220.

# GOLD MINERALOGY OF PORPHYRY GOLD DEPOSIT BIELY VRCH (SLOVAKIA)

[1]Jaroslav Kozák[#], [1]Peter Koděra,
[2]Jaroslav Lexa, [3]Martin Chovan, [1]Jana Brčeková

[1]     Department of Geology of Mineral Deposits, Comenius University, [#]kozakminerals@gmail.com
[2]     Geological Institute, Slovak Academy of Sciences
[3]     Department of Mineralogy and Petrology, Comenius University

Key words: porphyry gold, deposit, Biely vrch, alteration, stockwork, mineralization, ore body

## INTRODUCTION

Porphyry gold deposits are a relatively new type of gold deposits characterized by very low Cu:Au ratio. Porphyry gold deposit Biely Vrch is situated in northern part of the Middle Miocene Javorie stratovolcano in eastern part of the Central Slovakia Volcanic Field. It represents new porphyry type of ore mineralization in Slovakia with economic accumulation of gold ore – 42 Mt at 0.8 ppm Au (Hanes et al. 2010).

Parental intrusion at Biely Vrch is affected by hydrothermal alteration of various types. The dominant intermediate argillic (IA) alteration overprints earlier high-temperature K-silicate alteration and deeper Ca-Na silicate alteration. Ledges of advanced argillic alteration represent the youngest alteration stage (Koděra et al. 2010).

Alterations are accompanied by several generations of veinlets. The oldest biotite-magnetite (EB-type), amphibole-pyroxene-apatite and quartz-biotite-magnetite (A-type) veinlets are associated with K- and Ca-Na silicate alteration. Younger quartz veinlets with banded texture (B-type), pyrite (± chalcopyrite, sphalerite, galena, marcasite, molybdenite) veinlets and intermediate argillic veinlets are related to intermediate argillic (IA) alteration. The youngest generations of veinlets are represented by calcite-zeolite and advanced argillic (AA) veinlets (Koděra et al. 2010).

## GOLD MINERALIZATION

Gold grains from the Biely Vrch deposit are characterized by high homogeneity and relatively high fineness. Silver is the only significant element in addition to gold. Observed grains are anhedral with average size 1-10 μm, maximum up to 45 μm. Submicroscopic gold was confirmed by X-ray mapping. Gold in most samples occurs in altered matrix in the presence of quartz stockwork but mostly not directly in veinlets which is the typical feature of porphyry gold deposits in Chile (Muntean and Einaudi 2000). Whole rock analysis of quartz veinlets showed typical grades from 200 to 750 ppb of Au, but no significant differences between A-type and B-type veinlets have been observed.

Gold in high-temperature hydrothermal alterations (K-silicate and Ca-Na silicate)

associates with K-feldspar, basic to intermediate plagioclase, amphibole, biotite and magnetite. Gold fineness is relatively high (945-992). Average gold grades are 0.3 to 2 ppm Au but locally higher. Maximum grade (45.2 ppm Au) was documented in a sample hosting impregnations of gold in basic hydrothermal plagioclase filling a banded quartz veinlet.

The most abundant occurrence of gold is in rocks affected predominantly by intermediate argillic alteration that variably overprints earlier high-T alterations. Here the gold has similar fineness (969-996) and variably associates with illite, I-S, chlorite, epidote (±REE), Fe-Ti oxides and rare sulphides (pyrite, chalcopyrite, Fe-rich sphalerite, galena).

Gold from samples affected by advanced argillic alteration associates with kaolinite, dickite, pyrophyllite, alunite, dumortierite and vuggy silica. Gold has the highest fineness (990-998) which is probably caused by remobilisation by acid hydrothermal fluids. However, in two samples affected both by intermediate and advanced argillic alteration gold showed significantly lower fineness (870-880).

Geochemical GIS modeling shows that distribution of gold in deeper parts of the system (> 500 m) positively correlates with distinct zones of K-silicate alteration within Ca-Na silicate zone of alteration. Au grades are also increased on boundaries of xenoliths affected by intermediate argillic alteration due to some geochemical barrier for Au precipitation from fluids (Hanes et al. 2010).

Most of the early gold has probably precipitated below 380°C, as indicated by low Ti-concentrations of quartz hosting rare gold grains (< 8 ppm Ti, which is detection limit of Ti in Ti-in-quartz geothermometry; Thomas et al. 2010). Microanalyses of fluid inclusions in quartz veinlets show main contribution of gold to the hydrothermal system by Fe-K-Na-Cl salt melt transporting ~ 10 ppm Au and coexisting with hydrous vapor of very low density. The Au/Cu ratio in these inclusions is similar to bulk metal ratio in the Biely Vrch deposit (Koděra et al. 2014). This mineralization process is fundamentally different from Au transport and precipitation in other gold-rich porphyry systems, where gold is typically deposited by expanding dense vapor (Williams-Jones and Heinrich 2005).

REFERENCES

HANES, R., BAKOS, F., FUCHS, P., ŽITŇAN, P. & KONEČNÝ, V. (2010): Exploration results of Au porphyry mineralization in the Javorie stratovolcano. *Miner. Slov.* **42**, 15-32.
KODĚRA, P., LEXA, J., BIROŇ, A. & ŽITŇAN, J. (2010): Gold mineralization and associated alteration zones of the Biely vrch Au-porphyry deposit. *Miner. Slov.* **42**, 33-56.
KODĚRA, P., HEINRICH, CH. A., WÄLLE, M. & LEXA, J. (2014): Magmatic salt melt and vapour: Extreme fluids forming porphyry gold deposits in shallow volcanic settings. *Geology.* **42**, (in press, *doi:10.1130/ G35270.1*)
MUNTEAN, J. L. & EINAUDI, M. T. (2000): Porphyry Gold Deposit of the Refugio District, Maricunga Belt, Northern Chile. *Econ. Geol.* **95**, 1445-1472.
THOMAS, J. B., WATSON, E. B., SPEAR, F. S., SHEMELLA, P. T., NAYAK, S. K. & LANZIROTTI, A. (2010): TitaniQ under pressure: the effect of pressure and temperature on the solubility of Ti in quartz. *Contrib. Mineral Petrol.* **160**, 743-759.
WILLIAM-JONES, A. E. & HEINRICH, C. A (2005): Vapor transport of metals and the formation of magmatic-hydrothermal ore deposits. *Econ. Geol.* **100**, 1287-1312.

# MINERALOGICAL AND CHEMICAL CHARACTERISTIC OF THE MINERAL COATINGS DEVELOPED ON THE STEEL WELL FROM GAS RESERVOIR

[1]Jana Krajčová[#]

[1]      Department of Geological Sciences, Masaryk University, Brno, Czech Republic
[#] j.krajcova@centrum.cz

Key words: mineral crust, steel well, natural gas, extracting natural gas, gas reservoir, mineral coatings

## INTRODUCTION

This presentation is mainly focused on a mineral coatings developed on the steel well from gas reservoir. The coating affects the permeability of the well and caused that gas can not go through the well fluently.



Fig. 1. General view on the steel well

The aim of my study was a steel well (Fig. 1). About 120 cm long well is almost completely covered with crust. The thickness of the crust is around 1 to 5 mm. There are some places where the coating is missing, but it is likely caused by manipulation with the filter. The crust is hard and brittle. The color varies from light brown to rust. It depends on chemical propositions, thickness of the layers or other factors. Some parts of the crust were carefully cut of the well to characterize its composition. To determine the chemical and mineralogical composition of the crust developed on the well electron microscope JEOL, electron microprobe Cameca SX 100 and XRF were used.

## RESULTS

After using EMS to analyze the composition of the crust could be said that the biggest part of the crust (about 75 %) consist of rounded quartz grains (Fig. 2.). These grains come from sand packing of the well. They are originally loosely arranged, and the packing was therefore porous. Four mineral phases were identifying as cement, using EMP studies. Quartz grains and cement forms the incrustation that negatively affects the permeability of the well. Most common cement is calcite, which contains magnesite and siderite components. The second most important cement components are some argillaceous minerals represented

probably by mixture of kaolinite and illite. Some holes are filled by gel–amorphous, strongly hydrated Si-Al phase. It could be formed on expense of primary quartz, which exhibit traces of dissolution along rims. Small barite grains were detected in the cement too.
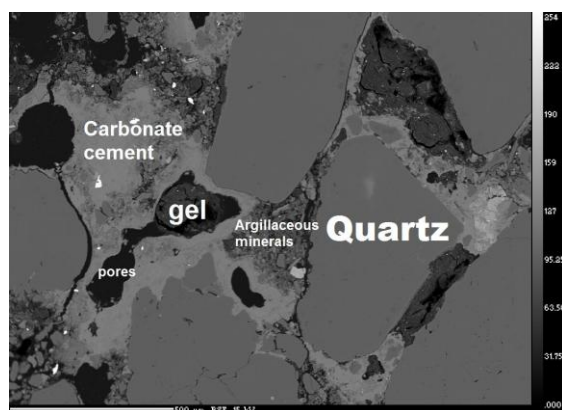


Fig. 2. Quartz grains cemented by carbonate cement and argillaceous minerals.

According to XRF analyze results was found that the coatings on the well are inhomogeneous and the content of particular minerals in different parts of the well varies. Overall, the ten measurements were made, each after every 10 cm of the well. I can allocate two groups of the incrustation with different composition. The first (measurements 5 and 11, Fig. 3.) is rich in K components and has a lower content of Ca, whereas the second group (measurements 4 and 10, Fig. 3.) is rich in Ca component and having a smaller contain of K.

| MEASURING | S | CL | K | CA |
|---|---|---|---|---|
| #4 | 18590 | 622 | 40890 | 67592 |
| #5 | 14539 | 1558 | 74106 | 56094 |
| #10 | 4368 | 387 | 33756 | 98974 |
| #11 | 37086 | 2620 | 150502 | 64837 |

Fig. 3. XRF analyze

If we compare the mineral composition described above with the XRF results, we can suppose that the Ca rich domains are enriched on calcite, whereas illite will be probably more wide-spread in the K rich parts of the crust.

RESUME

Quartz grains have origin in the sand packing. The cement was possibly derived from surrounding rocks via reaction of flushing fluids with these country rocks. This is valid especially for calcite and gel. Clay minerals could be of clastic origin as well. Barite could be a primary constituent of flushing fluids, and could be mechanically trapped in the sand packing. To explain origin of the crust in detail, additional data about surrounding rocks, nature of the fluids circulating in the rocks as well as the composition of the flushing are needed. The mineralogical study of the coating should help to eliminate its growing.

# ASSESSING THE GOLD ASSOCIATION OF HODRUŠA MINE ORE CONCENTRATE AND TAILINGS BY THE MEANS OF AUTOMATED MINERALOGICAL ANALYSIS

[1]Veronika Králová[#], [2]Marek Dosbaba

[1]     TESCAN Brno s. r. o., [#]veronika.kralova@tescan.cz
[2]     TESCAN ORSAY HOLDING, a.s.

Key words: automated mineralogy, ore characterization, gold ore, concentrates, processing efficiency, electron microscopy

## INTRODUCTION

Scanning electron microscope is a powerful tool for detailed understanding of mineralogical samples. In comparison with traditional optical methods, which are often laborious and time consuming, using a scanning electron microscope equipped with various types of detectors can speed up processing of the samples and help to simplify mineral species identification. Automated mineralogy analyzers enable to acquire and process mineralogical data automatically.

TESCAN Integrated Mineral Analyzer (TIMA) is based on a scanning electron microscope, equipped with backscattered electron detector (BSE) and silicon drift energy-dispersive X-ray detectors (EDX). Also other detectors, like a secondary electron detector (SE) or a cathodoluminescence detector (CL) can be used to acquire additional information about samples. BSE and EDX data, acquired from a sample, are combined and processed automatically in several data processing modules to measure mineral abundance, mineral liberation and association, particle and grain sizes, or bright particles.

The capabilities of this device will be explained on Hodruša gold mine concentrates.

## HODRUŠA GOLD DEPOSITE

The Hodruša gold mine (Baňa Rozália) is currently the only producer of gold in central Europe. It is situated in central Slovakia in Štiavnické Mountains. The gold deposit was formed as a result of extensive hydrothermal activity during the late stage of Štiavnica stratovolcano evolution in Miocene. The deposit is hosted by andesites and its porphyries (Chernyshev et al. 2013).

The mine originally produced copper ores from the Rosalia vein. The new era begun in 1991 after the new Svetozár vein system (NWN-SES striking and SW dipping) had been found on the XIV level. The gold mineralization is a result polyphase process. The oldest stage is represented by mesothermal gold – carbonate – quartz association, which was followed by several stages of epithermal

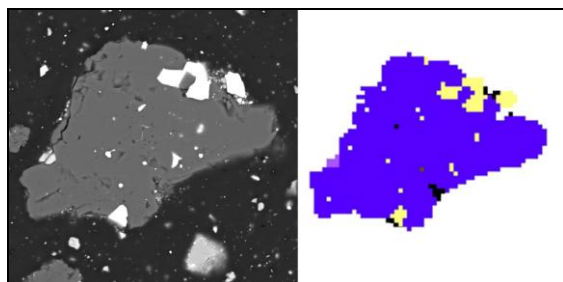gold – base metal association (Maťo et al. 1994).



Fig. 1. BSE image (left) and phase map (right) of single gold containing particle (gold – yellow, quartz – blue, sphalerite – violet). View filed is 170 μm.

METHODS & RESULTS

Two types of samples were provided by the company operating the Rozália mine – the concentrate and the tailings from the processing. The size of the particles in both types of samples ranged from 1 μm to 400 μm (P80 =18 μm). The powdered samples were then mounted into 30 mm epoxy resin blocks and coated with 10 nm of carbon.

TESCAN Integrated Mineral Analyser (TIMA) was used to acquire BSE and EDS data the under following conditions 25 kV and 5 nA. Pixel spacing was set to 3 μm. The tailing was scanned using bright phase search (BPS) mode whereas the concentrate was scanned using liberation analysis (LA). Both modules are capable of providing information on gold association but the BPS leaves out areas of low backscattered electron signal level (silicates, common sulphides etc.) in order to focus only on particles containing very bright phases.

The gold occurs extremely scarcely in waste. It was found only in one particle. It was locked in quartz, which prevented it from being separated during ore beneficiation.

The gold content in concentrate reaches up to 0.02 %, which corresponds well with the data from fire assay. Approximately 40

% of all gold grains are completely liberated.

The gold is most commonly associated with quartz (see Fig. 1) and calcite regarding the gangues minerals. Association with secondary iron oxide is common as well. The iron oxide probably formed on the expense of primary pyrite during ore processing. Other sulphides lock gold in following order sphalerite, chalcopyrite, pyrite and galena.

The automated mineralogical analysis is capable of providing results similar to the traditional approach but it allows faster evaluation of larger samples. Its results are more reliable from the statistical point of view and so it complements the traditional approach very well. Automated analysis can provide information on liberation degree in addition. Such task would be hardly achievable by traditional means.

REFERENCES

CHERNYSHEV, I.V., KONEČNÝ, V.LEXA, J., KOVALENKER, K.V., JELEŇ, S., LEBEDEV, V. A.& GOLTSMAN, Y. V. (2013): K-Ar and Rb-Sr geochronology and evolution of the Štiavnica Stratovolcano (Central Slovakia). *Geologica Carpathica*. **64**, 4, 327-360.

MAŤO, Ľ., SASVÁRI, T., BEBEJ, J., KRAUS, I., SCHMIDT, R. & KALINAJ, M. (1996): Štruktúrne kontrolovaná žilná mezotermálna zlato-kremeňová a epitermálna drahokovovo-polymetalická mineralizácia v hodrušskom rudnom poli, stredoslovenské neovulkanity. *Mineral. Slov.* **28**, 6, 455-490.

# CLINOPTILOLITE TUFF AT RACOŞ AND MATEIAŞ
## (PERŞANI MTS, CENTRAL ROMANIA)

[1]Ferenc Kristály [#], [2]Szabolcs Orbán,
[3]Alpár Kovács

[1]      Institute of Mineralogy and Geology, University of Miskolc, [#]askkf@uni-miskolc.hu
[2]      Faculty of Bilogy and Geology, Institute of Geology, Babeş–Bolyai University, Cluj-Napoca
[3]      S.C. GeoAnalyst S.R.L., Ojdula

## INTRODUCTION

The villages of Racoş and Mateiaş are located in the south-eastern corner of the Transylvanian basin. The geology of the region is characterized by the presence of large zeolite bearing volcanic tuffs and tuffaceous formations. The thickness of layered outcrops varies between several meters up to several tens of meters. Material belonging to the most extensively zeolitized parts is readily identified due to the characteristic pistachio green color. These tuffs are also known as Perşani-tuffs, and they belong to the Dej Tuff Formation. This formation is widespread in the Transylvanian basin and resulted from the resedimentation of rhyolitic tuffs (Szakács 2014). Significant outcrops were investigated from Maramureş-basin (Cochemé et al. 2003), and central part of Transylvanian basin (Seghedi et al. 2000) also. The main zeolite was identified as clinoptilolite, with mixed cation content, but mordenite was also observed (Seghedi et al. 2000). Our aim is to give a mineralogical and chemical characterization of these tuffs from Racoş and Mateiaş area, as a first step towards assigning an economical importance.

## MATERIALS AND METHODS

In the outcrops the material has a laminated–bedded structure, with minor variation in color and variable biotite content. Samples from the material collected from two larger outcrops, a former open-pit exploitation and a natural outcrop. They were prepared for X-ray powder diffraction (XRD), thermal analysis (TG-DTG-DTA), X-ray fluorescence spectrometry (XRF), optical microscopy (OM) in thin section and scanning electron microscopy with energy dispersive X-ray spectrometry (SEM+EDS).

## RESULTS

Grain size of investigated zeolite tuffs is generally < 1 mm, minor fluctuations are observed between the laminar segments. XRD quantitative mineralogy was obtained by Rietveld-refinement. It revealed the presence of clinoptilolite as dominant rock forming mineral, with 68 to 72 wt. %.

Cristobalite, in tetragonal form, is characteristic with 12-20 wt. %. Minor quartz (2-5 wt. %), plagioclase (2-5 wt. %), K-feldspar (~ 1 wt. %) and biotite (~ 1 wt. %) was detected. The presence of titanomagnetite and ulvöspinel was considered possible based on several matching peaks. The appearance of weak ~ 4.5 Å and ~ 3.5 Å peaks indicates the presence of clay minerals in traces. XRF results supported the XRD mineralogy, loss on ignition (~ 10 % et) covering the clinoptilolite water content. The main alkaline cation is K (~ 3 wt. % as $K_2O$), while Na (~ 3 wt. % as $Na_2O$) and Ca (~ 3 wt. % as CaO) are lower. Among trace elements, Ba (600-900 ppm), Sr (350-450 ppm) and Rb (100-110 ppm) show higher concentrations, probably related to the rhyolitic origin. Mn, Ti and P contents are in the minor elements range, also.

OM evidenced zeolitization of glass fragments and matrix also. Plagioclase and quartz grains are observed as hipidiomorphic, while biotite rarely has pseudoheaxagonal, idiomorphic lamellas. Peculiarity of zeolitization is the frequent replacement of glass shards by clinoptilolite crystals with the preservation of shard morphology. The ratio of replaced shard grains and other elements suggests an original high glass ratio tuff. SEM+EDS measurements showed that clinptilolite is mixed cation series, mostly with K and Ca as dominant cation. The Ca and Na ration displays some fluctuation between the different parts of thick tuff beds. Plagioclase has an intermediary composition, and appears more abundant than K-feldspar. Grain size distribution, based on BSE images, is made up by biotite: (1) plagioclase and quartz in the 0.1-1 mm range, (2) zeolitized shards, ulsvöspinel and pore filling clynoptilolite in the 0.01-0.1 mm range and (3) zeolitized matrix and clay minerals in the < 0.01 mm range. The biotites are high annite members, with considerable $TiO_2$ (~ 3 wt. %) content.

## RESULTS

A strong zeolitization transformed a high K-content acidic tuff into the clinoptilolite tuff. If results are interpreted according to Szakács (2014), the remobilized material was a rhyolite tuff with dacitic contributions. Cristobalite could be formed partly during zeolitization, from excess silica, but also may represent primary phase. However, it is not present as reactive silica. The minor element content is limited and abundances are low, not posing toxicity risks. Ba is linked to barite, observed by SEM+EDS. The green color is caused by the minor nanocrystalline clay minerals (Fig. 1.), possibly an illite-glauconite mixture.
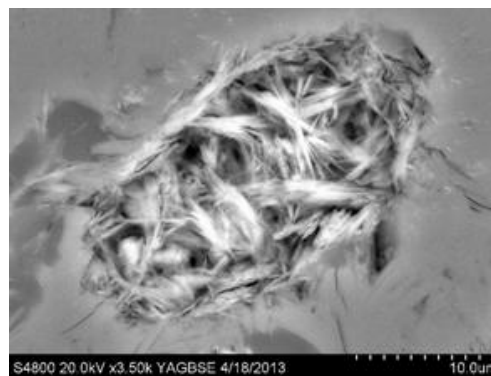


Fig. 1. Clay mineral aggregates of fibrous nanocrystals.

## REFERENCES

SEGHEDI, I., SZAKÁCS, A., VANGHELIE, I. & COSTEA, C. (2000): Zeolite formation in the lower Miocene tuffs, North-Western Transylvania, *Romania. Rom. J. Mineralogy*, **80,** 11-20.

COCHEMÉ, J. J., LEGGO, P. J., DAMIAN, G., FULOP, A, LEDESERT, B. & GRAUBY, O. (2003): The mineralogy and distribution of zeolitic tuffs in the Maramureş basin, Romania. *Clays and Clay Minerals*, **51/6,** 599-608.

SZAKÁCS, A. (2014): Magma of the Dej tuff: composition, nature and origin. BKF conference proceedings, Cluj Napoca, 238-242.

# THE KOJETICE COTICULES: AN IMPORTANT GEOLOGICAL AND AGE MARKER WITHIN THE MOLDANUBIAN ZONE?

[1]Lukáš Krmíček[#], [2]Rolf L. Romer,
[3]Uwe Kroner, [4]Milan Novák, [4]Radek Škoda

[1]     Institute of Geology, v.v.i., Academy of Sciences of the Czech Republic, Rozvojová 269, CZ-165 00 Praha 6, Czech Republic, [#]l.krmicek@gmail.com
[2]     Deutsches GeoForschungsZentrum GFZ, Telegrafenberg, D-14473 Potsdam, Germany
[3]     TU Bergakademie Freiberg, Department of Geology, B. v. Cotta Str. 2, D-09596 Freiberg, Germany.
[4]     Department of Geological Sciences, Masaryk University, Kotlářská 2, CZ-611 37 Brno, Czech Republic

## INTRODUCTION

The name *coticule* was first used for spessartine-bearing quartzites (Renard 1878) that represent metamorphosed fine-grained Mn-rich sedimentary rocks. Based on metamorphic conditions and the composition of the siliciclastic sedimentary protolith, coticules contain different Mn-minerals such as carpholite, hausmannite, or Mn-versuvianite. Although the Mn-rich sediments of the type locality were deposited on the continental shelf, the term *coticule* also was incorrectly applied to metamorphosed Mn-rich deep marine deposits and even exhalites.

Within Variscan Europe and Acadian North America, coticules *sensu* Renard (1878) occur in sedimentary units deposited on the continental shelf and typically are of Ordovician age (Romer et al. 2011). Most importantly, they seem to be restricted to the Avalonian shelf.

The provenance of the meta-sedimentary rocks of the Monotonous (Ostrong) and Variegated (Drosendorf) units of the Moldanubian Zone is not well-constrained. There are, however, rare occurrences of Mn-rich sedimentary rocks. We investigate whether these rocks show the geochemical and isotopic features of coticules from the Avalonian shelf, e.g., those from Nova Scotia (Canada) and the Ardennes (Belgium), which would provide a provenance proxi, and whether they also have an early Palaeozoic age.

## CONSTRAINTS FOR COTICULE FORMATION

Mn-rich sediments form when redox-controlled dissolution and precipitation of Mn (and Fe) keeps pace with siliciclastic input, i.e., in sediment-starved settings. Early Palaeozoic coticules on Avalonia formed when sediment input from Avalonia was drastically reduced and the subordinate sediment component derived from Gondwana became chemically and isotopically distinct in the coticule-bearing layers, most prominently by negative $\varepsilon Nd_t$-values, elevated $^{87}Sr/^{86}Sr$, and the REE-pattern.

## Mn-association in Kojetice near Třebíč and comparison with "Avalonian" coticules

The Kojetice locality is situated in the Variegated Unit of Moldanubian Zone, about 4 km W of the Třebíč Massif. Dominant biotite–sillimanite gneisses contain common intercalations of graphite quartzites, calcite/dolomite marbles and orthogneiss. Rare fragments of Mn-rich metasedimentary rocks (spessartine, braunite, rhodonite > Mn-andalusite, tephroite, pyrophanite) occur in a field ~1 km S of Kojetice village. The investigated sample consists of dark-colored braunite-rich sections in a spessartine-quartzite matrix with Mn-rich andalusite to kanonaite (Novák and Škoda 2007).

The Mn-rich metasediments from Kojetice show the same REE pattern as coticules from the Ardennes and Nova Scotia and recent Mn-rich sediments (Fig. 1). They show different pattern and contents than deepwater and hydrothermal Mn-deposits. In addition they have very low $\varepsilon Nd_{450}$ values (-10 to -12), which is distinctly lower than for coeval normal Avalonia sedimentary rocks. The initial Sr isotopic composition falls in the range of 0.7163 to 0.7170, which is more radiogenic than typically encountered for Avalonia crust. The Kojetice coticules differ from Avalonian coticules by their high Ba content, which, however, is known from some modern settings.

### IMPLICATIONS

The Sr isotope data of the Kojetice coticules fall in isochron diagram on a reference line that corresponds an age of c. 450 Ma, which indicates that the Rb-Sr system has not been disturbed strongly during Variscan HT/LP metamorphism (c. 540–750 °C at ~ 2–4 kbar) and therefore the chemical composition of the rocks rather closely reflect the original signature.
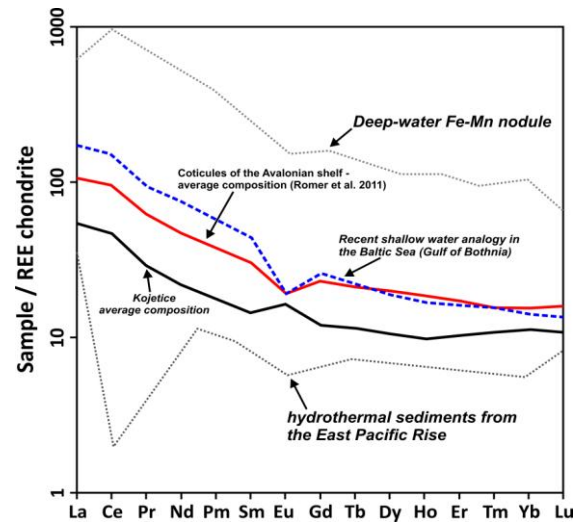


Fig. 1. Rare Earth Element (REE) pattern for Mn-rich sedimentary rocks deposited in different environments.

The REE pattern and contents, as well as the $\varepsilon Nd_t$ values that are characteristic for Gondwana-derived sediments indicate that the Kojetice coticules have a similar genesis as other Avalonian coticules and, thus, that the sedimentary rocks of the Variegated unit may have been deposited on Avalonia basement. Furthermore, at the time these Mn-rich sediments were deposited, Avalonia and Gondwana were not yet separated by a wide ocean.

### REFERENCES

Novák, M. & Škoda, R. (2007): Mn$^{3+}$-rich andalusite to kanonaite and their breakdown products from meta-manganolite at Kojetice near Třebíč, the Moldanubian Zone, Czech Republic. *J. Geosci.* **52**, 161-167.

Renard, A. (1878): Sur la structure et la composition minéralogique du coticule et sur ses rapportes avec le phyllade oligistifière. *Mém. Cour. Acad. R. Belge,* **41**, 1-42.

Romer, R.L., Kirsch, M., & Kroner, U. (2011): Geochemical signature of Ordovician Mn-rich sedimentary rocks on the Avalonian shelf. *Can. J. Earth Sci.* **48**, 703-718.

# TRACE-ELEMENT PARTITIONING IN A CALC – ALKALINE LAMPROPHYRIC SYSTEM

[1]Lukáš Krmíček[#], [1]Michaela Halavínová,
[1]Michael Tupý

[1]     Faculty of Civil Engineering, Brno University of Technology, Veveří 331/95, CZ-602 00 Brno, Czech Republic, [#]l.krmicek@gmail.com

Key words: Calc-alkaline lamprophyres, mineralogy, partition coefficients, Bohemian Massif

### INTRODUCTION

Knowledge of element partitioning between minerals and melts is crucial for geochemical modeling of magmatic systems. Element partitioning strongly depends, apart from pressure and temperature, also on the type of melt and changes with a higher degree of melt fractionation, i.e. lower MgO and higher $SiO_2$ contents (Fig. 1).

In fact, trace-element partitioning between mafic minerals and mantle-derived melt of lamprophyric composition has been discussed only in two papers. Foley et al. (1996) determined trace-element partition coefficients ($D$) for clinopyroxene and phlogopite in an alkaline dyke from Budgell Harbour in north-central Newfoundland using LA-ICP-MS. This moderately evolved dyke with Mg-number [mg# = molar $100 \times MgO/(MgO + FeO_t)$] of 60 was classified as monchiquite. In addition, Plá Cid et al. (2005) applied SIMS to determine trace-elements partitioning between clino-pyroxene and mica from mafic enclaves containing K-clinopyroxene and pyrope-rich garnet in the Piquiri Syenite Massif, southernmost Brazil. These variably evolved very high-pressure (3–5 GPa) mafic enclaves of intermediate com-position (mg# = 62–66) supposedly resemble calc-alkaline lamprophyres, but have a high agpaitic/peralkalinity index [molar $(K_2O + Na_2O)/Al_2O_3$] of 0.98–1.03 that makes them to straddle the boundary between alkaline and peralkaline rocks.
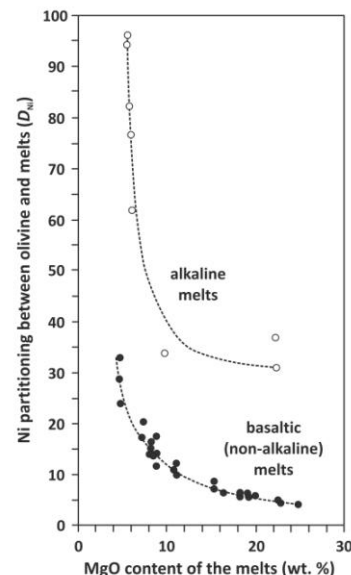


Fig. 1. Dependence of Ni partitioning between olivine and different types of melt with variable content of MgO. Partition coefficients $D_{Ni}$ significantly increase along with decrease of MgO content.

Olivine growing in alkaline environment shows $D_{Ni}$ 5–6 times higher (adopted from Foley et al. 2013).

The aim of our contribution is to present new data (for more detailed view see Krmíček et al. 2014) on the phlogopite/matrix, clinopyroxene/matrix, and clinopyroxene/phlogopite trace-element partitioning in a real calc-alkaline lamprophyric system with mg# close to a value of mantle-derived melts. The investigation was performed on a Variscan calc-alkaline (agpaitic index = 0.6) lamprophyre dyke of minette composition from the Bohemian Massif (Křižanovice, Teplá–Barrandian Unit). The studied Křižanovice lamprophyre is little affected by fractionation (mg# = 69) and contains compo-sitionally homogenous phenocrysts of mafic mica and clinopyroxene showing textures of coeval crystallization and – along chilled dyke margins – surrounded by aphanitic matrix.

## RESULTS

The partition coefficients between clinopyroxene and matrix were determined for 23 elements by laser ablation-inductively coupled plasma-mass spectrometry. Calculated $^{clinopyroxene/matrix}D$ values are very low, except for heavy rare earth elements (HREE) that range between 0.9 and 1.1. This suggests that **HREE can be concentrated in clinopyroxene during crystallization from lamprophyre melt.**

In phlogopite, only 15 elements had contents above their respective detection limits. Phlogopite/matrix partition coefficients are on average higher than 1 ($D_{Ba} = 1.1$, $D_{Rb} = 1.7$ $D_{Ti} = 1.5$) and extremely low ($\leq 0.02$) for light rare earth elements (LREE). On the other hand, $^{phlogopite/matrix}D$ values for the majority of HREE could not be determined.

Taken together, during simultaneous crystallization of clinopyroxene and phlogopite phenocrysts, Th, Zr, Hf, Y and LREE are preferentially partitioned into clinopyroxene and Ba with Rb and Ti into phlogopite. The contrasting fractionation behaviour of the two trace-element groups (Th, Zr, Hf and LREE vs. Ba, Rb, Ta and Ti) into clinopyroxene and phlogopite, respectively, will result in different trace-element signatures depending on the fractionation history of the rock. The two element groups will uncouple from each other if clinopyroxene *or* phlogopite crystallizes and will behave coherently if clinopyroxene *and* phlogopite crystallize.

## REFERENCES

FOLEY, S.F., JACKSON, S.E., FRYER, B.J., GREENOUGH, J.D. & JENNER, G.A. (1996): Trace element partition coefficients for clinopyroxene and phlogopite in an alkaline lamprophyre from Newfoundland by LAM-ICP-MS. *Geochimica et Cosmochimica Acta,* **60**, 629-638.

FOLEY, S.F., PRELEVIĆ, D., REHFELDT, T. & JACOB, D. (2013): Minor and trace elements in olivine as probes into early igneous and mantle melting processes. *Earth Planet. Sci. Lett.* **363**, 181-191.

KRMÍČEK, L., HALAVÍNOVÁ, M., ROMER, R.L., VAŠINOVÁ GALIOVÁ, M. & VACULOVIČ, T (2014): Phlogopite/matrix, clinopyroxene/matrix and clinopyroxene /phlogopite trace-element partitioning in a calc-alkaline lamprophyre: new constrains from the Křižanovice minette dyke (Bohemian Massif). *J. Geosci.* **59**, 87-96.

PLÁ CID, J., NARDI, L.V.S., ENRIQUE, P., MERLET, C. & BOYER, B. (2005): SIMS analyses on trace and rare earth elements in coexisting clinopyroxene and mica from minette mafic enclaves in potassic syenites crystallized under high pressures. *Contrib. Mineral. Petrol.* **148**, 675-688.

# MINERALOGY OF SOME METACARBONATE ROCKS FROM BURNED COAL-MINING DUMP IN PRZYGÓRZE (LOWER SILESIAN COAL BASIN) AND ITS ANALOGY TO "OLIVE" ROCKS FROM THE HATRURIM FORMATION

[1]Łukasz Kruszewski[#], [2]Justyna Ciesielczuk,
[2]Magdalena Misz-Kennan

[1]    Institute of Geological Sciences, Polish Academy of Sciences, Twarda 51/55, 00-818 Warszawa, Poland, [#]lkruszewski@twarda.pan.pl
[2]    University of Silesia, Faculty of Earth Sciences, Będzińska 60, 41-200 Sosnowiec, Poland

## INTRODUCTION

Thermal activity in an old coal-mining dump in Przygórze near Nowa Ruda has lead to the formation of vast complex of various pyrometamorphic rocks. The most common rocks are red, yellow and white metapelites (clinkers, "porcellanites"). Buchites and parabasalts are relatively rare. Metacarbonate formations are usually found as thin, powdery, yellowish or white covers on other rocks, and rarely as thin indistinct veins (Kruszewski et al. 2012).

However, huge white blocks rich in calcite, portlandite, thaumasite and/or ettringite, probably hydrocalumite-, fluorapophyllite- and rustumite-bearing also occur. Cellular, wood-like, yellowish-brown to greenish-brown, rounded metacarbonate rocks rich in clinopyroxene, melilite, calcite, leucite, and anorthite, were found within these blocks and also as loose fragments. The aim of our work was to investigate more deeply mineralogy and chemistry of them.

## MINERALOGY AND CRYSTAL CHEMISTRY

Typically for metacarbonate pyrometamorphic rocks, clinopyroxene is esseneite-rich, as described by its formula: $(Ca_{1.01}Na_{0.01})_{\Sigma 1.02}(Fe^{3+}_{0.66}Mg_{0.26}Ti_{0.11})_{\Sigma 1.03}(Si_{1.17}Al_{0.78})_{\Sigma 1.95}O_{5.93}$. Beside diopside, also hypothetical end-members like $CaFe^{3+}TiAlO_6$ and $CaMgTi_2O_6$ may take part in its build. Melilite is rich in gehlenite, åkermanite, ferrigehlenite and alumoåkermanite molecules, as suggested by the formula ($n$=30): $(Ca_{1.80}Na_{0.21}K_{0.01})_{\Sigma 2.03}(Al_{0.54}Mg_{0.28}Fe^{3+}_{0.18})_{\Sigma 1.00}(Si_{1.52}Al_{0.49})_{\Sigma 2.01}O_{7.06}$ with traces of Sr. Two types of leucite are present (1) $(K_{0.96}Na_{0.02}Ca_{0.01})_{\Sigma 1.00}(Al_{0.97}Fe^{3+}_{0.02}Fe_{0.02})_{\Sigma 1.01}Si_{\Sigma 2.00}O_{5.98}$ with traces of Ba, and (2) $(K_{0.83}Fe_{0.03}Na_{0.02}Mg_{0.02}Ca_{0.01}[]_{0.09})_{\Sigma 1.00}Al_{1.00}(Si_{\Sigma 1.68}Al_{0.42})_{\Sigma 2.10}O_{5.94}$ without Ba. A phase compositionally fitting to melilite is also found. Its enrichment in Ga and Sb is possible, though not yet confirmed. Leucite associates with "K-petalite", $(K_{0.73}Na_{0.21}Ca_{0.13})_{\Sigma 1.06}(Al_{0.54}Si_{0.28}Mg_{0.06}Fe^{3+}_{0.03}Fe_{0.02})_{\Sigma 0.93}Si_{4.00}O_{10.06}$ ($n$=5), and

$K_2Al_4Si_4O_{15}$ phase, $(K_{1.49}Na_{0.51})_{\Sigma2.00}(Al_{3.75}Mg_{0.08}Ca_{0.08}Fe^{2+}_{0.05}Ti_{0.04})_{\Sigma4.00}Si_{4.05}O_{15.01}$. Other alkali-rich minerals include Fe-bearing slightly barian K-feldspar, kalsilite/kaliophilite, albite and probably $(Na,Ca,K,Mg)_3(Si,Al,Fe)_7O_{14}$ phase. Mean formula of albite ($n=10$) is $(Na_{0.95}K_{0.04}Ca_{0.01}Fe_{0.01})_{\Sigma1.01}Al_{0.99}Si_{2.99}O_{7.99}$. Garnet (or garnet-like species) of one sample has the formula ($n=10$) $(Ca_{2.97}Mg_{0.03}K_{0.01})_{\Sigma3.01}(Fe^{3+}_{1.36}Al_{0.38}Mg_{0.13}Ti_{0.13})_{\Sigma2.00}(Si_{2.12}Ti_{0.87})_{\Sigma2.99}O_{11.97}$. It may represent a highly substituted andradite or its $Si_2Ti$-analogue. Mean composition of srebrodolskite-brownmillerite solid solution may be given as ($n=6$): $(Ca_{2.00}Mg_{0.02})_{\Sigma2.02}(Fe_{1.71}Al_{0.20}Mn^{3+}_{0.03}Si_{0.03}Ti_{0.02}[]_{0.02})_{\Sigma2.02}O_{5.01}$. Spinel-group or spinel-like species of one sample have mean composition of $(Fe^{3+}_{1.96}Al_{0.08}Si_{0.05})_{\Sigma2.09}(Mg_{0.64}Ca_{0.30}Mn_{0.03}[]_{0.03})_{\Sigma1.00}O_{4.05}$. The other sample contains spinel-like phase of mean ($n=4$) composition being $(Mg_{0.97}Ca_{0.09})_{\Sigma1.05}(Fe_{1.77}Ti_{0.11}Mn_{0.06}Si_{0.01})_{\Sigma1.95}Ti_{3.00}O_{10.00}$, ideally $MgFe_2Ti_3O_{10}$. Cuspidine ($n=12$) $Ca_{4.07}(Si_{2.00}O_7)F_{1.41}$ occasionally with very minor Mg, Ti and Al. Fluorapatite ($n=7$), with the formula $(Ca_{4.99}Sr_{0.01}Na_{0.01})_{\Sigma5.01}(PO_4)_{2.96}F_{0.97}$, is Si-, S-, As- and V-free. Perovskite of one of the samples analyzed ($n=3$) has formula $(Ca_{0.98}Mg_{0.02})_{\Sigma1.00}(Ti_{0.95}Si_{0.02}Fe^{2+}_{0.02}Al_{0.01})_{\Sigma1.00}O_{2.98}$ with trace but constant admixture of V, Nb and Zr. The other sample contains Ti-low perovskite, and may likely be referred to perovskite-(pseudo/para)wollastonite-ilmenite-ferrosilite solid solution, with the mean ($n=4$) formula $(Ca_{0.87}Fe^{2+}_{0.11}Mg_{0.02})_{\Sigma1.00}(Ti_{0.61}Si_{0.26}Al_{0.07}Fe^{3+}_{0.06})_{\Sigma1.00}O_{2.98}$.

## CONCLUSIONS

The metacarbonate rocks from Przygórze dump are somewhat analogous to the rocks from "olive" unit of the pyrometamorphic Hatrurim Formation, Israel (Vapnik et al. 2007). They include anorthite-diopside hornfels, while the typical "olive" rocks contain diopside-hedenbergite-esseneite, anorthite, calcite, zeolites, and minor apatite. These last rocks are supposed to be a product of hydrothermal reworking of a former hornfels. Hydrothermal activity in the Przygórze dump is manifested, e.g., in the presence of carbonate- and fluorite-bearing veins.

The Przygórze metacarbonate rocks differ from their Upper-Silesian counterparts in their high content of alkaline-rich minerals. Also, their apatite-group species characterize in absolute lack of Si and S, and only occasional and minor enrichment in Mg and Fe. Instead, they contain minor Na. Fluorine content nearly fulfilling the balance of the $X$ site is suggestible for the lack of $CO_3^{2-}+F^-$ coupled substitution at the $T$ site (in accordance to Fleet and Liu 2008).

## REFERENCES

FLEET, M. E. AND LIU, X. (2008): Accomodation of the carbonate ion in fluorapatite synthesized at high pressure. *Am. Mineral.* **93**, 1460-1469.

KRUSZEWSKI, Ł., CIESIELCZUK, J. AND MISZ-KENNAN, M. (2012): What have meteorites to do with coal fires? A case of Upper and Lower Silesian Coal Basins *Min. Spec. Pap.* **40**, 28-29.

VAPNIK, Y., SHARYGIN V. V., SOKOL E. V., SHAGAM, R. (2007): Paralavas in a combustion metamorphic complex: Hatrurim Basin, Israel, in: Stracher, G.B. (Ed.), Geology of Coal Fires: Case Studies from Around the World. The Geological Society of America, Reviews in Engineering Geology, vol. **XVIII**, 133-154.

# GOLD IN THE ROZÁLIA MINE AU DEPOSIT
## (HODRUŠA – HÁMRE, SLOVAKIA)

[1]Alexander Kubač[#], [2]Martin Chovan,
[1]Peter Koděra, [3]Jaroslav Lexa, [4]Peter Žitňan

[1]    Department of Geology of Mineral Deposits, Comenius University, Mlynská dolina G, 842 15 Bratislava, Slovakia, [#] alexander.kubac@gmail.com
[2]    Department of Mineralogy and Petrology, Comenius University, Mlynská dolina G, 842 15 Bratislava, Slovakia
[3]    Geological Institute, Slovak Academy of Sciences, Dúbravská cesta 9, 840 05 Bratislava, Slovakia
[4]    Slovenská banská, Ltd., Hodruša-Hámre, Slovakia

## INTRODUCTION

Epithermal Au-Ag mineralization occurs within the Hodruša-Štiavnica ore discrict in the central zone of the Štiavnica stratovolcano. It occurs as subhorizontal vein system of intermediate-sulfidation type at the base of pre-caldera andesite, close to the roof of a subvolcanic granodiorite intrusion. The veins are dismembered by younger quartz-diorite porphyry sills and displaced by steeply dipping base-metal veins and parallel structures, which are related to resurgent horst uplift in the caldera center (Koděra et al. 2005). Since 1992, the mineralization is exploited by Slovenská Banská, s.r.o. with total production about 5 tons of gold and a similar amount of gold is estimated in remaining resources. Average ore grade varies between 7 and 10 g/t Au. The combined Pb+Zn+Cu content is up to 0.3-0.5 wt.% and the Ag/Au ratio varies from 1:2 to 10:1 (Šály et al. 2008).

The mineralogy and mineral chemistry of the western part of deposit have been studied in detail by Maťo et al. (1996), who distinguished three stages of mineralization − mesothermal, early epithermal and late epithermal. Similar paragenetic chart created Šály et al. (2008) for eastern part of the deposit based on study of exploration drill hole samples.

## ORE TEXTURES

According to our detailed study of ore textures and mineral associations three evolution stages of mineralization were defined for eastern part of the deposit.

The first stage involves the formation of silicites (Qtz I) with massive and breccia texture. Silicite veins are barren and typically occur on the base of the second stage veins.

The second stage produced the principal gold ore within the deposit. This stage typically contains Mn-minerals (rhodonite, rhodochrosite, Mn-calcite). In breccia-cockade textures Mn-minerals with clinochlore cover altered rock fragments. Fragments are also covered by later thin layers of calcite and grey-colored quartz II, which are accompanied by galena,

sphalerite, chalcopyrite, pyrite, Au- and Ag-tellurides hessite and petzite. Quartz II is also often accompanied by carbonates of variable Mg-Ca-Fe composition (including dolomite, ankerite, calcite, siderite), illite, chlorite and K-feldspar. The milky quartz III with adularia crystalized to free spaces within breccia-cockade textures. In banded veins, galena, sphalerite, gold and tellurides crystallized dominantly on margins of veins. Quartz III occurs here in the central zone of veins. Banded veins are crosscut by veins of milky quartz IV that include thin veinlets with gold, galena, sphalerite and chalcopyrite. The third stage is represented by thin calcite veins and later quartz veins (quartz V), which both occur in andesite and quartz-porphyry sills.

## GOLD

Gold typically occurs with hessite and petzite in four different mineral assemblages, all formed during the stage 2.

The first assemblage is characterized by the presence of gold in the form of disseminated grains (< 20 µm) in quartz II, rhodonite, rhodochrosite and Mn-calcite or in aggregates with major sulphides – galena, sphalerite and chalcopyrite. Grain size of gold ranges from few µms to visible agregates (< 0.5 mm). Gold shows a strong affinity to galena. In high-grade ore, small gold inclusions (< 5 µm) were found in pyrite. The second assemblage is similar to the first one but Mn-minerals are replaced by Mg-Ca-Fe carbonates, adularia and illite.Gold in the third mineral assemblage typically creates aggregates with galena and sphalerite on the edges of banded veins. Middle part of the veins is filled by milky Qtz III with adularia.

Probably the youngest generation of gold occurs in a few millimeters thick veinlets with galena, sphalerite and chalcopyrite hosted by quartz IV.

Microprobe analyses of gold (57 analyses) show increased concentration of Ag from 9.99 to 26.78 wt. % and traces of Hg (0.06-0.23 wt. %). The highest fineness of gold (86.81-89.15 wt. % Au) was measured in association with Mn-minerals, while the lowest fineness of gold was determined in late quartz IV veins (73.78-75.96 wt. % Au). The most common occurrence of gold is within the second and third assemblage in the form of aggregates with galena and other sulphides. Based on this study, gold mineralization in the eastern part of the deposit has many similar features to the earlier-mined western part (Maťo et al. 2005), including major mineral assemblages, typical gold fineness, distinct affinity of gold to galena and typical ore textures. However, some differences have been also observed, such as the presence of low fineness gold in late milky quartz, common presence of Au- and Ag-tellurides and the presence of gold in rhodonite. Neither the rare occurence of high fineness gold (90.5-95.8 wt. % Au) was confirmed in this part of the deposit.

## REFERENCES

KODĚRA, P., LEXA, J., RANKIN, A. H. & FALLICK, A. E. (2005): Epithermal gold veins in a caldera setting: Banská Hodruša, Slovakia. *Miner. Deposita*, **39**, 921-943.

MAŤO, Ľ., SASVÁRI, T., BEBEJ, J., KRAUS, I., SCHMIDT, R. & KALINAJ, M. (1996): Structurally-controlled vein-hosted mezothermal gold-quartz and epithermal precious and base metal mineralization in the Banská Hodruša ore field, Central Slovakia neovolcanites. *Miner. Slov.* **28**, 455-490.

ŠÁLY, J., HÓK, J., LEPEŇ, I., OKÁĽ, M., RECK, V. & VARGA, P. (2008): Exploration of ore-bodies with precious-metal mineralization in the vicinity of the Hodruša-Svetozár deposit. *Final report, ŠGÚDŠ archive, Bratislava* (in Slovak).

# SYNTHESIS AND CRYSTAL STRUCTURE STUDY OF SOPCHEITE (AG$_4$PD$_3$TE$_4$) AND LUKKULAISVAARAITE (PD$_{14}$AG$_2$TE$_9$)

[1]František Laufek[#], [1]Anna Vymazalová,
[2]Tatiana L. Grokhovskaya, [1]Milan Drábek, [3]Jan Drahokoupil

[1] Czech Geological Survey, Geologická 6, 152 00 Praha 5, Czech Rep. [#]frantisek.laufek@geology.cz
[2] Institute of Geology of Ore Deposits, Petrology, Mineralogy and Geochemistry Russian Academy of Sciences, Staromonetnyi per. 35, Moscow 119017, Russia
[3] Institute of Physics of the AS CR v.v.i., Na Slovance 2, 182 21 Praha 8, Czech Rep

Key words: sopcheite, lukkulaisvaaraite, crystal structure, tellurides, platinum-group minerals

## INTRODUCTION

Sopcheite (Ag$_4$Pd$_3$Te$_4$) was established as a mineral by Orsoyev et al. (1982) during the study of Cu-Ni sulphide ores of the Monchegorsk layered complex, Kola Peninsula, Russia. Orsoev et al. (1982) provided a chemical and physical characterization of this mineral, however a detailed crystal structure analysis was lacking. The phase Pd$_{14}$Ag$_2$Te$_9$ was reported from Lukkulaisvaara layered intrusion, Russian Karelia, Russia as unnamed phase by Grokhovskaya *et al.* (1992) and Barkov et al. (2001). Recently Vymazalová et al. (2014) described this phase as a new mineral lukkulaisvaaraite. Both minerals occur in the forms of small anhedral grains in size not exceeding 100 μm, typically enclosed in chalcopyrite. Because of small size of natural grains and their intimate intergrown with other PGM-minerals, these minerals cannot be isolated in an amount for a proper structural characterization. Therefore, during our experimental study on Ag-Pd-Te system, we performed synthesis of both minerals and subsequently their crystal structure analysis.

## EXPERIMENTAL PROCEDURES

The synthetic analogues of minerals were prepared using silica glass tube technique. The stoichiometric amounts of elements were loaded into silica glass tubes. The evacuated tubes with their charges were heated at 350°C for several weeks. The resultant materials were characterized with powder and single-crystal X-ray diffraction, electron-microprobe analyses and optical microscopy. While the synthesis of sopcheite yielded crystals suitable for single-crystal diffraction analysis, the crystal structure of lukkulaisvaaraite was determined from powder diffraction data. The structural identity between the synthetic and natural materials was confirmed by an electron-backscattered diffraction study (EBSD).

## SOPCHEITE

Sopcheite, Ag$_4$Pd$_3$Te$_4$, crystallizes in *Cmca* space group ($a$ = 12.22 Å, $b$ = 6.14 Å, $c$ = 12.23 Å) with $Z$ = 4. The mineral shows a layered crystal structure, where the Pd atoms exhibit a square planar coordination by four Te atoms. The [PdTe$_4$] squares share two opposite Te-Te edges with adjacent [PdTe$_4$] squares forming layers parallel to (100). The layers imitates a distorted honeycomb nets and show AB-type stacking along the **a** axis. The layers of edge-sharing [PdTe$_4$] squares are connected

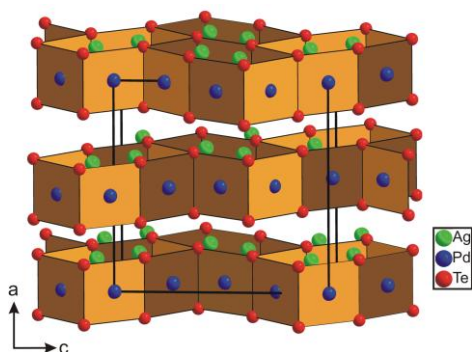by number of Ag-Te bonds running approximately in the [100] direction (Fig. 1)



Fig. 1. The crystal structure of sopcheite $Ag_4Pd_3Te_4$ in a polyhedral representation. The [$PdTe_4$] squares are emphasized.

## LUKKULAISVAARAITE

Lukkulaisvaaraite, $Pd_{14}Ag_2Te_9$, is tetragonal, with space group $I4/m$ ($a$ = 8.96 Å, $c$ = 11.82 Å) and $Z$ = 2. The crystal structure of this mineral is based on a three-dimensional framework, which is composed of two types of blocks of polyhedra. The first type consists of edge-sharing deformed [$PdTe_4$] tetrahedra, which are flattened along one of the $\bar{4}$ axes. Four of these flattened tetrahedra are linked into a [$PdTe_4$]$_4$ tetramer by sharing their common Te-Te edges. These tetramers form slabs parallel to (001). The second type of coordination polyhedra are [$PdTe_4$] squares. Each of the squares share two opposite Te-Te edges with adjacent squares forming layers parallel to (001) planes.
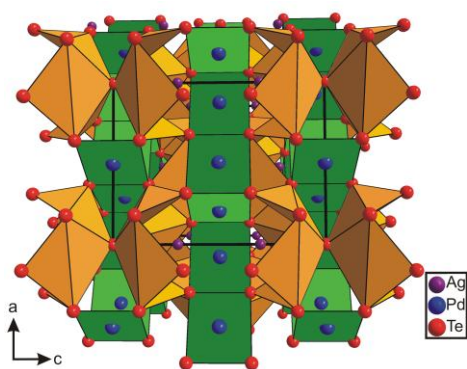


Fig. 2. Polyhedral representation of the lukkulaisvaaraite crystal structure (adapted from Vymazalová et al. 2014).

In the lukkulaisvaaraite crystal structure, these two types of blocks of polyhedra regularly alternate along the **c**-axis. The Ag atoms show square anti-prismatic coordination by Pd atoms (Fig. 2).

### RELATION TO OTHER MINERALS

The crystal structures of sopcheite and lukkulaisvaaraite are unique; there are no exact structural analogues. Both minerals show some structural similarities; nevertheless their structures differ considerably. Either phase shows presence of edge-sharing [$PdTe_4$] squares. However, the three-dimensional framework structure of lukkulaisvaaraite is in contrast to the layered structure of sopcheite. Similar structural features to the mineral sopcheite (i.e. layered structure, analogical structural function of Ag) was observed in synthetic ternary chalcogenides of Pd and alkali metals. The flattened tetrahedra, which are a hallmark of the lukkulaisvaaraite structure, were also found in palladseite $Pd_{17}Se_{15}$ (Geller 1962).

### REFERENCES

BARKOV, A.Y., MARTIN, R.F., TARKIN, M., POIRER, G., & THIBAULT, Y. (2001): Pd-Ag tellurides from a Cl-rich environment in the Lukkulaisvaara layered intrusion, northern Russian Karelia. *Can. Mineral.* **39**, 639-653.

GELLER, S. (1962): The crystal structure of $Pd_{17}Se_{15}$. *Acta Crystallographica*, **15**, 713-721.

GROKHOVSKAYA, T.L., DISTLER, V.V., KLYUNIN, S.F., ZAKHAROV, A.A. & LAPUTINA, I.P. (1992): Low-sulfide platinum group mineralization of the Lukkulaisvaara pluton, northern Karelia. *Int. Geol. Review*. **34**, 503-520.

ORSOEV, D.A., REZHENOVA, S.A. AND BOGDANOVA, A.N. (1982): Sopcheite, $Ag_4Pd_3Te_4$, a new mineral from copper-nickel ores of the Monchegorsk pluton. *Zapiski Vserossiyskogo Mineralogicheskogo Obshchestva*, **111**(1), 114-117.

VYMAZALOVÁ, A., GROKHOVSKAYA, T.L., F LAUFEK, F., RASSULOV V. I. (2014): Lukkulaisvaaraite, $Pd_{14}Ag_2Te_9$, a new mineral from Lukkulaisvaara intrusion, northern Russian Karelia, Russia. *Mineralogical Magazine* (submitted)

# MICROSCALE MINERALOGICAL AND TEXTURAL STUDY OF THE BOTTOM MANGANESE-OXIDE LAYERS AT THE ÚRKÚT DEPOSIT (HUNGARY)

[1]Máté Zs. Leskó[#], [1]Boglárka A. Topa,
[1]Tamás G. Weiszburg, [2]Tamás Vigh, [1]Tamás Váczi, [3]Zsolt Bendő

[1]     Department of Mineralogy, Eötvös Loránd University, Pázmány Péter sétány 1/C, H-1117 Budapest, Hungary, [#]lmate89@gmail.com
[2]     Manganese Mining and Processing Ltd., H-8409 Úrkút, Hungary
[3]     Department of Petrology and Geochemistry, Eötvös Loránd University, Pázmány Péter sétány 1/C, H-1117 Budapest, Hungary

Key words: microscale SEM and Raman study, manganese oxides, Úrkút, Hungary

### INTRODUCTION

During the Toarcian anoxic event manganese rich strata were deposited Europe-wide. One of the largest known manganese accumulations of this horizon is the Úrkút deposit (Bakony Mountains, Transdanubian Range, Hungary). There are two ore types in the Úrkút manganese deposit: carbonatic and oxidic.

The geological section we studied in the mine represents a transition between these types. In this research we focused on the lowermost manganese oxide bearing layers, which represent the first occurrence of manganese in the system (Fig. 1). These layers occur just above the footwall of the deposit and show massive, macroscopically unlayered texture. The manganese oxide mineral determined by bulk phase analytical methods are of too small grain size for proper optical identification, thus previously only speculations could be set up for the relationship between the observed textures and the mineral phases. The formation of these black ("oxidic") layers has been assumed to be the result of the postdiagenetic remobilization of the manganese related to pyrite oxidation (Vigh 2013). However, details of such a process have never been worked out, neither mineralogically, nor geochemically. The complex, micrometer-scale mineralogical study of the ore texture could provide new data to the better understanding of the system (Bíró 2014).
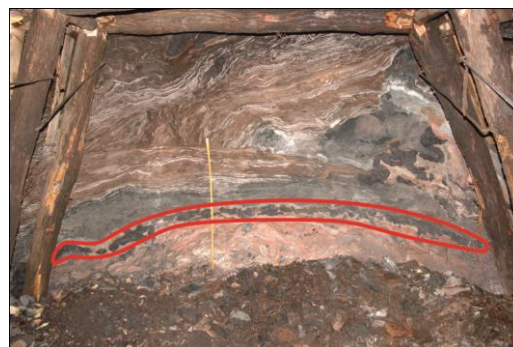


Fig. 1. The sampled section (the first occurrence of manganese within the dotted line)

### APPLIED METHODS AND RESULTS

In our study, after stereo and polarized reflected light microscopy observations, we combined X-ray powder diffraction

(XRD) to measure the average (bulk) mineralogical composition of the samples, scanning electron microscopy (SEM) to observe the micrometer scale textural features, X-ray microanalysis (SEM-EDX) for chemical analysis and Raman spectroscopy for identification of the minerals even at the micrometer size range.

It is the first time that oxidic manganese mineral phases, known before from bulk phase analyses only, can be connected to particular microtextural features. Raman spectroscopic fingerprinting was very effective in separating the different manganese oxide (-hydroxide) mineral phases at the micrometer scale.

The measurements revealed that these layers, macroscopically without stratification, are made up of thin sublayers with particular mineralogical and textural features. These sublayers contain mainly manganite and cryptomelane as dominant minerals, while other Mn-bearing phases (*e.g.* hollandite) are present in subordinate amount. Cryptomelane in the samples is fine-grained ($\leq$ 1 µm). Texturally it is present either as cavity filling matrix or in rounded aggregates, up to 100–200 µm in diameter, frequently around detrital mica crystals. Manganite appears mostly in two different euhedral crystal generations. Few µm thin, 40–60 µm wide platy manganite crystals form loose masses in separate sublayers (e.g. the uppermost sublayer in Fig. 2). The other manganite generation, stubby crystals of around 50 µm, fills post-sublayer-formation veins (e.g. the large vein crossing all sublayers in Fig. 2).

Both minerals replace also originally $CaCO_3$ fossils in various proportions. Some of these fossils were fully replaced, others preserved partially the original $CaCO_3$ material.

## CONCLUSIONS

The combined method allowed us, for the first time, to connect oxidic manganese mineral phases, known before from bulk phase analyses only, directly to

microtextural features. The studied samples, despite of the massive, bulk, unstructured appearance, preserved fine details of the originally carbonate dominated sedimentary features. The $CaCO_3$ to Mn-O-(OH) replacement process was slow and resulted in mineralogical and geochemical (sub) zonation parallel to the original strata. The observed textural characteristics support more a primary (synsedimentary? / syndiaganetic?) formation of the footwall connected oxidic layers, rather than a postdiagenetic oxidation related origin.

Detailed analysis of the oxidic sublayers, the replacement processes and the different veinlet generations show, that the formation of these massive bottom manganese oxide layers in Úrkút will have to be interpreted in a more complex way than it was expected earlier.


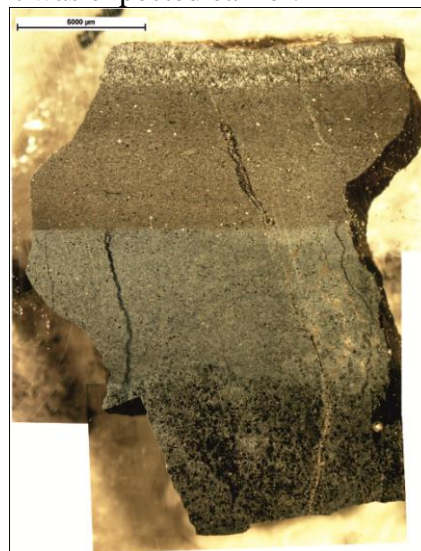
Fig. 2. Oxidic manganese layer (oriented) from Fig. 1, consisting four different, mm-sized sublayers. Scale bar: 5 mm

## REFERENCES

Bíró, L. (2014): Az úrkúti mangánérc-bányászat fúrásainak sztratigráfiai újraértékelése, *Földtani Közlöny* 144/1, p. 3–14.

Vigh, T. (2013): Mangánérctelepek, *In*: Pál-Molnár, E., Bíró, L., (eds.): Szilárd ásványi nyersanyagok Magyarországon, Szeged, p. 45–64.

# W-MINERALIZATION FROM GREISEN AT CETORAZ NEAR PACOV, CZECH REPUBLIC

[1]Lenka Losertová[#], [1]Zdeněk Losos

[1] Department of Geological Sciences, Masaryk University, Kotlářská 2, 611 37 Brno, Czech Republic, [#] lena.los@seznam.cz

Key words: wolframite, scheelite, greisen, huanzalaite component, chemical composition, Cetoraz near Pacov, Moldanubian zone

## INTRODUCTION

Studied locality is situated about 750 m NE from the Cetoraz village. The small tungsten deposit is surrounded by mostly moldanubian rocks, especially Pacov orthogneiss and sillimanite-biotite paragneiss. W-minerals occur in quartz veins and lenses with accompanying greisen. Greisenization is developed in endocontact of the orthogneiss, it has form of silicification and muscovitization (Jurák et al. 1987).

Ore mineralization of this greisen is represented by wolframite, scheelite, gahnite, pyrite, molybdenite, chalcopyrite and native bismuth. Cassiterite, galena and gold are only accessoric (Jurák et al. 1987).

Tungsten deposit was discovered in 60's by Prchlík and Jeřábek (1965). Consequent exploration revealed that the deposit has only low economic potential (Jurák et al. 1987). Němec and Tenčík (1976), Němec and Páša (1986) labeled the host rock as the meta-greisen.

Presented new data are summarized from recent studies by Losertová et al. (2013a) and Losertová et al. (2013b).

## RESULTS

Wolframite in quartz gangue is associated with scheelite and albite. Wolframite forms black tabular aggregates with size up to 10 cm. It is usually accompanied by scheelite crystals and aggregates of yellow-brown color and size from few mm to 1 cm.

Microscopic study revealed wolframite, scheelite and uncertain secondary phase of Fe and W, which is by chemistry closely related to some pyrochlore group minerals. This phase was temporarily labeled as ferritungstite.

Wolframite in BSE-image (Fig. 1.) is chemically homogenous and forms subhedral grains from 0.08 to 0.5 mm in size. Wolframite is composed of dominating ferberite (72–75 %), lower hübnerite (21–24 %) and small but unusual amount of rare huanzalaite (4 %) (Fig. 2.). Average chemical composition is $(Fe_{0,752}Mn_{0,227}Mg_{0,040}Ca_{0,001}K_{0,001})_{\Sigma1,021}(W_{0,987}Nb_{0,004}V_{0,004})_{\Sigma0,995}O_4$. Wolframite grains are often partially or fully replaced by ferritungstite. Unaltered wolframite is rare and sometimes contains inclusions of bismuth. Anhedral grains of scheelite are from 0.04 to 0.45 mm in size. Scheelite is chemically homogenous and close to its

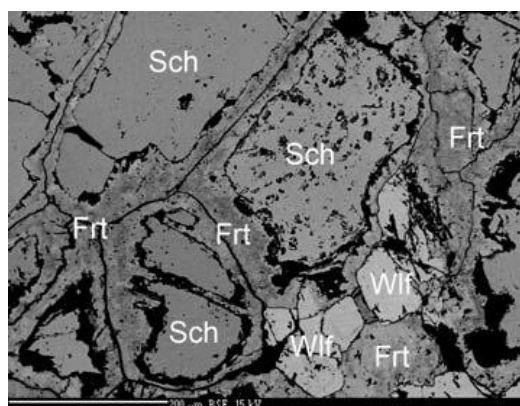ideal formula. Scheelite is replaced by ferritungstite too.



Fig. 1. Wolframite (Wlf) and scheelite (Sch) grains altered by ferritungstite (Frt).
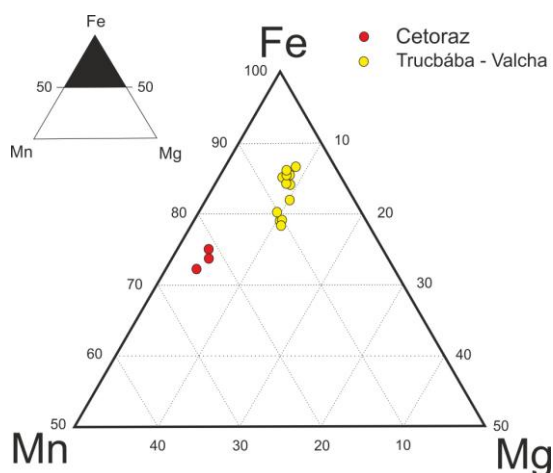


Fig. 2. Ternary plot of chemical composition of Mg-ferberite from Cetoraz near Pacov (Losertová et al. 2013a) and Trucbába–Valcha near Humpolec (Losertová et al. 2012).

## CONCLUSIONS

Magnesium-bearing wolframite and pure scheelite were analysed from quartz gangue of the (meta?) greisen near Cetoraz by Pacov. Wolframite composition is dominated in ferberite. Unusual is relatively high huanzalaite component (up to 4 %) and increased content of Nb. Similar unzonal Mg-rich ferberite with huanzalaite end member up to 11 % is known in Bohemian Massif only from placers of the locality Trucbába-Valcha near Humpolec. Even these low amounts of huanzalaite component in wolframites from Cetoraz and Trucbaba-Valcha are very rare in worldwide scale.

Wolframite from Cetoraz may be replaced by scheelite. Both wolframite and mainly scheelite are strongly altered and sometimes fully replaced by mineral close to ferritungstite.

## REFERENCES

JURÁK, L., HRANÁČ, P., PÁŠA, J., PROCHÁZKA, J., KARBAN, L., ANFT, A. & NOVOSÁD, I. (1987): Final report. Tungsten–Moldanubicum. *MS*, Geoindustria Jihlava, P 57675.

LOSERTOVÁ, L., HOUZAR, S., BUŘIVAL, Z. & LOSOS, Z. (2012): Wolframite from heavy-mineral assemblages at Trucbába-Valcha, Moldanubicum. *Acta Musei Moravie, Sci. Geol.* **97**, 2, 77–84.

LOSERTOVÁ, L., BUŘIVAL, Z., LOSOS, Z. & HOUZAR., S. (2013a): Mineral assemblage and chemical composition of Mg-wolframite and scheelite from Cetoraz by Pacov, Czech Republic. *Acta Musei Moravie, Sci. Geol.* **98**, 1, 41–48.

LOSERTOVÁ, L., BUŘIVAL, Z. & LOSOS., Z. (2013b): Mineralogy and chemical composition of Fe-gahnite from Cetoraz near Pacov, Czech Republic. *Bulletin mineralogicko-petrologického oddělení Národního muzea v Praze,* **21**, 1, 47–51.

NĚMEC, D. & PÁŠA, J. (1986): Regionally metamorphosed greisens of the Moldanubicum. *Mineralium Deposita,* **21**, 12–21.

NĚMEC, D. & TENČÍK., J. (1976): Regionally metamorphosed greisens at Cetoraz, The Bohemian-Moravian heights (Českomoravská vrchovina), Czechoslovakia. *Mineralium Deposita,* **11**, 210–217.

PRCHLÍK, I. & JEŘÁBEK, M. (1965): Tungsten mineralization from Cetoraz, west from Pacov. *Věstník Ústředního Ústavu Geologického,* **40** (1), 47–49.

# NB-TA OXIDE MINERALS IN ALLUVIAL PLACERS FROM KAMAKWIE, NW SIERRA LEONE: COMPOSITIONAL VARIATIONS AND EVOLUTIONARY TREND

[1]Jan Loun[#], [1]Milan Novák,
[1]Radek Škoda, [1]Renata Čopjaková, [2]Michaela Vašinová Galiová, [2]Lubomír Prokeš

[1] Department of Geological Sciences, Masaryk University, Kotlářská 2, CZ-611 37 Brno, Czech Republic, [#]loun.jan@seznam.cz

[2] Department of Chemistry, Masaryk University, Kotlářská 2, CZ, CZ-611 37 Brno, Czech Republic

Key words: columbite-tantalite, pegmatite, alluvial placers, Sierra Leone, "fingerprinting"

## INTRODUCTION

Columbite-tantalite group minerals („coltan" ore) are extensively mined from alluvial placers in Sierra Leone together with diamonds, gold and cassiterite. In this study chemical composition of columbite group minerals from placer deposits near Kamakwie (Northern Province, Sella Limba Chiefdom), NW Sierra Leone are presented.

## GEOLOGICAL SETTING

Most of Sierra Leone is underlain by rocks of Precambrian age (Archaean and Proterozoic). The Precambrian outcrops cover ~ 75 % of the country and typically comprises granite-greenstone terrain. It represents part of an ancient continental nucleus located on the edge of the West African Craton. The Archean basement can be subdivided into infracrustal rock (gneisses and granitoids), supracrustal rocks (containing greenstone belts), and basic and ultrabasic igneous intrusions. The Leonean orogenetic episode (2,950-3,200 Ma) commenced with the intrusion of a basic igneous suite (the Pre-Leonean amphibolites) and by the formation of a greenstone belt represented by the Loko Group which is now deeply eroded. Gold, cassiterite and columbite mineralization associated within portions of the Loko Group is probably related to a late Leonean granitisation event which accompanied the formation of the shear zones in the craton.

Deposits near Kamakwie are situated in a hilly terrain referred to as the Loko Hills. These prospects reflect the occurrences of greenstone belt lithologies of the Loko Hills Group. It is older than other greenstone belts in Sierra Leone and therefore has been subject to a greater degree of erosion. „Coltan" deposits are represented by swamp areas in the valley floors and river valleys close to these greenstone belt occurrences.

## COLUMBITE-GROUP MINERALS

The columbite-tantalite group minerals were found only in the shallow alluvial placers within the swamps, not in a primary source in situ due to deep tropical weathering of upper soil horizon.

Nevertheless, overall paragenetic, textural and compositional character of the assemblage suggests rare-element granitic pegmatite(s) as the parental rock of the Nb-Ta mineralization. Given the very high density of the targeted minerals, their often coarse grain size and frequent angular shapes, it is not expected they traveled great distances into areas of gentle relief.

The columbite group minerals were identified as abundant black loose fragments of euhedral crystals and nuggets of 0.X mm to X cm in size. Chemical composition corresponds to predominant ferrocolumbite, with rare ferrotantalite (ferrotapiolite?) [at. $Mn/(Mn + Fe) = 0.01–0.22$ and $Ta/(Ta + Nb) = 0.02–0.83$], which are either homogenous or show patchy irregular zoning. Based on minor and trace elements they are unusually rich in Ti ($\leq$ 1.9 wt. %), W ($\leq$ 2.7 wt. %), Sc (2100 ppm), Mg (6200 ppm) and Y+HREE ($\leq$ 250 ppm Y; $\leq$ 330 ppm REE). The chondrite normalized REE patterns show MREE and HREE enrichment with well visible tetrad effect on third and fourth tetrad and deep negative Eu anomaly.

An evolutionary trend in the columbite quadrilateral (Fig. 1) indicates very low degree of fractionation and F-poor environment (Černý 1992) similar to some beryl–columbite subtype pegmatites commonly derived from S-type granites. Other minerals in the heavy mineral assemblage ilmenite > magnetite, titanomagnetite, cassiterite, garnet (alm > spess > pyr), tourmaline (srl > drv) and monazite support their affinity to the columbite-bearing pegmatite(s).

## SUMMARY

In comparison with known columbite-tantalite compositions (e.g, Černý et al. 1992), very primitive composition in this study is quite unique and suggest very low activity of Ta relative to Nb in the parent melt and very low degree of fractionation. Any such extreme composition may be useful, along with trace elements

variability and geochronological information, for the „fingerprinting" of Ta ores. Mineralogical and geochemical characteristics of the Ta ores from Sierra Leone revealed specific features which can distinguish these deposits from those situated in conflict zone in the central Africa (cf. Melcher et al. 2014).
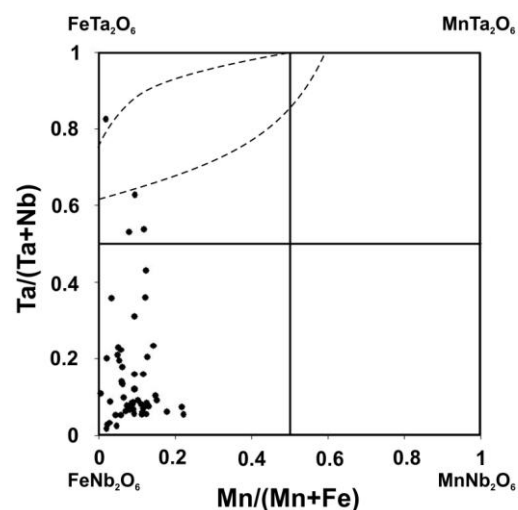


Fig. 1. Quadrilateral diagram (atomic proportions) of columbite-tantalite from Kamakwie, NW Sierra Leone.

## REFERENCES

ČERNÝ, P. (1992): Geochemical and petrogenetic of the mineralization in rare-element granitic pegmatites in the light of current research. *Appl. Geochem.* **7**, 393-416.

ČERNÝ, P., ERCIT, T. S., & WISE, M. A. (1992): The tantalite-tapiolite gap: Natural assemblages versus experimental data. - *Can. Mineral.* **30**, 587-596.

MELCHER, F., GRAUPNER, T., GÄBLER, H. E., SITNIKOVA, M., HENJES-KUNST, F., OBERTHÜR, T., GERDES A. & DEWAELE S. (2014): Tantalum-(niobium-tin) mineralisation in African pegmatites and rare metal granites: Constraints from Ta-Nb oxide mineralogy, geochemistry and U-Pb geochronology. *Ore Geology Reviews*. (in print)

# THERMODYNAMIC PROPERTIES OF SECONDARY COPPER MINERALS

[1]Juraj Majzlan[#], [1]Arne Zittlau,
[2]Martin Števko

[1]    Institute of Geosciences, Burgweg 11, University of Jena, D-07749 Jena, Germany,
[#] Juraj.Majzlan@uni-jena.de
[2]    Department of Mineralogy and Petrology, Comenius University, Bratislava, Slovakia

In this contribution, we report thermodynamic properties of a suite of secondary copper minerals. For all phase, enthalpies of formation were measured by acid-solution calorimetry and third-law entropies by relaxation calorimetry. From these data, we derived the Gibbs free energies of formation and the solubility products for all phases. Thermodynamic data were determined for brochantite (enthalpy of formation $\Delta_f H^o = -2194 \pm 7.0$ kJ·mol$^{-1}$, standard entropy $S^o = 343.1 \pm 3.4$ J·mol$^{-1}$·K$^{-1}$, Gibbs free energy of formation $\Delta_f G^o = -1824.9 \pm 7.1$ kJ·mol$^{-1}$), posnjakite ($\Delta_f H^o = -2468.2 \pm 7.0$ kJ·mol$^{-1}$, $S^o = 390.9 \pm 3.9$ J·mol$^{-1}$·K$^{-1}$, $\Delta_f G^o = -2043.4 \pm 7.1$ kJ·mol$^{-1}$), langite ($\Delta_f H^o = -2762.3 \pm 7.1$ kJ·mol$^{-1}$, $S^o = 397.9 \pm 4.0$ J·mol$^{-1}$·K$^{-1}$, $\Delta_f G^o = -2270.0 \pm 7.2$ kJ·mol$^{-1}$), antlerite ($\Delta_f H^o = -1733.6 \pm 5.3$ kJ·mol$^{-1}$, $S^o = 274.3 \pm 2.7$ J·mol$^{-1}$·K$^{-1}$, $\Delta_f G^o = -1453.6 \pm 5.4$ kJ·mol$^{-1}$), libethenite ($\Delta_f H^o = -1385.7 \pm 4.3$ kJ·mol$^{-1}$, $S^o = 162.2 \pm 1.6$ J·mol$^{-1}$·K$^{-1}$, $\Delta_f G^o = -1229.7 \pm 4.3$ kJ·mol$^{-1}$), olivenite ($\Delta_f H^o = -1000.3 \pm 4.6$ kJ·mol$^{-1}$, $S^o = 179.5 \pm 1.8$ J·mol$^{-1}$·K$^{-1}$, $\Delta_f G^o = -851.1 \pm 4.7$ kJ·mol$^{-1}$), pseudomalachite ($\Delta_f H^o = -3230.1 \pm 10.5$ kJ·mol$^{-1}$, $S^o = 374.5 \pm 3.7$ J·mol$^{-1}$·K$^{-1}$, $\Delta_f G^o = -2823.0 \pm 10.6$ kJ·mol$^{-1}$), kröhnkite ($\Delta_f H^o = -2791.6 \pm 3.5$ kJ·mol$^{-1}$), cyanochroite ($\Delta_f H^o = -4021.4 \pm 3.5$ kJ·mol$^{-1}$), and devilline ($\Delta_f H^o = -4409.1 \pm 7.8$ kJ·mol$^{-1}$). Using the new dataset, we modeled the water in the Jacobi adit near the village of Ľubietová (Slovakia), known for its massive precipitation of langite. The fluid discharged from fractures in the underground space is supersaturated with respect to langite, brochantite, and posnjakite but interestingly, it precipitates massively the least stable phase, that is, langite; brochantite is found only in traces. Chemical analyses combined with forward and inverse modeling with the software PHREEQC suggest that the strong enrichment of copper and other heavy metals in the water is a result of an interplay of oxidation dissolution of primary sulfides (pyrite, chalcopyrite), buffering of pH by carbonates (dolomite), and dissolution of the secondary copper minerals (malachite, native copper) either in the oxidation zone of the deposit or within the debris of the old mine dumps. Although native copper is not a common mineral in Ľubietová, using transmission

electron microscopy, we have observed abundant copper micro- or nanocrystals, which form by the interaction of copper-rich fluids and $Fe^{2+}$-bearing phyllosilicates (chlorites) in the host rocks of the deposit. We speculate that the re-oxidation of these crystals may seasonally contribute to a higher metal load in the water. These results indicate a remediation strategy, which may attempt to diminish the discharge of copper-rich water at this site, would have to target the primary ores, secondary oxidation zone, and the mine dumps. This option is probably not viable because of its very high cost and therefore, chemical cleanup of the discharged waters, currently implemented at the site, is a better way to deal with the pollution in Ľubietová.

# STUDY OF CHEMICAL COMPOSITION OF HYDROXYAPATITE IN BOVINE TEETH

[1,2]Radana Malíková[#], [1]Martin Ivanov

[1] Institute of Geological Sciences, Faculty of Science, Masaryk University, Kotlářská 2, 611 37 Brno, Czech Republic, [#] radanna@mail.muni.cz

[2] Department of Mineralogy and Petrology, National Museum, Cirkusová 1740, 193 00 Prague 9, Czech Republic

Key words: hydroxyapatite, bovine teeth, stable isotopes

## INTRODUCTION

Detection of stable isotopes by the modern analytical methods is widely applied in palaeontology and archaeology. Several directions in the study of stable isotope composition in biological material with hydroxyapatite matrice is used including $^{13}C/^{12}C$ and $^{15}N/^{14}N$ ratios; moreover, isotope ratio $^{87}Sr$ and $^{86}Sr$ is used for the solution of the problem of possible migrations (Bentley 2006, Price et al. 2002, Smrčka 2005). New mineralogical studies focused on the chemical composition of biominerals show significant variability in chemical composition of hydroxyapatite in natural environment (Kohn & Cerling 2002, Hinz & Kohn 2010).

Hydroxyapatite (OHAp) is the mineral of the most interest and relevance in biological and material sciences. In the mineral structure of hydroxyapatite with the ideal formula $Ca_5(PO_4)_3OH$ (and Ca/P stoichiometric ratio 1.67) numerous substitutions causing changes in physical processes in OHAp may occur (Skinner 2005, Wopenka and Pasteris 2005). Hydroxyapatite in fossil teeth can be affected by the character of natural environment, especially by the mineralogy, geochemistry and hydrology of the rock background.

## METHODS

Biological material with OHAp matrice – bovine teeth (*Bos primigenius* f. *taurus*) was used for the experiment. Some teeth were cut into cross sections, one tooth remained uncut. Some samples of tooth tissue remained with collagen, the others were deproteinated by hydrazine hydrate – $NH_2.NH_2.H_2O$ (Nielsen-Marsh & Hedges 1999) to simulate the process of fossilization. Then the teeth were saturated in solution of strontium.

Numerous simulation experiments were realised (fresh samples vs. deproteinated samples immersed in solutions of Sr) to determine the ability of the selected element to incorporate into the tooth tissue and structure of bioapatite. The samples were analysed by the method of electron microprobe.

## RESULTS

In fresh and deproteinated samples these elements were detected: Ca, P, Na, Mg, Cl, F, Sr, S, Si, Zn. The chemical composition of fresh and deproteinated samples differs slightly in the amount of minor and trace elements (Na, Mg, Sr, Si, Mb, S and K), the amount of matrice elements (Ca and P) has similar values.

It was proven from the simulation experiments that bioapatite occurring in fresh and deproteinated bovine tissue is not stable; it is able to incorporate strontium to its structure as a result of substitution exchanges. There is a different ability of incorporating strontium in certain parts of tooth tissue in both cases; strontium incorporated better into dentine than to enamel.

Very strong negative correlation between Ca and Sr in case of the deproteinated samples (correlation coeficient: -0.74 for enamel, -0.96 for dentine) reflects higher ability of stroncium incorporation than in fresh sample (correlation coeficient: -0.92 for dentine, no correlation for enamel).

Experiment with fresh whole tooth saturated in solution of strontium showed: strontium incorporated most easily into the root (cementum), than to the central part of the crown, and least to the upper part of the crown.

Results of the study aim to assess the suitability of utilization of bioapatite in bovine teeth for paleoenvironmental interpretations.

REFERENCES

BENTLEY, R. A. (2006): Strontium Isotopes from the Earth to the Archaeological Skeleton: A Review. *Journal of Archaeological Method and Theory,* **13**, 135-187.

HINZ, E. A., KOHN, M. J. (2010): The effect of tissue structure and soil chemistry on trace element uptake in fossils. *Geochimica et Cosmochimica Acta,* **74**, 3213-3231.

KOHN, M. J., CERLING T. E. (2002): Stable isotope composition of Biological Apatite. *Reviews in Mineralogy and Geochemistry,* **48**, 455-488.

NIELSEN – MARCH, C. M., HEDGES, R. E. M. (1999): Bone porosity and the use of mercury intrusion in bone diagenesis studies. *Archaeometry,* **41**, 65-74.

PRICE, T. D., BURTON, J. H., BENTLEY, R. A. (2002): The characterization of biologically available strontium isotopes ratios for the study prehistoric migration. *Archeometry,* **44**, 117-135.

SMRČKA, V. (2005): Trace elements in Bone Tissue. *Karolinum*, 213 p.

SKINNER, H. C. (2005): Biominerals. *Min. Mag.* **69**, 621-641.

WOPENKA, B., PASTERIS, J. D. (2005): A mineralogical perspective on the apatite in bone. *Materials Science and Engineering,* **25**, 131-143.

# MICROMINERALOGICAL INVESTIGATION OF THE ILMENITE RICH HEAVY MINERAL FRACTION OF THE FEHÉRVÁRCSURGÓ GLASS – SAND

[1]Izabella Rebeka Márkus[#], [1]Ferenc Kristály,
[1]Norbert Zajzon, [2]Sándor Nagy

[1]      Institute of Mineralogy and Geology, University of Miskolc, [#]iza.marks@gmail.com
[2]      Institute of Raw Material Preparation and Environmental Processing, University of Miskolc

Key words: quartz sand, rutile, zircon, monazite, Ti-oxides

## INTRODUCTION

Fehérvárcsurgó is a locality in Central-Hungary, siutated NW from the town of Székesfehérvár. The quartz sand from this locality is known since the end of the 18th century and used for glass manufacturing (Thamóné Bozsó and Baloghné Bozsó 2008), but the industrial scale extraction began only in 1961 (Kun 1989). The white silica sand contains 93–96 wt % of $SiO_2$ and low amount of Fe-minerals, total $Fe_2O_3$ content being between 0.24–0.89 % (Kun 1989), which makes it proper raw material for glass industry after refinement.

## GEOLOGICAL BACKGROUND

The late Pannonian quartz sand is situated in the Mór-trench, which separates the Bakony and Vértes mountains. The carbonatic rocks of the Triassic substrata surround the region, which in the upper Pannonian was a closed lagoon and coastal plain (Kun 1989). The quartz-sand, formed in the nearest 300–400 m width zone to the one-time beach, is of glass-sand quality and the sand formed in the farther zone is of foundry quality. The Pannonian-beds are 80–100 m thick (Varjú 1966), the lower 2/3 is built up of clay and just the upper 1/3 is quartz sand.

The quartz-sand is enriched in heavy-mineral fraction, being undesirable for the glass-sand production. The utilization as a glass industry raw-material requires the separation of heavy- and rare earth minerals. The waste becomes a form of enrichment of these minerals and gives a secondary raw material for critical elements (Nagy 2013).

## MATERIAL AND METHODS

The samples were prevailed from the waste material of the glass-sand production plant. The heavy-mineral fraction was separated on the basis of density from the quartz. The obtained fraction was divided to sub-fractions on the basis of magnetism. They were separated to sub-fractions with weak field magnetic separation (0.1 A, 0.5 A, 5 A). In the next step the residue was separated based on density, we obtained a fraction lighter than cca. 4 kg/dm$^3$ and a fraction heavier which later was further divided, based on conductivity. We performed optical microscopy, X-ray powder diffraction and scanning electron microscope analysis combined with energy

dispersive X-ray spectrometry on the samples. We performed stereomicroscopy observation during the preparation of samples for electron microscopy. We identified first the grains based on their morphology and color, and then we determined the chemical composition by SEM+EDS. From each sample we selected mineral grains of different color and shape. These grains were placed on adhesive carbon foil for scanning electron microscopic investigations.

## RESULTS AND DISCUSSION

The most frequent mineral was the ilmenite, followed by rutile in the samples. The yellow colored, translucent staurolite grains were also present in each sample. The non-magnetic fraction resulted from the magnetic separation at 5 A has the most diverse composition, beside the ilmenite and rutile, it contained staurolite, amphibole, epidote, garnet, zircon and monazite. The nonmagnetic fraction which was lighter than 4 kg/dm$^3$ contained a few grains of ilmenite, rutile, staurolite and was more abundant in quartz, kyanite, tourmaline and amphibole. The magnetic samples resulted from the magnetic separation at 0.5 and 0.1 A shoved similar composition but with different ratios of ilmenite and rutile, some quartz with a few grains of zircon. In the sample lighter than 3 kg/dm$^3$ besides quartz we identified chlorite, staurolite, clay-minerals and few rutile grains. In the samples lighter than 4 kg/dm$^3$ we identified corundum, rutile, staurolite and monazite. The mineral grains in most cases were rounded, anhedral, except partly for the zircon grains, the ilmenite, of which corners and edges were rounded but the ditrigonal crystal shape could be recognized (Fig. 1.) and the tourmaline, which was elongated, ditrigonal prismatic. Based on their chemical composition we could separate different groups of ilmenite. The first group is which contained just Fe an Ti in 1:1 ratio, next group is which contained also just Fe and Ti, but not in 1:1 ratio, another group is the ilmenite with significant Mg substitution. Some ilmenite with Mg, Al and Si substitution could be observed also. The Ti-oxides have a few percent of Fe substitution, and in some cases with minor Nb content. The very low magnetite content is an interesting feature in the heavy mineral spectrum of the sand.
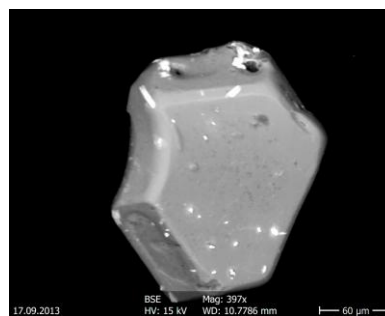


Fig. 1. Platy ditrigonal ilmenite with rounded edges and corners (BSE image, whit grains are residual Na-politungstenate)

## REFERENCES

BÁROSSY, GY.-NÉ. (1958): The sedimentological investigation of the pannonain quartz-sand from Fehévárcsurgó (Dunántúl). *Földtani Közlöny*, **88/2**, 228-236.

VARJÚ, GY. (1966): Non-metallic industrial minerals. *In* Geology of our mineral deposits, 238-312.

KUN, B. (1989): 25 years of the National Ore- and Mineral Mining, 153-166.

NAGY, S., CSŐKE, B., ZAJZON, N., KRISTÁLY, F., PAP, Z., KALICZNÉ, P.K., SZÉP, L. & MÁRKUS, I. (2013): Basic experiments of refuse of glass sand from Fehérvárcsurgó in the interest of recovery of critical elements. *B. K. L.-Bányászat*, **146**/5-6, 58-65.

# NEW MINERALOGICAL AND GEOCHEMICAL RESULTS ON THE OPALS FROM BĂILE CHIRUI (HARGHITA MTS., ROMANIA)

[1]Izabella Rebeka Márkus [#], [1]Ferenc Kristály,
[2]Alexandru Szakács

[1]      University of Miskolc, Institute of Mineralogy and Geology, [#]iza.markus@gmail.com
[2]      Sapientia Hungarian University of Transylvania, Department of Environmental Studies

## INTRODUCTION

The South-Harghita Mts. is the southernmost part of the Călimani-Gurghiu-Harghita Neogene volcanic chain, the last eruption taking place only a few ten thousand years ago. The volcanism was followed by strong, partially still active post-volcanic activities, like mineral water springs, thermal- and mesothermal waters, $CO_2$ and $H_2S$ emanations, opal- and carbonatic spring deposits. One of the most significant opal deposits of the Harghita Mts. is at Băile Chirui. The geological research in the area was aimed at siderite prospecting, thus little information is known about the opals.

## GEOLOGICAL BACKGROUND

The Călimani-Gurghiu-Harghita range is a 160 km long mountain chain, part of the East-Carpathians volcanic arc. The volcanism started in the Upper Miocene, 11.9±0,7 Ma ago in the Călimani Mts., migrated southwards through the Giurghiu Mts., and ended in the South-Harghita Mts. 35-42 Ka ago (Pécskay et al. 1995). The intermediary calc-alkaline and alkaline volcanism in the South-Hargitha (Mason et al. 1998) resulted in basalt-andesites, andesites, dacite and in the southernmost part shoshonites and banakites (Szakács et al. 1993). The calc-alakaline magma shows enrichments in $SiO_2$, $K_2O$, $Na_2O$, Sr, Ba, Th and U from north to south (Seghedi et al. 1986). In the same direction a change from normal calc-alkaline to a high K-concentration magmatism is observed (Szakács et al. 1993). As the result of post-volcanic activity, frequently opal deposits occur, together with siderite usually linked to mineral water springs. At Băile-Chirui the opal occurs as a mix of brown, black and yellowish to white colors and cream colored sideritic opal.

## SAMPLES AND METHODS

We selected samples based on their type and color: white, black, brown, the alternated outer part of the brown and a sideritic opal sample. We performed optical microscopic observations (OM), X-ray powder diffraction (XRD) measurements, differential thermal analysis (DTA), scanning electron microscopy combined with energy dispersive spectrometry (SEM+EDS) and

inductively coupled plasma optical emission spectroscopy (ICP-OES).

## RESULTS AND DISCUSSION

In thin sections by OM we observed, besides the few μm sized opal crystalline aggregates, goethite, siderite and organic matter. In the case of sideritic opal sample the opal and siderite co-precipitation texture was distinguished. With SEM+EDS we could observe concentrically alternating opal and siderite beds, grown over an opal or siderite core (Fig. 1.), associated sometimes with framboidal pyrite. Another texture type is the sideritic matrix, in which the places of former minerals filled with opal is observed. In the black sample the stringiness of the organic matter was visible. The outer white part of the brown opal shoved a spherical, strongly altered, spongy texture. Based on the XRD result each sample contained more than 50 %
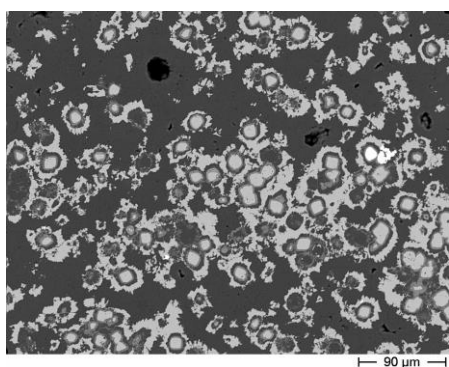


Fig.1. Rhythmic siderite and opal precipitation, with euhedral siderite crystals in the core, formed in the first stage.

amorphous material. The sideritic opal sample, showed a high, 28.3 %, siderite content, as expected. The tridymite and cristobalite content of the sample was very different. Based on these results, we could not classify the samples neither as opal-A nor opal-CT, more likely they are a mixture of this two. The ratio calculated with tridymite and cristobalite can be interpreted as opal-CT and the amorphous part as opal-A.

The DTA investigations conducted on the black opal have confirmed the presence of organic matter. The sample changed its color to white, shoved strong exothermic reactions, and a significant weight loss. The sideritic opal sample also showed a significant weight loss, because of the $CO_2$ release. In the case of the other sample we could also observe weight loss, this being the result of FeO(OH) dehydration. The white alteration rim of the brownish yellow opals also has high organic matter content, probably of microbial origin.

The results of ICP-OES analysis shoved high content of the trace elements Co, Cr, Cu and V, and from the REE group the Nb is dominant. In the sideritic opal significant amount of Mn, Zn and Ni could be observed, the first two as substitutions in the siderite and the later one in the pyrite. Compared to the result of the chemical analysis of the surrounding formations (Seghedi et al. 1986), we can assume that the Co, Cr, Cu, V and Nb are enriched in the post volcanic phase.

## REFERENCES

MASON, P. R. D., SEGHEDI, I., SZAKÁCS, A., DOWNES, H. (1998): Magmatic constrain on geodynamic models of subduction in the East Carpathians, Romania, *Tectonophysics*, **297**, 157-176.

PÉCSKAY, Z., EDELSTEIN, O., SEGHEDI, I., SZAKÁCS, A., KOVACS, M., CRIHAN, M., BERNAD, A. (1995): K-Ar datings of Neogene-Quaternary calc-alkaline volcanic rocks in Romania, *Acta Vulcanologica*, **7(2)**, 53-61.

SEGHEDI, I., GRABARI, G., IANC, R., TĂNĂSESCU, A., VÂJDE, E. (1986): Rb, Sr, Zr, Th, U, K distribution in the Neogenevolcanics of the South-Harghita Mountains, *D. S. Inst. Geol. Geofiz.* **70-71/1**, 453-473.

SZAKÁCS, A., SEGHEDI, I.,PÉCSKAY, Z., (1993): Pecularities of South Harghita Mts as a terminal segment of the Carpathian Neogene to Quaternary volcanic chain, *Rev. Roum. Géologie,* **37**, 21-36.

# RARE – EARTH MINERALS FROM THE HALIMBA BAUXITE

[1]Izabella Rebeka Márkus[#]

[1]        Institute of Mineralogy and Geology, University of Miskolc, [#]iza.markus@gmail.com

Key words: REE content of bauxite, REE-phosphates, xenotime-(Y), baddeleyite

## INTRODUCTION

Halimba is situated in the south-western part of the Bakony-mountains in Central-Hungary. This is a well known region for its numerous karst-bauxite deposits (Halimba is one of them). Our aim was the identification of REE containing mineral phases, their relationships with textural elements and the possibility of their enrichment in size fractions obtained by wet sieving.

## GEOLOGICAL BACKGROUND

The karst-bauxite deposit from Halimba covers an area of 8 $km^2$, being the largest continuous karst-bauxite deposit in Europe (Bárdossy 2007). The substrata of the deposit varies, the Norian dolomites of the Haupt Dolomite Formation being the most frequent, which is partially overlain by the upper Rhetian-Norian carbonates and marls of the Kössen Formation and the carbonates of the same age of the Dachstein Limestone Formation (Pataki 2002). The bauxite was deposited in a fluvial-floodplain environment, and it is enriched in bauxite extraclasts. The texture can be characterized as bauxitic-wackstone or packstone with iron rich ooids, pisoids and intraclasts (Juhász 1988, Bárdossy 2007). The cover of the bauxite deposit is the Santonian conglomerates and marls of the Csehbánya Formation, the Jákó Marl Formation and the Ugod Limestone Formation.

## MATERIALS AND METHODS

The samples were prevailed from the Halimba-subterranean mine. Based on the previous bulk rock ICP-MS results, we selected a sample with high REE content on which we made detailed mineralogical investigations. We studied the whole, unprocessed sample and also the different size fractions obtained with wet sieving. The applied methods were X-ray powder diffraction (quantitative data was obtained by Rietveld-refinement), X-ray fluorescence spectrometry and scanning electron microscopy combined with energy dispersive X-ray spectrometry.

## RESULTS AND DISCUSSION

On the whole sample based on XRD results we identified boehmite, hematite, anatase, rutile and kaolinite. In the fractions > 1 mm and 500 μm obtained with wet sieving, the mineralogical composition was slightly different. We identified boehmite, hematite, anatase, rutile and zircon. Kaolinite was absent. In the fractions > 212 μm, >125 μm and > 63 μm the zircon was absent. In the fractions > 45 μm and < 45 μm beside the boehmite,

hematite, anatase and rutil the kaolinite appeared. The amount of kaolinite in the original sample was 3-5 %, in the > 45 μm fraction 5-4 % and in the < 45 μm fraction 11-8 %, showing that the clay mineral content of the bauxite can be decreased efficiently by wet sieving. The amount of zircon was around 0.2-0.5 wt % in both sample. During the Rietveld-refinement a residual peak persisted at 6.118 Å, which we identified as lepidocrocite (*200*) with Al-substitution. Although it is considered a rare mineral in bauxites, the solid solution between bohmite-lepidocrocite is known (Wolska et al. 1992), but this case needs further investigations.

We made SEM observations on the whole sample and the fractions > 500 μm, > 45 μm, < 45 μm. The original sample showed a specific oolitic, pisolitic wackstone texture. We identified monazite and xenotime-(Y) enriched in REE. The xenotime was enriched in Gd, Dy, Er, Yb, while the monazite in Nd, La and Sm. The xenotime grains were angular, xenomorph, appearing always inside the ooides. The monazite is more frequent, it can be found in the ooids and their matrix too. Beside these two minerals, we observed a large quantity of zircon in the ooid/pisoids and the matrix too, and in few cases baddeleyite. In the > 500 μm fraction we identified monazite and xenotime with similar REE enrichment like in the first sample, except few grains of monazite in which beside Nd, La, Sm the Eu and some Th and Ca could also be observed. Also in this sample we found xenotime with very low REE content. In the > 45 μm fraction size sample, we identified the above-mentioned REE containing minerals. We also observed U containing xenotime grains, which could not be observed in other samples. In the < 45 μm sample we identified monazite with La, Nd Sm enrichment, Ca is also present, but based on other EDX measurements made on the ground mass, Ca could be observed to, so it is possible to be simply enrichment of the ground mass. We also observed the presence of Cr and Na in the groundmass. The xenotime grains showed similar composition like in other samples. The xenotime and monazite grains in all samples were around 5-10 μm in size. In the case of the last two samples we could not determine if the grains were part of the ground mass or in the ooids/pisoids because the samples size fraction is smaller than the size of these (20-30 μm).The REE containing mineral grains were more abundant in the coarser fraction.

Based on XRF analyses $Al_2O_3$ content decreased with the size fraction, while the $SiO_2$ content increased. This can be explained with the increasing amount of kaolinite. The MgO and CaO content was the highest also in the < 45 μm fraction. Sr and Zr also shoved enrichment in the smaller grain sizes, while the Cr has a decreasing tendency.

## REFERENCES

BÁRDOSSY, G. (2007): The Halimba bauxite deposite. 119 p.
JUHÁSZ, E. (1988): Sedimentological features of the Halimba bauxite and paleogeographic reconstruction. *Acta Geol. Hungarica,* **31/1-2,** 111-136.
WOLSKA, E., SZAJDA, W., PISZORA, P. (1992): Determination of solid solution limits based on the thermal behaviour of aluminium substituted iron hydroxides and oxides. *Journal of Thermal Analysis*, **38**, 2115-2122.
Pataki, A. (2002): Geological results of the research between 1995-2001 on the Halimba bauxite deposit. *Földtani Kutatás,* **34/1,** 27-37. (in Hungarian)

# LIANDRATITE FROM KARKONOSZE PEGMATITES, SUDETES, SW POLAND

[1]Witold Matyszczak[#]

[1]    University of Warsaw, Institute of Geochemistry, Mineralogy and Petrology
[#] witold.matyszczak@gmail.com

Key words: liandratite, Karkonosze, pegmatites.

## INTRODUCTION

Liandratite, of the ideal formula $U^{6+}(Nb,Ta)_2O_8$, is a rare secondary mineral, first described in pegmatites from Madagascar (Mücke and Strunz 1978) as a oxidation product of petscheckite, $U^{4+}Fe(Nb,Ta)_2O_8$; it forms 1-2 mm thin translucent, yellow coatings on petscheckite.

Since that time barely a few contributions about this mineral was presented in literature (Lumpkin and Ewing 1996, Lumpkin 2001, Abd El-Naby 2009, Matyszczak 2008).

The both mentioned oxides occur in metamict state and annealing provides to restoration of the structure corresponding to synthetic $U^{6+}Ta_2O_8$.

Little is known about the chemical composition of liandratite. Lupkin (2001) reported the U-site total significantly higher than theoretical, together with a presence other elements in the structure like K, Ba, REE, Fe, Al. These facts indicate that chemical composition of liandratite is more complex than it was originally suggested.

## CHEMICAL COMPOSITION

Liandratite is a common secondary mineral in the investigated pegmatites. It fills cracks, forms crusts (with a maximum thickness of 40 μm), inclusions or pseudomorphic substitutions after various Nb-Ta-Ti minerals (with a maximum size ca. 90 μm) e.g. fergusonite, aeschynite-euxenite group minerals, pyrochlore supergroup minerals or columbite (Fig. 1).
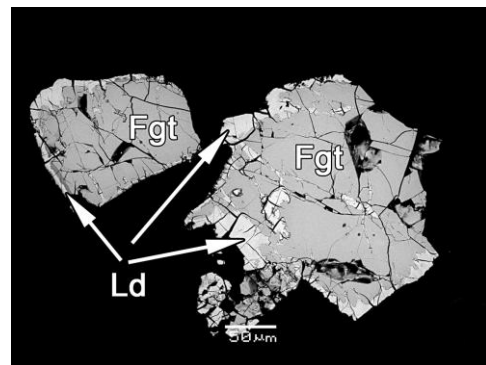


Fig. 1. SEM-BSE microphotography of fergusonite-(Y), labeled Fgt, with a thin crust of liandratite (Ld).

Chemical analyses reveal, in addition to the main elements such us U, Nb, Ta, Ti typical of liadratite, also less common Si, P, Zr, Al, Fe YREE, Ca, Bi and Pb. Chemical formula after recalculation to 8 atoms of oxygen shows that total amount of cations on U- site is ranges between

1.18 and 1.50. It is mainly occupied by $U^{6+}$ which usually exceeds theoretical 1.00 *apfu* and reaches up to 1.27 *apfu* (60.02 wt. % $UO_3$). Amount of other cations ($YREE^{3+}$, $Ca^{2+}$, $Th^{4+}$, $Bi^{3+}$, $Pb^{2+}$, $Mn^{2+}$) does not exceed 0.34 *apfu* (6.94 wt. % $\sum YREE_2O_3+CaO+ThO_2+Bi_2O_3+PbO+MnO$). Nb-site is mainly occupied by $Nb^{5+}$ (0.83-1.47 *apfu*; 18.2-34.10 wt. % $Nb_2O_5$), $Ti^{4+}$ (0.20-0.59 *apfu*; 0.26-7.78 wt. % $TiO_2$), $Ta^{5+}$ ($\leq 0.23$ *apfu*; $\leq 8.41$ wt. % $Ta_2O_5$), $Fe^{3+}$ (0.04-0.18 *apfu*; 0.50-2.48 wt % $Fe_2O_3$), $Zr^{4+}$ ($\leq 10$ *apfu*; $\leq 2.14$ wt. % $ZrO_2$) and $W^{6+}$ ($\leq 0.03$ *apfu*; $\leq 1.22$ wt. % $WO_3$). Often there occur: $Al^{3+}$ ($\leq 0.28$ *apfu*; 0.14-2.41 wt % $Al_2O_3$), $Si^{4+} \leq 0.32$ *apfu*; $\leq 3.19$ wt. % $SiO_2$) and $P^{5+}$($\leq 0.20$ *apfu*; $\leq 2.47$ wt. % $P_2O_5$). The presence of the last mentioned cation group in the structure, sometimes in very significant amounts, is sometimes controversial due their small ionic radii. The main cations in this position are eight-fold coordinated (Villars et al. 2008) but $Si^{4+}$, $P^{5+}$ as well as $Al^{3+}$ do not occur in such coordination. Moreover, the 8-fold coordinated main cations radii, e.g. $Nb^{5+}$ are about 50 % larger than those of 6-fold coordinated of $Si^{4+}$ and $P^{5+}$. In case of $Al^{3+}$ the difference in ionic radius relative to $Nb^{5+}$ is less than 30 %. Thus means that probably only small part of $Al^{3+}$ revealed by microprobe is included in the structure, if at all. Most of the above-mentioned cations, potentially occupying the U- and Nb-sites were described as possible isomorphic ones in liadratite (Lumpkin and Ewing 1996) as well as in isostructural petscheckite (Mücke and Strunz 1978, Tomašić et al. 2004). Only the presence of Si, P and partially Al does not agree with the data presented in literature. Probably these elements do not occur in the original structure of liandratite, but like in other metamict minerals, were included in areas being amorphic as submicroscopic intergrowths or adsorbed in structural voids like e.g. $SiO_2$ or $Al_2O_3$ (Ercit 2005).

Liandratite is a common secondary Nb-Ta-Ti mineral in Karkonosze pegmatites.

Its small sizes, complex chemical composition and not exactly determined structure make it an interesting object to further investigations.

## REFERENCES

ABD EL-NABY, H. H. (2009): Role of geochemical alteration on the formation of secondary Zr and U-bearing minerals in El Asthan trachyte, central Eastern Desert, Egypt. *Journal of Mineralogical and Petrological Sciences,* **104**, 37-51.

ERCIT, T. S. (2005): Identification an alteration trends of granitic-pegmatite-hosted (Y,REE,U,Th)–(Nb,Ta,Ti) oxide minerals: a statistical approach. *Can. Mineral.* **43**, 1291-1303.

LUMPKIN, G. R. (2001): Alpha-decay damage and aqueous durability of actinide host phases in natural systems. *Journal of Nuclear Materials*, **289**, 136-166.

LUMPKIN, G. R., EWING, R. C. (1996): Geochemical alteration of pyrochlore group minerals: betafite subgroup. *Am. Mineral.* **81**, 1237-1248.

MATYSZCZAK, W. (2008): A U-(Nb,Ta,Ti) oxide mineral from Podgórzyn – a preliminary report. *Mineralogia Special Papers,* **32**, 113.

MÜCKE, H., STRUNZ, H (1978): Petscheckite and liandratite, two new pegmatite minerals from Madagascar. *Am. Mineral.* **63**, 941-946.

TOMAŠIĆ, N., GAJOVIĆ, A., BERMANEC, V., RAJIĆ, M. (2004): Recrystallization of metamict Nb–Ta–Ti–REE complex oxides: a coupled X-ray-diffraction and Raman spectroscopy study of aeschynite- (Y) and polycrase-(Y). *Can. Mineral.* **42**, 1847-1857.

VILLARS, P., CENZUAL, K., DAAMS, J., GLADYSHEVSKII, R., SHCHERBAN, O., DUBENSKYY,V., MELNICHENKO-KOBLYUK, N., PAVLYUK, O., SAVYSYUK, I., STOYKO, S., SYSA, L. (2008): $UTa_2O_8$. *In* SpringerMaterials - The Landolt-Börnstein Database (P. VILLARS, P., K. CENZUAL, ed.). (http://www.springermaterials.com). Springer-Verlag Berlin Heidelberg.

# MANGANESE OXIDES AND OXYHYDROXIDES FROM BANSKÁ ŠTIAVNICA, ĽUBIETOVÁ AND SELCE (CENTRAL SLOVAKIA)

[1]Stanislava Milovská[#], [1]Jarmila Luptáková,
[1,2]Stanislav Jeleň, [1]Adrian Biroň, [3]Peter Lazor, [2]Ľuboš Polák

[1]     Geological Institute, Slovak Academy of Sciences, Ďumbierska 1, 974 01 Banská Bystrica, Slovakia, [#]milovska@savbb.sk
[2]     Department of geography, geology and landscape ecology,  Faculty of Natural Sciences, Matej Bel University, Tajovského 40, 974 01 Banská Bystrica, Slovakia
[3]     Department of Earth Sciences, Geocentrum, University of Uppsala, Villavägen 16, 752 36 Uppsala, Sweden

Key words: Mn oxides, coronadite, cryptomelane, pyrolusite, birnessite, Raman spectroscopy

## INTRODUCTION

The samples of Mn oxides and oxyhydroxides from oxidation zones of 3 localities in Central Slovakia region were studied.

Many naturally-occurring minerals of this group tend to be poorly-crystalline and/or nanocrystalline, with not fully resolved crystal structures. Forming of mixtures and contamination with silicates and quartz is common. Main structural units are [$MnO_6$] octahedra sharing edges or corners to form chains and networks, their arrangement being unique for particular mineral species (Julien et al. 2004).

## METHODS

Raman microspectroscopy was employed to characterize the poorly crystalline Mn-phases. Analyses were performed on LabramHR 800 with Czerny-Turner type spectrometer using 532 and 633 nm excitation wavelengths in range 70 -1300 cm$^{-1}$. Interval between of 3000-4000 cm$^{-1}$ was also checked for presence of $H_2O$/OH vibrations.

In addition, supplementary analytical methods were used such as XRD, SEM-EDS, WDS, and XRF.

## RESULTS

Coronadite and probably birnessite type layered Mn oxyhydroxides compose microcrystalline collomorphous aggregates in samples from shallow parts of veins Terézia and Špitaler on precious metal deposit Banská Štiavnica. The minerals are associated with subhedral pyrolusite grains. Coronadite and cryptomelane occur as thin layers covering cavities in quartz. Cryptomelane and coronadite are minerals with characteristic tunnel structure. Their space group is I2/m and Raman spectra are almost identical. Tetragonal pyrolusite has rutile structure containing single chains of distorted octahedra running along the *c*-axis.

Cu-bearing asbolane (lampadite?) with Ba-birnessite or/and hollandite were identified in samples from dumps and from the Reiner adit (Upper Ladislav adit) opened in oxidation zone of the Cu-deposit Ľubietová. Raman spectra show that these minerals occur also as microcrystalline mixtures. Asbolane and birnessite are species with layered structure and water and/or metal cations occupying the interlayer (Manceau et al. 1987; Julien et al. 2003). Hollandite is monoclinic (space group I2/m) with octahedra shared by edges and corners in 2 x 2 configuration and Ba occupying tunnel cavities.

Mn oxides were also determined in Permian sediments hosted U-mineralisation from locality near Selce village. Comparison of Raman spectra suggests the presence of the mineral with layered structure of birnessite, asbolane or lithiophorite group. Preliminary XRF study shows high content of K, Cu and U. Coordination or possible contamination with Cu and U is not clarified yet.

REFERENCES

GOLDEN, D. C., DIXON, J. B., CHEN C. C. (1986): Ion exchange, thermal transformations, and oxidizing properties of birnessite. *Clays & Clay Miner,* **34**, 511-520.
JULIEN, C., MASSOT, M., BADDOUR-HADJEAN R., FRANGE, S., BACH S., PEREIRA-RAMOS J. P. (2003): Raman spectra of birnessite manganese dioxides. *Solid State Ionics*. **159**, 345-356.
JULIEN, C. M., MASSOT, M., POINSIGNON, C. (2004): Lattice vibrations of manganese oxides Part I. Periodic structures. *Spectrochim. Acta Part A,* **60**, 689-700.
MANCEAU, A., LLORCA, S., CALAS, G., (1987): Crystal chemistry of coabalt and nickel in lithiophorite and asbolane from New Caledonia. *Geochimica et Cosmochica. Acta,* **63**, 105-113.

# ADVANCED SCANNING MODE FOR AUTOMATED PRECIOUS METAL SEARCH IN SEM

[1]David Motl[#], [1]Veronika Králová,
[2]Vítězslav Ambrož

[1]    TESCAN Brno s. r. o., [#]david.motl@tescan.cz
[2]    TESCAN ORSAY HOLDING, a.s.

Key words: scanning electron microscopy, automated mineralogy, bright phase search, heavy minerals

TESCAN has developed a new automated mineralogy solution for analyses in the field of mining and mineral processing. TESCAN Integrated Mineral Analyzer (TIMA) combines BSE and EDX data to measure automatically mineral abundance, mineral liberation and association, and grain sizes. Now, an advanced scanning mode for precious metal search was implemented to widen practical applications of this device.

The advanced scanning mode is dedicated above all to precious metals particle search, but also other materials can be analyzed. Polished resin block samples of various materials and particle sizes were processed. In the case of precious metals particle search, the number of interest particles is very low in comparison to the number of all particles in a sample; there are only few bright phases per sample block, usually. The main task is to analyze a sample block as quickly as possible and acquire data only for particles which include such bright phases.

Comparing some other analyzers capable of acquiring EDX data from elemental geometric shapes only, the advanced scanning mode supported by the TIMA can drive the electron beam over an arbitrary irregular shape (see Fig. 1), following closely a particle boundary. This makes the whole process of data acquisition fast and effective, and allows obtaining precise results from the analysis which are not disturbed with redundant data.
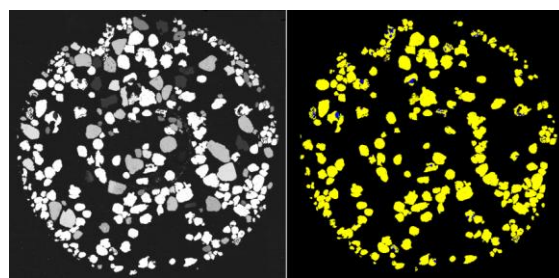


Fig. 1. BSE image of all grains present in the sample (left) and identified bright phases only (right). View field is 11 mm.

# IMPACT OF DIVERSE OXYGEN FUGACITY ($FO_2$) DURING GREENSCHISTS FACIES METAMORPHISM ON FE-TI OXIDES IN MAFIC ROCKS – A CASE STUDY FROM ST. JONSFIORDEN AND EIDENBUKTA AREAS, CENTRAL WESTERN SPITSBERGEN

[1]Krzysztof Nejbert[#], [1]Justyna Domańska – Siuda,
[2]Krzysztof Michalski, [3]Geoffrey Manby

[1]  Uniwersytet Warszawski, al. Żwirki i Wigury 93, 02-089 Warszawa, [#]knejbert@uw.edu.pl
[2]  Instytut Nauk Geofizycznych PAN, ul Księcia Janusza 64, 01-452 Warszawa
[3]  Natural History Museum, Cromwell Road, London, UK

Key words: origin of Fe-Ti oxides, greenschists metamorphism, magnetic petrology, Svalbard

## INTRODUCTION

Metamorphosed mafic magmatic rocks within the Precambrian calcareous metapelites and marbles in the St. Jonsfjorden and Eidenbukta ares from the Central Western Spitsbergen have been selected for magnetic petrology and rock magnetic study. The protoliths of the examined rocks were small Neoproterozoic dolerite sills/dykes, and mafic volcanic rocks recognized in the Precambrian successions. These rocks were subjected to greenschist facies metamorphism during the Caledonian Orogeny (Ohta 1985).

## PETROGRAPHY

The examined mafic rocks contain clinopyroxene, albite, biotite, apatite, pyrrhotite, ilmenite and magnetite that are preserved only in metavolcanites (Fig. 1C). In all the examined metadolerite samples only the titanite pseudomorphs after magnetite were observed (Fig. 1A-B). The fine-grained groundmass was highly recrystallized during greenschist facies metamorphism and consists of fine-grained intergrowths of albite, actinolite, epidote, chlorite, titanite, anatase, biotite, quartz, Ca-Mg carbonates, goethite, and sulphides. Ferromagnetic minerals within the groundmass consist of magnetite, pyrrhotite, hematite and goethite.

## FE-TI OXIDES

The ferromagnetic minerals which formed during the magmatic stage were recrystallized during greenschist facies metamorphism accompanied by a high activity of $CO_2$-rich aqueous fluids expelled from the host rocks. High oxygen fugacity ($f$O$_2$) during these processes caused breakdown of ilmenite and the whole Ti-rich magnetite into titanite. Moreover, oxyexsolved hematite in the ilmenite has been completely dissolved. The opposite processes took place in the metavolcanic rocks where the fluids have $f$O$_2$ close to QMF buffer and this preserve magnetite phenocrysts and supported growth of metamorphic magnetite in the groundmass (Fig 1C).
The three-component IRM acquisition curves (Lowrie 1990) show significant

changes of slope on demagnetization curves of the metadolerite samples (Fig. 2). Noticeable distinct temperatures around 275-350ºC and 500-575ºC are characteristic for pyrrhotite and magnetite, respectively. The temperatures above 575-600ºC (Fig. 2B) can be related to existence of the hematite. The magnetite recognized on some metadolerite IRM diagrams probably represent metamorphic phase that could grow during the breakdown of pyrrhotite to pyrite (see Ramdohr 1980).
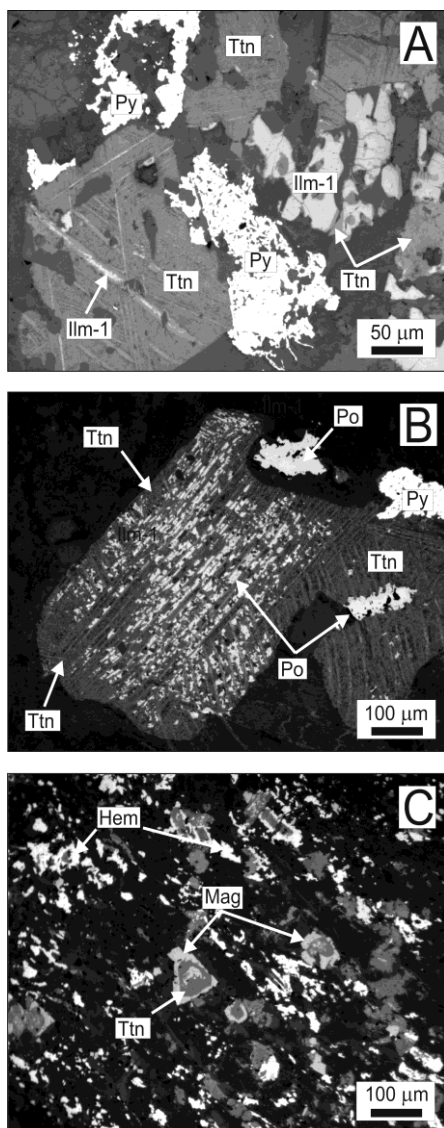


Fig. 1. Petrology of magnetic phases from metadolerite (A, B) and metavolcanite (C). Abbreviations: Ilm-ilmenite, Mag-magnetite, Po-pyrrhotite, Py-pyrite, and Ttn-titanite.
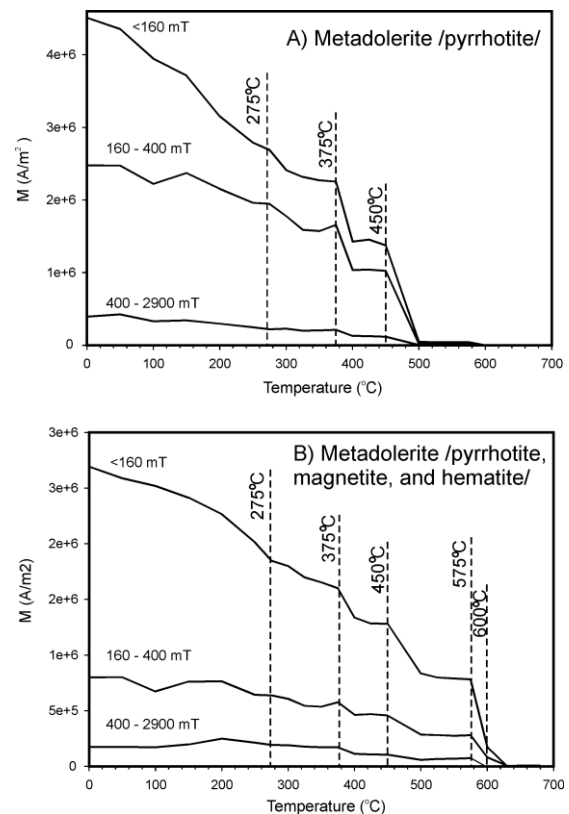


Fig. 2. Three-component IRM acquisition curves (Lowrie 1990) of metadolerites from St. Jonsfiorden. The curves show demagnetization of different coercivity fractions existing in two metadolerite samples. M-normalized magnetization of the samples.

REFERENCES

LOWRIE, W. (1990): Identification of ferromagnetic minerals in a rock by coercivity and unblocking temperature properties. *Geophys. Res. Lett.* **17**, 159-162.
OHTA, Y. (1985): Geochemistry of Precambrian igneous rocks between St. Jonsfjorden and Isfjorden, central Western Spitsbergen, Svalbard. *Polar Res.* **3**, 49-67.
RAMDOHR, P. (1980): *The Ore Minerals and their Intergrowths*, Pergamon Press, Oxford, 1205 p.

# MINERAL CHEMISTRY OF AESCHYNITE AND EUXENITE MINERAL GROUPS IN MUSCOVITE PEGMATIE FROM CENTRAL PART OF THE SUWAŁKI ANORTHOSITE MASSIF, NE POLAND

[1]Krzysztof Nejbert[#], [1]Witold Matyszczak,
[2]Marcin Błaszczyk

[1] Uniwersytet Warszawski, al. Żwirki i Wigury 93, 02-089 Warszawa, [#]knejbert@uw.edu.pl
[2] Instytut Nauk Geologicznych PAN, ul. Twarda 51/55 , 00-818 Warszawa

Key words: aeschynite-(Nd), polycrase-(Y), NYF pegmatite, Suwałki Anorthosite Massif, Poland

## INTRODUCTION

The Suwałki Anorthosite Massif (SAM) occurring in the basement of the East-European Platform in NE Poland is cut by numerous granitic pegmatite veins with thickness ranging from a few cm to ca. 8 m (Juskowiak 1971, Kubicki and Ryka 1982). The CHIME age of the examined pegmatite samples, 1438 +/- 48 Ma, corresponds to the Mesoproterozoic anorogenic activity, responsible for development of anorthosite-rapakiwi granite (AMCG) formation in the Laurentia-Baltica (Zhao et al. 2004).

## TEXTURE AND MINERALOGY

The thickest pegmatite veins within the SAM show classical well developed zoning. Starting from the contact with the host rocks the following zones are present: (I) fine- to medium-grained aplite zone, (II) coarse-grained blocky feldspar zone, in places with well visible feldspar-quartz graphic intergrowths, (III) quartz-euhedral feldspar intergrowths, and (IV) massive quartz core. The most evolved pegmatites are muscovite enriched, and one example of such pegmatite (GMS-2) was selected for the study. The examined pegmatite sample was very coarse-grained. The rock-forming minerals consist of K-feldspar (from 3 to 4 cm in size), albite, quartz, muscovite (up to 1 cm), and Fe-Ti oxides. The accessory phases in the examined muscovite pegmatite comprise apatite, zircon, monazite-(Ce), cheralite, Nb-bearing rutile, Nb-bearing titanite, pyrite, chalcopyrite, barite, malachite and rare Nb-rich phases that occur as grains, up 300 μm in diameter.

## MINERAL CHEMISTRY

Based on the statistical approach proposed by Ewing (1976) and Ercit (2005), numerous complex (Y, REE, U, Th) - (Ti, Nb, Ta) oxides that belong to aeschynite and euxenite mineral groups were recognized. They are represented by aeschynite-(Nd), polycrase-(Y), and uranopolycrase. Discrimination between aeschynite-(Nd) and polycrase-(Y) were done using discrimination formulae of Ercit (2005): [LREE > 0.326* $TiO_2$ - 0.06 $Nb_2O_5$ + 3.1 [wt. % oxide]. Additionally, predominance of Ti over Nb in the B site,

and $UO_2/ThO_2 > 1$ indicate the presence of polycrase-(Y) (for details see Ewing 1976, Ercit 2005). The aim of this presentation is to show mineral chemistry of these complex oxides.

The aeschynite–(Nd) have $TiO_2$ content ranging from 19.49 to 26.75 wt. % (0.89-1.21 *apfu*), $Nb_2O_5$ from 17.82 to 26.34 wt. % (0.51-0.71 *apfu*), $Ta_2O_5$ from 2.18 to 5.48 (0.04-0.09 *apfu*), $UO_2$ from 7.96 to 18.02 wt. % (0.10-0.25 *apfu*), $ThO_2$ 0.41-6.82 wt. % (0.01-0.10 *apfu*), $Nd_2O_3$ from 2.57 to 6.24 wt. % (0.06-0.13 *apfu*), $Ce_2O_3$ from 2.59 to 5.09 wt. % (0.06-0.11 *apfu*), $Y_2O_3$ from 1.68 to 3.87 wt. % (0.05-0.13 *apfu*), CaO from 3.03 to 5.92 wt. % (0.21-0.40 *apfu*), and FeO from 0.39 to 2.33 wt. % (0.02-0.12 *apfu*). The total REE are from 11.66 to 24.30 wt. %. The $SiO_2$ reaches up to 7.17 wt. % (0.44 *apfu*). The $U/(U+Th)$ varies from 0.66 to 0.98.

The examined polycrase-(Y) grains have $TiO_2$ content ranging from 19.51 to 23.48 wt. % (0.92-1.11 *apfu*), $Nb_2O_5$ from 18.85 to 26.23 wt. % (0.54-0.75 *apfu*), $Ta_2O_5$ from 2.10 to 4.21 (0.04-0.07 *apfu*), $UO_2$ from 7.22 to 19.01 wt. % (0.10-0.27 *apfu*), $ThO_2$ 1.30-3.28 wt. % (0.02-0.05 *apfu*), $Y_2O_3$ from 3.06 to 16.99 wt. % (0.10-0.57 *apfu*), CaO from 2.73 to 4.30 wt. % (0.19-0.29 *apfu*), and FeO from 0.63 to 4.42 wt. % (0.03-0.23 *apfu*). The $SiO_2$, $Ce_2O_3$ and $Nd_2O_3$, reach up to 6.54 wt. % (0.41 *apfu*), 2.70 wt. % (0.06 *apfu*) and 3.05 wt. % (0.07 *apfu*), respectively. The total REE are from 6.96 to 13.95 wt. % and $U/(U+Th)$ varies from 0.70 to 0.91.

The uranopolycrase was observed only as small intergrowths within polycrase-(Y). The examined grains have $TiO_2$ content ranging from 22.26 to 29.34 wt. % (1.06-1.33 *apfu*), $Nb_2O_5$ from 15.32 to 22.00 wt. % (0.45-0.60 *apfu*), $Ta_2O_5$ from 2.16 to 4.17 (0.04-0.07 *apfu*), $UO_2$ from 20.21 to 28.10 wt. % (0.28-0.41 *apfu*), $ThO_2$ 0.43-3.57 wt. % (0.01-0.05 *apfu*), $Nd_2O_3$ from 0.43 to 2.24 wt. % (0.01-0.05 *apfu*), $Ce_2O_3$ from 0.64 to 2.94 wt. % (0.01-0.07 *apfu*), $Y_2O_3$ from 1.19 to 6.01 wt. % (0.04-0.20 *apfu*), CaO from 2.86 to 4.25 wt. % (0.20-

0.27 *apfu*), and FeO from 0.69 to 2.34 wt. % (0.04-0.12 *apfu*). The total REE are from 5.99 to 10.23 wt. %. The $SiO_2$ reaches up to 6.56 wt. % (0.41 *apfu*). The $U/(U+Th)$ varies from 0.85 to 0.98.

FINAL REMARKS

The presented data revealed complex mineralogy of (Y, REE, U, Th) - (Ti, Nb, Ta) oxides that belong to aeschynite and euxenite mineral groups. The most evolved muscovite-rich pegmatite, described from the SAM (Juskowiak 1971), can be classified into muscovite–rare-elements (MSREL-REE) or euxenite subtype of the rare-element class (REL-REE) (see Černý, Ercit 2005). The dominance of aeschynite-(Nd) and polycrase-(Y) within the accessory associations indicates that the examined pegmatite belongs to the NYF family (*ibid.*).

REFERENCES

ČERNÝ, P. & ERCIT, T. S. (2005): The classification of granitic pegmatites revisited. *Can. Mineral.* **43:** 2005-2026.

ERCIT, T. S. (2005): Identification an alteration trends of granitic-pegmatite-hosted (Y,REE,U,Th)–(Nb,Ta,Ti) oxide minerals: a statistical approach. *Can. Mineral,* **43:** 1291-1303.

EWING, R. C. (1976): A numerical approach toward the classification of complex, orthorhombic, rare-earth, $AB_2O_6$-type Nb–Ta–Ti oxides. *Can. Mineral,* **14:** 111-119.

JUSKOWIAK, O. (1971): Skały plutoniczne NE Polski. *Biul. Inst. Geol.*, **245**: 7-172.

KUBICKI, S. & RYKA, W. (1982): Atlas geologiczny podłoża krystalicznego polskiej części platformy wschodnio-europejskiej. WG Warszawa, 24 p.

ZHAO, G., SUN, M., WILDE, S. A. & SANZHONG, L. (2004): A Paleo-Mesoproterozoic supercontinent: assembly, growth and breakup. *Earth. Sci. Rev.,* **67:** 91-123.

# ORIGIN OF COOKEITE FROM POCKETS IN THE OLDŘICH PEGMATITE, DOLNÍ BORY – HATĚ, MOLDANUBIAN ZONE, CZECH REPUBLIC

[1]Milan Novák[#], [2]Dalibor Všianský,
[1]Josef Staněk, [1]Marek Dosbaba

[1] Department of Geological Sciences, Masaryk University, Kotlářská 2, 611 37 Brno,
[#] mnovak@sci.muni.cz
[2] Research Institute for Building Materials, Hněvkovského 65, 617 00 Brno

## INTRODUCTION

Cookeite, a late mineral occurring in complex (Li) granitic pegmatites, typically replaces or overgrows primary Li-rich minerals (spodumene, lepidolite, petalite, elbaite), and commonly is associated with clay minerals, carbonates and zeolites. Pegmatite dike Oldřich from Dolní Bory-Hatě with rather primitive mineralogical and geochemical signature represents an unusual example of cookeite occurrence, where it is not associated with other Li-rich minerals. Mineral assemblage and chemical composition of cookeite and discussion of its origin are presented.

## THE PEGMATITE DESCRIPTION

The pegmatite Oldřich forms a symmetrically zoned dike, ~ 35 m thick and up to ~ 800 m long, NNW striking and steeply dipping. The internal structure consists from the contact inwards of: (i) a border zone of an outer granitic unit (Kfs + Qz + Plg + Bt ± Mu); (ii) a graphic unit (Kfs + Qz > Ab + Qz), and (iii) a core built up by blocky microcline (crystals up to 3 m in diameter) and large masses of quartz (milky > rose > smoky). (iv) An intermediate albite unit is commonly located between graphic zone and blocky microcline or blocky quartz, respectively. The mineral assemblages, abundance of the individual minerals and their chemical compositions suggest very low activity of F, moderate activities of B (common schorl and sekaninaite) and P (common apatite, moderate contents of P in feldspars) and generally low contents of Li concentrated in common Li-bearing sekaninaite, very rare triphylite and late cookeite.

## COOKEITE

Highly porous fine-grained beige aggregates of cookeite, up to 15 cm in size, occurred in pockets lined with albite and quartz. Sheet-like folded grains, up to ~ 100 μm in diameter, are associated with masses and veinlets of pale brown siderite, up to 1 cm in size, and very rare small grains of pyrite. Also small admixture of quartz (1 %) was revealed by powder XRD study but not detected using electron microprobe. Electron microprobe data

(EMP) and wet chemical analyses (WCHA) of cookeite yielded very similar results. Cookeite is moderately enriched in Si (3.21-3.29 apfu EMP; 3.31-3.32 apfu WCHA) and poor in Al (4.51-4.65; 4.55-4.56 apfu) relative to the ideal formula LiAl4(Si3Al)O10(OH)8. Low concentrations of Fe (Fe2+≤ 0.08 EMP; 0.03-0.04 Fe3+ and 0.02 Fe2+apfu WCHA), Mg (≤ 0.04; 0.07 apfu), and K (≤ 0.15; 0.09 apfu) were found. The WCHA also yielded 2.19 wt. % Li2O; 0.78 apfu Li, 0.06 apfu Ca and 7.76-7.77 pfu OH. The EMP analyses of associated siderite gave moderate to low concentrations of Mg (0.11-0.17 apfu), Mn (0.07-0.06 apfu) and traces of Ca (0.01 apfu).

<div align="center">DISCUSSION</div>

Chemical composition of cookeite with rather low concentration of Li (2.19 wt. % $Li_2O$; 0.77 *apfu*) and minor Mg and Fe is rather distinct from most cookeite analyses in granitic pegmatites (see e.g., Černý 1970, Julien et al 1996). These data are similar to cookeite from Al-rich mica schists and metabauxites. We also found quite a high content of K, which is comparable with cookeite from Barrhorn metabauxite (Julien et al. 1996) and indicates a presence of muscovite (or other mica) domains in the cookeite structure.

Cookeite precipitated from hydrothermal fluids at temperature below ~ 400°C, possibly as low as 300°C, but higher than ~ 270°C (Vidal & Goffé 1991) for $P_{H2O}$ = 2 kbar derived from abundant andalusite and common almost end-member sekaninaite. These conditions are consistent with those given for the cookeite formation in granitic pegmatites (Julien et al. 1996) and with the conditions derived for hydrothermal stage in granitic pegmatites (London 2008). Lithium-enriched sekaninaite (up to 0.55 wt. % $Li_2O$; Černý et al. 1997) is very likely source of Li for formation of cookeite in pockets. It was replaced by a mixture of micaceous minerals, ferrogedrite,

chloritoid and andalusite (Schreyer et al. 1993). Because sekaninaite is quite common mineral and its alteration is mostly very strong, it may have supplied enough Li into circulating fluids at 450-300°C when Li is mobile (Julien et al. 1996). Sekaninaite as a source of Li is also supported by the assemblage cookeite + foitite + albite found in pseudomorphs after sekaninaite from the pegmatite dike No. 1 located ~ 500 m E of the pegmatite dike Oldřich (unpubl data of MN).

<div align="center">REFERENCES</div>

ČERNÝ, P. (1970): Compositional variation in cookeite. *Can. Mineral*. **10**, 636-647.

ČERNÝ, P., CHAPMAN, R., SCHREYER, W., OTTOLINI, L., BOTTAZZI, P. & MCCAMMON, C. (1997): Lithium in sekaninaite from the type locality, Dolní Bory, Czech Republic. *Can. Mineral*. **35**, 167-173.

JULIAN, M., BARONNET, A. & GOFFÉ, B. (1996): Ordering of the stacking sequence in cookeite with increasing pressure: An HRTEM study. *Am. Mineral*. **81**, 67-78.

LONDON, D. (2008): Pegmatites. The Can. Mineral., Special Publications, **10**, 1–347.

SCHREYER, W., BERNHARDT, H.-J. & MEDENBACH, O. (1993): Ferrogedrite, siderophyllite, septechamosite, andalusite and chloritoid as alteration products of sekaninaite (ferrocordierite) from the Dolní Bory pegmatite, Moravia. *Geol. Geof*. **34**, 141-147. (in Russ.).

VIDAL, O. & GOFFÉ, B. (1991): Cookeite $LiAl_4(Si_3Al)O_{10}(OH)_8$: Experimental study and thermodynamic analysis of its compatibility relations in the $Li_2O-Al_2O_3-SiO_2-H_2O$ system. *Contrib. Miner. Petrol*. **108**, 72-81.

# CARBONATE MINERALIZATION IN LAKE BALATON

[1]Ilona Nyirő-Kósa[#], [1]Éva Tompa,
[1]Mihály Pósfai, [2]András Domonkos

[1]     Dept. of Earth & Env. Sci., Univ. Pannonia, Veszprém, 8200 Hungary, [#]kosaili@gmail.com

Key words: shallow lake, carbonate, Mg-calcite, dolomite

## INTRODUCTION

Calcite precipitation in hardwater lakes is a common phenomenon. Lake Balaton is a large (~ 600 km$^2$), shallow lake. Mostly carbonate minerals dominate in its sediment, including Mg-calcite that precipitates from the lakewater (Müller and Wagner 1978; Cserny 2003), diagenetic protodolomite (Müller 1970), allochthonous calcite and dolomite from the catchment area and aragonite from shells. In this study we focus on the compositions and structures of various carbonate minerals. We discuss the possible autochthonous formation of dolomite in the lake and the influence of biota on the mineralogical character of the sediment.

## SAMPLES AND METHODS

Sediment cores and freshly precipitated minerals were collected either by placing sediment traps under the ice (in order to avoid the resuspension of sediments by wind-driven turbulence) or by filtering lakewater. Pellets (aggregates of undigested mineral particles) produced by filtering organisms were collected by the dissection of zooplankton individuals. We used X-ray powder diffraction analysis to study the Mg/Ca ratios in calcite and dolomite, by inferring compositions from the variations of cell parameters. Individual carbonate crystal morphologies, microstructures and compositions, as well as mineral matter reprocessed by filtering organisms were studied using scanning and transmission electron microscopies (SEM and TEM, respectively).

## RESULTS

There are changes both in water chemistry and mineralogical composition of carbonate minerals along the West-East direction. The MgCO$_3$ content of calcite varies between 2 and 17 mol % and increases from West to East, showing an obvious relationship with the water chemistry. The most abundant Mg-calcite particles are elongated, few μm-large mesocrystalline aggregates (Figs. 1a). The other widespread carbonate species, dolomite, form smaller, euhedral crystals (Fig. 1b). We observed a change in the cell parameters of dolomite from the West to the East, with the parameters deviating from the values of stoichiometric dolomite in the eastern part of the lake.

Filtering organisms produce pellets of about 100 μm large which mostly consist of sediment grains. Pellets from the

Eastern Basin are poor in organic matter and rich in bare, mesocrystalline Mg-calcite particles, the surfaces of which differ from those of freshly precipitated particles.

In summary, our results show that the nature and the spatial distribution of carbonate minerals that precipitate from the water of Lake Balaton are determined primarily by water chemistry which, in turn, is governed by the available water budget. The detrital and primary mineral grains are further processed by the biota, changing the original size distribution of the particles. Studies are in progress to explore the origin of dolomite with anomalous lattice parameters, and the roles of organisms in reprocessing the mineral matter.

REFERENCES

MÜLLER, G. (1970): High-magnesian calcite and protodolomite in Lake Balaton (Hungary) sediments. *Nature*, **226**, 749-750.

MÜLLER, G., WAGNER, F. (1978): Holocene carbonate evolution in Lake Balaton (Hungary): a response to climate and impact of man. – *In* - Matter, A (M.E. Tucker, ed.): *Modern and ancient lake sediments, Blackwell Scientific Publications,* **2**, 57-81.

TULLNER, T., CSERNY, T. (2003): New aspects of lake-level changes: Lake Balaton, Hungary. *Acta Geol. Hun.*, **46**, 215-238.
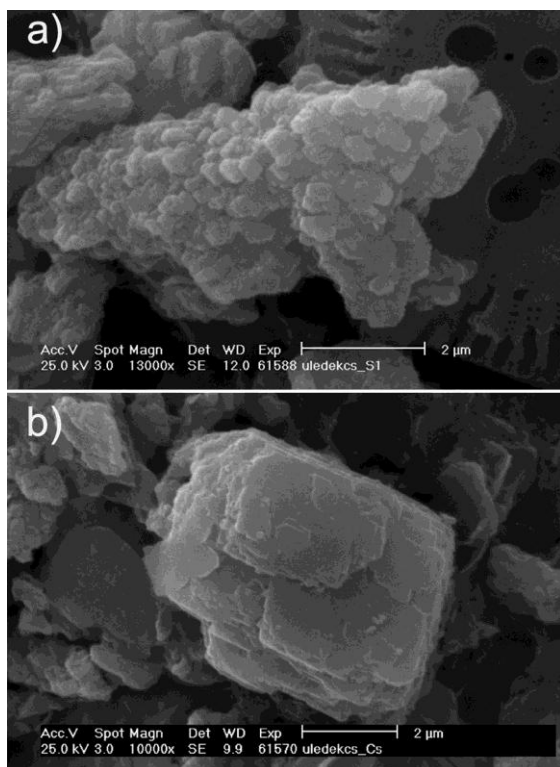
Fig.1. Carbonate minerals in the sediment of Lake Balaton. a) SEM image of a Mg-calcite aggregate; b) TEM bright-field image of Mg-calcite: crystallites are in a consensus crystallographic orientation; c) SEM image of a dolomite grain.

# COMPLEX SOLID SOLUTION SERIES OF APATITE SUPERGROUP MINERALS AND ALLANITE-(CE) BREAKDOWN IN THE A-TYPE GRANITE BOULDER, THE PIENINY KLIPPEN BELT, WESTERN CARPATHIANS, SLOVAKIA

[1]Martin Ondrejka[#], [1]Pavel Uher,
[1]Peter Bačík, [1]Libor Pukančík, [2]Patrik Konečný

[1] Department of Mineralogy and Petrology, Faculty of Natural Sciences, Comenius University, Mlynská dolina G, 842 15, Bratislava, Slovakia, [#]mondrejka@fns.uniba.sk
[2] Geological Survey of Slovak Republic, Mlynská dolina 1, 817 04 Bratislava, Slovakia

## INTRODUCTION

In this contribution, we present the post-magmatic alteration and breakdown phenomena of primary magmatic accessory fluorapatite and allanite-(Ce) to producing a unique assemblage of britholite group minerals including britholite-(Y), fluorbritholite-(Y) and fluorcalciobritholite as well as secondary monazite-(Ce), *REE* carbonates [bastnäsite-(Ce), synchysite-(Ce)] and other minerals in A-type granite near Stupné.

The investigated sample represents equigranular, medium-grained biotite granite with subhedral-grained structure with anhedral to subhedral quartz perthitic K-feldspar, $Or_{82-96}Ab_{04-18}An_{00-01}$, albitic plagioclase, $Ab_{91-98}An_{01-08}Or_{00-01}$, biotite and epidote. Accessory minerals of the Stupné granite include zircon, fluorapatite, allanite-(Ce), ilmenite, magnetite, and pyrite.

Allanite-(Ce) and fluorapatite form scattered crystals of euhedral to subhedral shape, usually up to 0.5 mm and 100 µm in size respectively, associated with partly chloritized biotite (annite), quartz, feldspars and in some places also with zircon, ilmenite, titanite and Nb rich rutile.

The allanite crystals are commonly partly to fully replaced by secondary minerals, which are represented by *REE* carbonates [namely bastnäsite-(Ce), synchysite-(Ce)], epidote, chlorite and pure calcite, while the fluorapatite is overrimed by secondary *REE*-Y bearing accessory minerals in some places or they form relatively scarce inclusions, usually ~5 to 30 µm in size, scattered in quartz or in interstices in quartz and K-feldspars. These mineral phases are mostly represented by yttrium-rich members of the britholite group (classified in the apatite supergroup, Pasero et al. 2010): britholite-(Y) $Ca_2(Y,REE)_3(SiO_4)_3OH$, fluorbritholite-(Y), $Ca_2(Y,REE)_3(SiO_4)_3F$; fluorcalciobritholite $Ca_3(Y,REE)_2(SiO_4)_2(PO_4)F$, and

"calciobritholite"
$Ca_3(Y,REE)_2(SiO_4)_2(PO_4)OH$, a hydroxyl-dominant analogue of fluorcalciobritholite. The chemical compositions are highly variable with a different $REE$/Ca, P/Si and F/OH ratio reflecting a complex isomorphic solid solution among the britholite end members.

### DISCUSSION

Identified minerals of the britholite group in the A-type granite boulder incorporated in Cretaceous flysch sequence of the Pieniny Klippen Belt, Western Carpathians, Slovakia are the first described occurrence in the West-Carpathian area and belong to a relatively rare occurrences of the britholite-group minerals in granitic rocks s.s.

According to textural relationships, it can be predicted the late-magmatic origin and partial replacement, eventually accretion of britholite on primary, early-magmatic fluorapatite in the environment rich in fluorine-bearing fluids, which is a typical feature of A-type granitic suites.

The allanite breakdown is probably connected with an activity of hydrothermal fluids rich in Ca, F, and $CO_2$ which are able to degrade allanite with simultaneous precipitation of secondary REE carbonates, calcite and titanite in some places. The REE fluorocarbonates can form at a relatively wide temperature range (up to ~ 750 °C) but association bastnäsite + synchysite + fluorite is considered as a low-temperature assemblage (Williams-Jones and Wood 1992). Bastnäsites can be stable from hydrothermal to magmatic conditions that $F^-$ enriched species can form in an environment relatively low in F content, and that $OH^-$ species are rare and occur only in low-temperature environments essentially devoid of F (Hsu 1992).

### REFERENCES

HSU, L. C. (1992): Synthesis and stability of bastnaesites in a part of the system (Ce, La)-F-H-C-O. *Mineral. Petrol.* **47**, 87-102.

PASERO, M., KAMPF, A. R., FERRARIS, C., PEKOV, I. V., RAKOVAN, J. & WHITE, T. J. (2010): Nomenclature of the apatite supergroup minerals. *Eur. J. Mineral.* **22**, 163-179.

WILLIAMS-JONES, A. E. & WOOD, S. A. (1992): A preliminary petrogenetic grid for REE fluorocarbonates and associated minerals. *Geochimica et Cosmochimica. Acta,* **56**, 725-738.

# PRELIMINARY STUDY OF MN – (HYDRO)XIDES IN THE WESTERN CARPATHIANS

[1]Daniel Ozdín[#], [1]Gabriela Kučerová,
[1]Martin Števko, [2]Stanislava Milovská

[1]    Department of Mineralogy and Petrology, Faculty of Natural Sciences, Comenius University, Mlynská dolina G, SK-842 15 Bratislava, Slovakia, [#]ozdin@fns.uniba.sk
[2]    Geological Institute of the Slovak Academy of Sciences, Ďumbierska 1, SK-974 01 Banská Bystrica, Slovakia

Key words: Mn-oxides, todorokite, hollandite supergroup, limnosilicite, Slovakia

## INTRODUCTION

In the Western Carpathians there was a long known the occurrence of Mn-oxides and hydroxides, mainly of Cenozoic limestones and dolomites (e. g. Rojkovič 2002, 2003; Pauliš et al. 2003) and Mn ore mineralization especially in Paleozoic rocks in the Spiš-Gemer Ore Mountains, where the Čučma was the most significant deposit (Rojkovič 2001). Later, Mn-hydroxides were also described from oxidation zone of hydrothermal base and precious-metal veins hosted in Neovolcanites in Banská Štiavnica (e.g. Háber et al. 2002), and from the cave environment (Bónová et al. 2009), and also from travertines (Bónová et al. 2012). Large amount of various black dendrites in different geological environments, diverse rocks of different ages, were not sufficiently identified and these dendrites were mostly determined as psilomelane or wad. Our preliminary study of Mn oxides in the Western Carpathians indicates that different mineral phases occur in genetically variable environment.

## METHODS

Manganese minerals were analyzed by a Cameca SX-100 electron microprobe in a wavelength-dispersive mode (State Geological Institute of Dionýz Štúr, Bratislava). Powder X-ray diffraction data were collected with a BRUKER D8 Advance diffractometer and were analyzed by thermal analysis (Derivatograph Q-1500D) in Faculty of Natural Sciences, Comenius University in Bratislava. Micro Raman spectroscopy was carried out on LabRAM-HR 800 spectrometer (Horiba Jobin-Yvon) using excitation laser at 532 and 633 nm (Geol. Inst. of SAS in B. Bystrica).

## RESULTS

Black dendrites in opals generated by residual weathering processes of serpentinite body at the locality Hodkovce are probably formed by romanèchite, which contains up to 0.6 wt. % FeO, 0.5 wt. % $V_2O_3$ and mainly up to 4.5 wt. % NiO and 1.2 wt. % CoO. In limnosilicite from the locality Dúbravica, there are very thin veins composed from radial aggregates of hollandite, whose chemical composition is characteristic by a variable

content of BaO (5.98-13.47 wt. %) and $K_2O$ (0.16-1.32 wt. %). On the locality Hriňová-Krivec in andesite tuffs, Mn mineralization is accompanied by a separate opal veins. Manganese minerals are represented by the minerals from cryptomelane-hollandite series. Pyrolusite was identified in the oxidation zone of hydrothermal base metal veins at Banská Štiavnica and Hodruša-Hámre. It contains up to 1.04 wt. % $SiO_2$, 0.46 wt. % CaO, 0.70 wt. % ZnO and up to 0.32 wt. % FeO. We also determined todorokite with variable content of $Na_2O$. Todorokite from Banská Štiavnica contains up to 9.3 wt. % ZnO. Zn-rich cryptomelane (up to11.7 wt. % ZnO) forms worm-like aggregates in assemblage with crystalline pyrolusite. In this association there was also another Mn oxide observed, which contain up to 19.9 wt. % ZnO and thus is close to chalcophanite or woodruffite. All Mn oxides from Banská Štiavnica and Hodruša-Hámre deposits show increased contents of Zn and Cl (up to 0.8 wt. %).

In oxidation zones of siderite deposits Sirk and Krásnohorské Podhradie crystalline pyrolusite was identified. The content of $Fe_2O_3$ in hollandite at Krásnohorské Podhradie deposit is up to 2.52 wt. % and at Sirk deposit cryptomelane contains only 0.6 wt. % $Fe_2O_3$. Manganese oxides are genetically younger in comparison with Fe oxides. They have very small substitution of Fe↔Mn, but goethite has increased content of $Mn_2O_3$ (~ 4 wt. %).Black dendrites in clay limestones (ruin marble) from the Horná Breznica occurrence consist of ranciéite and probably romanèchite or hollandite. Both minerals show variable chemical composition and strong isomorphism of Fe↔Mn. Content of BaO in romanèchite is up to 13.52 wt. %. Chemical composition of both minerals are characteristic by increased content of $SiO_2$ (up to 5.7 wt. %), $Al_2O_3$ (up to 4.1 wt. %), MgO (up to 0.8 wt. %) and $K_2O$ (up to 0.9 wt. %). Ranciéite was identified from Kolíňany quarry in association with hydroxylapatite and crandallite in limestone fissures. It contains (in wt. %): 1.1 $Na_2O$, 1.8, $Al_2O_3$, 1.0 MgO, 4.7-8.8 CaO, 1.0 $K_2O$ and 4.6 ZnO. In alkaline environment (limestones) ranciéite is the most common phase, which is in contrast with acidic environment (opals, silicites, quartz veins) were Mn oxides are represented mainly by the minerals of hollandite supergroup.

REFERENCES

BÓNOVÁ, K., BAČÍK, P. & BÓNA, J. (2012): Hexahydrite and ranciéite from Holocene travertine and calcareous tufa in the Vyšné Ružbachy locality (Spišská Magura Mts., Northern Slovakia). *Bull. mineral.-petrolog. odd. Nár. Muz. (Praha)* **20**, 94-100.

BÓNOVÁ, K., BAČÍK, P. & DERCO, J. (2009): Pyrolusite and ranciéite from the Skalistý potok Cave (Slovenský kras Mts., Eastern Slovakia). *Miner. Slov.* **41**, 511-518.

HÁBER, M., JELEŇ, S., KOVALENKER, V.A., GORSHKOV, A.A., SIVTSOV, A.V. & SHKOLNIK, E.I. (2002): Todorokite from Terézia vein of the Banská Štiavnica deposit. *In Zborník Mineralogie Českého masivu a Západních Karpat. Olomouc,* 31-36.

PAULIŠ, P., ŠEVCŮ, J., KOPISTA, J. & ZEMAN, M. (2003): Ranciéite from Malá Vieska near Košice. *Bull. mineral.-petrolog. odd. Nár. Muz. (Praha)* **11**, 209-210.

ROJKOVIČ, I. (2001): Early Paleozoic manganese ores in the Gemericum Superunit. Western Carpathians, Slovakia. *Geolines,* **13**, 34-41.

ROJKOVIČ, I., AUBRECHT, R. & MIŠÍK, M., (2003): Mineral and chemical composition of manganese hardgrounds in Jurassic limestones of the Western Carpathians. *Geol. Carpath.* **54**, 317-328.

# CHEMISTRY VARIATIONS IN GUSTAVITE FROM KUTNÁ HORA ORE DISTRICT

[1]Richard Pažout[#]

[1]   Central laboratories, Institute of Chemical Technology Prague, Technická 5, CZ-166 28, Prague 6, Czech Republic; [#] richard.pazout@vscht.cz

Key words: lillianite homologues, gustavite, substitutions, Kutná Hora, compositional trends

## INTRODUCTION

A new, previously unknown Bi-sulphosalt mineralization has been found in the Kutná Hora polymetallic ore district, Central Bohemia, Czech Republic. The largest group of studied sulphosalt minerals belongs to the lillianite homologous series, especially gustavite.

Crystal structures of these suplhosalts consist of galena-like layers separated by Pb in a trigonal-prismatic coordination. Members of the series (homologues) are distinguished by the width of the galena-like layers (Makovicky and Karup-Møller 1977). This is expressed as the number $N$ of octahedra which can be established from the structure or from the results of chemical analyses by microprobe. Most frequent is $N = 4$ (e.g. gustavite, $^4$Gus). Especially interesting in the Kutná Hora ore district is the transition of Bi-dominant members (gustavite − ideal end member $AgPbBi_3S_6$) to Sb-dominant members (andorites - ideal end member $AgPbSb_3S_6$) in various degrees of substitutions. There are two major substitutions occurring in lillianite homologues:

1) $Ag^+ + Bi^{3+} <=> 2Pb^{2+}$, the percentage of this substitution is marked as $L_{\%}$, ($Gus_{100}$).

2) $Bi^{3+} <=> Sb^{3+}$, is given as Bi/(Bi+Sb). So Bi-pure ideal gustavite is $^4Gus_{100}^{100}$.
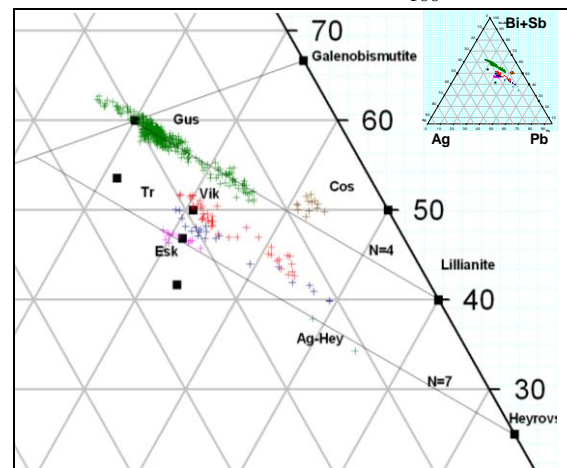


Fig. 1. Ternary diagram of the system $(Bi_2S_3+Sb_2S_3)$ - $Ag_2S$ - PbS showing the gustavite substitution $Ag^+ + (Bi,Sb)^{3+} \leftrightarrow 2Pb^{2+}$ (gustavite - lillianite solid solution) in 426 point analyses of lillianite homologues with Bi > Sb from Kutná Hora. Green - gustavite-lillianite solid solution - points with $N = 4$ ($^4$L), red - vikingite solid solution - points with $N = 5.5$ ($^{4.7}$L), blue - treasurite solid solution - points with $N = 6$ ($^{4,8}$L), violet - eskimoite solid solution - points with $N = 7$ ($^{5,9}$L), ), light blue - heyrovskyite solid solution - points with $N = 7$ ($^{7,7}$L), brown - cosalite.

## TYPES OF GUSTAVITE

Oversubstituted gustavite $Gus_{103.4-113.1}$ was found in 5 samples (26 points analyses). It is characterized by high Sb content $(Bi/(Bi+Sb) = 0.62-0.75$. No Sb-free oversubstituted gustavite was found. Example $Gus_{113}$:
$Ag_{1.09}Pb_{0.84}(Bi_{2.13}Sb_{0.97})_{3.10}S_{5.97}$
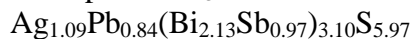
"Normal" gustavite $Gus_{85-100}$ is the most frequent (320 point analyses). Average N = 4.01, average $Bi/(Bi+Sb) = 0.74$ (0.51 – 0.97). The Bi-richest samples have the composition $Gus_{90-98}$.

Undersubstituted gustavite $Gus_{60-85}$. Although a miscibility gap was proposed to exist between $Gus_{55}$ and $Gus_{85}$ [10], gustavite with this composition was determined in 57 point analyses which are characterized by low Sb contents with average $Bi/(Bi+Sb) = 0.86$. Example $Gus_{62}$:
$Ag_{0.64}Pb_{1.74}(Bi_{2.30}Sb_{0.26})_{2.56}S_{6.05}$
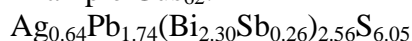
## TRENDS

Concerning the relations between the gustavite substitution $(Ag + (Bi, Sb) = Pb)$ and chemical N and Sb content within individual multicompositional grains (three or more different gustavite or andorite compositions within one grain with no phase boundary), two major and several weak trends have been observed in analyzed samples (Tab. 1).

|         | Sb | L% | N | Typical of |
|---------|----|----|----|------------|
| trend A | ↑  | ↑  | ↓  | gustavite (Bi>Sb) |
| trend B | ↑  | ↓  | ↑  | andorite (Sb>Bi) |
| trend C | ↑  | →  | →  |            |
| trend D | ↑  | ↑  | →  |            |

Tab. 1. Trends observed within multicompositional grains of gustavite and andorite

The trends concerning the increasing Sb for Bi substitution (i.e. decreasing $Bi/Bi+Sb$ ratio) in relation to the gustavite substitution, L% and $N_{chem}$ are hereafter denoted as trends A, B,C and D: Trend A -

with Sb content increasing (↑), L% increases (↑), N decreases (↓)
Trend B - with Sb ↑, L% ↓, N ↑. Trend C - with Sb ↑, L% does not change (→), N does not change (→), and trend D - with Sb ↑, L% ↑, N →. Trends A and B are most common, trends C and D are less frequent.
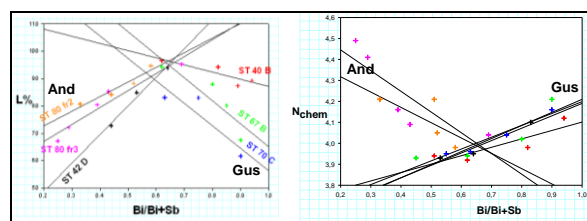


Fig. 2. Trends within multicompositional grains of gustavite and andorite. Left diagram: Sb content vs. L%: Sb increases - L% increases, typical of gustavite; Bi increases L% increases - typical of andorite. Right diagram: Sb content vs. N: Sb increases - N increases, typical of andorite; Bi increases N increases - typical of gustavite.

Trend A is the most frequently encountered and is typical of gustavite compositions (Bi > Sb) within one grain. There is a positive correlation between Sb content and the extent of gustavite substitution (oversubstituted gustavite is Sb-rich), simultaneously accompanied by the decrease of N.

Trend B is typical of andorite compositions (Sb > Bi) within one grain and it is an exact opposite of the trend A, with L% decreasing with increasing Sb (fizelyite is poorer in Bi than quatrandorite), accompanied by the increase of N.

## REFERENCES

MAKOVICKY, E., KARUP-MØLLER, S. (1977): Chemistry and crystallography of the lillianite homologous series, part I. General properties and definitions. *N. Jb. Mineral. Abh.* **130**, 265–287.

# NICKEL, CHROMIUM AND COBALT – BEARING MINERALS IN VARIOUS ULTRABASIC ROCKS OF LOWER SILESIA (SOUTHWESTERN POLAND)

[1]Artur Pędziwiatr[#], [1]Jakub Kierczak,
[2]Jarosław Waroszewski

[1]   University of Wrocław, Institute of Geological Sciences, 30 Cybulskiego St., 50-205 Wrocław, Poland, [#]artur.pedziwiatr@ing.uni.wroc.pl
[2]   Wrocław University of Environmental and Life Sciences, Department of Soil Sciences and Environmental Protection, 25/27 C.K. Norwida St., 50-375 Wrocław, Poland

Key words: ultrabasic rocks, serpentine soils, weathering, nickel, chromium, cobalt

## INTRODUCTION

The weathering of ultrabasic rocks (peridotites and serpentinites) leads to formation of specific soils named as serpentine soils which are characterized by low Ca/Mg ratio and low content of nutrients such as: N, P and K. Serpentine soils contain also significant amounts of trace elements, especially: Ni, Cr and Co. All these characteristics cause that soils developing on ultrabasic rocks are infertile and toxic to plants. Thus, identification of Ni, Cr, Co-bearing minerals in ultrabasic rocks is important as a first step in assessment of mobility and bioavailability of trace elements in related soils (Massoura et al. 2006). Olivines, pyroxenes and serpentines are major Ni-bearing phases in ultrabasites (Morrison et al. 2009). Olivines and pyroxenes are more susceptible to weathering than serpentines thus mobility of elements in soils may depend on type of ultrabasic parent material. The major minerals containing elevated Cr concentrations are chromite, magnetite and clinochlore (Morrison et al. 2004). Chromium-bearing minerals are generally resistant to weathering, thus mobility of this element is lower than mobility of Ni (Kierczak et al. 2007; Morrison et al. 2004).

The aims of our study were: (1) to identify Ni, Cr, Co-bearing phases in various types of ultrabasic rocks from Lower Silesia (southwestern Poland), (2) to present and compare chemical composition of these minerals from investigated rocks (peridotites and serpentinite).

## RESULTS

We examined three different ultrabasic rocks from the Fore Sudetic Block (Szklary Massif and Radunia) and from the Sudetes (Żmijowiec). Ultrabasites from Szklary Massif and Radunia are represented by serpentinised peridotites, whereas this from Żmijowiec is classified as serpentinite.

Serpentinised peridotite from Szklary Massif is composed of olivine (35-40 vol. %), serpentine (40-50 vol. %) and tremolite (10-15 vol. %) as major minerals. Chromium-magnetite (8-10 vol. %) and

clinochlore (5 vol. %) are minor components of this rock. Serpentinised peridotite from Radunia contains serpentine (48 vol. %) and olivine (40 vol. %) as major minerals. Minor components of studied rock is magnetite (11 vol. %), whereas diopside (1 vol. %) and clinochlore (< 1 vol. %) are accessory. Serpentinite from Żmijowiec is mainly composed of serpentine (97 vol. %) with accessory magnetite (3 vol. %).

Principal Ni-bearing phases in all studied ultrabasites are magnetites and Cr-magnetites. The highest Ni concentration is observed for Cr-magnetite from Szklary Massif (average 0.78 wt. %) whereas magnetite from Radunia contains approximately 0.68 wt. %. Magnetite from Żmijowiec is relatively Ni-poor comparing to these from two other sites and average Ni concentration in this mineral is 0.27 wt. %. Olivine and serpentine also constitute a source of Ni in studied rocks. These minerals contain much lower concentrations of Ni comparing to magnetites but they are volumetrically major constituents of ultrabasites, thus they are also important Ni carriers. Olivines from both peridotites are characterized by similar Ni content (approximately 0.23 wt. %). Serpentine from peridotites contains similar amounts of Ni (approximately 0.17 wt. %), whereas this from Żmijowiec lower concentrations of Ni (0.1 wt. %). Magnetite is the most important Cr-bearing mineral in all studied rocks. Magnetites from Szklary Massif and Radunia, contain approximately 8.73 and 7.91 wt. % of Cr respectively, whereas this from Żmijowiec is characterized but distinctly lower Cr concentrations (approximately 4.76 wt. %). Clinochlore is identified as a second Cr-bearing mineral in studied rocks. Average Cr concentration in clinochlore from Szklary Massif is 0.7 wt. %, whereas in ultrabasite from Radunia it is slightly lower (approximately 0.55 wt. %).

Similarly to the previously described trace elements, cobalt is mostly bound in magnetite. This element is distributed in similar concentrations in all studied ultrabasites and reaches up to 0.7 wt. % in magnetite from Radunia.

## CONCLUSIONS

Our study shows that among all minerals identified in investigated utrabasites, magnetites contain the highest concentrations of Ni, Cr and Co. However, because of the fact that they are resistant to weathering, mobility of trace elements from these minerals is rather limited. Olivines and serpentines also contain important concentration of Ni. Furthermore, they are major phases in all studied ultrabasic rocks and display higher susceptibility to weathering. Hence, olivine and serpentine both represent a potential source of Ni in serpentine soils.

Serpentine and magnetite from peridotites contain higher concentrations of Ni and Cr than serpentine and magnetite from serpentinite. Thus, higher potential environmental risk related with Ni contamination of serpentine soils is connected with peridotites than serpentinites.

## REFERENCES

KIERCZAK, J., NEEL, C., BRIL, H. & PUZIEWICZ, J. (2007): Effect of mineralogy and pedoclimatic variations on Ni and Cr distribution in serpentine soils under temperate climate. *Geoderma*, **142** (1-2), 165–177.

MASSOURA, S. T., ECHEVARRIA, G., BECQUER, T., GHANBAJA, J., LECLERC-CESSAC, E. & MOREL, J. L. (2006): Control of nickel availability by nickel bearing minerals in natural and anthropogenic soils. *Geoderma*, **136**(1-2), 28–37.

MORRISON, J. M., GOLDHABER, M. B., LEE, L., HOLLOWAY, J. M., WANTY, R. B., WOLF, R. E. & RANVILLE, J. F. (2009): A regional-scale study of chromium and nickel in soils of northern California, USA. *Applied Geochemistry*, **24**(8), 1500–1511.

# CRYSTAL CHEMISTRY OF THE SAMARSKITE – GROUP MINERALS: IMPLICATIONS FOR THE CLASSIFICATION

[1]Adam Pieczka[#]

[1] Department of Mineralogy, Petrography and Geochemistry, AGH - University of Science and Technology, Mickiewicza 30, 30-059 Kraków, Poland; [#] pieczka@agh.edu.pl

Key words: samarskite group, crystal-chemical relationships, classification

The samarskite group (SG) comprises a group of commonly completely metamict and pervasively altered U–Y–*REE*–Fe–Ca niobates of general stoichiometry $ABO_4$ (Sugitani et al. 1985; Warner and Ewing 1993). Both *A* and *B* sites have octahedral coordination and are distinct one from another by different sizes of occupants. The *A* site is occupied by greater $U^{4+}$, $Th^{4+}$, $Y^{3+}$, $REE^{3+}$, $Fe^{2+}$, $Fe^{3+}$ and $Ca^{2+}$ cations with minor $Na^+$, $Mg^{2+}$, $Al^{3+}$, $K^+$, $Mn^{2+}$, $Zr^{4+}$, $Sn^{4+}$, $W^{6+}$ and $Pb^{2+}$, whereas the *B* site is predominantly occupied by $Nb^{5+}$, minor $Ta^{5+}$ and $Ti^{4+}$ (Nillsen 1970; Sugitani et al. 1985; Warner and Ewing 1993). Iron can be present as $Fe^{2+}$ and $Fe^{3+}$ in the *A* site, except a Nb+Ta+Ti deficiency in the *B* site supplemented by, at least, a part of $Fe^{3+}$. $Fe^{2+}$ or $Fe^{3+}$ can even predominate the *A*-site population, however, the respective end-members are not distinguished, mainly because the $Fe^{2+}$ and $Fe^{3+}$ contents calculated by charge-balance may represent *post*-metamictization values (Hanson et al. 1998). $Ti^{4+}$ is commonly related to the *B* site, but in the case of a high sum of the *B*-site cations, it can be also located at the *A* site (Sugitani *et al*. 1985; Warner and Ewing 1993). As $Nb^{5+}$ is almost always the dominant *B*-site cation, mineral species in the SG are defined by the predominant *A*-site cation (Hanson et al. 1999): $U^{4+}$ in **ishikawaite**, (U,Fe,Y,Ca)(Nb,Ta)O₄ (Kimura 1922; Fleischer and Mandarino 1995), $Y^{3+}+REE^{3+}$ in **samarskite-(Y)**, (Y,*REE*,U,Fe³⁺)(Nb,Ta)O₄ (Sugitani *et al*. 1985, Hanson et al. 1988; 1989), $Yb^{3+}+Y^{3+}+$

$REE^{3+}$ in **samarskite-(Yb)**, (Yb,Y,*REE*,U,Ca,Fe²⁺)NbO₄ (Simmons et al. 2006), and $Ca^{2+}$ in **calciosamarskite**, (Ca,Fe,Y)(Nb,Ta,Ti)O₄ (Ellsworth 1928, Fleischer and Mandarino 1995). The crystal-chemical relationships between the *A*- and *B*-site cations have been studied on a set of 494 EMP analyses, representing minerals of the SG in term of canonical values CV1 and CV2 of the *three-group model* (Ercit 2005). The set comprised 189 analyses of SG minerals originated from the Piława pegmatitic system in the Góry Sowie block, Poland; 295 analyses of Warner and Ewing (1993); 5 analyses of Hanson et al. (1998); 4 analyses of Hanson et al. (1999); and the analysis of type samarskite-(Yb) (Simmons et al. 2006). All compositions were normalized in relation to 4 O *apfu*, with the assumption of valence charge-balance and such a value of $Fe^{3+}/Fe_{total}$ ratio to reduce excesses in the cation totals over two structurally available sites. In the case, when a cation total was close to, but still higher than 2 *apfu*, even if the entire Fe were assigned to $Fe^{3+}$, an additional, necessary portion of $O^{2-}$ was attributed to a small content of $OH^-$ to reduce the remaining surpluses to 2 *apfu*. In the calculations, $W^{6+}$ has been accepted as the *B*-site cation in accord to the wolframite structure model of SG minerals. Considered the presence of $W^{6+}$ in $Fe^{2+}$-rich, Ca-free, but also in $Fe^{2+}$-poor, Ca-rich compositions, the substitution (1) $^A(Fe^{2+}/Ca^{2+}) + {}^BW^{6+} \rightarrow {}^AR^{3+} + {}^BR^{5+}$ was accepted as responsible for the $^BW^{6+}$ presence. The balance of total cations' charge only by $O^{2-}$ allows to

derive the following substitutions of the *A*- and *B*-site cations: (2) $^A R^{2+} + {}^A R^{4+} \leftrightarrow 2\,{}^A R^{3+}$

(3) $^A R^{2+} + {}^{A,B} R^{5+} \leftrightarrow {}^A R^{3+} + {}^{A,B} R^{4+}$

(4) $^A R^{3+} + {}^{A,B} R^{5+} \leftrightarrow {}^A R^{4+} + {}^{A,B} R^{4+}$.

For compositions with Nb+Ta+W ≤ 1 *apfu* no significant excess of $R^{2+}$ ($Ca^{2+}$) should exist, which may question the existence in nature of calciosamarskite species, except a possibility created by the substitution:

(5) $^A R^{2+}(Ca^{2+}) + OH^- \rightarrow {}^A R^{3+}(Y^{3+}, REE^{3+}) + O^{2-}$
Crystal-chemical relationships $^A R^{2+}$–$^A R^{3+}$, $^A R^{3+}$–$^A R^{4+}$ and $^A R^{4+}$–$^A R^{2+}$ display data points disseminate along the lines 1:2, 2:1 and 1:1, respectively, with small displacements below or above the tie-lines as results from the substitutions (3) and (4) in the *A* and *B* sites. The displacements can be easily corrected according to the equations, what result in transfers of the data sets nearer, or even on the tie-lines. Plotting in the $^A R^{2+}$–$^A R^{3+}$–$^A R^{4+}$ triangle locates the data points along the tie-line $R^{3+}$–$(R^{2+}_{0.5} R^{4+}_{0.5})$ that marks the trend of the main substitution (2) standing in members of the SG, with deviations below the tie-line or above it as previously. The compositions allowing the fitting to the samarskite formula only with $Fe_{total} = Fe^{3+}$ and assumption of $OH^-$ show the highest deviations from the direction. If equation (2) is accepted as the main substitution at the *A*-site, we can present the composition of a SG mineral with Nb+Ta+W = 1 *apfu* in the form $^A(R^{3+}_{a} R^{2+}_{(1-a)/2} R^{4+}_{(1-a)/2})$ $^B(Nb,Ta,W)O_4$, where *a* denotes the content of 3-valent cations, and *(1-a)/2* content of $R^{2+}$ cations is already corrected by the substitution (1). The composition defines stoichiometry of two groups of end-members, $R^{3+}NbO_4$ and $(R^{2+}_{0.5} R^{4+}_{0.5})NbO4$ forming a solid solution corresponding to the SG. In consequence, end-members in the SG should be definied as $(Y_{0.5}Fe^{3+}_{0.5})NbO_4$ on the one hand, and $(U_{0.5}Fe^{2+}_{0.5})NbO_4$ and $(U_{0.5}Ca_{0.5})NbO_4$ on the other, because $(Y,REE)NbO_4$ and $FeNbO_4$ correspond already to the fergusonite and ixiolite groups, respectively. Substitution (5) marks the last possible trend of compositional evolutions of SG minerals to members of the pyrochlore group as the main alteration products, accordingly to the equation $2YNbO_4 + 2Ca^{2+} + 2OH^- = 2CaNbO_3\,OH$ $(=Ca_2Nb_2O_7 \cdot H_2O) + 2Y^{3+} + 2O^{2-}$. It can be related to an excess of $Ca^{2+}$ cations not coupled with $^A R^{4+}$ in species forming the group, and the apparent presence of $OH^-$ at the anionic sites of partly altered SGM. Stoichiometry of the defined end-members corresponds to the following general formula $A^1A^2Nb_2O_8$ already earlier supposed by Warner and Ewing (1993), where $A^1$ and $A^2$ denote two coupled lattice positions preferred by *A*-site cations with larger and smaller ionic radii, respectively.

REFERENCES

ELLSWORTH, H. V. (1928): A mineral related to samarskite from the Woodcox Mine, Hybla Ontario. *Am. Mineral.* **13**, 63–65.

ERCIT, T. S. (2005): Identification and alteration trends of granitic-pegmatite-hosted (Y,REE,U,Th)–(Nb,Ta,Ti) oxide minerals: a statistical approach. *Can. Mineral.* **43**, 1291–1303.

FLEISCHER, M. & MANDARINO, J. A. (1995): Glossary of Mineral Species 1995. *Min. Rec.* Tuscon, Arizona, 280 p.

HANSON, S. L., SIMMONS, W. B. JR. & FALSTER, A. U. (1998): Nb–Ta–Ti oxides in granitic pegmatites from the Topsham pegmatite district, Southern Maine. *Can. Mineral.* **36**, 601–608.

HANSON, S. L., SIMMONS, W. B., FALSTER, A. U., FOORD, E. E. & LICHTE, F. E. (1999): Proposed nomenclature for samarskite-group minerals: new data on ishikawaite and calciosamarskite. *Min. Mag.* **63**, 27–36.

KIMURA, K. (1922): Ishikawaite: a new mineral from Ishikawa, Iwaki. *J. Geol. Soc., Tokyo* **29**, 316–320 (in Japanese).

NILSSEN, B. (1970): Samarskites: Chemical composition, formula and crystalline phases produced by heating. *Norsk Geol. Tidsskrift,* **50**, 357–373.

SIMMONS, W. B., HANSON, S. R. & FALSTER, A. U. (2006): Samarskite-(Yb): A New species of the samarskite group from the Little Patsy pegmatite, Jefferson County, Colorado. *Can. Mineral.* **44**, 1119–1125.

SUGITANI, Y., SUZUKI, Y. & NAGASHIMA, K. (1985): Polymorphism of samarskite and its relationship to other structurally related Nb-Ta oxides with the αPbO$_2$ structure. *Am. Mineral.* **70**, 856–866.

WARNER, J. K. & EWING, R. C. (1993): Crystal chemistry of samarskite. *Am. Mineral.* **78**, 419–424.

# EXPANDING THE KNOWLEDGE OF $U^{6+}$ MINERAL TOPOLOGIES

[1]Jakub Plášil[#]

[1]       Institute of Physics, ASCR, v.v.i., Na Slovance 2, Praha 8, 182 00, Czech Republic, [#]plasil@fzu.cz

Key words: uranyl, crystal structure, topology, isomerism

## INTRODUCTION

$U^{6+}$ minerals and compounds, containing in their structures uranyl ion, $UO_2^{2+}$, are important products of uraninite and spent nuclear fuel weathering (Plášil 2014). The crystal chemistry of $U^{6+}$, which is crucial for knowledge of physico-chemical properties of these phases, underwent extensive step forward in last two decades (Burns et al. 1997; Burns 2005; Krivovichev and Plášil 2013). Recently, several new $U^{6+}$ minerals were discovered, providing us new insights into the complex structure topologies.

## $U^{6+}$ CRYSTAL CHEMISTRY − GENERAL REMARKS

$U^{6+}$ forms most frequently two triple axial U-O bonds, resulting in which results in formation of a uranyl ion, $[UO_2]^{2+}$. This, in turn, can further be coordinated in the equatorial plane by four, five or six ligands, leading to square, pentagonal, or hexagonal bipyramidal coordination, respectively. The geometrical characteristics for these coordinations have been reviewed in detail by Burns et al. (1997) and Burns (2005), giving the typical bond lengths for the distinct coordination geometries. In general, the strong directional anisotropy of bond distribution observed in the typical uranyl coordination geometries favors the formation of low-dimensional structures, consisting of 2D layers, or 1D chain structures of U-oxide bonds, with a strong prevalence of layered structures. The structural sheets or layer of polymerized $U^{6+}$-coordination polyhedra usually contains additional cations most commonly coordinated in tetrahedral anionic groups (as $SO_4^{2-}$, $PO_4^{3-}$, $AsO_4^{3-}$, $SiO_4^{4-}$).

The topologies of the structural units of $U^{6+}$ minerals and compounds can be represented by corresponding graphs (Burns et al. 1996; Burns 1999, 2005), in order to simplify and classify them.

## SELDOM TOPOLOGIES OF $U^{6+}$ MINERALS

Topologically unique sheet was found in the structure of mathesiusite, $K_5(UO_2)_4(SO_4)_4(VO_5)(H_2O)_4$ (Plášil et al. 2014a), an extremely rare mineral from Jáchymov. It is based upon $[(UO_2)_4(SO_4)_4(VO_5)]^{5-}$ clusters, which arise from linkages between corner-sharing quartets of uranyl pentagonal bipyramids, defining a square-shaped void at the center, occupied by $V^{5+}$. The very similar sheets were found in synthetic uranyl chromates, containing $Li^+$, $Mg^{2+}$ and $(NH_4)^+$ (Unruh et al. 2012). These differ from mathesisusite sheet in orientation of vertices of

tetrahedral elements; they are geometrical isomers. The sheet in synthetic Cs-uranyl-tungstate (Sykora et al. 2004) is then a topological isomer. The similar way of adoption of $W^{5+}$ polyhedra into the structure was found also in the infinite chain in synthetic $Rb^+$ uranyl tungstate (Alekseev et al. 2006),

Crystal structures of meisserite, $Na_5(UO_2)(SO_4)_3(SO_3OH)(H_2O)$ (Plášil et al. 2013b), bluelizardite, $Na_7(UO_2)(SO_4)_4Cl(H_2O)_2$ (Plášil et al. 2014b) and belakovskiite, $Na_7(UO_2)(SO_4)_4(SO_3OH)(H_2O)_3$ (Kampf et al. 2013), the new minerals from Blue Lizard mine in Utah, USA, are unique among minerals, although, some of the topological features has been observed yet in structures of inorganic compounds. Structure of meisserite is based upon infinite $[(UO_2)(SO_4)_3]$ chains, similar to these observed in synthetic uranyl molybdates (Krivovichev and Burns 2003). Bluelizardite is interesting in particular for $Cl^-$ present in the structure and it possesses $[(UO_2)_2(SO_4)_8]$ cluster, similar to the cluster found in $Na^+$-$Tl^+$-uranyl molybdate (Krivovichev and Burns 2003). Structure of belakovskiite contains isolated $(UO_2)(SO_4)_4$ cluster. This cluster is topological isomer to the clusters found in synthetic uranyl sulfates (e.g., Hayden and Burns 2002) containing a bidentate linked $SO_4$ tetrahedra.

REFERENCES

ALEKSEEV, E. V., KRIVOVICHEV, S. V., DEPMEIER, W., ARMBRUSTER, T., KATZKE, H., SULEIMANOV, E. V. & CHUPRUNOV, E. V. (2006): One-dimensional chains in uranyl tungstates: Syntheses and structures of $A_8[(UO_2)_4(WO_4)_4(WO_5)_2](A = Rb, Cs)$ and $Rb_6[(UO_2)_2O(WO_4)_4]$. *J. Solid State Chem.* **179**, 2977-2987.

BUNRS, P. C. (2005): $U^{6+}$ minerals and inorganic compounds: Insights into an expanded structural hierarchy of crystal structures. *Canad. Mineral.* **43**, 1839-1894.

BURNS, P. C., EWING, R. C. & HAWTHORNE, F. C. (1997): The crystal chemistry of hexavalent uranium: Polyhedron geometries, bond-valence parameters, and polymerization of polyhedra. *Can. Mineral.* **35**, 1551-1570.

HAYDEN, L. A. & BURNS, P. C. (2002): A novel uranyl sulfate cluster in the structure of $Na_6(UO_2)(SO_4)_4(H_2O)_2$. *J Solid State Chem.* **163**, 313-318.

KAMPF, A. R., PLÁŠIL, J., KASATKIN, A. V. & MARTY, J. (2013): Belakovskiite, IMA 2013-075. CNMNC Newsletter 18, December 2013, page 3252. *Min. Mag.* **77**, 3249-3258.

KRIVOVICHEV, S. V. & BURNS, P. C. (2003): Crystal chemistry of uranyl molybdates. VIII. Crystal structures of $Na_3Tl_3[(UO_2)(MoO_4)_4]$, $Na_{13}Tl_3[(UO_2)(MoO_4)_3]_4(H_2O)_5$, $Na_3Tl_5[(UO_2)(MoO_4)_3]_2(H_2O)_3$ and $Na_2[(UO_2)(MoO_4)_2](H_2O)_4$. *Can. Mineral.* **41**, 707-720

PLÁŠIL., J., KAMPF, A. R., KASATKIN, A. V., MARTY, J., ŠKODA, R., SILVA, S. & ČEJKA, J. (2013b): Meisserite, $Na_5(UO_2)(SO_4)_3(SO_3OH)(H_2O)$, a new uranyl sulfate mineral from the Blue Lizard mine, San Juan County, Utah, USA. *Min. Mag.* **77**, 2975-2988.

PLÁŠIL, J., KAMPF, A. R., KASATKIN, A. V. & MARTY, J. (2014a): Bluelizardite, $Na_7(UO_2)(SO_4)_4Cl(H_2O)_2$, a new uranyl sulfate mineral from the Blue Lizard mine, San Juan County, Utah, USA. *J. Geosci.* **58**,

SYKORA, R. E., McDANIEL, S. M. & ALBRECHT-SCHMITT, T. E. (2004): Hydrothermal synthesis and structure of $K_6[(UO_2)_4(CrO_4)_7]$ $6H_2O$: A layered uranyl chromate with a new uranyl sheet topology. *J. Solid State Chem.* **177**, 1431-1436.

UNRUH, D.K., QUICKSALL, A., PRESSPRICH, L., STOFFER, M., QIU, J., NUZHDIN, K., WUB, W., VYUSHKOVA, M. & BURNS, P. C. (2012): Synthesis, characterization, and crystal structures of uranyl compounds containing mixed chromium oxidation states. *J Solid State Chem.* **191**, 162-166.

# MINERALOGICAL AND PETROGRAPHICAL CHARACTERIZATION OF FABOVA HOĽA GRANITOID COMPLEX (WESTERN CARPATHIANS)

[1]Libor Pukančík[#], [1]Martin Ondrejka

[1] Comenius University in Bratislava, Faculty of Natural Sciences Department of Mineralogy and Petrology, [#] pukancik@fns.uniba.sk

Key words: granitoid rocks, Fabova Hola, monazite dating, petrology

## INTRODUCTION

Fabova hoľa granitoid complex is a part of Kráľova hoľa zone, Veporic Unit, Western Carpathians, Slovakia. The studied area is 15 square km large and consists mainly of granitoid rocks. There were 8 samples analyzed by microprobe in State Geological Institute of Dionýz Štúr in Bratislava.

## RESULTS

Petrographical study has confirmed the presence of four basic types of granitoid rocks which have I- and S-type affinity according to SIAM classification of granitoid rocks.

The first type is represented by mainly granites to granodiorites of the Vepor type (e.g. FAH-2) which dominate in the area. This type consist of porphyric, white to gray K-feldspar often perthitized, baueritized sagenitic biotite muscovite, quartz, and altered albitic plagioclases. Accessory minerals of the Vepor type granitoids include zircon, fluorapatite, monazite-(Ce), allanite, epidote-clinozoisite and sagenitic titanite (chain-dispersed titanites in biotite).

The second type of studied rocks is represented by equigranular, medium grained biotite granodiorites of the Ipeľ type (e.g. FAH-6), which are slightly deformed and contain weakly perthitic white K-feldspars, quartz, albitic plagioclases which are completely sauseritizied, strongly baueritizied biotite with sagenitic titanite inclusions, muscovite + sericite. The accessory mineral assemblage is represented by zircon, fluorapatite, monazite-(Ce), sagenitic titanite, rutile, epidote-clinozoisite.

The third type of granitoids is represented by porphyritic biotite granodiorites of the Ipeľ type (e.g. FAH-4) with large euhedral phenocrysts of pinkish K-feldspars. Quartz forms anhedral, occasionally subhedral to euhedral grains, with distinct deformation and undulatory extinction. Albitic plagioclase is moderately sericitized biotite, epidote-clinozoisite and muscovite is also present. Identified accessory minerals are represented by zircon, fluorapatite, monazite-(Ce), allanite, epidote, titanite, magnetite, ilmenite, pyrite and goethite.

Finally, the fourth type is represented by Sihla type granodiorites to tonalites (e.g. FAH-8), which have a relatively

homogeneous mineral composition, represented by greenish plagioclase, moderately chloritized biotite aggregates show distinct pleochroism of greenish to brown colour. Accessory assemblage is represented by large euhedral primary titanite, post-magmatic dendritic titanite II., euhedral allanite, zircon, fluorapatite and magnetite.

In addition to the basic mineralogical and petrological characteristics of rock-forming and accessory minerals and the study of their chemical composition there were made more than 170 spot analyses used for monazite dating. Calculated ages confirm the expected Carboniferous (Lower Mississippian) age of granitoids (Fig. 1): 346±7 Ma (FAH-5) and 353±4 Ma (FAH-7). In the sample FAH-7 there were also confirmed younger alpine reworking event.
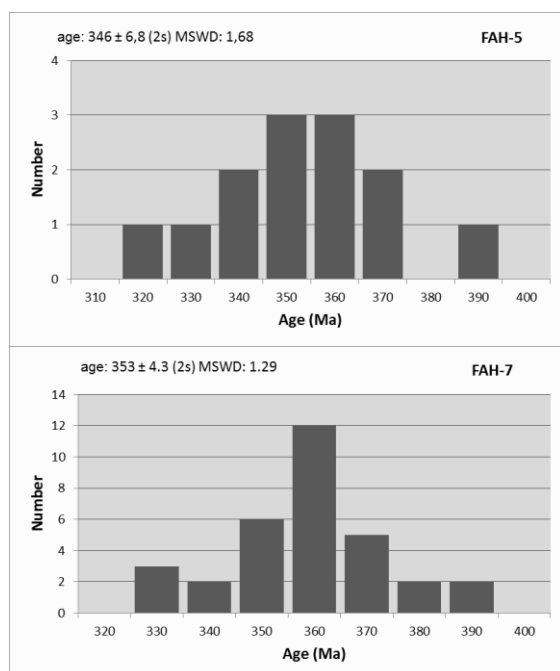
Fig. 1. Diagrams showing calculated Carboniferous ages in samples FAH-5 and FAH-7.

# MINERALOGICAL STUDY OF SYNTHETIC AND NATURAL TRIPUHYITE FESBO4

[1]Petra Rusinová [#], [1]Gabriela Kučerová,
[1]Bronislava Voleková–Lalinská

[1] Comenius University in Bratislava, Faculty of Natural Sciences, Department of Mineralogy and Petrology, Mlynská dolina, 842 15 Bratislava, Slovakia, [#]rusinova@fns.uniba.sk

Key words: tripuhyite, synthesis, Fe:Sb molar ratio, Powder X-ray diffraction, Electron microprobe, XRD microdiffraction

## INTRODUCTION

The first description of tripuhyite comes from cinnabar-bearing gravel of Tripuhy Ouro Preto, Minas Gerais, Brazil (Husak and Prior 1897). The chemical formula of mineral is $Fe^{3+}Sb^{5+}O_4$, the crystal structure is tetragonal, with the space group $P4_1/mnm$, unit cells are: $a = 4.63$ Å, $c = 3.06$Å, $V = 65.43$ Å$^3$, $Z = 2$ (Berlepsch et al. 2003). Natural tripuhyite has yellowish brown, lemon-yellow, brown-black color and forms fibrous to fine-grained aggregates of crystal. In natural occurrences, tripuhyite is a product of stibnite and pyrite alteration in the oxidation zone of some hydrothermal antimony deposits, on supergene tailings, dumps and mines. It contains high concentration of both Fe and Sb, and forms in slightly alkaline or neutral pH conditions (Mitsunobu et al. 2011, Majzlan et al. 2011).

The physical and chemical properties of Sb-accumulating ferric oxides have been investigated to a limited extent. Even for tripuhyite, there is no available data for the solubility and stability for the bulk and nanoparticulate solids. Therefore, further research involving both field and laboratory study is needed.

This contribution reports the study of tripuhyite grains synthesised under different conditions (Fe, Sb, As content in solution, temperature, time), and compares chemical composition of these grains with natural specimens from Čučma deposit.

## EXPERIMENTAL

Tripuhyite was synthesized following the method of Diemar (2008). Aqueous solutions was mixed from $(NH_4)_2\mathbf{Fe}(SO_4)_2 \cdot 6H_2O$ and $K\mathbf{Sb}(OH)_6$:

$$Fe(NH_4)_2(SO_4)_2 \cdot 6H_2O + KSb(OH)_6 \rightarrow \mathbf{\underline{FeSbO_4}} + H_2SO_4 + H_2O + (NH_4)_2SO_4$$

## RESULTS

Synthesized tripuhyite was identified by the powder XRD; the patterns were consistent with published data of pure tripuhyite. Experimental studies have confirmed the ability of tripuhyite crystallization from the solution of various chemical compositions. The most consistent molar ratio for the crystallization of tripuhyite is Fe : Sb 1 : 2 (Fig. 1), which is in accordance to data of

Diemar (2008). The bulk concentrations of major elements measured by the electron microprobe are summarized in Tab. 1.

| Synthetic samples | | |
|---|---|---|
| | *Fe:Sb 1:2* | *Incorporation of As* |
| **Fe** | 16.97 – 23.53 wt% | 13.82 – 05.16 wt% |
| **Sb** | 42.16 – 55.27 wt% | 52.02 – 54.43 wt% |
| **As** | – | up to 1.8 wt % |
| Natural samples | | |
| **Fe** | 7.42 – 47.18 wt% | |
| **Sb** | 12.36 – 46.85 wt% | |
| **As** | up to 3.88 wt% | |

Tab. 1: Contents of Fe, Sb and As in tripuhyite samples

Preliminary studies showed the ability of tripuhyite to incorporate As from solution with consequent reduction of the Fe content and increase of the Sb content in the final product (Tab.1).

The incorporation of As into crystal structure changes observed lattice parameters and unit cell volume in these samples (V = 65.43–66.35 A$^3$). The correlation coefficient between the major elements documents a high negative correlation between (Sb + As) and Fe (r = -0.9361). A comparison of the Sb–Fe and As–Fe relationship shows that the decrease in Fe content is more dependent on an increase in the As content, which has a higher negative correlation to Fe (r = -0.9218).

The crystallization of tripuhyite was confirmed at wide range of pH values (1–10) and temperature of environment. Variability of Fe and Sb in natural samples of tripuhyite from the Čučma deposit is displayed in Fig. 1 and Tab.1. Studied tripuhyite grains have higher contents of Ca, Mg and Pb. Tripuhyite was identified with XRD microdiffraction.

We expect that increased Fe content in the solution could result in the crystallization of goethite. In contrast, Sb oxides would probably crystallize with the increased proportion of Sb in solution.

However, we have not yet been able to confirm this assumption in laboratory conditions.

REFERENCES

BERLEPSCH, P., ARMBRUSTER, T., BRUGGER, J., CRIDDLE, A.J., GRAESER, S. (2003): Tripuhyite, FeSbO$_4$, revisited. *Min. Mag.* **67**, 1, 31-46.
DIEMAR, G. A. (2008): Supergene dispersion of antimony and geochemical exploration model for antimony ore deposits, PhD. Thesis, 25 p.
HUSSAK, E., PRIOR, G. T. (1897): On tripuhyite, a new antimonate of iron, from Tripuhy, Brazil. *Min. Mag.* **11**, 302-303.
MAJZLAN, J., LALINSKÁ, B., CHOVAN, M., BLÄSS, U., BRECHT, B., GÖTTLICHER, J., STEININGER, R., HUG, K., ZIEGLER, S. & GESCHER, J. (2011): A mineralogical, geochemical, and microbiogical assessment of the antimony- and arsenic-rich neutral mine drainage tailings near Pezinok, Slovakia. *Am. Mineral.* **96**, 1-13.
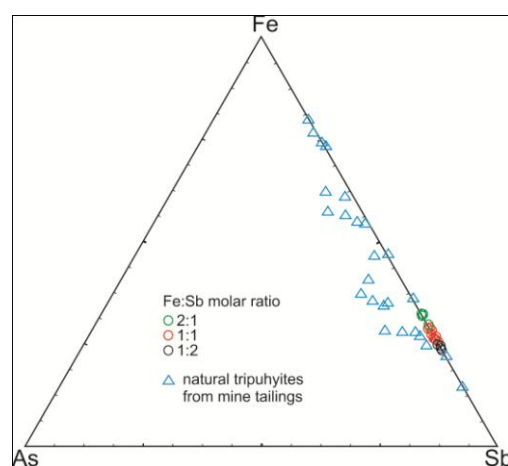


Fig 1. Ternary diagram showing relative Fe, As, and Sb content in natural and synthetic tripuhyite grains.

# ASSOCIATION OF HG AND TL SELENIDES FROM THE URANIUM DEPOSIT ZÁLESÍ, RYCHLEBSKÉ HORY MOUNTAINS, CZECH REPUBLIC

[1]Jiří Sejkora, [1,2]Ivo Macek,
[1]Pavel Škácha, [1,3]Petr Pauliš, [4]Vlastimil Toegel

[1] Department of Mineralogy and Petrology, National Museum, Cirkusová 1740, Praha 9, CZ-193 00, Czech Republic; [#]jiri_sejkora@nm.cz
[2] Dept. of Geological Sciences, Masaryk University, Kotlářská 2, CZ-611 37 Brno, Czech Republic
[3] Smíškova 564, Kutná Hora, CZ-284 01, Czech Republic
[4] Medlov 251, CZ-783 91, Uničov, Czech Republic

Key words: Hg selenides, Tl selenides, Cu selenides, EPMA data, Zálesí deposit, Czech Republic

## INTRODUCTION

The abandoned small uranium deposit Zálesí is situated near the southern margin of the Zálesí settlement, about 6.5 km SW of Javorník in the Rychlebské hory Mountains, Czech Republic. The deposit was discovered during the regional uranium exploration and mined from Galleries I. - III. on five levels at vertical intervals 50 m. Over 400 t of uranium was worked-out there during 11 years (1958-1968). The studied samples were collected on the mine dumps in the area of outcrops of the Pavel structure during several past years.

## GEOLOGY

Thirty hydrothermal veins and two stockworks are hosted by the folded and metamorphosed Paleozoic sequence of the Strónia Group belonging to the Orlice-Snieznik crystalline complex. The primary mineralization of the deposit originated in three mineralization stages - uraninite, arsenide and sulphide and can be classified as close to the so-called "five-element" formation (U-Ni-Co-As-Ag). Majority of the primary Se mineralization is related to the uraninite stage, the occurrence of Bi selenides (ikunolite - laitakarite) in bismuth of the arsenide stage was found sporadically only (Fojt et al. 2005). The primary and supergene Se mineralization of this ore deposit were recently studied by Fojt, Škoda (2005), Pauliš et al. (2006), Sejkora et al. (2004, 2006, 2011, 2012), and Topa et al. (2010).

## METHODS OF STUDY

Polished samples mounted in the epoxy resin were studied using the ore microscope Nikon ME600L (National Museum, Prague) and the quantitative chemical data were collected with the electron microprobe Cameca SX100 in the wavelength dispersive mode (National Museum, Prague).

## RESULTS

**Tiemannite** is abundant in the studied samples; it forms grains up to 1 mm in size; association with hakite, eukairite, klockmannite, Ag-Cu-Tl selenides and molybdomenite was observed. Tiemannite usually contains minority contents of Cu (up to 0.10 *apfu*; 2.27 wt %). Empirical formula: $(Hg_{0.99}Cu_{0.02})_{\Sigma1.01}(Se_{0.98}S_{0.01})_{\Sigma0.99}$.

**Hakite** was found as rare irregular grains up to 100 μm in tiemannite aggregates; umangite and molybdomenite were also found in the association. Empirical formula: $(Cu_{9.21}Ag_{0.39})_{\Sigma9.60}(Hg_{1.97}Zn_{0.03})_{\Sigma2.00}(Se_{12.93}S_{0.09})_{\Sigma13.02}$.
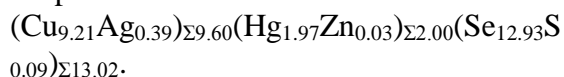
**Ag-Cu-Tl selenide** forms very rare irregular grains up to 80 μm in size in association with eukairite, umangite and tiemannite. Its chemical composition is not directly corresponding to any known mineral phase in Cu-Tl-Se system (bukovite, crookesite, sabatierite). Its metals/Se ratio (1.77) is close to sabatierite ($Cu_6TlSe_4$) but it differs in significant Ag contents (10.80-14.91 wt. %). The determined Ag contents correlate negatively with both Tl and Cu. Empirical formula: $Cu_{4.99}Ag_{1.09}Tl_{0.95}Se_{3.98}$.

**Eucairite** occurs as grains up to 100 μm in association with Ag-Cu-Tl selenide, umangite, tiemannite and molybdomenite. It contains minor contents of Tl up to 0.24 wt%. Empirical formula: $Cu_{1.01}Ag_{1.03}Se_{0.96}$.

**Klockmannite** forms irregular grains up to 200 μm in tiemannite aggregates. It usually contains minority contents of Ag (up to 0.06 *apfu*; 4.32 wt %) and Hg (up to 0.02 *apfu*; 2.74 wt %). Empirical formula: $(Cu_{0.98}Ag_{0.02})_{\Sigma1.00}(Se_{0.96}S_{0.04})_{\Sigma1.00}$.

**Umangite** was found as irregular grains up to 100 μm in size which partly replaces older eukairite and Ag-Cu-Tl selenide; tiemannite was also observed in the association. Empirical formula: $Cu_{3.00}(Se_{1.98}S_{0.02})_{\Sigma2.00}$.

REFERENCES

FOJT, B., DOLNÍČEK, Z., KOPA, D., SULOVSKÝ, P. & ŠKODA, R. (2005): Paragenesis of the hypogene associations from the uranium deposit at Zálesí near Rychlebské hory Mts., Czech Republic. *Čas. Slez. Muz. Opava (A)*, **54**, 223-280. (in Czech)

FOJT, B. & ŠKODA, R. (2005): $Bi_4Se_3$ and ikunolite-laitakarite from the uranium deposit Zálesí near Javorník, the Rychlebské hory Mts. *Acta Mus. Moraviae, Sci. geol.* **90**, 99-107. (in Czech)

PAULIŠ, P., ŠKODA, R. & NOVÁK, F. (2006): Demesmaekerite from uranium deposit Zálesí in the Rychlebské hory Mts. (Czech Republic). *Acta Mus. Moraviae, Sci. geol.* **91**, 89-95. (in Czech)

SEJKORA, J., PAULIŠ, P. & MALEC, J. (2004): The supergene selenium mineralization at the uranium deposit Zálesí, the Rychlebské hory Mts. (Czech Republic). *Bull. mineral.-petrolog. Odd. Nár. Muz. (Praha),* **12**, 174-179. (in Czech)

SEJKORA, J., ŠKODA, R. & PAULIŠ, P. (2006): Selenium mineralization of the uranium deposit Zálesí, the Rychlebské hory Mts., Czech Republic. *Miner. Polonica, Spec. Papers,* **28**, 196-198.

SEJKORA, J., MAKOVICKY, E., TOPA, D., PUTZ, H., ZAGLER, G. & PLÁŠIL, J. (2011): Litochlebite, $Ag_2PbBi_4Se_8$, a new selenide mineral species from Zálesí, Czech Republic: description and crystal structure. *Can. Mineral.* **49**, 639-650.

SEJKORA, J., PLÁŠIL, J., LITOCHLEB, J., ŠKÁCHA, P. & PAVLÍČEK, R. (2012): A selenide association with macroscopic umangite from the abandoned uranium deposit Zálesí, Rychlebské hory Mountains (Czech Republic). *Bull. mineral.-petrolog. Odd. Nár. Muz. (Praha)*, **20**, 187-169. (in Czech)

TOPA, D., MAKOVICKY, E., SEJKORA, J. & DITTRICH, H. (2010): The crystal structure of watkinsonite, $Cu_2PbBi_4Se_8$, from the Zálesí uranium deposit, Czech Republic. *Can. Mineral.* **48**, 1109-1118.

# TRACE ELEMENTS IN BOHEMIAN GARNETS

[1,2]Jan Soumar[#], [1,3]Roman Skála,
[3]Šárka Matoušková

[1]    Institute of Geochemistry, Mineralogy and Mineral Resources, Faculty of Science, Charles University, Albertov 6, 128 43 Prague 2, Czech Republic, [#] jansoumar@centrum.cz
[2]    Department of Mineralogy and Petrology, National Museum, Cirkusová 1740,193 00 Prague 9, Czech Republic
[3]    Institute of Geology, AS CR, v.v.i., Rozvojová 269, 165 00 Prague 6, Czech Republic

Key words: garnet, trace elements, REE, Bohemia

## INTRODUCTION

Samples from traditional Bohemian garnet localities (Třebívlice, Kuzov (Central Bohemian Uplands)), Zadní Ždírnice, Vestřev (Krkonoše Piedmont Basin)), and other locations (Bořetice, Ratboř (Kolín area)) were analyzed for contents of trace elements. Shape of the REE curve normalized to CI chondrite can indicate the source rock of the peridotitic garnet − lherzolite or harzburgite.

## METHODS

Samples were analyzed in the Laboratory of Geological Processes at the Institute of Geology AS CR, Prague using a sector field ICP-MS (inductively coupled plasma − mass spectrometer) ELEMENT 2 (ThermoFisher Scientific) with a New Wave UP213 laser ablation system.

## SOURCE ROCKS

The source rocks of garnets in the Central Bohemian Uplands are described as predominant garnet lherzolites with some wehlites and dunites (Kopecký and Paděra 1974 in Seifert and Vrána 2005). Vrána (2008) describes the source rock in the Kolín area as olivine-rich pyropic ultramafic rock often with lherzolite composition. Source rock of garnets from the Krkonoše Piedmont Basin is unknown; however, garnet composition is characteristic for garnet peridotite Martínek and Štolfová (2009).

## RESULTS

Chondrite normalized REE pattern in all analyzed samples shows a typical curve for lherzolitic garnets with significantly depleted LREE, gradual increase through MREE and a plateau of enriched HREE (Fig. 1), which confirms information published so far. The enrichment or depletion can also be illustrated by normalizing the measured contents to a primitive mantle garnet composition, e.g., garnet from lherzolite xenolite J4 from Jagersfontein (Stachel et al. 1998) (Fig. 2). In this case the values fluctuate around the primitive mantle garnet composition with the exception of LREE that are

substantially depleted. The garnet from Kuzov shows the strongest depletion especially in cerium.

Concentrations of other trace elements increase with their increasing distribution coefficient (Stachel et al. 1998). Chondrite normalized pattern shows depletion for Ba (mostly below the detection limit), Rb, Sr, and enrichment in Ti, Zr and Y (Fig. 3).
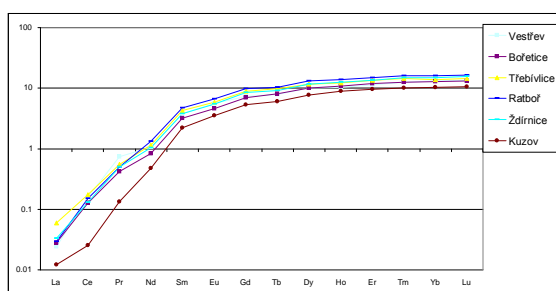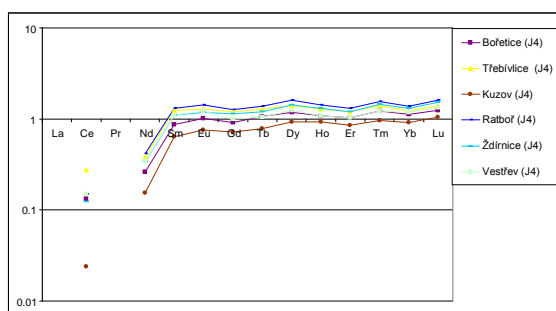


Fig. 1. REE normalized to chondrite CI.



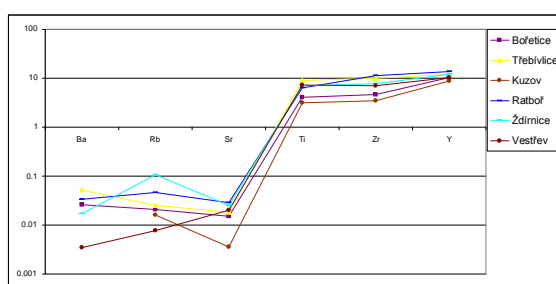Fig. 2. REE normalized to a primitive mantle garnet composition from lherzolite xenolite J4.



Fig. 3. HFSE normalized to chondrite CI.

REFERENCES

KOPECKÝ, L., PADĚRA, K. (1974): Baenderung der ultramafitischen Gesteine in der Bohrung T-7 Staré bei Třebenice (Nordboehmen). *Minerogenesis*. Bulgarian Academy of Sciences (Geological Institute), Sofia, 161–169.

MARTÍNEK, K., ŠTOLFOVÁ, K. (2009): Provenance study of Permian non-marine sandstones and conglomerates of the Krkonoše Piedmont Basin (Czech Republic): exotic marine limestone pebbles, heavy minerals and garnet composition. *Bulletin of Geosciences,* **84**, (3), 555–568.

SEIFERT, A. V., VRÁNA, S. (2005): Bohemian garnet. *Bulletin of Geosciences*. Vol. **80**, No. 2 113–124.

STACHEL, T., VILJOEN, K. S., BREYA, G., HARRIS, J. W. (1998): Metasomatic processes in lherzolitic and harzburgitic domains of diamondiferous lithospheric mantle: REE in garnets from xenoliths and inclusions in diamonds. *Earth and Planetary Science Letters,* **159**, 1–12.

VRÁNA, S. (2008): Mineral inclusions in pyrope from garnet peridotites, Kolín area, central Czech Republic. *Journal of Geosciences,* **53**, 17–30.

# GEOCHEMISTRY OF THE GRANITE PORPHYRY FROM ĽUBIETOVÁ CRYSTALLINE COMPLEXES (WESTERN CARPATHIANS)

[1]Ján Spišiak[#], [2]Pavel Siman

[1] Faculty of Natural Sciences, Matej Bel University, Tajovského 40, 97401 Banská Bystrica, Slovakia[#] jan.spisiak@umb.sk

[2] Geological Institute, Slovak Academy of Sciences, Dúbravská cesta 9, P.O. Box 106,840 05 Bratislava 45, Slovakia

Key words: granite porphyre, crystalline complexes, geochemistry, Rb/Sr, Western Carpathians

## INTRODUCTION

In the space of the Ľubietová zone, granite porphyry, locally even granodiorite porphyrite, creates several NE-SW oriented bodies (Fig. 1).
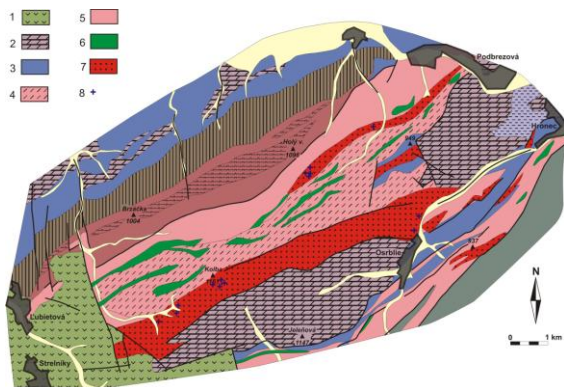


Fig. 1 simplified geological sketch of Ľubietová crystalline complexes; 1 – volcanic rocks (Badenian- Sarmatian), Veporic unit: 2 – Ramsau dolomite (Middle Triassic): 3 – quartzites, sandstones and conglomerates (Lower Triassic) 4 – paragneisses (Lower Palaeozoic), 5 – mylonitized orthogneisses (Lower Palaeozoic) 6 – amphibolites (Lower Palaeozoic), 7 granite porphyries, 8 – study samples.

We took samples from three areas: Ľubietová, Predajňanské Čelno and Osrblie. All samples are similar in petrographic composition. Their mineral compositions are simple: phenocrysts are composed mainly of quartz (partly magmatic resorbed), rarely altered biotites and plagioclases, and the matrix is composed of sericite, fine-grained quartz and feldspars.

From geochemical point of view these rocks have a peraluminous character and compositions between rhyolites – trachydacites and dacites (Fig. 2).
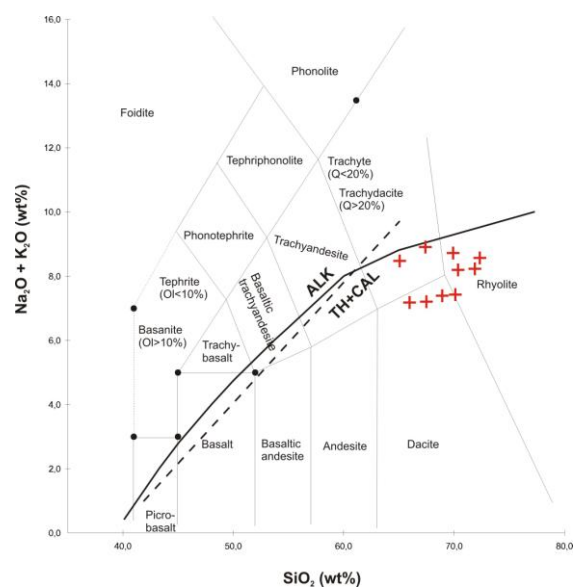


Fig. 2 TAS diagram for granite porphyry from Ľubietová crystalline complexes.

Based on the other geochemical characteristics, the studied rocks correspond to volcanic-arc granites, and/or syn-collisional granites (Fig. 3).
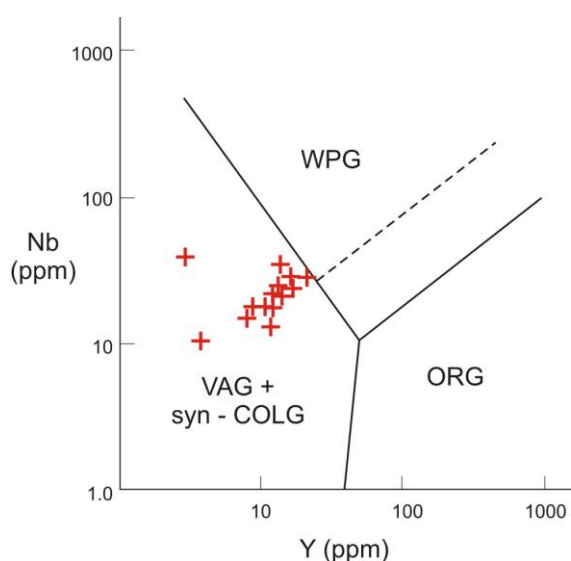


Fig. 3 The Nb-Y and Rb–(Y+Nb) discrimination diagrams for granites (after Pearce et al. 1984); WPG–within–plate granites, VAG–volcanic arc granites, syn-COLG–syn-collisional granites, ORG–ocean ridge granites.

The occurrences of these rocks in Upper Permian conglomerates in the Predajná basalt strata according Vozárová (1979) suggest a Lower Permian age. The most precise dating is with grant porphyry zircon from the area of Kelemen tunnel in Predajňanské Čelno – 273±4 Ma (Vozárová et al. 2010). Broska et al. (1993) point to a similarity of volcanite zircon typology Harnobis series and porphyrite–microgranite from Kelemen tunnel in Predajňanské Čelno. Monazite dating from granite porphyry from Osrblie (vz. NT-4) showed a Middle Permian age, and/or magma generating in the Guadalupian 265±9 Ma, Bezák et al. (2008). Our most recent dating of Rb/Sr isotopic system at 184±9 Ma (analyzed at IGEM Moscow, Philips PW-2400), falling within the Lower Jurassic, represents the age of the last thermal and tectonic event in the Ľubietová crystalline complex, which reached the closing temperature of Rb/Sr isotopic system. The initial ratio is $^{87}Sr/^{86}Sr$ = 0.709320. So, considering the previous findings in the age of granite porphyries 273±4 Ma (Vozárová et al. 2010), 265±9 Ma (Bezák et al. 2008) and Rb/Sr 184±9 Ma (our own finding), we can assume that in the Lower Jurrassic, there occurred a thermal event connected with re-activation of the age of these porphyries. This event may have been connected with the evolution of the Meliata Ocean.

REFERENCES

BEZÁK V., BROSKA, I., KONEČNÝ, P., PETRÍK, I. & KOŠLER, J. (2008): Permský magmatický komplex v severnom veporiku: interpretácia z nových datovaní kyslých magmatitov. *Min. Slov.* **40**, 127–134.

BROSKA, I., VOZÁR, J., UHER, P., JAKABSKÁ, K. (1993): Typológia zirkónu z permských ryolitov-dacitov a ich pyroklastík. In: RAKÚS, M. - VOZÁR, J. (eds.): Geodynamický model a hlbinná stavba Západných Karpát. Vyd. GÚDŠ Bratislava, 151–158. (in Slovak).

PEARCE, J. A., HARRIS, N. B. W., TINDLE, A. G. (1984): Trace element discrimination diagrams for tectonic interpretation of granitic rocks. *J. Petrol.* **25**, 956–983.

PETRÍK, I. (1996a): Genetická interpretácia ortorúl, migmatitov a granitoidov ľubietovského pásma Veporika. Čiastková záverečná správa, MS, Archive GSSR, Bratislava, 18. (in Slovak)

UHER, P., PUTIŠ, M., ONDREJKA, M., KOHÚT, M. & SERGEEV, S. (2008): Postorogenne granity typu A v Západných Karpatoch–nove výsledky datovania zirkonu metódou SHRIMP. *Min. Slov.* **40**, Geovestník. (in Slovak)

VOZÁROVÁ, A., LEPEKHINA E., VOZÁR, J., RODIONOV, N. (2010): In situ U-Pb (SHRIMP) zircon age dating from the Permian volcanites of the Northern Veporicum. ŠGÚDŠ, Bratislava, Conference Proceedings, 49 p.

# REE MINERALS FROM PHONOLITE IN THE MECSEK MTS., HUNGARY

[1]Sándor Szakáll[#], [1]Norbert Zajzon,
[2]Béla Fehér

[1]   Institute of Mineralogy – Geology, University of Miskolc, Miskolc, Hungary,
[#]askszs@uni-miskolc.hu
[2]   Herman Otto Museum, Miskolc, Hungary

Key words: REE-minerals, phonolite, Mecsek Mts.

## INTRODUCTION

Lower Cretaceous alkali magmatism is known in the Mecsek Mts., South Hungary, which has a differentiated series from basalt to phonolite (Harangi 1994). The rare earth element (REE) concentration is increased during the magmatic differentiation (Huemer 1997). As part of a bigger project we investigated the REE content of the phonolites, especially focused on mineralogical (electron microprobe (EPMA) and X-ray diffraction (XRD)) investigations of REE minerals. This is the first detailed mineralogical investigation on REE minerals of the phonolite.

## RESULTS AND DISCUSSION

The phonolites contain the highest amount of $\sum$REE+Y (550–600 ppm) among the different magmatites from the area, according to our ICP-MS data. The phonolite is enriched in LREE and shows negative Eu anomaly in the spider diagram (Fig. 1) of the chondrite normalized values (Anders and Grevesse 1989).
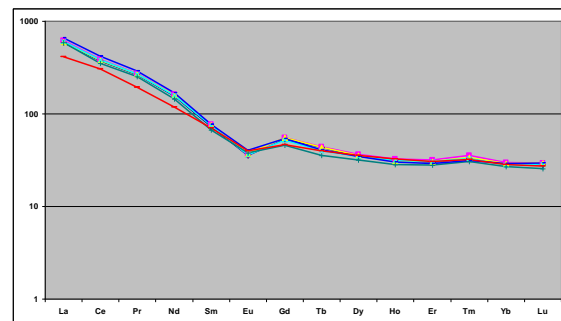


Fig. 1. Chondrite normalized (Anders and Grevesse 1989). REE values of the Mecsek phonolites. The red line represents an altered phonolite sample.

Detailed mineralogical investigation was performed on phonolites from the Szászvár-Hosszúhetény area. Numerous REE minerals were identified (Tab. 1) by EPMA and XRPD (many for the first time from the area).

| Oxides | |
|---|---|
| Aeschynite-(Ce) | $(Ce,Ca,Fe,Th)(Ti,Nb)_2(O,OH)_6$ |
| Fluornatro-pyrochlore | $(Na,Pb,Ca,Ce,U)_2Nb_2O_6F$ |
| *REE-rich Mn-oxide* | |
| | |
| **Carbonates** | |
| Ancylite-(Ce) | $SrCe(CO_3)_2(OH)\cdot H_2O$ |
| Bastnäsite-(Ce) | $(Ce,La)F(CO_3)$ |
| Calcioancylite-(Ce) | $(Ca,Sr)Ce_3(CO_3)_4(OH)_3\cdot H_2O$ |

| | |
|---|---|
| Lanthanite-(Ce) | $(Ce,La)_2(CO_3)_3 \cdot 8H_2O$ |
| | |
| **Phosphates** | |
| Cheralite | $CaTh(PO_4)_2$ |
| Monazite-(Ce) | $(Ce,La,Nd,Th)PO_4$ |
| Monazite-(La) | $(La,Ce,Nd,Th)PO_4$ |
| *REE-rich apatite* | |
| | |
| **Silicates** | |
| Bafertisite | $Ba(Fe,Mn)_2TiOSi_2O_7(OH,F)_2$ |
| Britholite-(Ce) | $(Ce,Ca)_5(SiO_4,PO_4)_3(OH,F)$ |
| Calciocatapleiite | $CaZrSi_3O_9 \cdot 2H_2O$ |
| Cerite-(Ce) | $(Ce,Ca)_9(Mg,Fe)Si_7(O,OH,F)_{28}$ |
| Eudialyte | $Na_4(Ca,Ce)_2(Fe^{2+},Mn^{2+})$ $ZrSi_8O_{22}(OH,Cl)_2$ |
| Joaquinite-(Ce) | $Ba_2NaCe_2FeTi_2Si_8O_{26}(OH) \cdot H_2O$ |
| Nacareniobsite-(Ce) | $Na_3Ca_3(Ce,La)(Nb,Ti)(Si_2O_7)_2$ $OF_3$ |
| *REE-rich smectite* | |
| *unknown Ca-Na-Zr-silicate* | |

Tab. 1. REE-containing minerals from phonolite, Mecsek Mts.

10–30 µm subhedral or anhedral crystals of monazite-group minerals, REE-rich apatite, britholite-(Ce) and fluornatropyrochlore represent the primary REE-mineral phases of the rock, beside the dominant rock-forming minerals (alkali pyroxenes, nepheline, K-feldspars and albite).

This primary assemblage was remobilized by hydrothermal fluids forming new REE-phases in the miarolitic cavities and among the crystals. REE-containing carbonates, such as ancylite-(Ce), calcioancylite-(Ce), lanthanite-(Ce), bastnäsite-(Ce) and silicates: joaquinite-(Ce), nacareniobsite-(Ce), cerite-(Ce) were formed during this process. Chemical zoning is common in both the carbonates and silicates. This involves partial substitution of different REEs and also the substitution of Nb for Ti, but sometimes substitution of Ca by U and Th was also observed. The hydrothermally formed REE-phases have a crystal size of 40–60 µm, which is bigger than the size of the primary REE-phases. The joaquinite-(Ce) aggregates have biggest size (400–600 µm)

and they are characteristic in the miarolitic cavities (Fig. 2). They are usually accompanied by Na-containing zeolites (natrolite, analcime).



Fig. 2. Joaquinite-(Ce) (pale grey), Nb-rich joaquinite-(Ce) (dark grey) and ancylite-(Ce) (white) from Köves Hill, Hosszúhetény. BSE image.

The second remobilization of the REE is happened because of surface weathering. The REE accumulates in supergene minerals, such as smectites and Mn-oxides. Even REE-zoned smectites were observed in the samples.

REFERENCES

ANDERS, E. & GREVESSE, N. (1989): Abundances of the elements: meteoritic and solar. *Geochimica et Cosmochimica Acta,* **53**, 197-214.

HARANGI, SZ. (1994): Geochemistry and petrogenesis of the Early Cretaceous continental rift-type volcanic rocks of the Mecsek Mountains, South Hungary. *Lithos,* **33**, 303-321.

HUEMER, H. (1997): Multistage evolution of a volcanic suite in the Eastern Mecsek Mountains, Southern Hungary. *Mineralogy and Petrology,* **59**, 101-120.

# PRELIMINARY DATA ON EXTREMELY EVOLVED MIAROLITIC NYF PEGMATITE OF THE STRZEGOM – SOBÓTKA MASSIF, SUDETES, SW POLAND

[1]Eligiusz Szełęg[#], [2]Adam Szuszkiewicz,
[3]Marcus Waelle

[1] Faculty of Earth Sciences, University of Silesia, Sosnowiec, Poland, [#]eligiusz.szeleg@us.edu.pl
[2] Institute of Geological Sciences, University of Wrocław, Wrocław, Poland
[3] Institute of Geochemistry and Petrology, ETH, Zurich, Switzerland

## INTRODUCTION

The Strzegom-Sobótka massif is located in the central part of the Sudetes at the NE margin of the Bohemian Massif about 50 km SW from Wrocław. It is a Late-Variscan post-tectonic shallow-level pluton built of granodiorite, monzogranite and two-mica granite. The hornblende-biotite monzogranite, that constitutes its western part, is associated with miarolitic pegmatites (Janeczek 2007 and references therein). The pegmatites show rare-element enrichment and contain a number of NYF-signature minerals including fluorite, fergusonite, formanite, tantalaeschynite, allanite, gadolinite, topaz, amazonite and others (Szełęg and Galuskina 2010). Typically they display high fluorine and low boron activities. The pegmatites range from primitive to highly evolved though no systematic investigations on chemical fractionation trends have been carried out so far.

## SAMPLES AND RESULTS

For the study we have chosen Li-Fe-Mn mica, microcline and columbite-group minerals (CGM) from the topaz-bearing pegmatite that, to our knowledge, represents the most evolved Strzegom pegmatite ever described (Szełęg and Szuszkiewicz 2010). The pegmatite vein consists of miarolitic cavities hosting quartz, microcline, albite and micas accompanied by topaz, phenakite, schorl-dravite, fluorite, zeolites and others. The cavities, up to 30x100 cm large, are surrounded by blocky feldspar, graphic and marginal biotite-rich granitic zones grading into the granite host. The studies were carried out using EMPA and LAICPMS.

**Microcline** samples include amazonite (Ab < 3.3 %) from the graphic zone and 4 cavity-grown creamy crystals (Ab < 2.9 %). Significant trace elements concentrations are (in ppm): Rb=1784-5136, Cs=7-141, Ba < 180, Ga=7-66 and Tl=12-50. Amazonite has less Cs (7-42 ppm) and more Pb (159-269 ppm) than other samples (Pb=8-119 ppm). K/Rb is from 74.9 to 25.9 and Rb/Cs from 27.2 to 76.3 (67.8-329.8 in amazonite) (Fig. 1). The cavity-grown Li-Fe-Mn mica shows well-pronounced colour zoning from purple core to yellow-brownish oscillatory rim. It contains (in wt %) 40.56-51.06 $SiO_2$, 19.19-23.40 $Al_2O_3$, 2.63-10.40 MnO, 2.11-9.61 FeO, 2.49-5.63 $Li_2O$, < 0.13 MgO, 8.38-10.33 $K_2O$, 1.39-4.67 $Rb_2O$ and < 0.32 $Na_2O$, $^{IV}Al/^{IV}Si$ changes from 0.34 to 0.15 and $^{VI}Al$ remains roughly constant at 1.03-0.94 *apfu* (calculated to 22 cations). The composition corresponds to **Fe-rich polylithionite-masutomilite** (Fig. 2) and to

our knowledge reaches the highest known Mn concentration of that series (Tischendorf et al. 2007 and references therein).
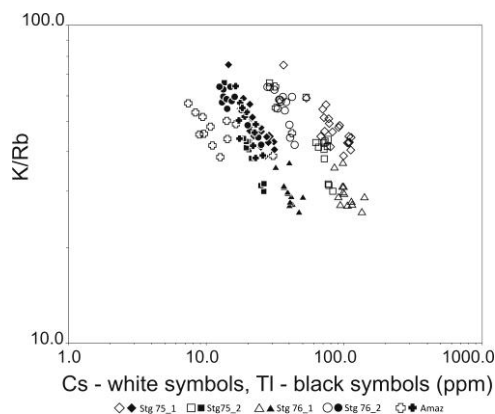


Fig. 1. K/Rb vs Cs and Tl fractionations in microcline. Amaz–amazonite, Stg–cavity-grown normal microcline.
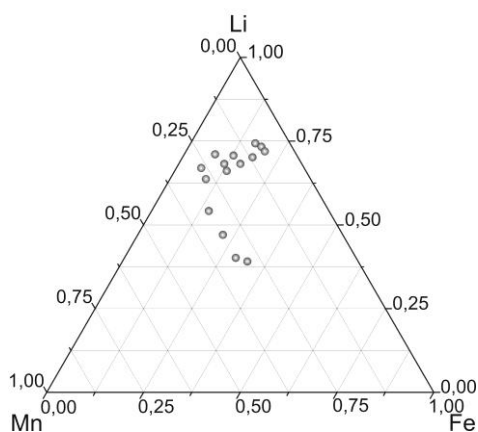


Fig. 2. Li-Fe-Mn octahedral site occupancy in masutomilite-Fe-rich polylithionite; $^{VI}Al$ almost constant at 1.03-0.94 *apfu* (calculated to 22 cations).

The mica is very rich in F: 5.31-7.76 wt % (1.24-1.67 *apfu*). The mica shows also elevated concentrations (in ppm) of 364-5258 Cs, 9-113 Be, 33-114 Ga, 52-198 Tl, 5-114 Nb, 3-56 Ta and 25-231 Sn as well as minor B, Sc, P and Pb. Fractionation indices are high: K/Rb=1.6-6.7, K/Cs=15.1-210.9 and Nb/Ta=0.2-2.1.

**CGM** are present within the cavities and the adjacent blocky feldspars zone. The older generation is represented by columbite-(Mn) (Fig. 3) with indistinct zones and sectors enriched in Ta and W. It contains (in wt %) 15.60-18.29 MnO, 2.34-4.32 FeO, 0.10-0.26 $Sc_2O_3$, 45.47-62.96 $Nb_2O_5$, 8.78-13.72 $Ta_2O_5$, 3.60-21.99 $WO_3$, 0.04-5.05 $SnO_2$ and 0.73-1.35 $TiO_2$. The cavity-grown generation is distinctly zoned with reversed Ta-Nb and Mn-Fe fractionations from tantalite-(Mn) to columbite-(Mn) (Fig. 3). It contains 11.74-

15.34 MnO, 0.24-5.17 FeO, 0.24-0.64 $Sc_2O_3$, 13.38-59.56 $Nb_2O_5$, 12.22-57.58 $Ta_2O_5$, 1.08-22.30 $WO_3$, 0.07-12.66 $SnO_2$ and 0.82-3.50 $TiO_2$.
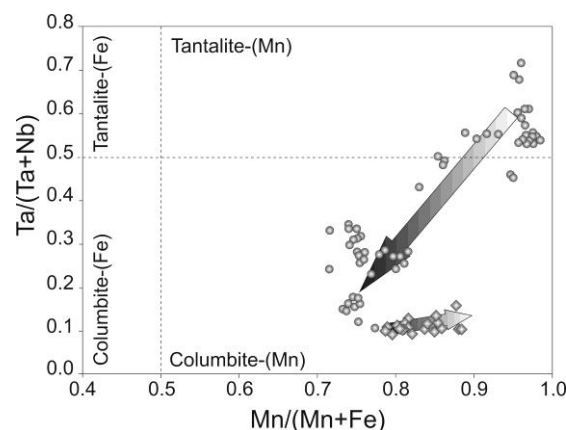


Fig. 3. Fractionation trends of CGM in the Ta/(Ta+Nb) vs Mn/(Mn+Fe) quadrilateral. Diamonds: earlier CGM, circles: cavity-grown CGM.

CONCLUSIONS

1. The described NYF pegmatite shows a very high degree of geochemical fractionation.
2. In CGM the initial increase of Mn is replaced at the pocket stage by a reversed Mn-Fe and Ta-Nb fractionation trends.
3. K-feldspar shows typical K/Rb, K/Cs and K/Tl fractionation paths.
4. The crystallization at the pocket stage took place from a fluid markedly enriched in Mn, Rb, Cs, Li, F and Be.

REFERENCES

JANECZEK, J. (2007): Intragranitic pegmatites of the Strzegom-Sobótka massif – an overview. *In* Granitoids in Poland (A. Kozłowski, J. Wiszniewska, eds). *AM Monograph*. **1**, 193-201.

SZEŁĘG, E. & SZUSZKIEWICZ, A. (2010): Topaz, lepidolite and phenakite-bearing pegmatite from Żółkiewka quarry, Strzegom-Sobótka granite massif, Lower Silesia, SW Poland. *Mineralogia-Special Papers*. **37**, 112 p

SZEŁĘG, E. & GALUSKINA, I. (2010): Mineralogy of Lower Silesia, Poland. *Acta Mineralogica-Petrographica, Field Guide Series*, **17**, 1-15.

TISCHENDORF, G., FÖRSTER, H.-J., GOTTESMANN, B. & RIEDER, M. (2007): True and brittle micas: composition and solid-solution. *Min. Mag.* **71**, 285-320.

# OCCURRENCES OF NATIVE SILVER IN URANIUM AND BASE – METAL DEPOSIT PŘÍBRAM (CZECH REPUBLIC)

[1,3]Pavel Škácha[#], [2]František Knížek,
[3]Jiří Sejkora

[1]     Mining Muzeum Příbram, Hynka Kličky Place 293, Příbram VI [#]skachap@seznam.cz
[2]     Příbram VII/127
[3]     National Museum, Cirkusová 1740, 193 00 Praha 9 – Horní Počernice

Key words: silver, dyscrasite, base-metal, uranium and base-metal deposit Příbram

## INTRODUCTION

Silver occurrences in the uranium and base-metal deposit Příbram (Czech Republic) were well-known during the whole period of mining (1948–1991), but only small parts of them were objects of exploration and following mining. On the one hand, silver was exploited from galena (in the form of isomorphous admixtures), or base-metal raw from several base-metal bearing veins in the deposit. The total amount of silver mined from this type of raw in the period 1955–1989 is 17.3 t (Collective 1990). On the other hand, silver contained in high-grade silver ores was mined in the shaft No. 21 in a total amount of 11.1 tons (Litochleb et al. 2003).

## DESCRIPTION OF SILVER LOCALITIES

Native silver was found in the uranium mine operations in Třebsko in the shaft No. 7 (Kašpar et al. 1985). Silver wires up to 3 cm growing in grey calcite gangue in association with galena and uraninite were found there. Other, smaller occurrences of silver were found in the shaft No. 3 –

Kamenná, but there are no references in available literature. Very fine samples of silver wires were found in the Lešetice shaft, its occurrence in the vein L1 is better known only (Řídkošil et al. 1992). Large silver found in the vein B117, 6th level in the shaft No. 6 – Brod is relatively well documented. Silver occurred as pseudomorphs after dyscrasite up to 15 cm in length there (Rus and Blüml 1966). Silver in the form of wires in cavities of calcite was found in the vein J152, 10th level of the shaft No. 9. Occurrence of silver and high-grade silver ores in the ore-node Háje, shaft No. 21 (mined in the years 1985–1991) was the best-documented one. Silver was found in several veins in forms of silver pseudomorphs after dyscrasite, wires, plates and impregnations in surrounding rocks in Háje. The richest vein was the H14F between the 8th and 6th level. Up to several cm long columnar silver aggregates, which are pseudomorphs – partially or completely replaced – of silver after dyscrasite are typical for this vein. The vein, originally comprised of arsenic, dyscrasite and calcite, was affected by younger solutions in lower parts (the level

of 7th floor of the mine), arsenic was leached totally and dyscrasite was replaced with a mixture of native silver and allargentum. Arsenic was preserved around the level of the 6th floor and forms matrix for silver and allargentum columnar pseudomorphs growing in calcite. Dyscrasite with both generations of intact arsenic was found just above this occurrence. Silver pseudomorphs after dyscrasite also occurred on the 7th level of the H14F3 vein (Škácha et al. 2013) and on the 10th level of the H64A vein in the shaft No. 21. Other forms of silver, especially wires or irregular aggregates, were found in the veins H14F, H14F3, H64A, H61Z and H14I. The northern occurrence of native silver appears in the vein Bt1 of the shaft No. 10, vein node Háje. It was found in the form of dull pseudomorphs after dyscrasite and wires there.

CONCLUSION

Native silver in the Příbram uranium and base-metal deposit occurs in several forms. The most interesting one is its occurrence in the form of silver pseudomorphs after prismatic dyscrasite crystals, which were found in many veins in several parts of the deposit. It was possible to observe mineralization sequence of the main minerals in these veins thanks to the knowledge of the exact position of collected specimens from the veins H14F and H14F3. The oldest is arsenic I with growing dyscrasite crystals, which were wrapped by arsenic II. Under the influence of younger solutions in deeper parts of the ore mineralized area, arsenic was partly or completely dissolved and dyscrasite was replaced by silver or other Ag-bearing minerals. Silver wires and plates are also products of these younger mineralization processes.Genesis of native silver in the uranium and base-metal deposit is explained by the regeneration of silver from the underlying galena accumulations (Petroš 1982).

REFERENCES

COLLECTIVE (1990): Závěrečná zpráva projektu předběžného průzkumu 1986-1989, komplexní uran-polymetalické ložisko Příbram, Surovina: Pb, Zn, Ag. Textová čast. MS DIAMO SUL. (in Czech)

KAŠPAR, P., ŘÍDKOŠIL, T. & ŠREIN, V. (1985): Silver-rich minerals from Třebsko near Příbram, Central Bohemia, Czechoslovakia. *N. Jb. Miner.* **1**, 19-28.

LITOCHLEB, J., ČERNÝ, P., LITOCHLEBOVÁ, E., SEJKORA, J. & ŠREINOVÁ, B. (2003): Ložiska a výskyty nerostných surovin v oblasti středních Brd a Podbrdska. *Bull. mineral.-petrolog. Odd. Nár. Muz.* **11**, 57-86. (in Czech)

PETROŠ, R. (1982): Geologická pozice nových výskytů stříbrných rud na Příbramsku. *Vlast. sbor. Podbrdska,* **22**, 39-50. (in Czech)

RUS, V. & BLÜML, A. (1966): Výskyt ryzího stříbra v jihozápadní části haťského pásma. *Věstník ÚUG*, **41**, 425-430. (in Czech)

ŘÍDKOŠIL, T., KAŠPAR, P., KNÍŽEK, F. & ŠREIN, V. (1992): Porovnání vývoje stříbrné mineralizace žíly Pošepný ve Vrančicích se zrudněním žíly L1 v Lešeticích na příbramském uranovém ložisku. *Sbor. konf. Stříbrné minerální asociace v Československu.* Donovaly, 131-135. (in Czech)

ŠKÁCHA, P., SEJKORA, J., KNÍŽEK, F., SLEPIČKA, V., LITOCHLEB, J. & JEBAVÁ, I. (2012): Výskyty unikátního monometalického stříbrného zrudnění na žíle H14F3 mezi 7. a 9. patrem šachty č. 21 Háje, příbramský uran-polymetalický revír (Česká republika). *Bull. mineral.-petrolog. Odd. Nár. Muz.* **20**, 2, 230-254.

# CONTRIBUTION TO CHEMICAL COMPOSITION OF CHALCOPHYLLITE, PSEUDOMALACHITE AND OLIVENITE GROUP MINERALS FROM ŠPANIA DOLINA – PIESKY, SLOVAK REPUBLIC

[1]Martin Števko[#], [2]Jiří Sejkora

[1]  Comenius University, Faculty of Natural Sciences, Department of Mineralogy and Petrology, Mlynská dolina, 842 15 Bratislava, Slovak Republic [#]stevko@fns.uniba.sk

[2]  Department of Mineralogy and Petrology, National Museum, Cirkusová 1740, 193 00, Prague 9, Czech Republic

Key words: chalcophyllite, cornwallite, pseudomalachite, libethenite, chemical composition, Piesky deposit, Špania Dolina, Slovak Republic

## INTRODUCTION

The Špania Dolina-Piesky deposit which is located about 10 km north of Banská Bystrica in the Starohorské vrchy Mts. (Slovak Republic), once was very important producer of copper in Europe and is also well known for rich suite of various supergene minerals, mostly copper carbonates, sulfates and arsenates. An extensive hydrothermal stockwork to impregnation ore mineralization at Piesky deposit is hosted in Late Paleozoic (Permian) sandstones and conglomerates and it is represented by two principal primary ore minerals: tetrahedrite and chalcopyrite (Michňová and Ozdín 2010, Sejkora et al. 2013). By the *in-situ* weathering of these ore minerals, especially tetrahedrite an interesting association of copper arsenates like chalcophyllite, clinoclase, cornwallite-pseudomalachite, libethenite and tangdanite was formed (Števko and Sejkora 2012). Here we would like to present preliminary results from our systematic research of three such supergene phases from Piesky deposit: chalcophyllite, minerals of pseudomalachite group and libethenite.

## METHODS

Chemical composition of supergene minerals was quantitative studied using a Cameca SX 100 electron microprobe (Laboratory of Electron Microscopy and Microanalysis of the Masaryk University and Czech Geological Survey in Brno, Czech Republic) at following conditions: accelerating voltage 15 kV, sample current 10 nA, beam diameter 5 μm. These standards and X-ray lines were used: albite (Na Kα), sanidine (K, Al Kα), $Mg_2SiO_4$ (Mg Kα), fluorapatite (P, Ca Kα), almandine (Fe Kα), spessartine (Si, Mn Kα), Ni (Ni Kα), Co (Co Kα), lammerite (As, Cu Lα), gahnite (Zn Kα), $SrSO_4$ (S Kα), vanadinite (Pb, Cl Kα) and Sb (Sb Lβ).

Chalcophyllite belongs to the most common supergene copper arsenate minerals at the studied locality. It forms well developed tabular crystals with characteristic hexagonal shape, which are up to 5 mm in size and are often associated together with azurite or barite in cavities or at fissures of mineralized rocks. The color of chalcophyllite crystals ranges from emerald green to pale green with vitreous to pearly luster and are transparent to translucent in dependence on degree of dehydration. Except Cu and Al only minor contents of Fe (up to 0.22 *apfu*) were detected in cation position of studied chalcophyllites. Much more interesting is content of Sb (up to 0.81 *apfu*) and especially P, which value is usually up to 0.29 *apfu*, but highest detected content was 1.78 *apfu*. Such high content of phosphorus in chalcophyllite is quite unusual and similar, but still lower contents of P were up to now reported just by Read (1986) from Maharahara occurrence, New Zeland. Locally also contents of Cl (up to 0.20 *apfu*) were observed in chalcophyllite from Piesky.

Minerals of the pseudomalachite group occurs at the Piesky deposit as pale to dark green botryoidal crusts up to several cm$^2$ in size, which replace and cover crystalline aggregates of older azurite or tangdanite. In the BSE images a very complex oscillatory chemical zoning is characteristic for the most of the studied specimens. This phenomenon is caused by an extensive As↔P substitution. The content of P is very variable (from 0.04 to 1.73 *apfu*) and such complex composition of pseudomalachite group minerals, which represent nearly complete solid solution between cornwallite and pseudomalachite has not yet been observed in nature.

Libethenite is rare species at the Piesky deposit. It forms well developed long prismatic crystals up to 0.8 mm with light to olive-green color, which are often grouped to the radial aggregates or crystalline crusts in cavities of mineralized rocks. Its chemical composition is characteristic by the high content of As (from 0.28 to 0.35 *apfu*), which suggests existence of at least incomplete solid solution between libethenite and olivenite.

Described supergene phases were formed by the *in-situ* weathering of tetrahedrite group minerals (tetrahedrite with minor but regular content of As), which was the main source of Cu and As. The main source of P was most probably apatite, which is accessory constituent of the mineralized rocks and it was dissolved by the acid solutions, which were produced by the decomposition of ore minerals.

REFERENCES

READ, A. J. (1986): Chalcophyllite and other rare hydroxy-sulfates from Maharahara, New Zealand. *Mineralogical Record,* **17**, 199–204.
MICHŇOVÁ, J. & OZDÍN, D. (2010): Genetic study of the primary hydrothermal mineralization in Špania Dolina and Ľubietová ore districts (Slovakia, Western Carpathians). *Acta Mineralogica-Petrographica, Abstract Ser.* **6**, 237.
SEJKORA, J., ŠTEVKO, M. & MACEK, I. (2013): Příspěvek k chemickému složení tetraedritu z Cu ložiska Piesky, rudní revír Špania Dolina, střední Slovensko. *Bull. mineral.-petrolog. Odd. Nár. Muz. (Praha)*, **21**, 89–103.
ŠTEVKO, M. & SEJKORA, J. (2012): Supergene arsenates of copper from the Piesky deposit, Špania Dolina, Central Slovakia. *Acta Mineralogica-Petrographica, Abstract Ser.* **7**, 130.

# RAMAN SPECTROSCOPY OF XENOTIME-(Y) FROM PÍSEK GRANITIC PEGMATITES

[1,2]Eva Švecová[#], [1,2]Zdeněk Losos,
[1]Renata Čopjaková, [1]Radek Škoda, [3]Jaroslav Cícha

[1]     Institute of Geological Sciences, Masaryk University, Kotlářská 2, 611 37 Brno, Czech Republic,
        [#]211679@sci.muni.cz
[2]     CEITEC, Masaryk University, Kotlářská 2, 611 37 Brno, Czech Republic
[3]     Prácheň Museum, Velké nám. 114, 397 24 Písek, Czech Republic

Key words: xenotime, recrystallization, Raman spectra, degree of metamictization, uranium, thorium, granitic pegmatites, Bohemian Massif

### INTRODUCTION

Xenotime-(Y) from the albite unit of the beryl-columbite Písek granitic pegmatites (Czech Republic) have been studied with focus on contents of U and Th and degree of metamictization via Raman spectroscopy.

### METHODS

Raman spectra of xenotime were measured by Horiba Jobin Yvon LabRam-Hr system using 473 nm laser in the region 900-1100 $cm^{-1}$ and evaluated by PeakFit v4 software package. Degree of metamictization has been estimated in terms of FWHM (full width at half maximum) values, position and intensity of the most intense Raman band (~ 995 $cm^{-1}$). Chemical composition was determined by Cameca SX100 electron microprobe.

### XENOTIME OCCURRENCE AND COMPOSITION

Primary xenotime-(Y) forms euhedral crystals (up 2 mm) usually in assemblage with tourmaline, zircon, monazite-(Ce) and Y, REE, Ti, Nb-oxides. Primary xenotime (I) has variable content of U (0.5-6.5 wt. % $UO_2$) and Th (0.2-4.1 wt. % $ThO_2$) with high U/Th ratio (1.2-4.0). Inner core (Ia) with medium U and Th content is commonly overgrown by high U, Th domain (Ib) and the outer rim (Ic) is often U, Th poor. Intermediate high U, Th zone of primary xenotime is often altered (Fig. 1). Altered domains (II) show enrichment of Th (up 9.6 wt. % $ThO_2$), Zr, Ca, Fe, F and depletion of U, Y, P with low U/Th ratio (0.1-1.3). Interaction between primary xenotime and pegmatite derived fluids led locally to the formation of secondary xenotime (III) as product of xenotime (I, II) recrystallization. Recrystallized xenotime domains at outer parts of xenotime I grains are typically full of tiny cheralite, or zircon inclusions. Moreover, altered domains (II) of primary xenotime can be partly recrystallized with occurrence of tiny secondary xenotime. Xenotime III has low $UO_2$ (0.3-2.3 wt. %) and $ThO_2$ (0.1-1.8 wt. %) contents.

### RAMAN SPECTROSCOPY RESULTS

Raman spectra of xenotime show commonly very strong doublet at 985-999 $cm^{-1}$ and 1055-1057 $cm^{-1}$ related to the internal modes of $PO_4$ group (Fig. 1).
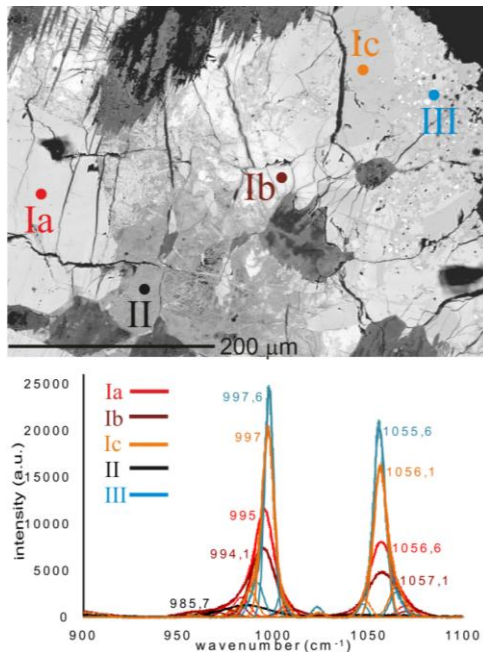


Fig. 1. BSE image and representative Raman spectra of xenotime.

According to position- values of the main peak (985-999 $cm^{-1}$), its FWHM, and intensity, the xenotime is well to poorly crystalline. Negative correlation between position (and intensity respectively) and FWHM value of the main peak (Fig. 2) reflects degree of metamictization and U and Th content in xenotime.

Primary unaltered xenotime (I) is moderately to well crystalline. The peak position shifts from 996.4-997.1 for low U, Th domain (Ic) to 991.4-994.7 $cm^{-1}$ for high U intermediate domain (Ib). With increasing U and Th content the FWHM increases (from 7.0-8.3 $cm^{-1}$ for low U, Th outer domains (Ic) to 11.1-17.8 $cm^{-1}$ for high U, Th intermediate domains (Ib) and intensity of peak decreases (Fig. 1).

Altered domains (II) of primary xenotime (Fig. 1) show peak position 985.7-996.0 $cm^{-1}$, very low peak intensity and rather high but variable FWHM values (8.2-29.5 $cm^{-1}$), which reflects their

metamict state. Secondary xenotime (III) is well crystalline with peak position of 995.3-998.5 $cm^{-1}$ and low values of FWHM (5.0-8.3 $cm^{-1}$). The intensity of this peak is high especially in inclusion rich domains compared with recrystallized xenotime in altered domains (Fig. 2).

Calculated total cumulative dose of the α-decay events (based on U and Th content in xenotime and age of 339 Ma) positively correlates with FWHM for unaltered xenotime (Ia,b,c, III). The altered domains show rather irregularly scattered behavior of the cumulative dose vs. FWHM which confirms open system for U and Th during the alteration processes.
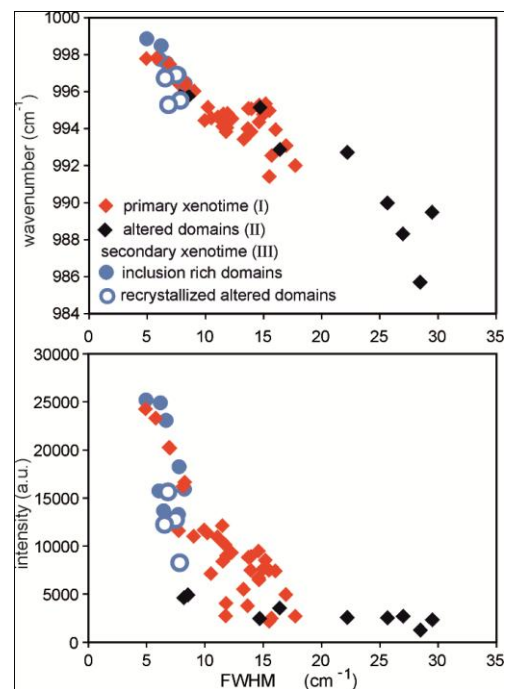


Fig. 2. Correlation between peak position, intensity of the peak and FWHM value of the main Raman peak.

# BIO-ASSISTED SYNTHESIS OF MAGNETIC FILAMENTS

[1]Éva Tompa[#], [2]Balázs Tóth,
[2]Ferenc Vonderviszt, [1]Ilona Nyirő-Kósa, [1]Mihály Pósfai

[1]  Department of Earth and Environmental Sciences, University of Pannonia, Hungary,
[#]eva.tompa88@gmail.com
[2]  Bio-Nanosystems Laboratory, University of Pannonia, Hungary

Key words: magnetite nanofibers, flagellin, Mms6 protein

## INTRODUCTION

A promising approach to synthesize nanostructured materials is to use design principles extracted from biological systems. Magnetotactic bacteria form intracellular, membrane-bound magnetic nanoparticles called magnetosomes with controlled dimensions and morphologies, and assemble them into chains. The bacteria use this magnetic system for navigating along the magnetic field lines of the Earth (Faivre and Schüler 2008). Isolated magnetosomes as well as magnetosome chains have numerous potential applications in bio- and nanotechnology (Lang et al. 2007).

At the center of our study is the idea that 1D magnetic nanostructures can be built in vitro by experimentally combining two known bacterial functions: flagellar filament formation and magnetic nanoparticle synthesis. Flagellar filaments are composed of thousands of flagellin subunits (Muskotál et al. 2010). Our strategy is to construct recombinantly expressed flagellin variants containing iron-binding motifs. The flagellins are then utilized for the construction of filaments displaying periodically repeated recognition sites on their surfaces that have strong affinity to bind iron from solution. These filaments may serve as templates for the formation of magnetite nanofibers.
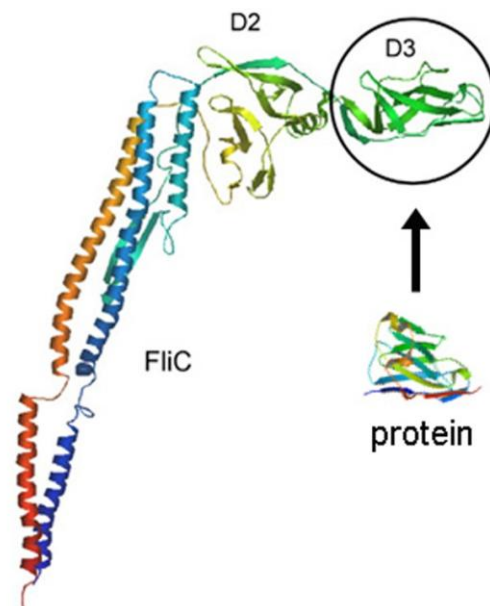


Fig. 1. Design of the FliC-Mms6Cterm fusion construct. The hypervariable D3 domain of *Salmonella* flagellin was replaced by the C-terminal part of the Mms6 protein from the magnetotactic bacterium strain *Magnetospirillum gryphiswaldense*.

## RESULTS

Several types of flagellin-based fusion proteins were created by inserting iron-binding segments, such as the C-terminal part of the Mms6 magnetosome protein that is known to be involved in magnetite synthesis in magnetotactic bacteria (Arakaki et al. 2003), in place of the highly variable D3 domain of flagellin from *Salmonella* (Fig. 1). The motility of cells having the mutagenized flagella was preserved, indicating that the folding of the flagellin protein was not affected (Fig. 2). Moreover, the mutagenized flagellin proteins were still able to self-organize *in vitro*.
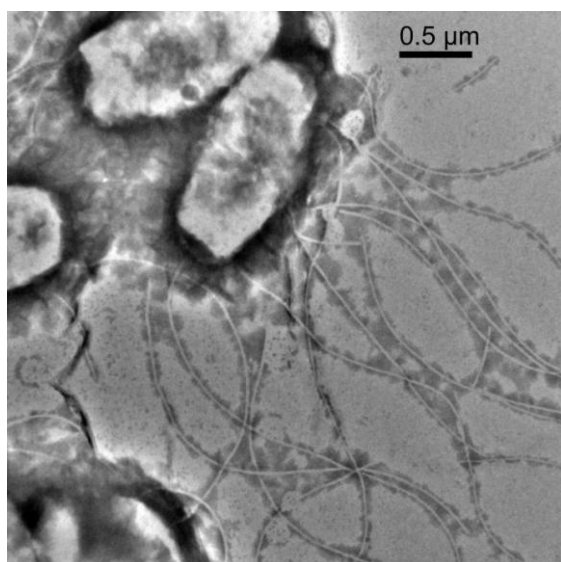


Fig. 2. Bright-field transmission electron microscope image of *Salmonella* cells that possess the mutagenized flagella. In order to enhance image contrast, the sample was stained with

The mutagenized filaments were used as templates for the formation of 1D iron oxide nanostructures, by nucleating magnetite on the filaments directly from iron-containing solutions. Iron concentration, rate of iron addition, pH and temperature were varied, and the solid products of the crystal nucleation experiments were studied using transmission electron microscopy. Our initial experiments brought mixed success: conditions under which the filaments were preserved in the solution did not typically favor the formation of magnetite. Instead, other iron oxides such as ferrihydrite nucleated on the mutagenized filaments. Further experiments are under progress to fine-tune the conditions for magnetite nucleation.

REFFERENCES

ARAKAKI, A., WEBB, J. & MATSUNAGA, T. (2003): A novel protein tightly bound to bacterial magnetic particles in *Magnetospirillum magneticum* strain AMB-1. *Journal of Biological Chemistry*. **278**, 8745-8750.

FAIVRE, D. & SCHÜLER, D. (2008): Magnetotactic bacteria and magnetosomes. *Chemical Reviews*. **108**, 4875-4898.

LANG, C., SCHÜLER, D. & FAIVRE, D. (2007): Synthesis of magnetite nanoparticles for bio- and nanotechnology: genetic engineering and biomimetics of bacterial magnetosomes. *Macromolecular Bioscience*. **7**, 144-151.

MUSKOTÁL, A., SEREGÉLYES, CS., SEBESTYÉN, A. & VONDERVISZT, F. (2010): Structural basis for stabilization of the hypervariable D3 domain of *Salmonella* flagellin upon filament formation. *Journal of Molecular Biology*. **403**, 607-615.

# HALOGEN – RICH BIOTITES FROM THE DETVA, BIELY VRCH AU-PORPHYRY DEPOSIT (SLOVAKIA): COMPOSITIONAL VARIATIONS AND GENETIC ASPECTS

[1]Pavel Uher[#], [2]Peter Koděra,
[3]Jaroslav Lexa, [1]Peter Bačík

[1]  Dept. of Mineralogy and Petrology, Comenius University, Mlynská dolina G, 842 15 Bratislava, Slovakia, [#] puher@fns.uniba.sk
[2]  Dept. of Mineral Deposits, Mlynská dolina G, 842 15 Bratislava, Slovakia
[3]  Geological Institute, Slovak Academy of Sciences, Dúbravská cesta 9, 840 05 Bratislava, Slovakia

Key words: biotite, annite, phlogopite, halogen-rich mica, Au-porphyry deposit, saline brine, altered intermediate rocks

## INTRODUCTION

Halogen anions (F and Cl) substitute hydroxyl (OH) or oxygen in several groups of rock-forming silicate minerals, e.g. in tourmalines, amphiboles and micas. Fluorine-rich to F-dominant members of the mica group occur in geological environments with high F activity, especially in highly-fractionated granites and granitic pegmatites. Chlorine-rich micas (> 1 wt. % Cl) are generally very rare in natural conditions, they were described only in some specific assemblages, e.g. in some skarns, gneisses, metamorphic banded iron formation rocks, and metasomatized volcanic or volcano-clastic rocks with hydrothermal overprint (e.g., Tracy 1991; Oen and Lustenhouwer 1992; Nash and Connor 1993; Léger et al. 1996). In our contribution, we describe a composition and possible origin of unique halogen-rich members of biotite solid solutions in altered Miocene andesite to diorite porphyry from the Detva, Biely Vrch Au-porphyry deposit in the Javorie stratovolcano, central Slovakia.

## RESULTS

Biotite form irregular aggregates (20 to 300 μm across) of anhedral crystals, rarely pseudomorphs after amphibole or pyroxene in quartz veinlets or in altered groundmass of the host rock. Biotite associates with fluorapatite, rutile, ilmenite, magnetite and hercynite, it is partly replaced along rims by chamosite and clay minerals (illite, hydrobiotite or vermiculite). Two polished thin sections from the boreholes DVE-1 (depth 58.5 m) and DVE-4 (depth 66.4 m) were investigated in detail by optical study, BSE and electron microprobe. Biotite formulae were calculated on the basis of 12 anions. Four basic compositional and genetic types of biotite could be recognized:

(1) Annite to phlogopite (DVE-1 OH with increased contents of Cl (1.8-5.5 wt. %; 0.25-0.76 *apfu*) and F (1.0-3.1 wt. %; 0.26-0.76 *apfu*);

(2) Cl-dominant analogue of annite with the highest concentrations of Cl (5.9-7.45 wt. %; 0.85-1.08 *apfu*) and mildly enriched contents of F (0.9-1.6 wt. %; 0.24-0.43 *apfu*);

(3) Phlogopite to fluorophlogopite with lower concentrations of Cl (0.6-1.1 wt. %; 0.07-0.15 *apfu*) but with the highest F enrichment (3.6-4.9 wt. %; 0.82-1.13 *apfu*);

(4) Annite to siderophyllite with lower concentrations of Cl (1.2-2.4 wt. %; 0.15-0.32 *apfu*) and moderately increased F (2.6-3.1 wt. %; 0.63-0.78 *apfu*). Moreover, Cl-rich biotites (type 1 and 2) show high concentrations of Ba (up to 4.4 wt. % BaO; $\leq 0.15$ *apfu*) and Ti (max. 3.1 wt. % $TiO_2$; 0.20 *apfu*). Due to larger ionic radius of $Fe^{2+}$ and Cl vs. Mg and F, strong positive correlations of Fe vs. Cl and Mg vs. F are observed (Fe-F and Mg-Cl avoidance). Compositional variations indicate following substitutions: $MgFe^{2+}_{-1}$, $ClF_{-1}$, $TiO_2(Fe^{2}+,Mg)_{-1}(OH,F)_{-1}$, and $Ba^TAlK_{-1}Si_{-1}$.

CONCLUDING REMARKS

Biotites from the Detva, Biely vrch Au-porphyry deposit reveal unique compositions with presence of the new member of the mica group: Cl-dominant analogue of annite. The "chloro-annite" with up to 7.45 wt. % Cl attains the highest content of this element ever reported in the mica group (Cl-dominant analogue of ferrokinoshitalite from Sterling Hill skarn, N. Jersey contains max. 7.15 wt. % Cl, Tracy 1991; annite from Nora, Sweden shows $\leq 5.5$ wt. % Cl). Beside of biotites, amphibole-group minerals from deeper part of the Detva, Biely Vrch deposit locally also show distinctly K, Fe, Cl-rich compositions. They represent a complex solid solution between hastingsite, potassic-hastinsite, a new Cl-analogue of hastingsite, and the most widespread chloro-potassichastingsite with up to 5.0 wt. % Cl ($\leq 1.43$ *apfu*). Fluorapatite to chlorapatite, rarely, F-rich titanite ($\leq 2.8$ wt. % F), and fluorite have been also detected. Moreover, exceptional *X*-site vacant, Mg, Al-rich oxy-tourmaline member attains here up to 0.45 wt. % Cl (the highest Cl content ever reported in the tourmaline supergroup), and a unique grain of $Ca_2(PO_4)Cl$ phase ("chlor-spodiosite") with ~ 16.5 wt. % Cl have been identified. The recently discovered Detva, Biely Vrch porphyry gold deposit (34 t Au at 0.8 g/t Au) shows an exceptionally low Cu/Au ratio (0.018 wt. % Cu/ppm Au). It evolved in very shallow level of 500 to 1000 m bellow the paleosurface. Due to a low pressure environment, this Au-deposit was formed from nearly anhydrous Fe-K-Na-Cl salt melts containing ~ 10 ppm Au, coexisting with hydrous vapor of very low density (Koděra et al. 2014). Interaction of these fluids or melts with host andesite to diorite porphyry in the temperature range 725-400 ºC created high-temperature Na-Ca and K-silicate alterations, including precipitation of minerals with extremely high Cl and/or F contents.

REFERENCES

KODĚRA, P., HEINRICH, C. A., WÄLLE, M. & LEXA, J. (2014): Magmatic saltmelt and vapor: Extreme fluids forming porphyry gold deposits in shallow subcolcanic settings. *Geology,* **42**, *doi: 10.1130/ G35270.1.*

LÉGER, A., REBBERT, C. & WEBSTER, J. (1996): Cl-rich biotite from Black Rock Forest, Cornwall, New York. *Am. Mineral.* **81**, 495-504.

OEN, I. S. & LUSTENHOUWER, W. J. (1992): Cl-rich biotite, Cl-K hornblende, and Cl-rich scapolite in meta-exhalites: Nora, Bergslagen, Sweden. *Econ. Geol.* **87**, 1638-1648.

NASH, J. T. & CONNOR, J. J. (1993): Iron and chlorine as guides to stratiformCu-Co-Au deposits, Idaho Cobalt Belt, USA. *Mineral. Deposita,* **28**, 99-106.

TRACY, R. J. (1991): Ba-rich micas from the Franklin Marble, Lime Crest and Sterling Hill, New Jersey. *Am. Mineral.* **76**, 1683-1693.

# ILVAITE FROM THE ABANDONED SKARN DEPOSIT MALEŠOV NEAR KUTNÁ HORA (CZECH REPUBLIC)

[1]Luboš Vrtiška[#], [1]Jiří Sejkora,
[1]Radana Malíková, [2]Pavel Černý

[1] Department of Mineralogy and Petrology, National Museum, Cirkusová 1740, 193 00 Prague 9, Czech Republic, [#] lubos_vrtiska@nm.cz
[2] Gorkého 257, 261 02 Příbram IV

## INTRODUCTION

Within the Czech Republic, ilvaite $(Ca(Fe,Mn)_2^{2+}Fe^{3+}OSi_2O_7(OH))$ was described as a rare mineral often in a microscopic form from the following occurrences: Vysoká Pec near Kraslice (Reh 1932a), Zlatý Kopec near Jáchymov (Reh 1932b), Županovice (Němec 1964), quarry in Zámčisko near Kouty nad Desnou (Fojt et al. 1997) and Vlastějovice quarry (Šrein pers. com. 2014).

## GEOLOGICAL SETTING

The magnetite skarn deposit Malešov (located 5 km SW from Kutná Hora), mined until 1957 (Pauliš 2003), is an approximately 300 m thick inhomogeneous body with NE-SW elongation situated in gneiss and migmatite complex in the Kutná hora crystalline complex. Surrounding rocks are represented by two-mica ortho-gneiss covered by cretaceous calcareous sandstones in the surroundings southern of the deposit. The deposit is mostly formed by garnet-pyroxene and pyroxene-amphibole skarn with following mineral association: garnet, pyroxene, amphibole, magnetite, epidote, oligoclase-andesine, calcite and quartz (Pauliš 2003).

## METHODS OF STUDY

Chemical composition of mineral phases was studied using EPMA Cameca SX100 (National Museum, Prague; Faculty of Science, MU Brno) in WD mode. The X-ray powder diffraction data were measured on the Bruker D8 Advance diffractometer (National Museum, Prague).

## CHARACTERIZATION OF STUDIED SAMPLES

The studied ilvaite samples from the occurrence Malešov come from surface exploration work and were found in 1970s by P. Černý. The samples up to 9 x 6 cm in size are formed by black coarsely crystallized ilvaite aggregates up to 2 cm in size abundantly pervaded by veins filled with sulphides, calcite and amphibole.

## ILVAITE

Ilvaite forms black subhedral grains with a size around 4 mm. Its powder X-ray pattern corresponds with the theoretical

values calculated from the crystal structure data of ilvaite (Finger and Hanzen 1987). Unit-cell parameters of the studied ilvaite were compared with published data in Tab. 1. The results of the EPMA study (mean of 10 point analyses) CaO 14.16, FeO 32.38, MgO 0.61, MnO 2.63, ZnO 0.04, $Al_2O_3$ 0.31, $Fe_2O_3$ 16.88, $SiO_2$ 29.52, $H_2O$ (calc.) 1.82, total 98.34 wt% on the basis of 6 *apfu* – gave the empirical formula $(Ca_{1.03}Mg_{0.06})_{\Sigma1.09}$ $(Fe_{0.87}Al_{0.02})_{\Sigma0.89}$ $(Fe_{1.85}Mn_{0.15})_{\Sigma2.00}$ $O(Si_{2.01}O_7)(OH)_{0.83}$. Isolated grains of Mn-rich ilvaite up to 1 mm in size in association with quartz and calcite were also observed in studied samples. Their chemical composition (mean of 6 point analyses) can be expressed as $(Ca_{0.96}Mg_{0.02})_{\Sigma0.98}$ $(Fe_{0.94}Al_{0.04})_{\Sigma0.98}$ $(Fe_{1.58}Mn_{0.42})_{\Sigma2.00}$ $O(Si_{2.07}O_7)(OH)_{0.77}$.

|  | this paper | Finger and Hazen 1987 |
|---|---|---|
| $a$ [Å] | 13.012(2) | 13.0103(5) |
| $b$ [Å] | 8.8038(9) | 8.8039(4) |
| $c$ [Å] | 5.8515(6) | 5.8517(3) |
| $\beta$ [°] | 90.17(1) | 90.209(5) |
| $V$ [Å³] | 670.3(1) | 670.26 |

Tab. 1. Unit-cell parameters of the studied ilvaite in comparison with published data

## ASSOCIATED MINERALS

Ilvaite occurs associated mostly with pyrite with As content up to 2 wt %, chalcopyrite, calcite, amphibole, quartz and andradite (Fig. 1). Microscopic grains of cobaltite, $(Co_{0.95}Fe_{0.05})_{\Sigma1.00}As_{0.95}S_{1.04}$ forming elongated euhedral grains up to 1.1 mm surrounded by quartz and a mineral from the stannite group forming subhedral grains up to 10 μm in pyrite were also found in the association.

## CONCLUSION

Occurrence of ilvaite in the skarn deposit Malešov near Kutná Hora is unique especially in its abundance and size of the aggregates in comparison with other occurrences of this mineral species in the Czech Republic.
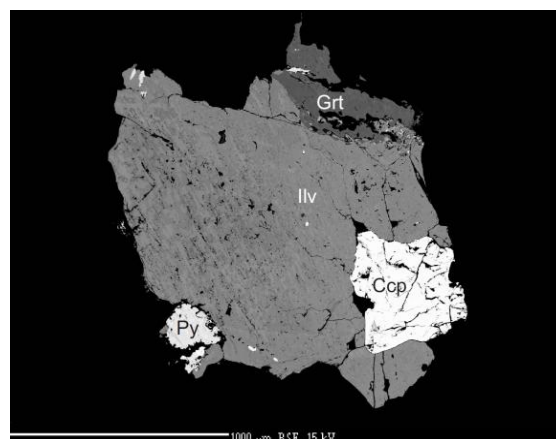


Fig. 1. Mineral association with ilvaite. Ilv-ilvaite, Grt-andradite, Py-pyrite, Ccp-chalcopyrite. BSE photo I. Macek.

## REFERENCES

FINGER, L. W., HANZEN, R. M. (1987): Crystal structure of monoclinic ilvaite and the nature of the monoclinic-orthorhombic transition at high pressure. *Zeitschrift fuer Kristallographie,* **179,** 415-430.
FOJT, B., HLADÍKOVÁ, J., KOPA, D., KRAUSOVÁ, D., SULOVSKÝ, P., VÁVRA, V., ZEMAN, J., ZIMÁK, J. (1997): Minerální a horninová asociace z lomu Zámčisko, Hrubý Jeseník. *Čas. Slez. Muz., (A),* **46,** 235-264.
NĚMEC D. (1964): Liévrit ze Županovic. *Čas. Mineral. Geol.,* **9,** 3, 333-335.
PAULIŠ, P. (2003): Malešov. *In Nejzajímavější mineralogická naleziště Čech II,* 78-80. Kuttna Kutná Hora.
REH, H. (1932a): Dissertation, Freiberg, *NJb 1932, BB65 A,* **18,** 46 in KRATOCHVÍL J. (1962): Topografická mineralogie Čech V, Nakl. Českosl. Akad. Věd, 100-101.
REH, H. (1932b): Beitrag zur Kenntnis der erzgebirgischen Erzlager. *NJbM, BB. 65A,* 1-86.

# WHITLOCKITE – GROUP MINERALS AND RELATED METASOMATIC PHOSPHATES FROM GRANITIC PEGMATITE AT LUTOMIA (SOWIE MTS BLOCK, SW POLAND)

[1]Adam Włodek[#], [1]Adam Pieczka

[1]     AGH University of Science and Technology, Department of Mineralogy, Petrography and Geochemistry, [#] wlodek@agh.edu.pl

Key words: phosphates, whitlockite, merrillite, pegmatite, metasomatism, Lutomia

## INTRODUCTION

Phosphate minerals from granitic pegmatite at Lutomia are represented by three main genetic associations: i) primary-magmatic; ii) secondary-metasomatic; iii) secondary-weathering. Primary magmatic phosphates are represented by lamellar intergrowths of graftonite, triphylite and sarcopside. Metasomatic phosphates occur in outer zones of primary phosphates lamellae and in thin veinlets cutting primary phosphates. Metasomatic assembly is represented by Ca-rich graftonite, wagnerite group minerals, alluaudite group minerals, kryzhanovskite and phases with compositions corresponding to the whitlockite group phosphates. Secondary weathering phosphates replace both primary and metasomatic minerals and occur mainly in border zones of phosphate nodules. Phosphates of this group are represented by several minerals including ferrisicklerite, heterosite, phosphoferrite, kryzhanovskite, ludlamite, vivianite, earlshannonite / whitmoreite, strunzite, hureaulite, beraunite, jahnsite group minerals, fluorapatite and $Mn^{2+}$-rich hydroxyapatite.

The most interesting phosphates belong to metasomatic assembly due to high textural diversity and large chemical variability, especially in whitlockite mineral group.

## WHITLOCKITE CRYSTAL CHEMISTRY

Whitlockite group includes five rare phosphate phases-two extraterrestrial minerals: merrillite $Ca_9NaMg(PO_4)_7$ and ferromerrillite $Ca_9NaFe(PO_4)_7$ and also terrestrial phases: whitlockite $Ca_9Mg(PO_4)_6(PO_3OH)$, strontiowhitlockite $Sr_9Mg(PO_4)_6(PO_3OH)$ and bobdownsite $Ca_9Mg(PO_4)_6(PO_3F)$. At the basis of chemical variations two main substitutions can be specified in whitlockite group minerals: $Mg^{2+}$ - $Fe^{2+}$ (and probable $Mn^{2+}$) substitution at Mg position and $Ca_{(Ca-Merr)}$ - $2Na_{(Merr)}$ - $2H_{(Whit)}$ - substitution at Ca(IIA') site (Hughes et al. 2006, Hughes et al. 2008). Data about bobdownsite given by Tait et al. (2011) show that one of the Ca positions occupied in whitlockite by hydrogen could also be occupied by fluorine. Despite of many investigations

about whitlockite group phosphates, there is no data documenting terrestrial samples with high $Na^+$ content and predominance of $Fe^{2+}$ over $Mg^{2+}$ at Mg position.

## METASOMATIC PHOSPHATES ASSEMBLY

Metasomatic changes in phosphate nodules from Lutomia pegmatite could be described as four-stage sequence: i) primary phosphates replacement by Ca-rich graftonite and alluaudite group minerals; ii) crystallization of granular wagnerite group phosphates, alluaudite group phosphates and kryzhanovskite; iii) crystallization of wolfeite (staněkite) / triploidite - alluaudite / hagendorfite symplectic intergrowths; iv) crystallization of whitlockite group minerals.

Electron microprobe was used to determine chemical compositions of all phosphates and contents of ions were calculated at the basis of $7P^{5+}$ atoms per formula unit for whitlockite, $12P^{5+}$ for alluaudite / hagendorfite and $1P^{5+}$ for wolfeite / triploidite.

Irregular crystals of whitlockite-type phase occurring in central parts of metasomatic veinlets reach up to 100 μm in length and 20 μm in thickness. Grains of this mineral associated with wagnerite group and alluaudite group phases show to be the last phosphates in metasomatic sequence. Due to high chemical diversity, individual grains could be assigned to several different phases.

At the Mg position substitution between $Mg^{2+}$ and $Fe^{2+}$ is evident and phase compositions changes in wide range (from $Mg^{2+}_{0.30}Fe^{2+}_{0.70}$ to $Mg^{2+}_{0.60}Fe^{2+}_{0.41}$). Role of manganese at Mg position seems to be negligible due to full occupancy by $Mg^{2+}$ and $Fe^{2+}$ and more probable presence of $Mn^{2+}$ at the one of the Ca positions. At the Ca position $Na^+$ shows to be main substituted cation and its content reaches up to 0.90 *apfu*. Other ions occurring at this position - $Mn^{2+}$ and $Sr^{2+}$ are less significant and their contents reach up to 0.62 *apfu* for manganese and up to 0.02

*apfu* for strontium. Role of fluorine and hydrogen seems to be negligible in Na-rich samples because of total cations charge is close to $21^+$ and $Na^+$ content is close to 1 *apfu*. According to the crystal chemistry, whitlockite-like phases from Lutomia should be described more likely as 'terrestrial merrillite' or 'terrestrial ferromerrillite' than 'Na-rich whitlockite'. However, actual data about whitlockite - type minerals show that samples with $Na^+$ content lower than 0.50 *apfu* and cations charge below $20.5^+$ could correspond more likely to whitlockite or bobdownsite and should be examined for water and fluorine content.

Related wagnerite group minerals show various chemical compositions with general formula $(Fe_{0.84-1.45}Mn_{0.42-1.11}Mg_{0.02-0.20})_{\Sigma=2}(PO_4)(OH)$, corresponding to both wolfeite (or staněkite) and triploidite end members. Alluaudite group minerals due to their chemical compositions correspond to several different phases including alluaudite (NaNa) or (Na[]) type and also hagendorfite (NaMn).

## REFERENCES

HUGHES, J. M., JOLLIFF, B. L., GUNTER, M. E. (2006): The atomic arrangement of merrillite from Fra Mauro Formation, Apollo 14 lunar mission: The first structure of merrillite from the Moon. *Am. Mineral.* **91**, 1547-1552.

HUGHES, J. M., JOLLIFF, B. L, RAKOVAN, J. (2008): The crystal chemistry of whitlockite and merrillite and the dehydrogenation of whitlockite to merrillite. *Am. Mineral.* **93**, 1300-1305.

TAIT, K. T., BARKLEY, M. C., THOMPSON, R. M., ORIGLIERI, M. J. EVANS, S. H., PREWITT, C. T., YANG H. (2011): Bobdownsite, a new mineral species from Big Fish River, Yukon, Canada, and its structural relationship with whitlockite-type compounds. *Can. Mineral.* **49**, 1065-1078.

# PRIMARY PHASES FROM SERPENTINITES FROM THE BRASZOWICE – BRZEŹNICA MASSIF (SW POLAND)

[1]Piotr Wojtulek[#], [1]Jacek Puziewicz,
[2]Theodoros Ntaflos

[1]  University of Wrocław, Institute of Geological Sciences, [#]piotr.wojtulek@ing.uni.wroc.pl
[2]  University of Vienna,  Department of Lithospheric Research

### INTRODUCTION

The Braszowice-Brzeźnica Massif (SW Poland) together with the Ślęża Ophiolite, Szklary Massif and Nowa Ruda Massif are considered as the parts of the Variscan Central-Sudetic Ophiolite. The Braszowice-Brzeźnica Massif (BBM) is located at the South end of the Niemcza Dislocation Zone and consists of gabbros and serpentinites. The ultramafic rocks occurring in the BBM are (from E to W) serpentinites with abundant relics of olivine and tremolite, lizardite-chrysotile serpentinites and antigorite serpentinites (Gunia 1992). The clinopyroxene and zoned chromite grains were found in the central part of the BBM (Mnich Hill) within antigoritic serpentinites.

### CHEMISTRY OF MINERALS

The clinopyroxene has the diopside composition. Two kinds of mineral occur: Cpx I (Mg# = 0.91-0.92, 0.7-0.8 wt. % $TiO_2$, 3.0-4.0 wt. % $Al_2O_3$, 1.0-1.4 $Cr_2O_3$ and 0.4 wt. % $Na_2O$) and Cpx II (Mg# = 0.93-0.97, < 0.4 wt. % $Al_2O_3$, < 0.2 $Cr_2O_3$ and < 0.2 wt. % MnO). Cpx I is enriched in REE relative to primitive mantle. The REE pattern is enriched in HREE relative to LREE and shows negative Eu anomaly. The spinel grains are zoned; chromite I occurs in a core whereas chromite II forms rims. Chromite I (Cr# = 0.49-0.51, Mg# = 0.42-0.45) contains < 0.70 wt. % $TiO_2$, < 0.65 wt. % MnO and 0.10 wt. % NiO. Chromite II (Cr# = 0.98, Mg# = 0.04) contains more MnO (< 2.00 wt. %) than chromite I.

### DISCUSSION

We interpret Cpx I and chromite as the primary phases of the pre-existing peridotite. Cpx I contains similar amount of the $Al_2O_3$, $Cr_2O_3$ and $Na_2O$ to primary diopsides described from the Marie Celeste FZ (cf. Hellebrand et al. 2002), Vulcan FZ, Discovery II and Indomed FZ (cf. Johnson et al. 1990). The $Al_2O_3$ and $Cr_2O_3$ contents in the Cpx I are also similar to secondary diopside originated from the melt-percolation reactions within thermal boundary layer (cf. Seyler et al. 2007; Wojtulek et al. 2010). We exclude the secondary, melt-percolation origin of the Cpx I, because percolation diopsides

contain much lower amounts of $TiO_2$ (< 0.05 wt. %) and $Na_2O$ (< 0.15 wt. %). The REE pattern of Cpx I is also more similar to residual diopsides that record the melt extraction episodes (Johnson et al. 1990, Norman 1998). The negative Eu anomaly indicates the presence of plagioclase in the pre-existing peridotite. Chromite I major element composition is similar to that occurring in primary chromites from oceanic peridotites of the Romanche and Kurchatov F.Z. (Dick and Bullen, 1984). The Cpx II, depleted in Al, Cr and REE relative to Cpx I and chromite II are the secondary phases. Cpx II formed at the expense of the Cpx I (forms often rims and fillings of fractures in Cpx I). Such alteration of the Cpx I and chromite I would happen at the ocean floor metamorphism stage (greenschist facies conditions) when the migrating fluids affected the primary peridotite mineralogy (cf. Gonzalez-Jimenez et al. 2009).

## REFERENCES

DICK, H. J. B., BULLEN, T. (1984): Chromian spinel as a petrogenetic indicator in abyssal and alpine-type peridotites and spatially associated lavas. *Contributions to Mineralogy and Petrology,* **86**, 54-76.

GUNIA P. (1992): Petrology of the ultrabasic rocks from the Braszowice-Brzeźnica Massif (Fore-Sudetic Block). *Geologia Sudetica,* **26**, 120-170.

JOHNSON, K. T. M., DICK, H. J. B., SHIMIZU N., (1990): Melting in the Oceanic Upper Mantle - an ion microprobe study of Diopsides in Abyssal Peridotites. *Journal of Geophysical Research,* **95**, 2661-2678.

NORMAN, M. D. (1998): Melting and metasomatism in the continental lithosphere: laser ablation ICPMS analysis of minerals in spinel lherzolites from eastern Australia. *Contributions to Mineralogy and Petrology,* **130**, 240-255.

SEYLER, M., LORAND, J. P., DICK, H. J. B., DROUIN, M. (2007): Pervasive melt percolation reactions in ultra-depleted refractory harzburgites at the Mid Atlantic Ridge, $15^020$"N: ODP Hole 1274A. *Contributions to Mineralogy and Petrology,* **153**, 303-632.

WOJTULEK, P., PUZIEWICZ, J., NTAFLOS, T. (2013): The origin of the non-serpentinic phases of the Gogołów-Jordanów serpentinite massif (SW Poland). *European Geosciences Union, General Assembly 2013, conference abstract.*

# BE-NB-W-SN-LI-TI-U-MN-PHOSPHATE-MINERALIZATION IN THE METARHYOLITE OF BÜKKSZENTKERESZT, NE-HUNGARY

[1]Norbert Zajzon[#], [1]Norbert Németh,
[1]Sándor Szakáll, [1]Ferenc Kristály, [1]Péter Gál, [2] Béla Fehér

[1]    Institute of Mineralogy – Geology, University of Miskolc, Miskolc, Hungary,
[#]nzajzon@uni-miskolc.hu
[2]    Herman Otto Museum, Miskolc, Hungary

Key words: fluorapatite, Be enrichment, Nb-W-zoned rutile, columbite, phlogopite-(F)

## INTRODUCTION

A previously known Mn-U-fluorapatite anomaly just nearby Miskolc, in the Bükk-Mts., Hungary became the target of a new research at the University of Miskolc for critical elements, like Be, Nb, Ta. On the frame of this work we investigated the mineralogy and geochemistry of the positive anomaly, the local environment and the host rock.

## GEOLOGY

The Mn-U-fluorapatite anomaly, with cca. 600 ppm U and 300 ppm Be was discovered in the early '70s by uranium exploration (Csáki and Csáki-né 1973). The host rock is a Ladinian-Carnian metarhyolite sequence, the Bagolyhegy Metarhyolite Formation. The stratovolcanic complex suffered prehnite-pumpellyite facies metamorphism ca. 80–90 Ma ago and it was folded and faulted in multiple phases, so syngenetic fabric and structures are strongly overprinted. The chemical composition is acidic and peraluminous (ASI = 1.2–2) (Tab. 1.). Most abundant rock forming minerals are quartz, sericite, K-feldspar and chlorite, but the formation contains silicified and albitized veins and K-metasomatite bodies with peculiar mineral parageneses.

| Rock type | $SiO_2$ | $Al_2O_3$ | $Na_2O$ | $K_2O$ | ASI | PI |
|---|---|---|---|---|---|---|
| *Felső-Bagoly Hill avg. of 19 sampl. (Szentpétery, Pantó in Balogh 1964)* | *75.8* | *12.1* | *2.6* | *5.5* | *1.39 (0.80–1.96)* | *0.67 (0.48–0.90)* |
| Chloritic metavolcanites | 63.4 | 16.0 | 3.6 | 5.3 | 1.36 | 0.55 |
| K-metasomatized, silicified metarhyolite | 68.4 | 12.7 | 5.3 | 10.8 | 0.78 | 1.27 |
| K-metasomatized, silicified metarhyolite with Na-depletion | 72.4 | 12.7 | 1.5 | 8.8 | 1.18 | 0.81 |
| albitized metarhyolite | 76.4 | 8.9 | 12.9 | 0.8 | 0.64 | 1.54 |

Tab. 1: Geochemistry of rock types at the Felső-Bagoly Hill; archive average and newly assayed sample data. ASI: aluminum saturation index, PI: peralkalinity index

## MINERALOGY

The uranium containing fluorapatite-Mn-oxide layer is a small body, only 20–30 cm thick. It is built up of zoned fluorapatite, quartz, smectite-15Å, cryptomelane, pyrolusite, todorokite, illite, nontronite, halloysite-10Å, fluorophlogopite, albite. Some barite, cassiterite and $TiO_2$ were also found by SEM. The bulk samples contain up to 22 wt % $P_2O_5$, 23 wt % MnO, 340 ppm Be, 600 ppm U, 320 ppm W, 40 ppm Sn, 53 ppm Tl. The $\sum$ REE usually is around 150–200 ppm, which is low, but the HREE / $\sum$ REE is around 0.4–0.5. The zoned fluorapatite has $CO_3^{2-}$ substitution in the $PO_4$ anionic site according to FTIR measurements, and also have 600–900 ppm Be and sometimes 400–500 ppm Li content, which varies, according to LA-ICPMS measurements. The Mn-oxides (cryptomelane and todorokite) usually contain more Be and Li, than the fluorapatite.
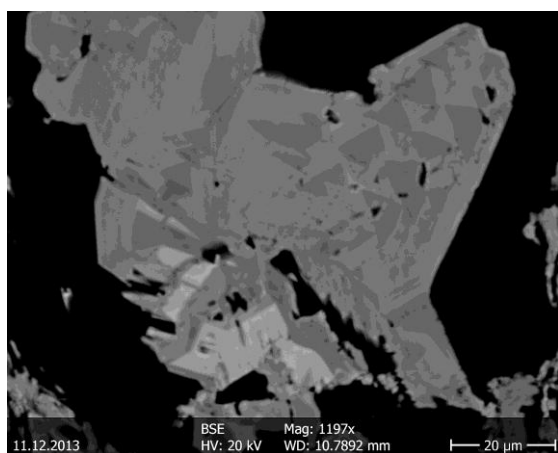


Fig. 1. W-(the most bright) and Nb-zoned rutile from Bükkszentkereszt, BSE image.

The fluorphlogopite contains the highest amount of Li above 1000 ppm. The K-metasomatite bodies and albite-quartz veins contain of quartz, orthoclase, albite, rutile with high W and Nb content, anatase, ilmenite, adularia, xenotime-(Y), monazite-(Ce), pharmacosiderite, cacoxenite, Nb-oxides columbite-Fe-Mn solid solution, cassiterite several sulfides, native gold and silver. The rutiles are usually strongly Nb and W zoned (Fig. 1.), containing columbite, cassiterite and xenotime-(Y) inclusions. The columbite can be homogenous or Ta-zoned.

## FORMATION OF THE MINERALIZATION

The rare minerals typically occur in veins. Ti, Nb, Li, Rb and REE are enriched in this material. Both mineralogical and trace element composition resemble to a REE pegmatite. The earlier suggested genetic model for the Mn-U-fluorapatite-Be enrichment was the Spor Mts. analogue (Kubovics et al. 1989). In the view of our new results it is not probable. It is partially because of the lack of zeolites, the rare occurrence of fluorite and no sign of carbonate replacement. The fluorapatite layer may be the product of hot spring activity related to the volcanism. Our suggested possible genetic models are 1. intrusion (aplite) or pegmatitic impregnation from a highly evolved magma in the final phase of the rhyolite volcanism or 2. K-metasomatism, with connected albite-quartz vein formation from a subsequent peralkaline volcanism (Carnian metabasalt formation).

## REFERENCES

BALOGH, K. (1964): Geological formations of the Bükk-hg. MÁFI year book 48/2, 245-553.
CSÁKI, F. & CSÁKI, F.-NÉ (1973): Összefoglaló jelentés a bükkszentkereszti kutatási területen 1969–1973 között végzett kutatómunkáról [Summary report on the prospecting at the Bükkszentkereszt area between 1969 and 1973]. Mecseki Érckutató Vállalat. MS. Mecsekérc Zrt., **Kővágószőlős**, 289 p.
KUBOVICS, I., NAGY, B., NAGY-BALOGH, J. & PUSKÁS, Z. (1989): Beryllium and some other rare element contents of acid volcanics (tuffs) and metamorphites in Hungary. *Acta Geol. Hung.* **32(1-2)**, 219-231.

# DUMORTIERITE FROM KRUCZE ROCKS: CRYSTAL STRUCTURE AND CHEMICAL COMPOSITION

[1]Sylwia Zelek[#], [1]Adam Pieczka,
[2]Katarzyna Stadnicka, [3]Eligiusz Szełęg

[1] Faculty of Geology, Geophysics and Environmental Protection, AGH University of Science and Technology, al. Mickiewicza 30, 30-059 Kraków, Poland, [#] zelek@geol.agh.edu.pl
[2] Faculty of Chemistry, Jagiellonian University, ul. R. Ingardena 3, 30-060 Kraków, Poland
[3] The Faculty of Earth Sciences, University of Silesia in Katowice, ul. Będzińska 60, 41-200 Sosnowiec, Poland

### INTRODUCTION

Dumortierite was first described in 1880 as a result of its occurrence in Chaponost, in the Rhône-Alps of France by M.E. Bertrand (Grawe 1928) and named after the French paleontologist Eugène Dumortier (1803-1873). In 1958 Claringbull and Hey established the general formula of dumortierite as $(Al,Fe)_7BSi_3O_{18}$, unit cell parameters and space group as Pmcn (ITC No.62). In 1965 Golovastikov published the results of the first crystal structure determination for dumortierite which indicated the presence of isolated silicate tetrahedra, borate triangles, and three kinds of Al/Fe octahedral chains, two of which involved face-sharing octahedra. A structure refinement by Moore and Araki (1978) provided detailed description of the structure and revealed that one of the chains containing face-sharing octahedra was not fully occupied. In 2013 Pieczka et al. revised the nomenclature of the dumortierite group. The newly constituted dumortierite supergroup, comprises two

groups with six minerals all isostructural with dumortierite, one of which is the first member of a potential third group. The supergroup, which has been approved by the CNMNC, is based on specific end-member compositions for dumortierite and holtite, in which occupancy of the Al1 site is critical. Dumortierite in Poland had been identified as an accessory mineral of Karkonosze aplites and pegmatites. In Krucze Rocks dumortierite forms aggregates of about 1cm in size containing violet-blue or grey-bluish needle-shaped crystals (Fig.1).

### METHODS

The chemical composition of the dumortierite crystals was determined using electron-microprobe CAMECA SX-100 equipped with Wavelength Dispersive Spectrometer (WDS). The single crystals of dumortierite were separated from the dumortierite aggregates occurring in the pegmatite fragments. X-ray intensity measurements of diffracted beams were carried out on SuperNova diffractometer

(Agilent Technologies) using graphite monochromated MoKα radiation.

## RESULTS AND DISCUSSION

The obtained data from EMPA indicated that crystals of the dumortierite consist of two different varieties: (*i*) a simple compositional variety forming a poorly-zoned matrix, and (*ii*) secondary veinlets of As-bearing dumortierite. The matrix has the following mean composition:
$(Al_{0.49(3)}Ti_{0.16(2)}Mg_{0.04(<1)}Fe^{2+}_{0.04(<1)}Nb_{0.01(<1)}\square_{0.26(1)})_{\Sigma=1.00}Al_{6.00}B_{1.00}(Si_{2.82(4)}Al_{0.17}As_{0.01(1)})_{\Sigma=3.00}$ $(O_{17.16(3)}OH_{0.82(3)})_{\Sigma=17.99}$ that corresponds to a complex solid solution of end-members: dumortierite (~ 53mol. %), OH-dumortierite (18 mol. %), [($Fe^{2+}$, Mg)-Ti] analogues of dumortierite (16mol.%), titanoholtite (12 mol. %), nioboholtite (1 mol. %). The dumortierite from Krucze Rock crystallized in orthorhombic Pnma (ITC No. 62) space group, with a=4.6935(1), b=11.7894(3), c=20.2197(6), V=1118.83 and Z = 4. The structure was solved using SIR92 and refined with SHELXL97 to R1 = 0.0306, R2=0.0778, S=1.129 on the basis of 2984 unique reflections. The structure is built of two interpenetrating sublattices with site occupancy factors 0.9445 and 0.0555, respectively. Both sublattices have a typical dumortierite structure. The sublattice I contains Ti(IV), Fe(II) and Al(III) in the position of Al1, and As(III) and Si(IV) in the position of Si2, whereas the sublattice II consists of Fe(II) and Nb(V) in the position of Al1, and As(III) and Si(IV) in position of Si1. It is worth noting that the sublattice II has been revealed due to detection and analysis of a pseudo-hexagonal close-packing of oxygen atoms. The coordination polyhedra for Al, Si and B in both sublattices have essentially the same geometry as those found in the original dumortierite structure. The position of Al1 is not fully occupied with vacancy comprising 0.156 of 0.5000 for the position 4 c .m. (Pnma). The common part of both sublattices contains B1, O8, O9, O10 and O11 atoms (in the position of O10 and O11 there are alternatively OH groups). The resulting chemical composition leads to charge compensation calculated with an assumption that the compound contains 0.8225 OH groups per chemical formula:
$(Al_{0.420}Ti_{0.195}Fe^{2+}_{0.065}Nb_{0.008}\square_{0.312})Al_{6.00}B_{1.00}(Si_{2.985}As_{0.010})(O_{17.178}OH_{0.822})$.



Fig1. (**a**) The aggregates of dumortierite crystals occuring in pegmatite from Krucze Rocks, Karpacz - Wilcza Poręba. (**b**) Single crystal of dumortierite for which the crystal structure analysis was described in this work.

## REFERENCES

GOLOVASTIKOV, N. I. (1965): The crystal structure of dumortierite. *SPhD*. **10**, 493-495.

GRAWE, O. R. (1928): The mineralogy of dumortierite. *In* A bulletin by The Mackay School of Mines Staff on the mineral dumortierite, Reno, Nevada, 7-19.

MOORE, P. B. ARAKI, T. (1978): Dumortierite, $Si_3B[Al_{6.75}\square_{0.25}O_{17.25}(OH)_{0.75}]$: A detailed structure analysis. *Neues Jb Miner Abh.* **132**, 231-241.

PIECZKA, A., EVANS, R. J., GREW, E. S., GROAT, L. A., MA, C., ROSSMAN, G. R., (2013): The dumortierite supergroup. I. A new nomenclature for the dumortierite and holtite groups. II. Three new minerals from the Szklary pegmatite, SW Poland: Nioboholtite, $(Nb_{0.6}\square_{0.4})Al_6BSi_3O_{18}$, titanoholtite, $(Ti_{0.75}\square_{0.25})Al_6BSi_3O_{18}$, and szklaryite, $\square Al_6BAs^{3+}_3O_{15}$. *Min. Mag.* **77**, (I) 2825-2839; (II) 2841-2856.

# BERYL-COLUMBITE PEGMATITES FROM ŠEJBY, NOVOHRADSKÉ HORY MTS., MOLDANUBIAN BATHOLITH, CZECH REPUBLIC

[1]Jiří Zikeš[#], [2]Petr Welser,
[3]Milan Novák

[1] Department of Geological Sciences, Masaryk University, Brno, Czech Republic, [#]379601@mail.muni.cz
[2] Fosil Partner a.s., Ostrava-Poruba, Czech Republic
[3] Department of Geological Sciences, Masaryk University, Brno, Czech Republic

## INTRODUCTION

Granitic pegmatites of beryl-columbite subtype are common in the Moldanubian Zone and three compositionally distinct groups were recognized (Novák et al. 2013): i) pegmatites with common primary muscovite, tourmaline and accessory garnet (spessartine-almandine), apatite, columbite-tantalite and cassiterite (e.g., Drahonín, Kácov); (ii) pegmatites with rare primary muscovite, minor to accessory cordierite, apatite, niobian (tantalian) rutile and ilmenite as typical Nb,Ta,Ti-oxide minerals (e.g., Věžná I, Písek region); (iii) pegmatites with Be-bearing phosphates (hurlbutite, herderite) and columbite related to granites of the Moldanubian Batholith (e.g., Šejby near Hové Hrady, Kostelní Vydří near Telč; Cempírek et al. 1999). Systematic research of the authors in the Novohradské hory Mts. revealed several new pegmatite dikes of this group in a close vicinity of Šejby and the results of geological and mineralogical research are presented therein.

## GEOLOGICAL SETTING AND INTERNAL STRUCTURE

Five zoned pegmatite dikes are situated in agricultural fields about 1.5 km NNW from Šejby near Nové Hrady, southern Bohemia. The individual dikes, ~ 2-4 m thick and several tens m long, are N- to NNE-striking and steeply dipping. High degree of weathering of host rocks does not enable to recognize whether the pegmatites are enclosed in Eisgarn granite or its gneiss envelope. The pegmatite dikes exhibit zoned internal structure consisting from the border of: (i) a fine- to medium-grained aplitic unit (Kfs + Qz + Plg + Bt), (ii) a coarse-grained granitic unit (Kfs + Qz + Plg + Bt + Ms), (iii) a blocky K-feldspar unit (Kfs > Qz > Ms), up to 2 m thick, and (iv) a quartz core (Welser and Zikeš 2013). Between granitic unit and blocky unit (v) graphic unit (Kf+Qz) is locally developed. (vi) Muscovite-rich elongated nests (Ms > Qz + Ab), ~ 15 cm in size, are locally present between granitic unit and blocky K-feldspar.

## MINERALOGY

Along with major and minor minerals (Kfs, Qz, Plg, Ab, Ms and Bt), yellowish to greenish beryl is a common accessory phase. Its columnar crystals, locally arranged in radial aggregates up to 15 cm in size, occur in blocky K-feldspar, and muscovite-rich aggregates. Small beige grains and coutings on surface of beryl crystals were identified using powder XRD as hurlbutite and herderite. They are likely alteration products of beryl. Greenish fluorapatite, in crystals, up to 2 cm in size, is a common accessory mineral in muscovite-rich aggregates but also in other units. Rare crandallite-group mineral and strengite were identified in some pegmatites as well. Black tabular crystals of Nb,Ta-oxides and their aggregates, up to 3 cm in size, are common. They occur in almost all pegmatite units but typically associated with beryl. Zoned columbite-(Fe) - tantalite-(Fe) and tapiolite-(Fe) were found mostly closely associated. Brown dipyramidal crystals of zircon, up to 8 mm in diameter, are also associated with beryl.

## DISCUSSION

Chemical composition of Nb,Ta-oxide minerals with Ta/(Ta+Nb) = 0.28-0.90 and Mn/(Mn+Fe) 0.22-0.24 and zircon with $UO_2$ ~ 6-9 wt. % and $HfO_2$ ~ 10 wt. % suggest high degree of fractionation of these beryl-columbite subtype pegmatites. Compositional trend of Nb,Ta-oxides in Šejby characterized by almost constant Mn/(Mn+Fe) and high variation in Ta/(Ta+Nb) is similar to other data from this region (e.g., Novák et al. 1994), and other F-poor beryl-columbite pegmatites in the Moldanubian Zone (Kostelní Vydří; Novák 1995) but distinct from beryl-columbite pegmatite in Věžná I (Černý et al. 2000).

The mineral assemblage of the pegmatites characterized by common beryl, Nb,Ta > Ti (common columbite-tantalite, rare tapiolite and absence of ilmenite and niobian rutile), high activity of P (common fluorapatite, Be-phosphates), and low activities of B (tourmaline is absent) and F typifies this specific type of beryl-columbite pegmatites in the Moldanubian Zone.

## REFERENCES

CEMPÍREK, J., NOVÁK, M. & VÁVRA, V. (1999): Hurlbutit z beryl-colubitového pegmatitu v Kostelním Vydří u Telče, západní Morava. *Acta Mus. Morav., Sci. geol.*, **84,** 45-48.

ČERNÝ, P., NOVÁK, M. & CHAPMAN, R. (2000): Subsolidus behavior of niobian rutile from Věžná, Czech Republic: a model for exsolution in phases with $Fe^{2+}$ >> $Fe^{3+}$. *Journ. Czech. Geol. Soc.*, **45,** 21-35.

NOVÁK M. (1995): Ferrocolumbit z beryl-columbitového pegmatitu v Kostelním Vydří u Telče, západní Morava. *Acta Mus. Morav., Sci. nat.*, **79,** 3-8.

NOVÁK, M., KADLEC, T. & GADAS, P. (2013): Geological position, mineral assemblages and contamination of granitic pegmatites in the Moldanubian Zone, Czech Republic; examples from the Vlastějovice region. *Journ. Geosci.*, **58,** 21-47.

NOVÁK, M., KLEČKA, M. & ŠREIN, V. (1994): Compositional evolution of Nb,Ta-oxide minerals from alkali-feldspar muscovite granites Homolka and Šejby southern Bohemia, and its comparison with other rare-element granites. *MinPet 94 Symposium, Mitteil. Österreich. Mineral. Gessel.*, **139,** 353-354.

WELSER, P. & ZIKEŠ, J. (2013): Pegmatity od Šejb v Novohradských horách. *Minerál*, **21,** 5, 387-409.

# AU-PORPHYRY MINERALIZATION AT KRÁĽOVÁ AND SLATINSKÉ LAZY, WESTERN CARPATHIANS, SLOVAKIA

[1]Juraj Žitňan[#], [1]Peter Koděra,
[2]Jaroslav Lexa, [1]Jana Brčeková, [1]Iveta Zvarová

[1]    Department of Geology of Mineral Deposits, Faculty of Natural Sciences, Comenius University, Bratislava, Slovakia, [#]jzitnan@gmail.com
[2]    Geological Institute, Slovak Academy of Sciences, Bratislava, Slovakia

## INTRODUCTION

Au porphyry mineralization in Western Carpathians has been recently discovered by EMED Slovakia. Kráľová and Slatinské lazy are located in western part of the Javorie stratovolcano, Initial Mineral Resource estimate totals 13.9 t Au at 0.29 g/t Au (Kráľová) and 2.5-5 t Au at 0.2-0.4 g/t Au (Slatinské lazy) (Hanes et al. 2010).

## RESULTS AND DISCUSSION

The Kráľová deposit (KVE drill holes) is associated with altered diorite to andesite porphyry. The ore body is locally cut by younger porphyry dykes which are maximum several meters thick.

The intrusive centre Slatinské lazy (SLE drill holes) is formed by andesite porphyry that is crosscut by magmatic-hydrothermal breccias. This porphyry gold occurrence is located at the edge of the hydrothermal center Klokoč-Podpolom that is hosting advanced-argillic alteration with gold and thus it can be a part of this system. Prevailing intermediate argillic alteration at KVE variably overprints earlier hybrid Ca-Na/K-silicate alteration.

Sericite alteration is the most widespread alteration type at SLE. Sericite, chlorite, calcite, K-feldspar and clay minerals replace mafic minerals and form irregular aggregates in groundmass. In some parts of the system, high temperature alteration was also determined. Anorthite, actinolite, diopside, biotite and magnetite are replacing mainly mafic minerals.The vein system of both localities is dominated by A-type and banded quartz veins. Vein quartz hosts four types of fluid inclusions: ubiquitous vapor inclusions, li-quid-rich fluid inclusions, salt melt inclu-sions and silicate glass inclusions (at Krá-ľová only). Raman spectroscopy showed that in salt melt inclusions all solid phases except one of the smaler grains are water free, indicating that these inclusions repre-sent an essentially anhydrous salt melt. Si-milar inclusions occur on other porphyry gold deposits in this district and are related to fluid exsolution from parental diorite magma in a relatively shallow depth (Ko-děra et al., 2014). Based on microprobe a-nalyses the silicate melt inclusions have ryolitic compositions. Oxygen isotope data from vein quartz and magnetite from both localities are consistent with magmatic origin of hydrothermal fluids.

Gold occurred in samples affected by Ca-Na/K-silicate alteration and intermediate alteration. Gold grains at Kráľová were identified in small quartz veins in association with chalcopyrite and bornite, and have increased concentrations of Ag (13-18 wt %) and Cu (2-4 wt %). Most of the gold grains at SLE are not hosted by quartz veinlets, but they occur in their broad vicinity within altered rock associated with chlorite, sericite, calcite, and plagioclase. Sometimes they were in association with galena, bornite and magnetite. Gold had increased concentration of Ag (7-21 wt %) and Fe (1.5-2.3 wt %).

In order to evaluate the pressure-temperature (P-T) path that magma and fluids followed during formation of the deposit, different types of mineral geothermometers have been used, especially their combination for proper calibration. Presence of garnet phenocrysts and Ti-in-quartz geothermobarometry (Thomas et al. 2010) on partially resorbed quartz phenolcrysts at KVE indicate that early evolution of the magma took place at the base of the lower crust in pressure of 9 kbar. Based on plagioclase-amphibole thermobarometry (Holland and Blundy 1994; Ridolfi et al. 2010) next stage of magma evolution took place at 865-915°C; at pressure 2-3.8 kbar in depth of 9-14 km. According to plagioclase-K-feldspar geothermometry (Putirka 2008) emplacement of fluid-saturated magma to the present position took place at 850°C in low pressure (1.0-1.5 kbar) environment of shallow depth (3.8-5.6 km). Early vein quartz started to form in range 660–580°C at ductile conditions. Large proportion of vein quartz has precipitated below 380°C, after fluid decompression due to change from lithostatic to hydrostatic pressure conditions. Most of the A-veins contained both early and late quartz with strong and weak CL response, respectively, as well as various transitional phases, overgrown or crosscutting in a complicated manner in several cycles. Resorbtion of early quartz grains with strong luminescence has been also often observed. Geothermometer TitaniQ applied at SLE showed that Ti contents are well corresponding to the intensity of cathodoluminiscence and show a broad continuous range of values from < 8 to 200 ppm (< 380 to 670°C). The different features of the Kráľová may be associated with different properties of the parental intrusion and more likely with significantly deeper erosion level of this locality.

## REFERENCES

HANES, R., BAKOŠ, F., FUCHS, P., ŽITŇAN, P., KONEČNÝ, V. (2010): Exploration results of Au porphyry mineralizations in the Javorie stratovolcano. *Min. Slov.* **42**, 15-33.

HOLLAND, T., BLUNDY, J. (1994): Non-deal interactions in calcic amphiboles and their bearing on amphibole-plagioclas thermometry. *Contrib. Mineral. Petrol.* **116**, 433-447.

KODĚRA, P., HEINRICH, C. A., WÄLLE, M., LEXA, J. (2014): Magmatic salt melt and vapor: Extreme fluids forming porphyry gold deposits in shallow subvolcanic settings. Geology, *doi:10.1130/G35270.*1

PUTIRKA, K. D. (2008): Thermometers and barometers for volcanic systems. *Rev. Mineral. Geoch.* **9**, 61-120.

RIDOLFI, F., REZULLI, A., PUERINI M. (2010): Stability and chemical equilibrium of amphibole in calc-alkaline magmas: an overview, new thermobarometric formulations and application to subduction related volcanoes. *Contrib. Mineral. Petrol.* **160**, 45-66.

THOMAS, J. B, WATSON, E. B., SPEAR F. S., SHEMELLA, P. T., NAYAK, S. K., LANZIROTTI A. (2010): TitaniQ under pressure: the effect of pressure and temperature on the solubulity of Ti in quartz. *Contrib. Mineral. Petrol.* **160**, 743-759.

# CRYSTAL CHEMISTRY AND EVOLUTION OF TOURMALINES ON SB DEPOSIT ČUČMA – GABRIELA, GEMERIC SUPERUNIT, SLOVAKIA

[1]Peter Bačík[#], [1]Jakub Dikej,
[1]Jana Fridrichová

[1] Comenius University in Bratislava, Faculty of Natural Sciences, Dpt. of Mineralogy and Petrology, Mlynská dolina, 842 15 Bratislava, Slovakia, [#]bacikp@fns.uniba.sk

Key words: tourmaline supergroup, crystal chemistry, disorder, octahedral sites

Gemeric superunit in the Eastern Slovakia is rich in occurrences of tourmaline. It is a common accessory mineral in granitic rocks and their derivatives (Broska et al. 1999), as well as a frequent gangue mineral on hydrothermal ore deposits. Moreover, it is actually a rock-forming mineral on small deposit of tourmalinites near Zlatá Idka which was examined as a possible deposit of tourmalines with a use as filling in radiation-shielding concrete (Chovan et al. 2003). However, tourmaline forms very rich accumulations also on heaps of siderite and mainly on Sb hydrothermal deposits which can be used as secondary sources of tourmaline.

Exceptionally rich accumulations of tourmaline are occurring in the belt of Sb hydrothermal veins near Rožňava. This contribution brings preliminary results on crystal chemistry and evolution of tourmaline from Čučma – Gabriela vein.

### GEOLOGICAL SETTINGS

Studied samples of tourmaline were found in stack material at deposit of Čučma – Gabriela, located on NNE from Rožňava in the Southern part of Gemeric superunit. Stibnite veins are a part of Bystrý potok Fm. formed by metasandstones, phyllites, carbonates and acid volcanites. The Gabriela vein is a part of vein belt stretching in NE-SW direction between Betliar, Čučma, Bystrý potok and Štofova dolina valley (Grecula et al. 2011). Stibnite is the most abundant ore mineral on this locality, forming massive aggregates most commonly in quartz, but also in dolomite. Pyrite is also present and usually forms complex aggregates with arsenopyrite. Other common ore minerals here include sphalerite, and less common galena, berthierite, chalcopyrite, tetrahedrite, pyrrhotite, various Sb sulphosalts and gold. From gangue minerals quartz is the most abundant along with tourmaline. Dolomite is also common. Siderite is present, but not very often mineral. Other gangue minerals are muscovite, chamosite, orthoclase, rutile, xenotime-(Y), monazite-(Ce), apatite and zircon (Klimko et al. 2009).

### CRYSTAL CHEMISTRY AND EVOLUTION OF TOURMALINE

Tourmaline from Čučma – Gabriela veins forms large (up to several cm to dm) aggregates of parallel prismatic to acicular black to grayish black crystals. It displays irregular to weak oscillatory chemical zoning (Fig. 1).
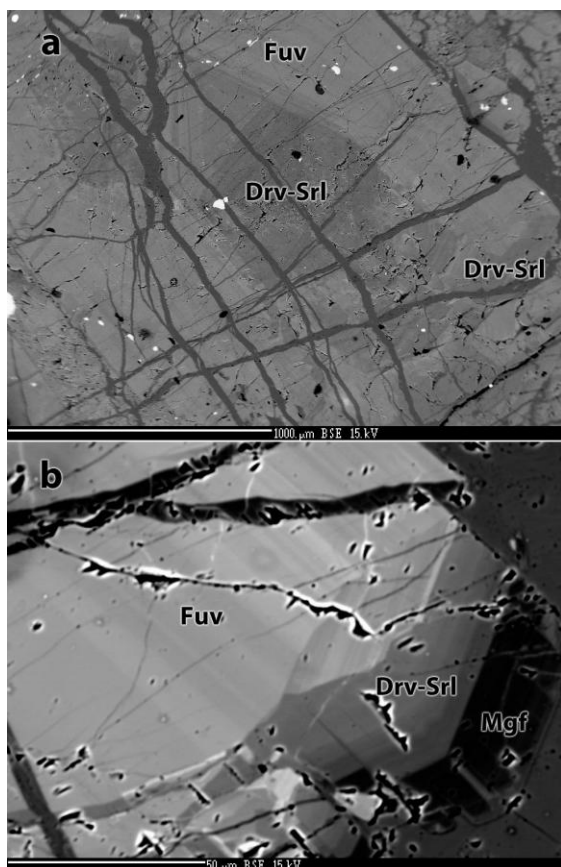
Fig. 1. BSE images of tourmaline from Čučma – Gabriela with distinct chemical zoning (Drv – dravite, Srl – schorl, Fuv – feruvite, Mgf – magnesio-foitite).

Chemical composition of tourmaline varies between calcic feruvite to alkali schorl/dravite in the majority of its mass but some of crystals have a rim zone with composition close to $X$-site vacant magnesio-foitite (Fig. 2 & 3a, b). Feruvite is volumetrically prevailing phase as also documented on lattice parameters $a$ = 15.9928(8) Å, $c$ = 7.2035(5) Å, V = 1595.6(2) Å$^3$ refined from bulk powder diffraction which are between those of schorl and feruvite. Relatively large value of $c$ parameter suggests a significant proportion of Mg in the $Z$ site while large value of $a$ parameter reflects the dominance of Fe in the $Y$ site.

Two dominant substitution mechanisms influence the composition of tourmaline from Čučma – Gabriela: uvite/feruvite $CaMgFe^{2+}(NaAlFe^{3+})_{-1}$ (Fig. 3c) and

magnesio-foitite $^X\square AlFe^{3+}(NaMgFe^{2+})_{-1}$ (Fig. 3d) substitution. The Ca content increases with the higher $Fe^{2+}/(Fe^{2+}+Mg)$ ratio (Fig. 3a) while the higher proportion of the $X$-site vacancy is connected with the enrichment in Mg (Fig. 3b). The change in composition from schorl/dravite to magnesio-foitite follows the ideal trend of substitution (Fig. 2b) which suggests that the deprotonization in the anionic $V$ and $W$ sites did not play any role in studied tourmalines.
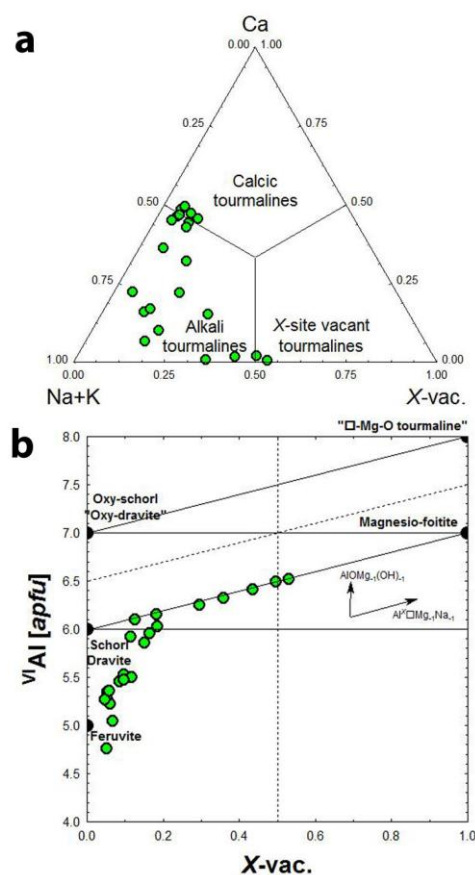


Fig. 2. Diagrams displaying chemical composition of tourmaline from Čučma: a) Ca-Na+K-$^X\square$; b) octahedral Al vs. $^X\square$.

The chemical composition and zoning of studied tourmalines reflects the small oscillations in the composition of hydrothermal fluids (variations in the proportion of Al, Mg, Fe, Na and Ca especially) producing feruvite to schorl/dravite and a significant compositional change in the latest stages of

the tourmaline crystallization producing magnesio-foitite. The presence of magnesio-foitite should not be attributed to the decrease in temperature as it is in case of schorl-to-foitite system in Gemeric granites (Broska et al. 1999). It can be the result of the decrease in proportion of Fe and Na in fluids. Similar but genetically reverse effect was observed in magnesio-foititic to schorlitic tourmaline from Detva – Biely vrch deposit where the oldest magnesio-foititic composition is the result of low Fe content in fluids and compositional transition to schorl was a result of the Fe enrichment (Bačík et al. *in prep.*).

REFERENCES

BROSKA, I., UHER, P., SIMAN, P. (1999): Sodium deficient schorl and foitite in the Spiš-Gemer granite, Eastern Slovakia. *Miner. Slov.* **31**, 507–512. (in Slovak)

CHOVAN, M., MORAVANSKÝ, D., OZDÍN, D., PRŠEK, J. (2003): Turmalíny – Zlatá Idka, mineralogická správa. *Unpublished manuscript, KMP PriF UK, Bratislava.*

KLIMKO, T., CHOVAN, M. & HURAIOVÁ, M. (2009): Hydrothermal mineralization of stibnite veins in the Spiš-Gemer Ore Mts. *Miner. Slov.* **41**, 115–132. (in Slovak)

GRECULA, P., KOBULSKÝ, J (EDS.) (2011): Vysvetlivky ku geologickej mape Spišsko-gemerského rudohoria 1: 50 000. ŠGÚDŠ, Bratislava.
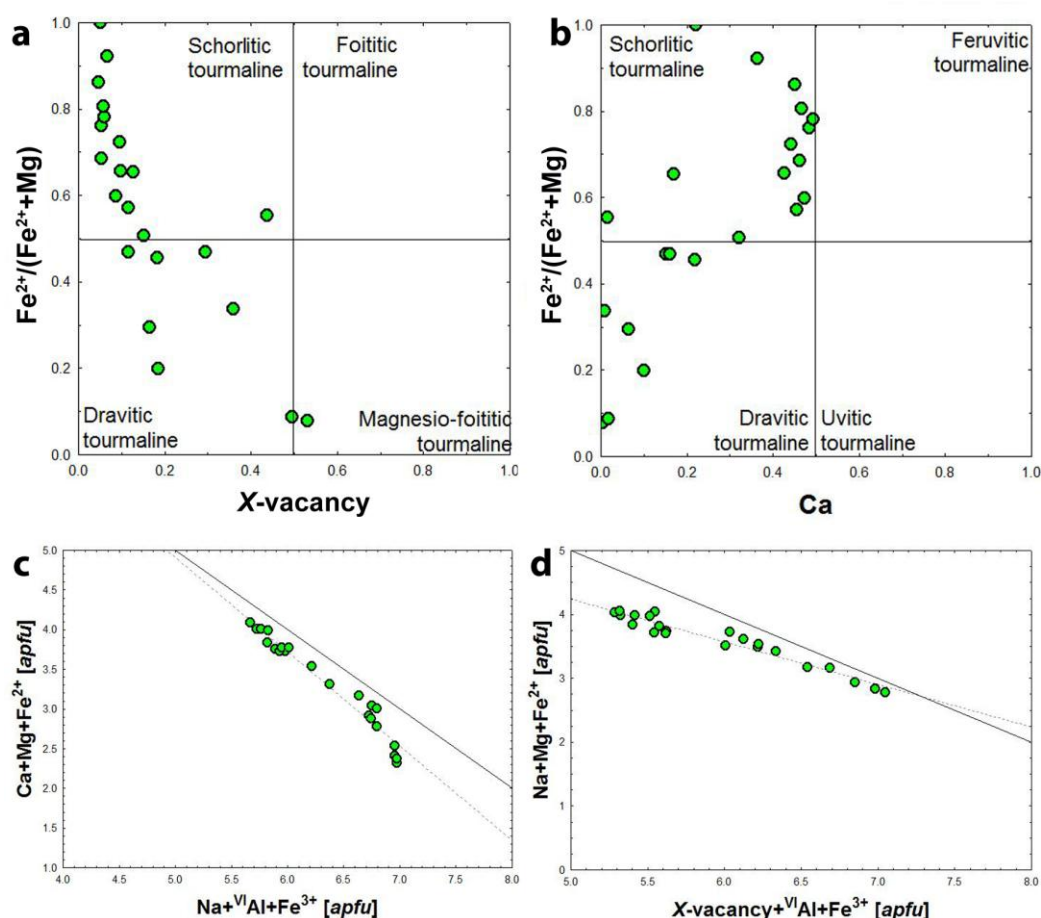


Fig. 3. Classification and substitution diagrams: a) $Fe^{2+}/(Fe^{2+}+Mg)$ vs. $^X\square$; b) $Fe^{2+}/(Fe^{2+}+Mg)$ vs. Ca; c) $Ca+Mg+Fe^{2+}$ vs. $Na+Al+Fe^{3+}$; d) $Na+Mg+Fe^{2+}$ vs. $^X\square+Al+Fe^{3+}$.

# AUTHOR INDEX

4ᵗʰ Central European Mineralogical Conference

Skalský Dvůr 2014